Perceptual and Motor Consequences of Intra-saccadic Perception

Dissertation zur Erlangung des akademischen Grades

doctor rerum naturalium (Dr. rer. nat.)

im Fach Psychologie

eingereicht an der Lebenswissenschaftlichen Fakultät der Humboldt-Universität zu Berlin
von

Richard Schweitzer, M.Sc.

Präsidentin der Humboldt-Universität zu Berlin
Prof. Dr.-Ing. Dr. Sabine Kunst

Dekan der Lebenswissenschaftlichen Fakultät
Prof. Dr. Bernhard Grimm

GutachterInnen:
Prof. Dr. Martin Rolfs
Prof. Dr. Karl R. Gegenfurtner
Prof. Thérèse Collins, Ph.D.

Tag der mündlichen Prüfung: 03.11.2020

Betreuer:

Prof. Martin Rolfs
Active Vision and Cognition, Institut für Psychologie, Humboldt-Universität zu Berlin.

Co-Betreuer (Berlin School of Mind and Brain):

Prof. John-Dylan Haynes
Theory and Analysis of Large-Scale Brain Signals, Bernstein Center for Computational Neuroscience Berlin.

Prof. Felix Blankenburg
Neurocomputation and Neuroimaging, Fachbereich Erziehungswissenschaft und Psychologie, Freie Universität Berlin.

Cite as: Schweitzer, R. (2020). *Perceptual and Motor Consequences of Intra-saccadic Perception* (Doctoral Dissertation, Humboldt-Universität zu Berlin, Berlin, Germany). doi: 10.18452/22148

”The perceptual experience of the stable, unbounded visual world comes from the information in the ambient array that is sampled by a mobile retina. The reason the world does not seem to move when the eye moves, therefore, is not as complicated as it has seemed to be. Why should it move?”

Gibson, 1966, *The Senses Considered as Perceptual Systems*, p. 256

Acknowledgements

This doctoral thesis would not have been possible without the support of many people, to whom I am eternally grateful for their important contributions on various levels.

To my supervisor Martin Rolfs, not only for the unique opportunity to conduct my research in a stimulating, open-minded, and trustful environment, full of cutting-edge methodological possibilities, but also for scientific advice and mentoring, honest feedback and valuable ideas, patience, and unconditional support, both personally and financially.

To all the members of Rolfslab. Both current and former student research assistants, Jan-Niklas Klanke, Clara Kuper, Polina Arbuzova, Luke Pendergrass, Olga Shurygina, Julius Krumbiegel, Tobias Richter, Hannah Wnendt, Aaron Vetter, Lea Krätzig, Lara Mbaye, for their help with data collection and their availability as pilot participants, as well as visiting students Emilia Maria Rehse and Yiğit Erigüç, whose great work I was glad to supervise. My PhD colleagues, Lisa Kröll, Frederik Geweke, Clara Kuper, Betty Kalogeropoulou, Olga Shurygina, Jan-Niklas Klanke, for everyday scientific and personal exchanges, as well as fun times at conferences and retreats. Carlos Cassanello for valuable literature and modeling suggestions. Anna Heuer for her advice on submitting, reviewing, and graduating. Sven Ohl for various references and discussions on modeling of response data, reverse correlation, and open science practices. Christine Kupper for her help with managing academic bureaucracy.

To Tamara Watson for welcoming, supervising, financially supporting, and introducing me to EEG research at Western Sydney University within the UA-DAAD project "Steady vision: the role of discontinuity and disruption", Tarryn Balsdon for challenging and intriguing collaborations, John Watson for sharing his insights in building LED setups, and the lively group of PhD students at the WSU's School of Psychology and Social Sciences for making me feel at home.

To the Berlin School of Mind and Brain and Studienstiftung des deutschen Volkes for both funding this doctoral project for 3 years and offering helpful courses, workshops, and conferences, as well as travel funding. Again I am greatly indebted to Martin Rolfs (DFG grants RO3579/2-1, RO3579/8-1, and RO3579/10-1) for generously extending this funding.

To Olaf Dimigen for his invaluable advice on EEG-eye tracking co-registration, preprocessing and deconvolution of EEG data, and his extremely useful and publicly available Matlab toolboxes.

To M&B-based co-supervisors Felix Blankenburg and John-Dylan Haynes for occasional helpful supervision meetings.

To M&B cohort 10 and colleagues at BCCN, who were greatly missed in Adlershof, for interesting scientific exchanges, mind-opening conversations, honest advice, and enjoyable get-togethers. To the regular's table of the psychology graduate students, organized by Richard Wundrack and Julia Baum, for providing an opportunity to meet fellow PhD students at the HU's Department of Psychology.

To the reviewers and members of the doctoral degree's committee, Rasha Abdel Rahman, Martin Rolfs, Karl Gegenfurtner, Thérèse Collins, and Elisa Filevich, who read and evaluated this thesis and made its defense a memorable experience.

To those deserving thanks, but whom I may have unintentionally forgotten – my gratitude and apologies.

To my parents, relatives, friends, and my partner Sabrina for continuous support, sincere encouragement, most welcomed distraction, and wholehearted presence in times of need.

Declaration of authorship

Hiermit erkläre ich,

- dass keine Zusammenarbeit mit gewerblichen Promotionsberatern stattfand.
- dass ich die dem angestrebten Verfahren zugrunde liegende Promotionsordnung zur Kenntnis genommen habe.
- dass die Dissertation oder Teile davon nicht bereits bei einer anderen wissenschaftlichen Einrichtung eingereicht, angenommen oder abgelehnt wurden.
- dass ich mich nicht anderwärts um einen Doktorgrad beworben habe bzw. einen entsprechenden Doktorgrad besitze.
- dass die Dissertation gemäß § 6 (3) auf der Grundlage der angegebenen Hilfsmittel und Hilfen selbstständig angefertigt worden ist.
- dass die Grundsätze der Humboldt-Universität zu Berlin zur Sicherung guter wissenschaftlicher Praxis eingehalten wurden.

Datum, Unterschrift

Abstract

Rapid eye movements, so-called saccades, are most likely the fastest and most frequent human movements. Even though saccades cause projections of static objects in the world to constantly shift across the retina at high velocities, thereby producing large amounts of motion blur, visual experience remains unimpaired by these disruptions. To explain this phenomenon, dedicated mechanisms of saccadic suppression were proposed that prevent the visual processing of intra-saccadic smear. Given the fact that, despite these mechanisms, intra-saccadic perception remains in principle possible, the consequential question arises whether it might have a functional value.

As saccades are fast and brief events, technical challenges when studying intra-saccadic perception were first addressed. Study I describes a custom LED-based anorthoscopic presentation setup capable of displaying text and images strictly during saccades. Furthermore, in study II, a novel online saccade detection algorithm enabled rapid, gaze-contingent display changes using a DLP projection system running at 1440 fps.

Making use of the latter, studies III and IV investigated whether intra-saccadic motion streaks, i.e., blurred traces routinely induced by stimuli moving at saccadic speeds, could serve as cues to establishing object correspondence across saccades. Study III showed that, during both saccades and fixation, motion streaks enabled perceptual matching of pre- and post-saccadic object locations, and that matching performance depended strongly on streak efficiency. Study IV further provided evidence that gaze correction triggered by intra-saccadic target displacements, that was previously found to be mainly driven by objects' surface features, could be facilitated by motion streaks, most likely even in the absence of conscious awareness. Finally, study V explored the subjective appearance and localization of intra-saccadic motion streaks, tasking observers to reproduce the trajectories of unpredictable target motion during saccades. The subsequent modeling of resulting response patterns suggested that retinal positions over time were combined with a damped representation of eye position to readily, though imperfectly, localize intra-saccadic input in world-centered coordinates.

Taken together, these results invite the intriguing hypothesis that intra-saccadic visual signals might indeed have an impact on trans-saccadic perceptual and motor processes, for instance, by linking object representations via spatiotemporal continuity. The potential role of intra-saccadic perception for active vision in more natural environments, as well as directions for future research, are discussed.

Zusammenfassung

Sakkadische Blickbewegungen sind die wahrscheinlich häufigsten und schnellsten aller menschlichen Bewegungen. Obwohl Sakkaden die wiederholte und rapide Verschiebung von Objektprojektionen über die Retina zur Folge haben, welche mit extremer Bewegungsunschärfe verbunden sein sollte, bleibt die bewusste Wahrnehmung davon unangetastet. Um dieses Phänomen zu erklären, wird angenommen, dass durch spezielle Mechanismen die Sehempfindlichkeit herabgesetzt wird, um die Intrusion von verschmierter visueller Information zu verhindern. Trotz verringerter Sehempfindlichkeit bleibt intrasakkadische Wahrnehmung jedoch prinzipiell möglich, wodurch sich die Frage nach ihrer potentiellen Funktion stellt.

Da Sakkaden sehr kurze Ereignisse sind, galt es zunächst die technischen Voraussetzungen ihrer Untersuchung zu schaffen. Studie I beschreibt eine individuell gefertigte LED-Installation, welche die ausschließlich intrasakkadische Präsentation von Text und Bildern ermöglicht. Studie II stellt zudem einen Algorithmus zur Detektion von Sakkaden vor, welcher es erlaubt blickkontingente Stimulusmanipulationen mithilfe eines DLP Projektionssystems mit einer Bildwiederholungsrate von 1440 Hz durchzuführen.

Studien III und IV untersuchten ob visuelle Bewegungsspuren (sog. *motion streaks*), welche durch die schnelle Bewegung von Objekten über die Retina erzeugt werden, Korrespondenz zwischen Objekten über Sakkaden hinweg herstellen könnten. Studie III konnte zeigen, dass diese Bewegungsspuren es Versuchsteilnehmern erlaubten einen präsakkadischen Stimulus aus zwei identischen postsakkadischen Stimuli heraus zu identifizieren, und diese Fähigkeit von der Deutlichkeit der Bewegungsspur abhing. Darüber hinaus stellte Studie IV fest, dass, falls Stimuli während Sakkaden versetzt wurden, Bewegungsspuren Korrektursakkaden zum ursprünglichen präsakkadischen Objekt zu unterstützen vermochten. Dies war möglich, selbst wenn Versuchsteilnehmer sich der Bewegungsspur nicht bewusst waren. Schließlich untersuchte Studie V die subjektive Wahrnehmung und Lokalisierung von intrasakkadischen Bewegungsspuren, welche durch unvorhersehbare Objektbewegung während der Augenbewegung induziert wurden. Die Modellierung der von Teilnehmern gezeichneten Berichte ergab, dass retinale Positionssignale mit einer zeitlich gedämpften mentalen Repräsentation von Augenposition kombiniert wurden, um so eine effiziente, wenn auch unvollkommene Lokalisation in weltzentrierten Koordinaten zu ermöglichen.

In ihrer Gesamtheit erlauben diese Ergebnisse die Hypothese, dass intrasakkadische visuelle Signale einen Einfluss auf transsakkadische perzeptuelle und motorische Prozesse haben könnten, z.B. indem sie Objektrepräsentationen durch raumzeitliche Kontinuität verbinden. Letztlich werden die mögliche Rollen intrasakkadischer Wahrnehmung im Kontext von natürlichen visuellen Umgebungen, sowie Möglichkeiten für zukünftige wissenschaftliche Untersuchungen, diskutiert.

Contents

1 Background **1**

1.1 The challenge of visual stability 1

1.2 Saccadic omission 3

1.2.1 Active accounts: Extra-retinal mechanisms of saccadic suppression 4

1.2.2 Passive accounts: Smearing, masking, shearing forces 7

1.2.3 Excursus: Visual evoked responses to intra-saccadic stimuli 11

1.3 Intra-saccadic motion smear 14

1.3.1 Motion streaks 18

1.3.2 Excursus: Tachistoscopic presentations of natural scenes during saccades . . 22

1.4 Research question 25

2 Summaries **27**

2.1 Study I. A build-it-yourself device for intra-saccadic presentations 27

2.2 Study II. An adaptive algorithm for fast and reliable online saccade detection 29

2.3 Study III. Motion streaks as cues to linking object locations across saccades 32

2.4 Study IV. Intra-saccadic motion streaks facilitate gaze correction 35

2.5 Study V. The reference frame of intra-saccadic perception 39

3 General Discussion **43**

3.1 The extent of intra-saccadic vision 44

3.1.1 What makes a good motion streak? 45

3.1.2 Motion streaks versus large-field smear 47

3.1.3 Omission of intra-saccadic motion streaks 49

3.2 The potential function of intra-saccadic vision 52

3.2.1 Spatiotemporal visual consequences of saccades 53

3.2.2 Object correspondence based on motion streaks 55

3.3 Methodological considerations and limitations 61

3.4 Future directions 63

4 References **65**

5 Appendix **77**

5.1 Original articles 77

5.1.1 Study I 77

5.1.2 Study II 84

5.1.3 Study III 103

5.1.4 Study IV 128

5.1.5 Study V 146

Abbreviations

2AFC	two-alternative forced-choice
BOLD	blood oxygenation level-dependent
cpd	cycles per degree of visual angle
dva	degrees of visual angle
dva/s	degrees of visual angle per second
EEG	electroencephalography
FA	false alarm, false positive result
FEF	frontal eye field
fMRI	functional magnetic resonance imaging
fps	frames per second
GABA	gamma-aminobutyric acid, inhibitory neurotransmitter
H-H	horizontal-horizontal, referring to the presentation of horizontally oriented gratings around and during horizontal saccades
ISI	interstimulus interval
LED	light-emitting diode
LGN	lateral geniculate nucleus of the thalamus
LIP/VIP	lateral/ventral regions of the intra-parietal cortex
MD	medial dorsal nucleus of the thalamus
MT/MST	medial/medial-superior temporal area of the primate brain
RF	receptive field
SC	superior colliculus

SEM standard error of the mean

SF Spatial frequency

SNR signal-to-noise ratio

SOA stimulus onset asynchrony

TAE tilt after-effect

TF temporal frequency

TRF temporal response function

V1 primary visual cortex

VEP visual evoked potential

VSTM visual short-term memory

1

Background

1.1 The challenge of visual stability

We often think of perception as placing a camera in front of a visual scene. Each photograph can be represented as a matrix of RGB values which can subsequently be used to detect edges, group them to segment individual objects, and extract their meaning and relation, in order to finally perform higher-level cognitive tasks. Although this model is compelling in many respects, the process of image acquisition in humans is strikingly different and more complex, as we constantly make step-like, rapid eye movements – so-called *saccades* – that sequentially re-orient our gaze to investigate small subsets of the visual scene that are selected for processing.

Saccades are not only the most frequent, but also the fastest movements humans are capable of. In fact, it is estimated that we make 173,000 saccades per day (Robinson, 1981) which can reach angular velocities of up to 1000 degrees per second (Bahill, Clark, & Stark, 1975). On the one hand, saccades (and eye movements in general; Martinez-Conde, Macknik, & Hubel, 2004) make human vision possible, as they allow the allocation of the region of sharpest vision of the non-homogeneous human retina – the *fovea* – to areas of interest in the visual scene, while at the same time counteracting fading that would otherwise occur if the retinal image were stable for prolonged periods of time (Ditchburn & Ginsborg, 1952; Riggs & Ratliff, 1952; Stevens et al., 1976). On the other

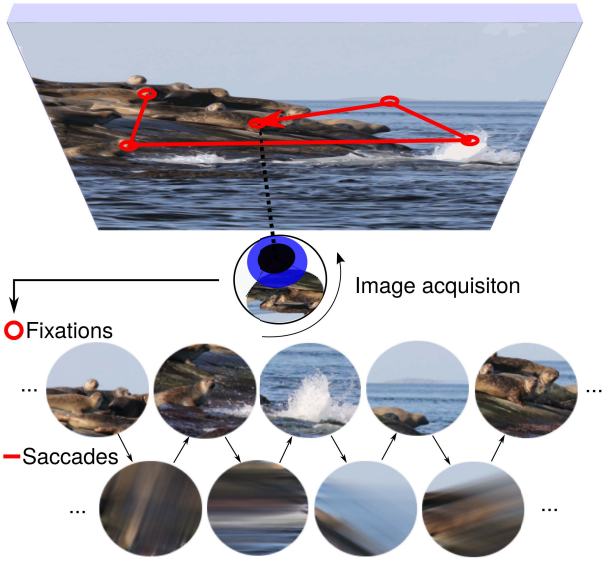

Figure 1.1: Active vision. When viewing a visual scene, the human eyes are in constant motion. While sequential fixations acquire snapshot-like pieces of information from the environment, saccadic eye movements quickly re-orient the direction of our gaze, thus shifting the visual image quickly across the retina and inducing a considerable amount of motion smear.

hand, this way of viewing the world (as illustrated in Figure 1.1) comes with (at least) two major challenges, framed as the problem of *visual stability*. First, saccades cause objects in the visual scene to rapidly change the locations of their retinal projections, creating a discrepancy between the retinotopic (where on the retina) and spatiotopic (where in physical space relative to eye and body) representation of object location. The visual system must thus keep track of object locations across saccades and seamlessly integrate visual input from discrete fixations (Aagten-Murphy & Bays, 2019; Higgins & Rayner, 2015; Melcher & Colby, 2008; Rolfs, 2015). Second, due to their high velocities, saccades induce dazzling jumps of the retinal image, as well as large-scale motion blur, so-called *intra-saccadic smear* (Binda & Morrone, 2018; Castet, 2010; Ross, Morrone, Goldberg, & Burr, 2001a). Indeed, as both simple and moving stimuli are integrated over considerable amounts of time in early vision (e.g., 100-120 ms; Barlow, 1958; Burr, 1981), one would expect moving retinal projections to appear smeared and extended in space, like photos taken with a moving camera and long exposure times (Burr, 1980). Strikingly, these immediate self-induced visual consequences of our own saccadic movements are never part of our stable and continuous experience of the world, but are – under normal viewing conditions – largely omitted from perception. The phenomenon of *saccadic omission* will be discussed in section 1.2.

To achieve stability, three distinct classes of information may be used, i.e., retinal information, proprioceptive ("inflow") information from stretch receptors in the eye muscle, and motor commands ("outflow") to the eye muscles (for extensive discussions, see Bridgeman, Van der Heijden, & Velichkovsky, 1994; MacKay, 1973; Wurtz, 2008). Adopting a Gibsonian view, one may argue that, as the visual world or "ambient optic array" (Gibson, 1966) is mostly static and contains an abundance of structured information, retinal information about the saccade-induced translation of the entire visual image may be sufficient to infer both whether an eye movement was made and whether a motion percept was induced by one's own movement or the movement of an external object in the world. However, when lightly pressing the outer canthus of one eye while occluding the other, the entire visual field moves similarly to how it should move during a saccade, suggesting that large-field visual references are not sufficient to eliminate the arising percept of an unstable world. Instead, it seems likely that extra-retinal signals would be taken into account.

A plausible candidate for such extra-retinal signals is proprioception, as stretch receptors from the six extra-ocular muscles may provide an accurate representation of eye position and compensate for retinal change. Throughout the literature, however, several findings contradict this view. First, although sufficiently available, proprioceptive information can not compensate for the visual consequences of an eye press. Second, even with paralyzed eye muscles, and therefore unchanging "inflow", illusionary jumps of the visual scene could still be perceived (Stevens et al., 1976). Similarly, oculomotor compensation and saccade accuracy remained largely unaltered in monkeys even if their proprioceptive afferents – the ophthalmic branches of the trigeminal nerve – were cut (Guthrie, Porter, & Sparks, 1983; Lewis, Zee, Hayman, & Tamargo, 2001). Finally, neural representations of the eye muscles in the monkey primary somatosensory cortex were shown to be contin-

gent upon saccade offset, often occurring with a delay of around 100 ms relative to saccade onset (Wang, Zhang, Cohen, & Goldberg, 2007). Proprioceptive signals are thus assumed to be too slow to counteract to perceptual change occurring early during the saccade (Wurtz, 2008), although they might still play a role in the estimation of visual direction (Bridgeman & Stark, 1991; Bridgeman et al., 1994; Gauthier, Nommay, & Vercher, 1990). Recent evidence suggests that information about eye position is already represented in V1 and that proprioceptive signals in the somatosensory cortex have a similar latency as those now found in V1 (Morris & Krekelberg, 2019).

In fact, most recent evidence suggests that predictions based on motor commands to the eyes – coined as *Willensanstrengung* (Helmholtz, 1866), *corollary discharge* (Sperry, 1950), or *efference copy* (Von Holst & Mittelstaedt, 1950) – serve as the basis for visual stability. The terms imply that the available feedforward signal is very close to or even a copy of the motor output, that could be available in real time or even prior to the initiation of the movement. Conveniently, the retinotopically organized superior colliculus (SC) projects not only to the midbrain and the pontine reticular formation, which further project to the oculomotor nuclei and the oculomotor nerve innervating the eye muscles, but also to the medial dorsal nucleus of the thalamus (MD), which projects to the frontal eye field (FEF), where also visual signals ascending via the visual pathways converge (Wurtz, 2008). Indeed, in the double-step paradigm (Hallett & Lightstone, 1976a), the inactivation of the monkey MD relay using GABA agonists (thus leaving SC and FEF intact) caused secondary saccades to be misguided towards the retinotopic location of the second target, suggesting that the transfer of information about the successfully executed primary saccade was impaired (Sommer & Wurtz, 2008). Moreover, the idea of the efference copy is compelling, as it explains illusionary jumps in the paralyzed eye (Stevens et al., 1976), as well as the movement of retinal afterimages in total darkness that occur as a consequence of saccades, but not as a consequence of tapping the eye ball (Grüsser, Krizic, & Weiss, 1987). Although efference-copy-based explanations of visual stability do not remain without criticism (e.g., Bridgeman, 2007), there is now good evidence that efference copies of the saccadic motor command are used to localize objects across saccades (Collins, Rolfs, Deubel, & Cavanagh, 2009), adjust the metrics of saccades (Collins & Wallman, 2012; McLaughlin, 1967), control the timing of saccadic suppression (Binda & Morrone, 2018; Ross et al., 2001a), and perform remapping of receptive fields and spatial attention (Cavanagh, Hunt, Afraz, & Rolfs, 2010; Rolfs, Jonikaitis, Deubel, & Cavanagh, 2011; Wurtz, 2018).

1.2 Saccadic omission

What is the fate of visual stimulation during saccades? It was first noted by Erdmann and Dodge (1898) that during reading, letters were perceived during fixations, but not during saccades. Dodge (1900) further described an easily replicable phenomenon, namely that one cannot see one's own eyes moving in a mirror, and proposed a "momentary visual anaesthesia" (p. 458). The idea is

compelling, as saccadic eye movements regularly induce a large amount of smear across the entire visual field, which is indeed never perceived under normal viewing conditions, despite being perceivable in principle (Campbell & Wurtz, 1978).

To date, most research has focused on visual or non-visual mechanisms that could eliminate smeared input during saccades: *saccadic suppression*. Although coined a mechanism (presumably with extra-retinal origin; Ross et al., 2001a; Binda & Morrone, 2018; Burr, Morrone, & Ross, 1994), the effect of saccadic suppression is an elevation of detection thresholds for brief stimulus presentations during saccades, often also briefly before and after the saccade, relative to detection thresholds for the same presentation during fixation. Volkmann (1962) first found that detection thresholds for dot patterns and recognition thresholds for words during saccades were approximately 0.5 log units higher than during fixation. As presentation durations amounted to 20 μs, retinal image smear could be ruled out as the cause of the observed threshold elevation, thus suggesting a central inhibitory mechanism. With respect to her findings, Volkmann (1962) observed that ”vision was never totally "blanked out" during eye movements” (p. 576) and that ”when one considers the ranges of luminance and stimulus-detail which we encounter every day in the visual scene, differences of these magnitudes are not impressive” (p. 578). This notion was also picked up by Campbell and Wurtz (1978) who argued that saccadic suppression (or, in their words, *saccadic attenuation*) does not explain the lack of vision during saccades, or, in other words, why one fails to notice the retinal consequences – attenuated by saccadic suppression or not – of one’s own saccades. This problem will be referred to as *saccadic omission* (Campbell & Wurtz, 1978; Ibbotson & Cloherty, 2009; Watson & Krekelberg, 2009).

It is still an ongoing matter of debate – for instance, see Castet, Jeanjean, and Masson (2001) versus Ross, Morrone, Goldberg, and Burr (2001b) – not only what the origin of the effect of saccadic suppression might be, but also which mechanisms contribute to the phenomenon of saccadic omission. Throughout the literature, two main accounts can be identified. Today’s pre-dominant view is that saccadic omission is realized by an extra-retinal mechanism of active saccadic suppression (for a collection of examples, see Castet, 2010), whereas there is a growing body of evidence suggesting that effects previously attributed to extra-retinal mechanisms could also be explained by purely visual factors, such as retinal smear, shearing forces on the retina, and masking. Below, both accounts and their respective evidence will be discussed in detail.

1.2.1 Active accounts: Extra-retinal mechanisms of saccadic suppression

In general, active accounts of saccadic suppression state that dedicated, extra-retinal brain mechanisms are in place that selectively suppress or eliminate intra-saccadic signals to enable saccadic omission and maintain visual stability.

There are several results that speak in favor of an extra-retinal contribution to saccadic suppression (for an extensive review, see Volkmann, 1986). First, although retinal smearing induced by saccades has been shown to impair detection performance (Mitrani & Yakimoff, 1970, 1971),

saccadic suppression was found even when the latter was controlled for by applying very brief presentation durations (Volkmann, 1962). Second, the effect could be replicated with nearly uniform backgrounds of homogeneous luminance (Burr, Holt, Johnstone, & Ross, 1982; Burr et al., 1994; Volkmann, Riggs, White, & Moore, 1978), as well as under complete Ganzfeld conditions (Riggs & Manning, 1982). Although these studies used longer presentation durations (10 – 20 ms), which would induce considerable smear in the retina, the applied stimuli – i.e., large horizontal gratings presented during horizontal saccades, sometimes to referred to as the *H-H paradigm* – were chosen to minimize smearing and contrast masking (Castet, 2010). The stimulus used by Riggs and Manning (1982) was instead a 10-ms decrement in illumination of the Ganzfeld. Third, saccadic suppression could also be found in complete darkness when observers detected the presence of visual phosphenes, i.e., small illusionary visual percepts produced by the 20-ms electrical stimulation of the eye (Riggs, Merton, & Morton, 1974), suggesting that even in the absence of other retinal stimulation that could potentially interact with the test stimulus, saccades could cause a threshold increase. Note, however, that other investigators, such as Brooks and Fuchs (1975) and Richards (1969), could not find meaningful saccade-related threshold increases in total darkness.

The most relevant argument in favor of the active account is however the finding that saccadic suppression is particularly strong for test stimuli with low spatial frequencies (SFs), as first shown by Volkmann et al. (1978) using the H-H paradigm. The authors argued that, as the stimulus is shifting horizontally across the retina, its horizontal orientation (i.e., parallel to the eye movement) should not induce any temporal frequencies and minimize smearing. Furthermore, even if saccades had a vertical component, the smearing should have had a stronger effect on high SFs than on low SFs, thus predicting the opposite result. The selectivity of saccadic suppression for low SFs becomes particularly striking when considering that low-SF gratings (down to 0.01 cpd) remained readily resolvable when moving at high velocities of up to 800 dva/s, whereas high-SF gratings became undetectable (Burr & Ross, 1982). This result contradicted previous results by Kelly (1979) who argued that (within a SF range from 0.2 to 10 cpd) contrast detection was virtually at chance above velocities of 100 dva/s, thereby explaining the loss of vision during saccades. The critical question that thus emerged was the following: While small or high-SF stimuli would be rendered invisible by the high velocities of saccades, ”why then is the observer not startled during a saccade by the sudden intrusion of low frequency components onto the scene?” (Burr & Ross, 1982, p. 483). While smearing, masking, or shearing effects (see subsection 1.2.2) should in principle affect all SFs equally, Burr et al. (1982), who replicated the specificity of saccadic suppression to low SF previously found by Volkmann et al. (1978), offered a mechanistic explanation: Low SFs were selectively suppressed to prevent the perception of motion that they would otherwise elicit when moving at saccadic velocities. Castet, Jeanjean, and Masson (2002) later showed that low SFs, such as 0.04 or 0.18 cpd, indeed elicited motion percepts when presented briefly during saccades, whereas higher SFs, such as 1.81 cpd, did not. However, this result also suggested that motion perception during saccades – despite being dampened by selective suppression processes – would be in principle possible. The idea of

motion-selective saccadic suppression was further supplemented with findings showing that contrast sensitivity was mainly impaired for patterns modulated in luminance, but not for equiluminant patterns modulated only in color (Burr et al., 1994; Knöll, Binda, Morrone, & Bremmer, 2011). This result suggested a selectivity to the magnocellular pathway as early as the lateral geniculate nucleus (LGN) in the thalamus, responsible for the fast neural processing of transient, low-SF, and motion signals (Purves et al., 2011). However, more recent experiments provided evidence that sensitivity to color is not unimpaired by saccadic suppression (Braun, Schütz, & Gegenfurtner, 2017).

Another interesting aspect of saccadic suppression – often used as an argument in favor of the role of active, extra-retinal mechanisms – is its time course. Latour (1962) first reported that an impairment of detection rate occurred already around 50 ms prior to saccade onset. A similar, but slightly less drastic early onset was found for the phenomenon of *saccadic suppression of displacement* (Bridgeman, Hendry, & Stark, 1975), and has ever since been replicated not only with various psychophysical measures (Diamond, Ross, & Morrone, 2000; Volkmann, 1986), but also with single cell recordings from various brain areas of the monkey, such as MT, MST, VIP, and LIP (Bremmer, Kubischik, Hoffmann, & Krekelberg, 2009; Crevecoeur & Kording, 2017; Ibbotson, Crowder, Cloherty, Price, & Mustari, 2008), all suggesting that neural excitability was proactively downregulated in anticipation of the saccade, not in response to retinal changes. Indeed, more than half of all measured neurons in monkey MT and MST were downregulated during image motion induced by saccades, but not when presenting comparable image motion during fixation (Thiele, Henning, Kubischik, & Hoffmann, 2002). Additional support for this view was provided by Thilo, Santoro, Walsh, and Blakemore (2004), who found that phosphenes induced by transcranial magnetic stimulation (TMS) remained unaffected by saccades when applied to the visual cortex, but not when applied to the retina. The authors thus argued that suppression must have taken place between the retina and the visual cortex, presumably in the LGN. Moreover, Sylvester, Haynes, and Rees (2005) used functional magnetic resonance imaging (fMRI) to show that saccades significantly modulated blood oxygenation level-dependent (BOLD) responses to full-field flicker in the LGN and (to a lesser degree) the primary visual cortex (V1), but not higher-level visual areas, such as V2, V3, or V5/MT. Interestingly, in contrast to prior evidence (e.g., Burr et al., 1994; Knöll et al., 2011), BOLD responses to equiluminant and achromatic flicker were equally downregulated during saccades. Notably, in complete darkness and absence of stimulation, saccades caused a positive BOLD response, highlighting the yet unclear relevance of ambient luminance for saccadic suppression (further discussed in subsection 1.2.2). For instance, Chahine and Krekelberg (2009) showed that, when the eyes were separated by a physical barrier, background luminance presented to one eye modulated suppression to a flashed target presented to the other eye. This result is evidence that the LGN cannot be the only site of saccadic suppression, as each of the nuclei receives input from the contralateral visual hemifield.

1.2.2 Passive accounts: Smearing, masking, shearing forces

Volkmann (1986) argued that in order to show the relevance of extra-retinal influences, experimenters would first need to carefully control for the inherent retinal differences between vision during fixation and saccades. As this was not always successful, it leaves the possibility that the effect of saccadic suppression – and the phenomenon of saccadic omission supposedly realized by the latter – could be explained by purely visual factors. A premise that best captures this alternative hypothesis comes from Woodworth (as cited by Matin, 1974, p. 902), stating that "vision with the rapidly moving eye ... does not differ essentially from vision with the resting eye ... given only the same retinal stimulation". Visual factors that might cause (or at least accompany) saccadic suppression involve retinal stimulation caused by saccades, spatiotemporal integration or smearing, visual masking – especially meta-contrast masking – and shearing forces on retinal photoreceptors (for reviews, see Matin, 1974; Castet, 2010). Strong evidence for the view that saccadic suppression has a retinal origin was provided by studies that simulated the visual consequences of saccades by presenting rapid image motion to the fixating eye or passively moved the eye, thus showing that the effect of saccadic suppression could also occur in the absence of extra-retinal signals, such as the efference copy. Other studies controlled for the retinal consequences induced by saccades and found the absence or reduction of saccadic suppression.

Richards (1968) found that passively moving the eye ball, e.g., by tapping or flicking the skin near the outer canthus, produced a rapid eye movement, well comparable to the duration and velocity of a saccade with an amplitude of 2–4 degrees. Test flashes were presented either 40 ms after the onset of active and passive eye movements or randomly during steady fixation periods. Strikingly, the expected increase of detection thresholds relative to fixation was of similar size for both active and passive eye movements. Even though in both conditions suppression may have been caused by efference signals co-occurring with both eye and finger movements, respectively (essentially to prepare for the disturbing visual consequences of either movement), it becomes clear that the resulting threshold elevation is clearly unable to counteract the percept of the entire visual world moving, whenever the eye ball is pressed.

Suppression effects with a similar time course to saccadic suppression could also be found when presenting rapid image motion to the fixating eye. For example, MacKay (1970) found that the likelihood of detecting a test flash on a uniformly illuminated circular projection screen decreased down to zero when the latter was rapidly moved by an electronic mirror system – even up to 50 ms prior to the onset of that movement. In a more recent study by Dorr and Bex (2013), observers were shown videos of natural scenes, which they explored under free-viewing conditions. In a second session, these eye movements were then replayed during fixation. Throughout the viewing, observers were tasked to detect contrast modulations in SF bands of either 0.375 – 0.75 cpd or 1.5 – 3 cpd, that were presented at various points around the onset of saccades. Surprisingly, in both active and passive viewing conditions, the authors found strikingly similar early-onset time courses of suppression for both low and high SF bands. These results suggest that, in more natural visual

environments, suppression was neither selective to low SFs nor specific to saccades. Furthermore, Brooks and Fuchs (1975) compared visual suppression occurring as the consequence of saccadic eye movement and saccade-like image movement during fixation in the context of uniform and patterned backgrounds of varying luminance. As also previously shown by Richards (1969) and Mitrani and Yakimoff (1971), they noted that the amount of suppression – in both saccade and fixation conditions – increased with the luminance of the background, and that in the absence of background luminance, i.e., in total darkness, no suppression was found. These results suggest that suppression is likely not related to the attenuation of intra-saccadic signals, but rather caused by the modulation of visual responses caused by large-field retinal image translations, or, in other words, "an amplification of the background activity following an eye movement" (Richards, 1969, p. 623). Watson and Krekelberg (2011) investigated saccadic suppression using the equivalent noise paradigm and provided corroborating evidence for this view: Suppression caused greater reduction of sensitivity when small amounts of Gaussian noise was added to the target than when large amounts were added. This result is compatible with a stimulus-independent reduction of response gain achieved by transient injections of noise, thus reducing the SNR across all visual detectors. Such noise injection may occur due to translations of structured backgrounds (Diamond et al., 2000) or due to motor noise induced by saccade planning and execution (Crevecoeur & Kording, 2017). Therefore, most classic studies took great care to measure saccadic suppression in Ganzfeld-like uniform conditions, but were mostly conducted in medium-luminance conditions (as an exception, see Riggs et al., 1974, who presented phosphenes instead of visual stimuli). Notably, patterned backgrounds produced larger suppression than uniform backgrounds (Brooks & Fuchs, 1975; Chekaluk & Llewellyn, 1990; Diamond et al., 2000). Surprisingly, however, patterned backgrounds impaired detection of punctate and small stimuli to a larger extent than patterned backgrounds, whereas diffuse and large stimuli were more strongly impacted by uniform backgrounds (Brooks & Fuchs, 1975). This result suggests that the effect of suppression – during both saccades and fixation – is subject to complex target-background relationships and does not selectively eliminate a restricted band of SFs.

The findings closely relate to the well-studied phenomena of visual masking. It is probably the most parsimonious approach to think of saccadic omission as the consequences of forward- and backward masking: As the brief and smeared intra-saccadic input is always enclosed within stable visual images, that can be thought of as high-intensity large-field masks with significantly longer durations, one might think that it is no wonder that intra-saccadic percepts rarely reach conscious awareness (Breitmeyer & Ganz, 1976; Breitmeyer & Öğmen, 2000). These ideas will be inspected more closely in section 1.3 on *intra-saccadic smear*. Even though it remains a matter of debate whether the effect of saccadic suppression can be attributed to masking, there is good evidence in favor of this account. For instance, Chekaluk and Llewellyn (1990) simulated a trans-saccadic sequence of images to the fixating observer, using tachistoscopic presentations. While the intra-saccadic interval consisted of a 50-ms presentation of either a mid-gray uniform screen or a vertically oriented striped pattern moving at approximately 400 dva/s, pre- and post-saccadic intervals were

each presented for 1.5 seconds and could be either patterned or uniform. Visual sensitivity was impaired – following a time course strikingly similar to those found in saccadic suppression studies (e.g., Ross et al., 2001a; Volkmann, 1986) – but only if the intra-saccadic interval was preceded and succeeded by a patterned background. For this effect to occur, it did not matter whether high-speed motion or a uniform gray screen was presented during the interval, suggesting that the transients induced by structured visual fields were sufficient to cause suppression. Recently, long-lasting suppression of neural responses was found as a result of sudden saccade-like image motion in ex vivo mouse and pig retinae (Idrees, Baumann, Franke, Münch, & Hafed, 2020). The extent of suppression was also determined by the SF content of the image background: Coarse, low-SF backgrounds produced larger suppression than fine, high-SF backgrounds. These results suggest that suppression may occur in the absence of extra-retinal signals and solely due to the processing dynamics on the retinal level. To study the time course of masking effects, Brooks, Impelman, and Lum (1981) explicitly manipulated pre- and post-saccadic mask onset relative to real and simulated saccades. Masks were presented at fixation targets (pre-saccadic mask) and saccade targets (post-saccadic mask), whereas the target stimulus location was always in-between the latter while the eye was in flight. Remarkably, pre-saccadic masks were most efficient at the onset of both real and simulated saccades, whereas post-saccadic masks were most efficient shortly saccade offset and produced prolonged threshold elevations up 300 ms after saccade offset. Mask luminance had a large impact on the extent of threshold elevations, thus mirroring the known effect of background luminance on saccadic suppression (cf. Brooks & Fuchs, 1975; Mitrani & Yakimoff, 1971; Richards, 1969). Although both target and mask were presented largely in the same retinal location, other studies could later show that a retinal overlap was not necessary to achieve a masking effect (Balsdon, Schweitzer, Watson, & Rolfs, 2018; Duyck, Collins, & Wexler, 2016), highlighting a possible special role of meta-contrast masking (Matin, Clymer, & Matin, 1972; Matin, 1974).

Another visual factor to have potentially contributed to saccadic suppression is image smearing. While the H-H paradigm (Volkmann et al., 1978; Burr et al., 1982) or extremely short presentation durations (Volkmann, 1962) were applied to minimize the potential effects of smearing, this factor remains an critical one. Matin (1974, p. 905) elaborated: “Since the eye is moving at very great speeds during most of the saccade, the time over which the luminance can be integrated at any given retinal point is small relative to the temporal integrating capacity of the eye. Thus, the effective stimulation at a given retinal point during a saccade ... is less than the effective stimulation when the same slit is presented to the stationary eye before or after the saccade.” To elucidate this point, when bright bands with either horizontal or vertical orientation were presented during a horizontal saccade, visual sensitivity decreased (relative to presentations during fixation) for vertical orientations, but not for horizontal orientations (Mitrani & Yakimoff, 1970). To further quantify the contributions of smearing and suppression, Mitrani and Yakimoff (1971) attempted to stabilize the detection target on the retina by moving it in the same direction as the saccade, and compared this condition to static targets during saccades (i.e., the effect of smearing) and to static targets

during fixation (i.e., the effect of suppression). The authors found that when presented on uniform backgrounds, threshold elevations caused by smearing and suppression were largely of the same size. On structured backgrounds, the effect of suppression was considerably larger than the effect of smearing, whereas in total darkness, no effect of suppression was found, while the effect of smearing persisted. This result suggests that image smearing might well contribute to suppression on uniform backgrounds. Clearly, these results also suggest that smearing could not fully account for suppression effects, unless some residual image smearing still occurred due to stimulus movement which did not fully match the velocity profile of the saccade.

A different way to briefly stabilize a stimulus on the retina while the eye is moving, was first described by Deubel, Elsner, and Hauske (1987), and has subsequently been used by various investigators (e.g., Castet & Masson, 2000; García-Pérez & Peli, 2001, 2011; Mathôt, Melmi, & Castet, 2015; Schweitzer & Rolfs, 2020): If gratings with an orientation orthogonal to their movement direction drift inside their aperture at high speeds, then the induced temporal frequencies (TFs) may be too high for the visual system to resolve, so that the stimulus becomes invisible (Burr & Ross, 1982; Deubel et al., 1987; Kelly, 1979). If an eye movement is made in the same direction as the drift movement, the stimulus' TF decreases, as relative (retinal) speed is reduced. As a consequence, the grating will be rendered visible for the brief amount of time during which the saccadic peak velocity matches the velocity of the stimulus movement. Moreover, due to the high TFs again present when the eye is at rest, pre- and post-saccadic masking is counteracted. Using this procedure, Castet and Masson (2000) found that motion perception during saccades was well possible, if saccadic peak velocities were slightly slower than the drift velocities of low-SF gratings (0.17 cpd), ideally inducing retinal TFs around 10–20 Hz. When TFs of 0 Hz occurred, observers reported a flashed, but not moving grating. A subsequent study found that pupillary constrictions occurred in response to the conscious perception of such fast-moving gratings presented during saccades (Mathôt et al., 2015). Furthermore, when low-SF gratings were presented as flickering in counterphase during saccades and were then replayed during fixation at TFs produced by those saccades, no significant decrease in contrast sensitivity was found (García-Pérez & Peli, 2011). Taken together, these results have intriguing implications. First, mechanisms of saccadic suppression are unable to prevent detection of low SFs and motion during saccades. Second, when the visual consequences of saccades – such as high retinal speeds, smearing, as well as pre- and post-saccadic masking – are accounted for, perception during saccades is not so different from perception during fixation.

The residual loss of sensitivity during saccades could be accounted for by the Stiles-Crawford effect, which describes the reduction of luminous efficiency (e.g., as measured by subjective brightness) of up to 80%, when light falls not directly, but obliquely onto the retina, for instance, when entering not in the center, but at the edge of the pupil (Westheimer, 2008). When an eye movement is made, shearing forces act upon the retina. "Like a bowl of jelly suddenly made to rotate, in which the greatest forces occur at the wall of the container" (Richards, 1969, p. 618), the sclera moving faster than the vitreous body causes photoreceptors to tilt away from the direction of the

ongoing eye movement. As photoreceptor responses are dependent on the angle of the incoming light, their tilt during an eye movement and the resulting reduction of responses to any stimulation could explain decreased contrast sensitivity during saccades. Although this hypothesis has rarely been investigated, Richards (1969) found that the Stiles-Crawford effect measured during fixation was indeed modulated during 5-degree saccades: The optimal direction of incoming light during saccades shifted by 0.6 mm, which corresponds to a change in receptor orientation of 2 degrees. Clearly, even though it contributes, the Stiles-Crawford effect could not account for 0.5-log-unit decreases in contrast sensitivity that were measured during saccades in various studies (Volkmann, 1986). Ross et al. (2001b) further argue that the Stiles-Crawford effect was mainly found in photopic vision while saccadic suppression could also be shown in dark-adapted observers, and that it is unable to explain the selectivity for low SFs found in many saccadic suppression studies (Ross et al., 2001a).

It is a recurring argument that passive accounts of saccadic suppression are unable to explain why contrast sensitivity during saccades is reduced especially (and in some studies exclusively, e.g., Burr et al., 1982, 1994) for low SFs. The hypothesis that the properties of the experimental setup, such as the SF content of the area surrounding the presentation screen, could have contributed to low-SF selectivity, was investigated by Idrees et al. (2020). The authors enveloped a circular, uniformly gray presentation area with noise fields, bandpass-filtered to either low or high SFs. Observers were tasked to detect Gabor patches of varying SFs presented both around saccades and movements of the surrounding noise field during fixation. Their results revealed clear visual suppression in both conditions, although saccades produced a greater reduction in sensitivity. With low-SF noise fields, suppression was strongest for low-SF targets, thus reproducing previous studies using uniform, mid-luminance backgrounds (cf. Burr et al., 1982, 1994; Volkmann et al., 1978). With high-SF noise fields, however, suppression in both conditions was equally strong for all tested target SFs. These results suggest that, even though the target was always displayed within the uniform presentation area and the surrounding noise fields were irrelevant to the task, the SF content of the entire visual scene strongly influenced to what extent certain SFs were suppressed (Idrees et al., 2020), an effect that is reminiscent of critical-bandwidth masking (Stromeyer & Julesz, 1972).

Although active accounts, stating that motion signals during saccades are actively suppressed to omit the sensory consequences of saccade-induced image motion, are widely accepted within the scientific community (Binda & Morrone, 2018), a number of purely visual mechanisms exist that could in principle achieve the same effect. To this day, it remains an ongoing discussion whether these visual mechanisms are able to fully explain the effect of saccadic suppression, let alone the phenomenon of saccadic omission.

1.2.3 Excursus: Visual evoked responses to intra-saccadic stimuli

García-Pérez and Peli (2011) found that contrast sensitivity to 0.2-cpd gratings was largely unaltered during saccades, as compared to fixation. This effect contradicted various saccadic suppression

studies (e.g., Burr et al., 1982, 1994; Volkmann et al., 1978) that have – using the H-H paradigm – described large sensitiviy differences between fixation and saccadic conditions. In contrast to those studies, García-Pérez and Peli (2011) asked participants to indicate the location of vertically oriented gratings of varying contrast, rapidly flickering in counterphase at 61 Hz, in either the upper or lower visual field. Whereas this stimulus was indiscriminable during fixation, this grating would become visible during saccades, due to the reduction of TFs. For instance, a 16-dva saccade, presumably with a peak velocity of 500 dva/s (Bahill et al., 1975), would induce a peak TF of 100 Hz on a static 0.2 cpd grating, thus rendering it invisible. The flicker-induced TF would thus reduce the saccade-induced TF to $\sim$40 Hz, thus lowering the grating's detection threshold (García-Pérez & Peli, 2001). In the fixation condition, the authors then presented TFs in the range of those previously induced by saccades. This paradigm was adopted (see Figure 1.2a) to measure visual evoked potentials (VEPs) in a co-registration approach involving eye tracking and electroencephalography (EEG) to be able to investigate the relationship between behavioral and neuronal responses to varying target contrasts. Unlike previous approaches in which the flickering stimulus was continuously present during the entire trial (e.g., Castet & Masson, 2000; Mathôt et al., 2015; García-Pérez & Peli, 2011), three frames (25 ms) of 60-Hz flicker were now presented gaze-contingently upon saccade onset, essentially to avoid the possibility of subliminal processing during fixation. In the fixation condition, the grating was presented at a TF of 54 Hz.

Gross, Vaughan, and Valenstein (1967) varied the onset of test flashes relative to saccade onset and showed that amplitudes of VEPs were greatly reduced when flashes occurred during saccades, compared to when test flashes occurring after saccade offset. These results were confounded with the retinal velocity of the applied 10-ms display, which is why this pilot study attempted a design that largely controlled for TFs induced by saccades. Due to the limited refresh rate of the 120-Hz ViewPixx EEG monitor, it was impossible to replay the exact saccade-induced consequences during fixation.

Together with Tamara Watson, five observers were tested in the EEG lab of the MARCS Institute for Brain, Behavior and Development at Western Sydney University. Figure 1.2b shows the average visual responses to targets with contrasts in a range from 17% to 100% (target absent at 0%) for each observer and experimental condition. In the saccade condition, both the typical spike potentials around saccade onset and lambda responses occurring 100 ms after saccade offset can be observed (Dimigen, Sommer, Hohlfeld, Jacobs, & Kliegl, 2011). They are followed by a negative peak around 200 ms after target onset and a positive peak again 100-150 ms later, which are present in both saccade and fixation conditions, and are generally considered part of a normal flash VEP (Odom et al., 2010). As the latter two peaks were clearly more distinct at higher target contrasts, we were able to compute the average amplitude of a VEP in each condition, i.e., the difference between local maxima and minima. As shown in the left panel of Figure 1.2c, psychometric curves did not reveal any reduction in sensitivity to lower contrasts in the saccade condition, if anything, it seemed like target discrimination performance was larger in the latter than during fixation. This may

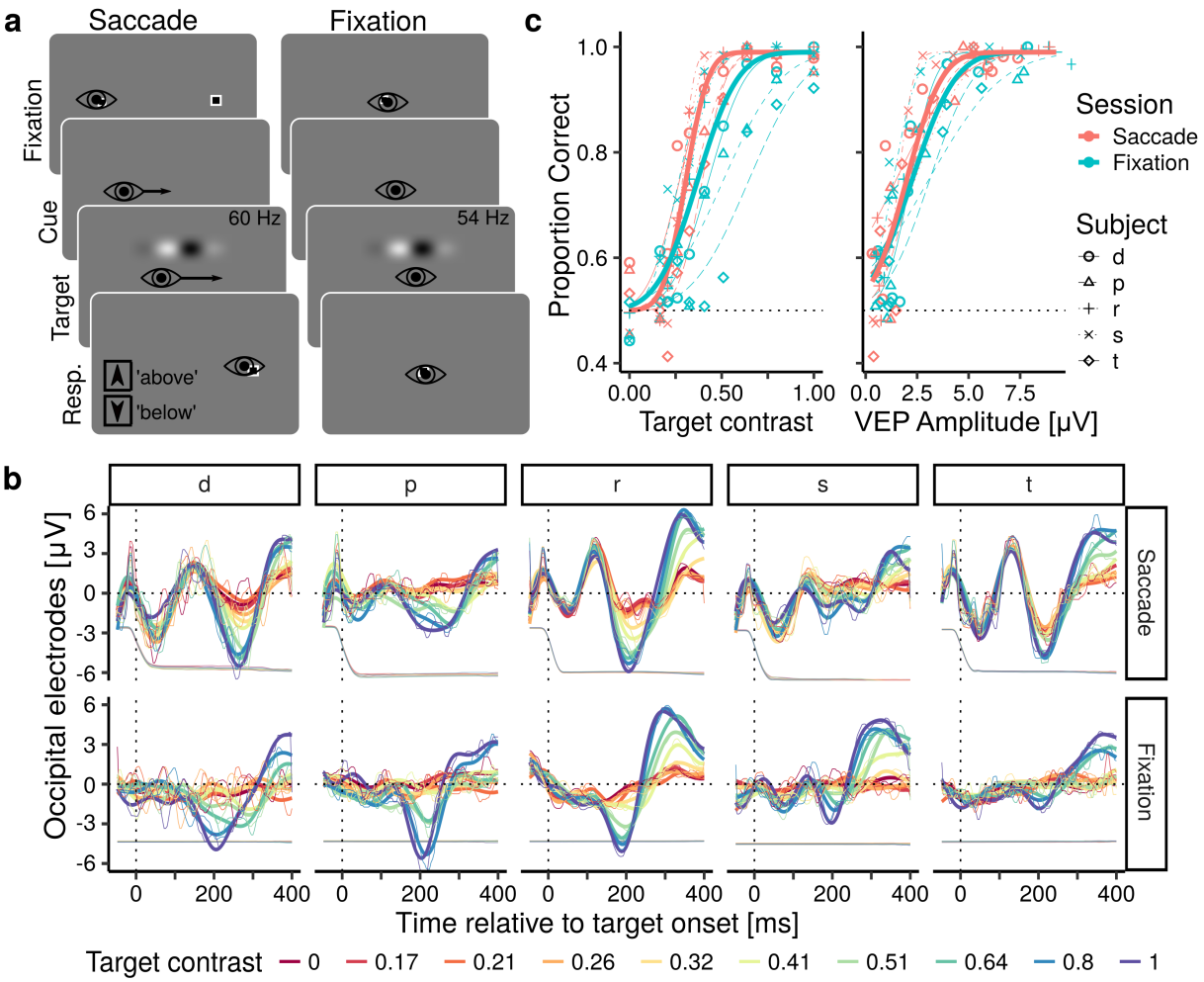

Figure 1.2: Visual evoked reponses to flickering gratings presented during saccades and fixation.
a In a two-alternative forced-choice task, observers indicated whether a 0.2-cpd vertically oriented grating was presented in the upper or lower visual field. In the saccade condition, three frames of 60-Hz flicker in counterphase were presented gaze-contingently during the saccade, whereas in the fixation condition temporal frequencies of 54 Hz were induced.
b Visual evoked potentials of five observers described by a mixed-effects generalized additive model, fitted separately for saccade (top row) and fixation conditions (bottom row), and involving target contrast as a numeric covariate. Ordinates show the mean of the central occipital electrode Oz and the adjacent electrodes. Solid lines show the model fit, thin lines show raw data averaged across all trials. Bottom trajectories represent the average gaze positions over time.
c Psychometric functions modeling the proportion of correct responses as predicted by target contrast (left panel) and mean VEP amplitude (right panel) in each condition and observer.

have been caused by a different phenomenal appearance of the target during saccades, which was reported by several observers. In fact, while during fixation the TF of the stimulus was constant, the quite variable, skewed velocity profile of the saccade induced a broader range of TFs on the retina, especially when considering that the exact physical onset time of the target stimulus varied relative to saccade onset. Moreover, in both fixation and saccade conditions, VEP amplitudes were equally well capable of predicting task performance (Figure 1.2c, right panel), suggesting that the relationship between target contrast, visual processing (as indicated by VEP amplitude) and behavioral responses during saccades is not as qualitatively different from fixation conditions as previously

suggested (e.g., Duffy & Lombroso, 1968; Gross et al., 1967). This pilot study further elucidates the feasibility of co-registering eye tracking and EEG in psychophysical tasks in order to investigate the visual responses to stimuli presented strictly during saccades.

1.3 Intra-saccadic motion smear

As outlined in subsection 1.2.1, considerable efforts were made to investigate the saccadic suppression to provide an explanation for why we do not perceive the retinal consequences of our own saccadic eye movements. Many studies suggested that saccadic suppression is driven by extra-retinal signals, but it remains yet probable that saccadic suppression could be explained by purely visual factors. Despite the prominence of the idea for active saccadic suppression that eliminates visual processing during the saccades, it is clear from most studies that the observed reduction of contrast sensitivity is unable to account for the subjective loss of vision during saccades (Castet, 2010; Matin, 1974; Volkmann, 1986). In fact, it can be elegantly demonstrated that intra-saccadic perception of motion and large-field smear is well possible (e.g., Campbell & Wurtz, 1978; Castet & Masson, 2000; Schweitzer, Watson, Watson, & Rolfs, 2019). What keeps us perceiving the latter when making saccades in rich natural environments?

This exact question was asked by Campbell and Wurtz (1978) who illuminated their laboratory room contingently upon saccade onset for varying durations using repetitive xenon flashes, thus briefly rendering the smeared scene visible. As expected, at very brief flash durations, such as 5 ms, the scene did not appear smeared, whereas large amounts of smear were perceived at durations around 50 ms. Importantly, when presentations were extended beyond saccade offset, observers perceived consistently less smearing, in fact, post-saccadic illumination durations of 40–50 ms were sufficient to leave observers with a single impression of a static, sharp scene. The authors further extended their illumination procedure to pre-saccadic intervals and found that visual sensitivity (as measured by Snellen charts) increased by up to one log-unit when illumination durations were further extended into pre- and post-saccadic intervals. These results suggest that the presence of a stable pre- and post-saccadic retinal image was sufficient not only to restore visual sensitivity, but also to omit the smeared image from conscious perception. Similarly, using large-field motion with the trajectory of simulated 6-dva saccades, Duyck, Wexler, Castet, and Collins (2018) showed that, even while fixating, the perceived amplitude of horizontal motion decreased by on average 4 dva when pre- and post-motion static masks were displayed for 40 ms or longer.

The capability to remove brief visual stimulations from conscious perception is a feature of forward and backward masking (Breitmeyer & Öğmen, 2000). Visual masking, especially backward masking, has recurrently been proposed as a parsimonious explanation for saccadic omission (Campbell & Wurtz, 1978; Castet, 2010; Matin, 1974; Volkmann, 1986), because it could explain findings of visual suppression both around saccades and during fixation (e.g., Brooks et al., 1981;

Brooks & Fuchs, 1975; Diamond et al., 2000; Idrees et al., 2020; MacKay, 1970). In their sustained-transient model, Breitmeyer and Ganz (1976) suggested that visual masking occurs due to inhibitory interactions between sustained and transient channels, which are commonly implicated in the processing of both structural and spatial information. P retinal ganglion cells, projecting to the parvocellular layers of the LGN, have smaller receptive fields, longer response latencies and responses longer sustained over time, while magnocellularly-projecting M ganglion cells have larger receptive fields, shorter response latencies, and short-lived, transient responses (Cleland, Dubin, & Levick, 1971; Croner & Kaplan, 1995; Enroth-Cugell & Robson, 1966). The sustained-transient model posits that forward masking can be realized within the sustained channel as a consequence of the center-surround organization of RFs, whereas backward masking is caused by transient channels laterally inhibiting sustained channels (Breitmeyer & Ganz, 1976). With respect to the early-onset time course of saccadic suppression, which can also be produced by presenting rapid image motion to the fixating eye (MacKay, 1970), the authors argue that ”transient stimulation produced by the saccade generates inhibition of sustained channels, which ... starts several tens of msec prior to the saccade and lasts some 100 msec or more” (Breitmeyer & Ganz, 1976, p. 26). The same logic would explain why intra-saccadic smear can be masked by post-saccadic input, as the unsmeared retinal image following the saccade can produce similar transients.

Despite its theoretical feasibility, masking-based explanations have not always been met without criticism. For instance, Ibbotson and Cloherty (2009) argued that ”backward masking relies on the mask being stronger than the stimulus during the antecedent saccade” (p. 494), which in fact might not always be the case, e.g., when a high-contrast intra-saccadic stimulus falls onto a low-contrast post-saccadic background. This would indeed be an issue in masking by noise or masking by structure, where the mask spatially overlaps with the target stimulus (Breitmeyer & Öğmen, 2000), and is a reasonable assumption for natural environments where smeared and static images always cover the entire visual field (as in the setup used by Campbell & Wurtz, 1978). It is important to note, however, that masking can similarly occur when test stimulus and mask are separated in both time and space, which is the case in para- and meta-contrast masking. In classic metacontrast masking paradigms, presentations of target stimuli are followed by non-overlapping, surrounding annular masks at varying SOAs. Breitmeyer (1978) found that the extent of metacontrast masking follows a type-B function with maximum masking efficiency at intermediate SOAs around 40 ms, a time course strikingly similar to the masking of large-field smear (Campbell & Wurtz, 1978) and motion (Castet et al., 2002; Duyck et al., 2018). In addition, metacontrast masking has been shown to be most efficient at greater visual eccentricities (for a review, see Breitmeyer & Ganz, 1976). Metacontrast masking has therefore received quite some attention as a potential visual mechanism for saccadic omission: Not only could post-saccadic stable input at one retinal location mask intra-saccadic smeared input previously picked up in a adjacent retinal location, but it would be conceivable that an earlier part of a smeared trace could be masked by successive parts of that same trace, thus reducing the overall amount of perceived smear (Matin, 1974).

Instead of studying large-field intra-saccadic smear, like Campbell and Wurtz (1978), most studies have focused on an instance of the latter, namely intra-saccadic motion streaks, which are induced by fast retinal motion of single stimuli (usually produced by oscilloscopes or LEDs) in an otherwise uniform, unstructured field. Although clearly experienced during high-speed retinal translations, motion smear can also be perceived at velocities much lower than saccadic velocities (Burr, 1980, 1981). Indeed, most experiments on motion streaks and their role in the discrimination of motion direction were conducted during fixation (or during smooth pursuit, e.g., Bedell, Tong, & Aydin, 2010), applying stimulus velocities much lower than saccadic velocities, and will therefore be discussed in subsection 1.3.1. The line of research relating to the more general question of motion deblurring (Burr & Morgan, 1997; Chen, Bedell, & Öğmen, 1995) will not be discussed.

In a classic study, Matin et al. (1972) reported the perceived lengths of intra-saccadic motion streaks induced by 4-dva horizontal saccades made across a narrow slit which was illuminated for varying durations, ranging from 1 to 300 ms. Perceived streak length depended on both luminance and illumination duration, first increasing monotonically, then peaking at durations of 20 – 40 ms, finally decreasing again when durations extended beyond saccade offset, thus mirroring well-established type-B U-shaped masking functions produced by metacontrast and backward masking (Breitmeyer & Ganz, 1976; Kahneman, 1968). As also predicted by masking processes, higher luminances led to significantly faster alleviation of perceived smearing due to increased post-saccadic mask energy, an effect that is strikingly similar to the multiplicative effect of background luminance on the magnitude of saccadic suppression (Brooks & Fuchs, 1975; Richards, 1969; Mitrani & Yakimoff, 1971). The results by Matin et al. (1972) suggest that even smear induced by highly salient stimuli (even when presented in dark field) could be reduced by simply extending intra-saccadic presentation into the fixation interval. Indeed, given that high target luminances were used, presentation durations larger than 100 ms (which are easily achieved by typical fixation durations in natural viewing, e.g., Laubrock, Cajar, & Engbert, 2013) caused the virtually complete elimination of smearing, which means that the target – extending even up to 3 dva in retinal space throughout the saccade – was perceived just as during fixation.

A similar task was applied by Bedell and Yang (2001), who compared the perceived length of motion streaks induced by saccades to streaks induced by fast stimulus motion during fixation. In saccade conditions, a bright dot was displayed upon saccade onset for 5–640 ms in front of a uniformly illuminated background, producing extended streaks on the retina during 4.6-dva saccades. After the saccade, a comparison line was presented whose length could be adjusted by the observer to match the perceived length of the intra-saccadic streak. In fixation conditions, observers fixated centrally while the test dot crossed a distance of 4.6 dva at varying speeds (50–200 dva/s). In saccade conditions, they found a strong attenuation of smear at longer presentation durations, following a time course similar to what was reported by Matin et al. (1972). Unlike these authors, however, they found no effect of test dot luminance on post-saccadic smear attenuation that would suggest metacontrast masking, which was most likely related to the illumination of their test field. In

fixation conditions, this attenuation pattern was significantly modulated: Perception of streak length while fixating was largely veridical and only a small underestimation of streak length was found when display durations exceeded movement durations. Across observers and conditions, smear was perceived as more extended during saccades (as compared to the respective fixation condition) at short presentation durations. This pattern was however reversed when saccade durations were exceeded. Bedell and Yang (2001) interprete this finding as evidence for additional smear-attenuating processes around the saccade, most likely attributable to extra-retinal signals, and propose a shortening of TRFs as a potential neural mechanism (Bedell et al., 2010). This idea had previously been developed by Burr and Morrone (1996). Although there is evidence for this view, there is also relevant critique of the applied method: Subjective reports may be inherently less reliable during saccades than during fixation, given that in normal viewing conditions smear during saccades is not consciously perceived and observers therefore have little expertise with the latter.

Therefore, more recently, a different – presumably more objective – paradigm was applied to study smear perception: By briefly dimming a bright LED at various time points throughout the saccade, observers were tasked to localize 5-ms gaps in the resulting intra-saccadic motion streak in the upper or lower visual field (Duyck et al., 2016). As long as the LED was illuminated only during the saccade, localization was quite accurate. With pre- and post-saccadic masks ($\sim$300 ms), however, localization performance was significantly impaired in all observers. With two additional experiments Duyck et al. (2016) showed not only that the effect of pre- and post-saccadic masks was similar in both normal and dichoptic viewing conditions, but also that masking could be achieved even when pre- and post-saccadic masks were displaced by up to 6 dva away from the streak-inducing target. These results suggest that the masking of intra-saccadic smear is not purely retinal in origin, as well as that a spatial overlap of intra-saccadic smear and extra-saccadic mask was not necessary for it to take effect. The latter feature is again reminiscent of metacontrast masking. In addition, the sudden pre- and post-saccadic displacement of the mask could independently have caused attentional distraction that impaired localization performance (Balsdon et al., 2018). Another objective paradigm to study the perception of streaks during real and simulated saccades was developed by Brooks, Yates, and Coleman (1980). These authors let observers detect vertical (orthogonal) target displacements while they made horizontal saccades. During fixation, the target moved rapidly at similar velocities and amplitudes as during real saccades. The proportion of correct responses was a linear function of target displacement size and was moreover strikingly similar in both real and simulated saccade conditions. This result was obtained regardless of whether the target was visible throughout the entire trial or only during its movement interval, and did not depend on the eccentricity of the presentation.

The studies reviewed in this chapter reveal that perception of intra-saccadic motion smear, whether induced by the entire visual field or by single stimuli, is possible. There are no conclusive results at this point to decide whether perception of smear during saccades is different from perception during fixation, as most studies were unable to fairly compare the two situations. There

is strong evidence, however, that smear can be significantly attenuated by prolonged presentations at the endpoints of motion trajectories. This effect, due to its time course, luminance-dependence, and its comparably weak spatial specificity, could be related to masking processes, especially metacontrast masking (for a review, see Matin, 1974). Despite criticisms (e.g., Ibbotson & Cloherty, 2009), this parsimonious visual-only mechanism, may be sufficient to explain saccadic omission: Intra-saccadic smear may be processed, but is removed from conscious awareness by masking.

1.3.1 Motion streaks

Motion in the retinal image can be described as a time-dependent two-dimensional vector field that has to be estimated locally from a time series of points in retinal space. As RFs for motion have a limited size (Anderson & Burr, 1987), the aperture problem arises, stating that if a certain RF measures the motion of a subset of an edge, then it can only extract the direction component perpendicular to the edge within the aperture, even though the detected motion could have been caused by an infinite number of motion directions (Hildreth, 1984).

Geisler (1999) first proposed that motion streaks could alleviate this problem, as 'streaky' motion of a stimulus would always activate both direction-selective and orientation-selective populations of neurons, each with an orientation tuning orthogonal and parallel to the direction of motion, respectively. On the one hand, direction-selective motion detectors are tuned in space and time (Adelson & Bergen, 1985). For instance, in (bi-)directional "Reichhardt detectors" two simple orientation-selective detectors sample from two positions in space and mutually inhibit each other, thus activating when an orientation is sequentially present in one, but not the other position (Reichardt, 1987). They therefore respond to moving, but not static orientations, orthogonal to the motion direction. On the other hand, simple orientation-selective detectors are tuned only in space. Therefore, they are not selective to motion itself, but could still respond to orientations parallel to the direction of motion. To provide an example, such a motion-streak unit would be optimally activated if a small stimulus moved through its RF. In this case, the direction-selective motion detector with a tuning orthogonal to the dot's motion direction would be activated due to the sequential appearance of the dot within its sub-units' respective RFs, while the orientation-selective detector with tuning parallel to the dot's motion direction would be activated due to the dot's appearance along the trajectory of its preferred orientation. This system would come with the advantage that both motion and motion direction could be extracted from a local RF, while optimally using available cues: If speed increases, then pure motion signals may become less reliable, but orientation signals from motion streaks may increase their reliability in this case.

A plethora of psychophysical studies provide evidence for the processing of motion streaks in the visual system, applying various techniques involving motion detection, masking, and adaptation. First, Geisler (1999) measured luminance thresholds for Gaussian blobs moving across dynamically changing line noise masks with either orthogonal or parallel orientation relative to the motion direction of the blob. Some populations of neurons in V1 have been shown to be selective for SF and

orientation, whereas others were selective for motion orthogonal to their preferred orientation (Hubel & Wiesel, 1968). Geisler (1999) found that above critical motion speeds (depending on the width of the presented blob) parallel masks were more effective in elevating detection thresholds than orthogonal masks, suggesting that especially fast-moving blobs produced larger responses in those populations that coded orientations parallel to the blob's motion direction. Similarly, fast-moving dot fields containing high- and low-luminance dots moving coherently in one direction were able to efficiently mask briefly flashed gratings when they were oriented parallel to the direction of dot motion (Alais, Apthorp, Karmann, & Cass, 2011). Maximum detection thresholds were reached around 70 ms after the onset of the dot field, suggesting that a certain integration time is needed to process motion streaks. As expected from backward and forward masking, thresholds were already elevated approximately 50 ms before motion onset and after motion offset. This masking effect was shown to occur both in monoptic and dichoptic viewing conditions and to have an orientation tuning around the direction of the masking dot field (Apthorp, Cass, & Alais, 2010). Apthorp, Cass, and Alais (2011) provided further evidence that this masking effect was also tuned to SF by measuring threshold elevations for gratings of varying SFs, again in both monoptic and dichoptic presentations. The authors found a rather broad tuning with maximal mask efficiency at lower SFs, but the introduction of a 42-second adaptation period prior to the test stimulus led to a narrowing of SF-tuning, largely resembling the SF content of the adapting dot fields (Apthorp et al., 2011). These results suggest that the processing of 'streaky' motion recruits an architecture of orientation-selective channels with SF tuning.

Evidence for motion streaks is also generated by experiments measuring the tilt after-effect (TAE). For instance, the adaptation to a grating oriented 10 degrees away from vertical caused the perceived direction of vertical motion to shift (Geisler, 1999). Crucially, significant repulsion occurred only at sufficiently high motion speeds, as, in this case, a significant TAE could be found for speeds of 10 dva/s, but not for speeds of 2.5 dva/s. Moreover, a pair of vertically aligned static dots were also subject to TAEs, which were however significantly smaller than the TAE produced by 'streaky' motion. These results were later elaborated on by Apthorp and Alais (2009), who showed that the adaptation to dot fields produced both TAEs, as well as tilt illusions. Instead of manipulating the speed of the elements in the dot fields as a measure of streak strength, they manipulated the number of frames which showed fixed-walk motion in one direction (as opposed to random-walk motion) while keeping the overall coherence constant at 50%. Using dot fields as adaptors, they found TAEs strikingly similar to those found with static adaptors: Similar to what was shown by Gibson and Radner (1937), TAE size varied as a function of relative orientation, while streak strength (i.e., fixed-walk motion duration) had a multiplicative effect on TAE size. Evidence from TAE experiments thus suggests that orientation-selective populations of neurons may indeed code motion direction.

Motion streaks might not only facilitate the coding of motion direction, but might also facilitate motion detection. Using a 2AFC task, M. Edwards and Crane (2007) let observers discriminate upward or downward motion direction from three-frame moving dot fields. They presented short (2

frames) or long (3 frames) streaks at speeds varying from 3 to 24 dva/s. Consistent with motion-streak theory, the authors found lower thresholds for motion direction discrimination when coherent motion extended further in space, but only at motion speeds higher than 10 dva/s. This effect, however, was only observed at moderate (20%) contrasts, not at low (6%) contrasts (M. Edwards & Crane, 2007). Their results suggest that the benefit of motion streaks was best described as an interaction of spatial distance and velocity, and not presentation duration alone, and that sufficient contrast was needed resolve the orientation of the motion streak. Burr and Ross (2002) used a similar motion-direction discrimination task, overlaying dot fields with noise, bandpass-filtered to a range of orientations either parallel or orthogonal to the dots' motion direction. They found that discrimination thresholds were higher for parallel masks (thus replicating Geisler, 1999) and that those thresholds were lowered with larger orientation filter bandwidths. Neither contrast sensitivity thresholds nor speed discrimination thresholds were systematically altered by the parallel/orthogonal or static/dynamic noise patterns, suggesting that noise masks specifically raised thresholds for motion direction discrimination. Further evidence for the relevance of motion streaks was provided by the investigation of motion signals from dynamic Glass patterns, which can be created by the superposition of a random noise pattern with a linear, concentric or radial transformation of the same pattern (Glass, 1969). As shown previously by Ross, Badcock, and Hayes (2000), these dynamic Glass patterns can create strong motion percepts of ambiguous direction, even though motion energy is random (see Supplementary video 3 in Burr & Thompson, 2011). Although these findings were explained differently in the original paper, they are consistent with the idea of the activation of motion streak detectors by dynamic Glass patterns: Although no consistent motion signal is present, the orientation-selective components of motion streak detectors would still be activated by the local structure of the Glass patterns (for an example, see Figure 3 in Glass & Smith, 2011), therefore locally signaling motion parallel to the alignment of pairs of dots (Burr & Thompson, 2011). Indeed, increasing the number of dots oriented coherently in pairs (thereby providing misleading motion direction signals) led to significant elevations of motion discrimination thresholds (Burr & Ross, 2002), showing that, even in the absence of effective motion energy, orientations created by aligned dots can be sufficient to provide erroneous motion direction information, and thus underlining the relevance of motion streaks for motion detection.

Having also used Glass pattern stimuli, compelling neurophysiological evidence for visual processing of motion streaks has been provided. For instance, recording from monkey MT and MST, Krekelberg, Dannenberg, Hoffmann, Bremmer, and Ross (2003) found that implied motion induced by Glass patterns modulated single cells' responses to actual motion: 26% of all recorded cells with directional tuning were affected by implied motion with respect to their preferred direction. In humans, fMRI revealed that Glass patterns affected processing in V1 and V2, and that implied motion was represented along the dorsal (but not the ventral) stream, suggesting that areas implicated in the processing of real motion were also recruited for implied motion. Krekelberg, Vatakis, and Kourtzi (2005) presented pairs of radial and concentric Glass patterns in either same-type or different-type

sequences and found that BOLD signal changes were larger in different-type sequences, suggesting adaptation to implied motion in early visual areas. These result patterns were similar, but slightly stronger for real motion, while the lateral occipital complex was active during both implied and real motion (Krekelberg et al., 2005). A similar approach was chosen by Apthorp et al. (2013), who presented sequences of alternating oriented gratings and dot fields (showing slow or fast coherent dot motion, respectively) whose orientation was always 90 degrees apart, and trained a multivariate pattern classifier on BOLD activity elicited by static oriented gratings. The classifier was then able to predict the direction of fast/'streaky' dot motion, but unable to decode the direction of slow dot motion from the BOLD signals. Notably, decoding accuracy was significantly above chance in V1 and V2, but not in higher-level visual areas, suggesting that motion streaks indeed recruited orientation-selective neuronal populations present in the early visual areas.

Finally, with the help of single-cell recordings, Geisler, Albrecht, Crane, and Stern (2001) measured neural responses to slow and fast motion from monkey and cat V1, presenting motion of both single spot stimuli and drifting plaid patterns with directions either orthogonal or parallel to the spatial-orientation preference of the RF. This convenient design allowed to quantify firing rate as a parallel-orthogonal ratio, varying across stimulus speeds. For moving spot stimuli, slow stimulus motion produced stronger responses to orthogonal directions, whereas above a critical speed (remarkably similar to the critical speeds determined with psychophysical measurements by Geisler, 1999) responses to parallel motion exceeded those to orthogonal motion. For drifting plaid patterns, SF tuning functions were band pass for orthogonal motion (with maximum responses around 2 cpd) and low pass for parallel motion (with maximum responses below 2 cpd), whereas temporal tuning functions were largely similar for parallel and orthogonal motion. Although this last result seems to disagree with the finding that increasing dot speed produces larger responses to parallel motion, it can be explained by the fact that plaid motion – unlike dot motion – should not produce any motion streaks. Crucially for the motion-streak hypothesis, the authors found a number of neurons that were direction-selective to parallel motion. While V1 neurons would be expected to be direction-selective to motion orthogonal to their preferred orientation, or not to be direction-selective at all (Hubel & Wiesel, 1968), direction-selectivity to parallel motion suggests that Reichardt-type detectors may exist that accumulate responses from two (or more) aligned and similarly orientation-selective RFs over time (Geisler et al., 2001). This kind of simple neural architecture would be ideal for the processing of motion streaks.

To conclude, investigations on the perception of motion streaks during fixation by using velocities significantly lower than saccadic velocities have important implications for intra-saccadic motion streaks. At saccadic velocities, when saccade-induced TFs exceed their temporal tuning, motion detectors in the sense of the Reichhardt model may become unable to resolve motion signals (Burr & Ross, 1982; Castet et al., 2002; Kelly, 1979). In contrast, motion-streak detectors might still be able to respond to high-speed stimulus motion, as motion streaks may still be picked up by orientation-selective cells with preferred orientations parallel to motion direction (Geisler et al., 2001). Even

though a sense of implied motion (Krekelberg et al., 2003, 2005) should thus be induced by intra-saccadic motion streaks, motion streaks were shown not to be immune to masking (Apthorp et al., 2010, 2011), as they most likely recruit the same neural architecture as the processing of orientation (Apthorp et al., 2013). Finally, motion streaks depend on motion velocity (Apthorp, Wenderoth, & Alais, 2009; Apthorp & Alais, 2009), motion distance (M. Edwards & Crane, 2007), and size of the inducing stimulus (Geisler, 1999; Geisler et al., 2001), and could therefore theoretically offer clues to more parameters than just motion direction.

1.3.2 Excursus: Tachistoscopic presentations of natural scenes during saccades

Inspired by the famous study by Campbell and Wurtz (1978), in which the laboratory room was briefly illuminated by a flashtube during saccades, we studied the appearance of smeared natural scenes tachistoscopically presented strictly during saccades. The Tscope mode of the VIEWPixx/3D monitor (Vpixx Technologies, Saint-Bruno, QC, Canada) allowed us to turn the display's scanning backlight on and off with sub-millisecond precision, so that intra- and post-saccadic scenes could be flashed in an otherwise almost completely dark environment. Stimulus material was collected from the Southhampton-York natural scenes (SYNS) dataset (Adams et al., 2016), resulting in nine subsets of 90 unique scenes, of which each belonged to one of nine scene categories, involving both natural and built environments. As illustrated in Figure 1.3a, observers made 16-dva horizontal saccades during which the first scene was presented at one of four presentation durations (8.3, 16.7, 25, 33.3 ms, i.e., multiples of one backlight scanning cycle), either as a colored or grayscale image. After an ISI of 500 ms, a second, post-saccadic scene was presented for the same presentation duration and in the same color condition. Observers subsequently decided whether this second scene was the same as the one presented intra-saccadicly, or a different one. Unlike the post-saccadic scene presented during fixation, the intra-saccadic scene would appear smeared due to the inherent speed of the saccade. As a consequence, it would seem to the observer that intra-saccadic scenes were always different from post-saccadic scenes, but we hypothesized that if some features of the scenes remained intact even during high-speed motion, then these features could be used to solve the task. Ultimately, identifying these features would allow some definition of what intra-saccadic smear in natural environments looks like.

Data of 22 observers was mainly collected by Yiğit Erigüç as part of his research internship (Pre-registration: `https://osf.io/bf246/?view_only=bff1084e94144acb94a8dde7204f07cf`). Average task performance is shown in Figure 1.3b and suggests that (except for one observer) scenes were clearly identified above chance level. Across presentation durations, colored scenes were correctly identified at a higher rate than grayscale scenes and performance decreased with increasing presentation durations in a similar manner for both color and grayscale scenes. These results are compatible with the interpretation that the amount of smear increases the longer in time and space the visual image travels across the retina, but it is equally possible that presentation duration was confounded with eye velocity during the presentation interval, i.e., the retinal velocity. Figure 1.3c

shows that at short presentation durations, which occur on average around the time of the saccade's peak velocity, average retinal velocity was only slightly below the peak velocity. Moreover, at longer presentation durations, as presentations extended into the deceleration phase of the saccade, retinal velocity decreased. Differences in retinal velocity were thus unlikely to account for the decrease of task performance at longer presentation durations, as they would predict the opposite pattern. In fact, observers' mean saccadic peak velocity only had a marginal effect on their task performance, especially at longer presentation durations (Figure 1.3d). This effect is especially striking given the wide range of saccadic peak velocities, which was caused by a large number of inaccurate saccades to the remembered position of the saccade target and a therefore large range of resulting saccade amplitudes.

Interestingly, the category of the scene presented during the saccade had a large influence on task performance over presentation durations (Figure 1.3e). Whereas differences between scene categories were negligible at short presentation durations, task performance for different scene categories ranged from slightly above chance level (e.g., woodland scenes) to 80% (e.g., natural environments and indoor scenes) at longer presentation durations. This result suggests that stimulus features of some natural scene categories might have been responsible for these large differences, rendering the scene more or less resolvable at high velocities. Clearly, task performance was determined by the similarity of intra- and post-saccadic scenes, but smearing would only affect the intra-saccadic scene. The same-different task allowed for two types of errors, i.e., mistaking the same post-saccadic scene for a different scene and mistaking a different post-saccadic scene for the same scene. Although the first type of error was twice as likely as the second, both errors could be attributed to natural scenes being distorted by smearing and certain determining features being rendered invisible during the saccade.

To determine which image features were most relevant to solving the task, two-dimensional power spectra were computed for every single scene image, resulting in power maps describing each stimulus on the dimensions orientation and spatial frequency. This procedure then allowed for the efficient comparison of pairs of scenes. For instance, Figure 1.3f shows the overall difference in power spectra between natural environments (the "easiest" category, yielding the highest task performance) and woodland scenes (the "hardest" category). On the one hand, scenes from the natural-environments category, involving coastal features, heath, and wetlands, contain higher energy in the low-SF domain and horizontal orientations, parallel to saccade direction in our task. On the other hand, woodland scenes are richer in high-SF content and vertical orientations, orthogonal to saccade direction. This result invites the intriguing hypothesis that low-SF information and orientations parallel to saccade direction may be able to explain the large performance differences between scene categories. The previously described analysis was therefore further extended. First, the stimulus set yielding maximum performance was identified and its power spectrum was chosen as the reference spectrum. Second, for each stimulus set, the mean absolute power difference to the reference spectrum was computed. Third, as shown in Figure 1.3g, mean task performance

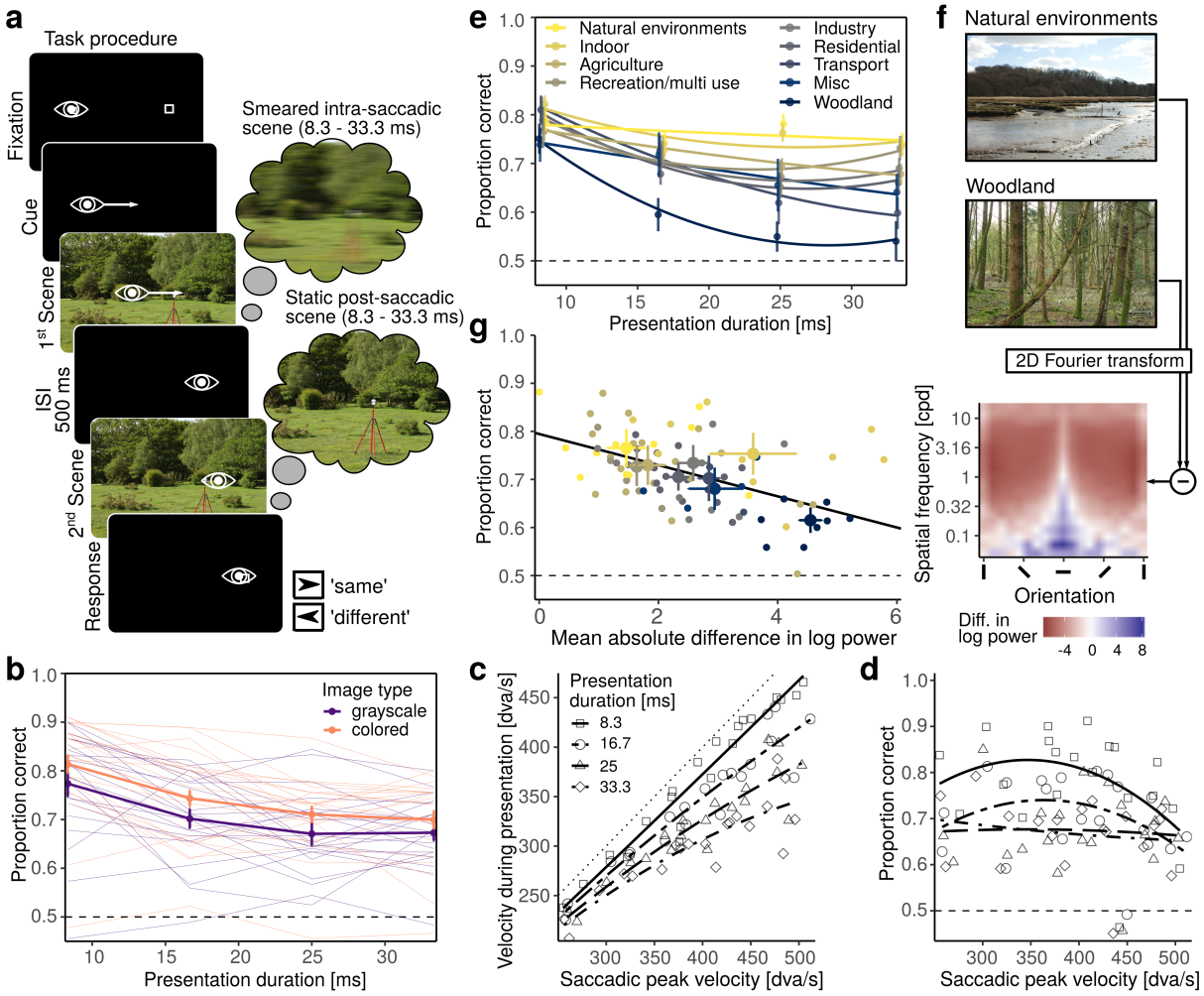

Figure 1.3: Intra-saccadic perception of tachistoscopically presented natural scenes.
a In each trial, two natural scenes were tachistoscopically presented in a same-different task. Both scenes were presented as colored or grayscale images. Observers' task was to indicate whether the first scene presented for 8.3, 16.7, 25, or 33.3 ms during the saccade was the same as the post-saccadic scene presented for the same duration.
b Task performance across 22 observers. Thin lines indicate individual observers, solid lines indicate the grand average with error bars representing the within-subject 95% confidence intervals.
c Mean saccadic velocity during presentation as a function of the observer's saccadic peak velocity.
d Relationship between each observer's average peak velocity and task performance in each experimental condition.
e Average task performance as function intra-saccadic scene category, as defined in the SYNS dataset (Adams et al., 2016), sorted by average task performance.
f Difference in log power between all natural environments (highest task performance) and woodland (lowest task performance) scenes in SF and orientation content. Blue indicates higher power in natural environments, red indicates higher power in woodland scenes.
g Relationship between task performance and difference in log power compared to the scene producing the highest task performance.

for each stimulus set was plotted against the mean difference in log power, revealing a significant negative linear relationship. This result suggests that the less horizontal and low-SF information natural scenes contained, the less identifiable they were to the observer, resulting in lower task performance.

Although saccade-induced smear in natural scenes has never been investigated, these finding are well in line with previous experimental findings. For instance, very low SFs ($<$ 0.1 cpd) remain largely resolvable at saccadic velocities, whereas high SFs are eliminated by the latter (Burr et al., 1982; Castet et al., 2002). Due to the high-luminance intra-saccadic presentation, saccadic suppression – presumably selective to low SFs – was unable to omit low-SF image content from conscious perception in the absence of pre- and post-saccadic masking (Brooks et al., 1981; Campbell & Wurtz, 1978; Duyck et al., 2018). Instead, high power in the low-SF domain predicted high task performance. Conversely, vertical orientations, especially those at SFs above 0.1 cpd, were predictors of low task performance. They have been shown to be most affected by smearing (Mitrani & Yakimoff, 1970; Volkmann et al., 1978) and induce high TFs that easily exceed the window of sensitivity between 1 and 30 Hz (Burr & Ross, 1982). This effect is strikingly evident in the woodland scenes, since, after having completed the experiment, observers frequently reported that they had never or rarely seen any trees during saccades, while they could indentify water, sky, beaches, or grassland with high confidence. To conclude, these results suggest that motion smear induced by saccades when viewing natural scenes contains meaningful information that allows for the discrimination of scene categories. Depending on the combination of saccade parameters (e.g., direction, amplitude, and velocity of the saccade) and scene content, visual features in certain SF and orientation passbands could in principle remain resolvable even at high retinal velocities.

1.4 Research question

Intra-saccadic visual input may be rich in information. As the world during a saccadic eye movement is usually stable, saccade-induced motion smear has a deterministic relationship to the metrics of the ongoing saccade, such as direction, amplitude, duration, and velocity.

Perception of motion streaks, caused by fast retinal translation of objects, has been thoroughly researched in fixating subjects and with stimulus velocities well below those of saccadic eye movements (subsection 1.3.1). These studies suggest that processing of motion streaks is grounded in motion and orientation detectors in early vision (Geisler, 1999; Geisler et al., 2001). Thus, motion streaks could enable the processing of motion even when induced TFs are too high to be resolved by motion detectors alone (Burr & Ross, 1982). These features make motion streaks the ideal model for studying motion smear in general, which should be ubiquitous to intra-saccadic visual experience (subsection 1.3.2; Campbell & Wurtz, 1978). Regardless of whether the effect of saccadic suppression is caused by active, extra-retinal mechanisms (subsection 1.2.1) or can be explained by purely visual-only processes (subsection 1.2.2), the reduction of contrast sensitivity around saccades is unable to account for the striking omission of intra-saccadic vision from conscious awareness, especially during natural vision. In fact, that intra-saccadic vision is in principle possible could be demonstrated by a plethora of studies (section 1.3). In addition to that, there is evidence that peri-saccadic information, which could not be detected above chance level, still shaped observers'

post-saccadic perception – even to the extent of contributing to visual illusions (Watson & Krekelberg, 2009). As a consequence, the question arises whether intra-saccadic vision can be simply considered an epiphenomenon or lab artifact, or whether it might actually contribute to processes of active vision, even in the absence of conscious awareness. Ultimately, intra-saccadic visual input may even provide important visual cues that – in addition to, or even instead of extra-retinal signals – contribute to solving the challenges of visual stability (section 1.1).

This doctoral thesis attempts to lay the groundwork for studying intra-saccadic vision. More than to what extent the latter is possible, the main goal is to investigate whether intra-saccadic vision could have a functional role in trans-saccadic perceptual and motor processes.

Studies I and II are methodological. The former deals with the possibility of using LED-based anorthoscopic presentations to study retinal smearing during saccades, whereas the latter focuses on the issue of online saccade detection for strictly intra-saccadic gaze-contingent presentations. Studies III and V investigate the perceptual consequences of continuous (and therefore streak-inducing) high-speed stimulus motion during saccades with respect to the matching of pre- and post-saccadic object locations, as well as the localization and phenomenal appearance of motion streaks in space. Finally, study IV examines the motor consequences of intra-saccadic vision, specifically, whether motion streaks could facilitate post-saccadic gaze correction in response to the intra-saccadic displacement of the initial saccade target.

2

Summaries

2.1 Study I. A build-it-yourself device for intra-saccadic presentations

Reference

Schweitzer, R., Watson, T., Watson, J., & Rolfs, M. (2019). The joy of retinal painting: A build-it-yourself device for intrasaccadic presentations. *Perception*, 48(10), 1020–1025.
doi: 10.1177/0301006619867868

Summary

By simply trying to see one's own eyes move in a mirror (Dodge, 1900), it can easily be demonstrated that (at least in normal, everyday visual environments) we are largely unaware of the extreme visual consequences that our own saccades should produce when they rapidly shift the entire visual image across the retina. Despite the widespread assumption that visual processing is shut down during saccades (for a non-exhaustive list of examples, see Castet, 2010), intra-saccadic perception of motion smear, as outlined in section 1.3, has been shown to be in principle possible. To be able to demonstrate the latter, study I (see subsection 5.1.1) describes a simple but potent build-it-yourself device that allows for stimulus presentations easily perceivable exclusively during saccades.

For complex visual stimuli to remain resolvable in the face of high saccadic velocities, one would normally need efficient retinal stabilization techniques (Mateeff, 1978; Mitrani & Yakimoff, 1971), gaze-contingently triggered and extremely short presentations durations (Campbell & Wurtz, 1978; Volkmann, 1962), or stimuli moving at high speeds in the direction of the saccade (Castet & Masson, 2000; Deubel et al., 1987; García-Pérez & Peli, 2001). Since all of these approaches require costly dedicated experimental setups, here we employed a presentation technique that uses the inherent retinal smearing due to saccadic speeds to its advantage. *Anorthoscopic* presentations show separate subsections of an image in a sequential manner, as if that image moved behind a narrow slit (Rock, 1981). We built an anorthoscopic presentation device based on four vertical LED strips (1m, 144 pixels) driven by a Raspberry Pi microcontroller. As illustrated in Figure 2.1a, image matrices were scaled to the number of available LEDs and presented column-wise from left to right at a refresh rate of approximately 1400 fps. On the one hand, when fixating, the anorthoscopic

stimulus appeared like a brief vertically oriented flash (Figure 2.1b, left). As presentation durations of 25 ms were used, sequential activations projected on the same part of the retina naturally underwent temporal summation, leaving the observer unable to resolve the image. On the other hand, when presentations happened to occur during saccades, sequential activations would be projected on different parts of the retina, thereby producing a retinal image extended in space (Figure 2.1b, right) that is briefly visible due to visual persistence (Anstis & Atkinson, 1967; Rock, Halper, DiVita, & Wheeler, 1987). This is the principle of *retinal painting* that was first proposed by Helmholtz (1866).

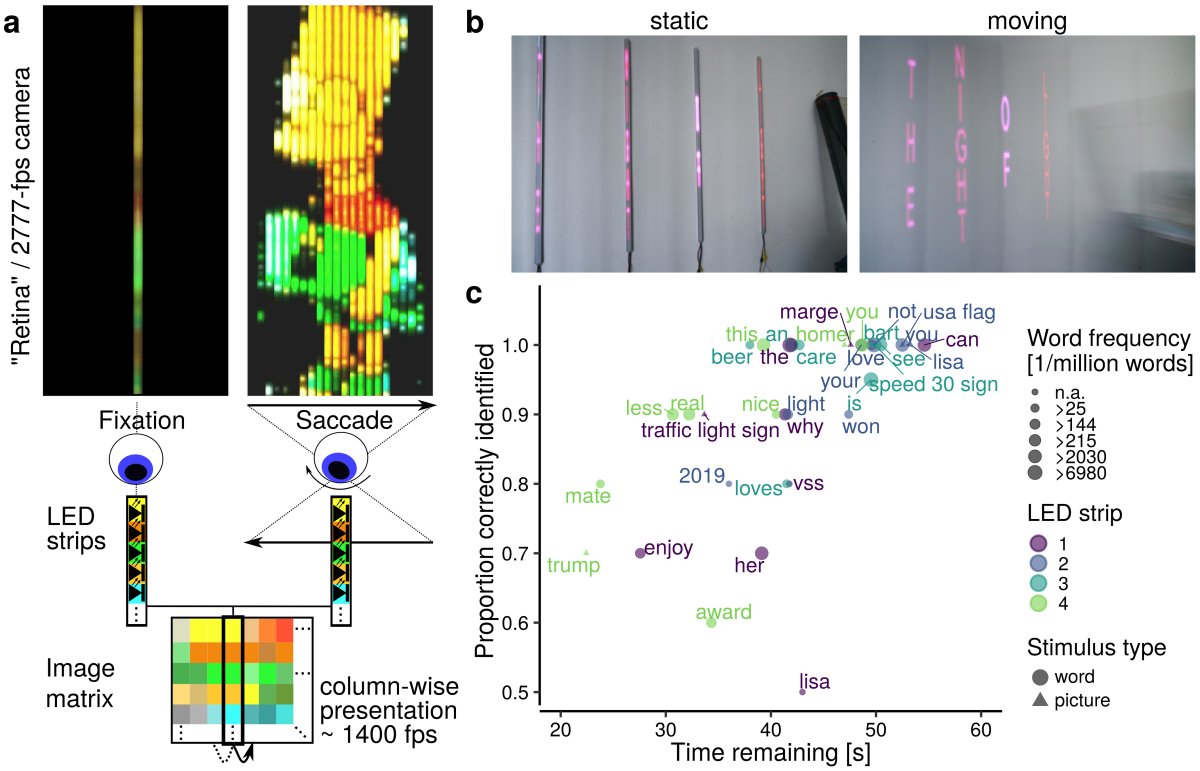

Figure 2.1: The principle of intra-saccadic retinal painting. **a** Image matrices are presented on vertical LED strips in an anorthoscopic fashion, i.e., column-wise, as if moving behind a narrow slit. Due to the device's high refresh rate, images are only briefly resolvable during saccades when individual LED strip activations fall on different parts of the retina (right column). This instance was simulated by the concatenation of individual activations recorded by a high-speed camera.
b Photographs taken with a static and rightward rotating camera (1/3-second exposure time).
c Results of the validation procedure. Observers were shown nine stimulus sets, each with four anorthoscopically presented words or images, which they had to identify within a time limit of one minute.

We validated our presentation technique by tasking ten observers to name sets of anorthoscopically presented text and images (nine sets, four stimuli per set, 1-minute time limit) without further instructions, except that moving one's eyes would be necessary. Overall identification performance was around 90% (words: 89%, images: 95%) and observers took on average 29 seconds to identify all four stimuli. Figure 2.1c shows the average discriminability of each stimulus.

In this study we built, implemented, and validated an anorthoscopic presentation technique that is – thanks to its high temporal resolution – well suited for the purposes of intra-saccadic stimulus presentation. Both text and images could be resolved at high accuracy when smeared (or "painted")

across the retina during saccades. This new application of retinal painting could not only be used to study visual processing around and during saccades, but could also be interesting for media-related applications, as these stimuli, even without actively attending to them, become highly salient when occurring during involuntary saccades.

2.2 Study II. An adaptive algorithm for fast and reliable online saccade detection

Reference

Schweitzer, R., & Rolfs, M. (2020). An adaptive algorithm for fast and reliable online saccade detection. *Behavior research methods*, *52*(3), 1122–1139.
doi: 10.3758/s13428-019-01304-3

Summary

As saccades are brief and fast events, timing-efficient gaze-contingent experimental setups and implementations are needed to perform strictly intra-saccadic stimulus presentations. To achieve display changes upon saccade onset, various sources of latencies have to be considered, ranging from end-to-end delays of eye tracking systems to the display's reaction time. While most of these latencies are hardware-related, saccade detection latency (i.e., the time from the physical onset of the saccade to the online decision that it has occurred) is determined by the algorithm used. Most experimental paradigms use either spatial-boundary or absolute-velocity techniques, which have significant shortcomings, respectively. Boundary techniques are robust, but detect saccades relatively late, whereas absolute-velocity thresholds provide early saccade detection, but suffer from high false alarm (FA) rates, especially when tracking noise is increased.

In study II (see published manuscript in subsection 5.1.2) we proposed and validated a velocity-based algorithm for online saccade detection (based on an approach to microsaccade detection described in Engbert & Kliegl, 2003; Engbert & Mergenthaler, 2006) that remedies these problems, providing early saccade detection with high robustness to noise. As described in Figure 2.2a, the algorithm computes a two-dimensional velocity threshold $\eta_{vx,vy}$ based on the median-based standard deviations $\sigma_{vx,vy}$ of previously collected velocity samples (multiplied by a free threshold scaling parameter λ), thus adaptively estimating tracking noise. Noisy samples are further accounted for by in-built smoothing and interpolation. In order to further increase robustness, for instance against blinks, an optional direction criterion θ limits detections to a specified range of saccade directions ($\theta_{min} - \theta_{max}$).

To evaluate the proposed algorithm's performance compared to the widely used spatial-boundary and absolute-velocity techniques, all three algorithms' detection latency and accuracy was measured in a large-scale simulation involving more than 30,000 saccades of varying amplitudes and directions, collected at sampling rates of 500 and 1000 Hz. Results suggested that the proposed

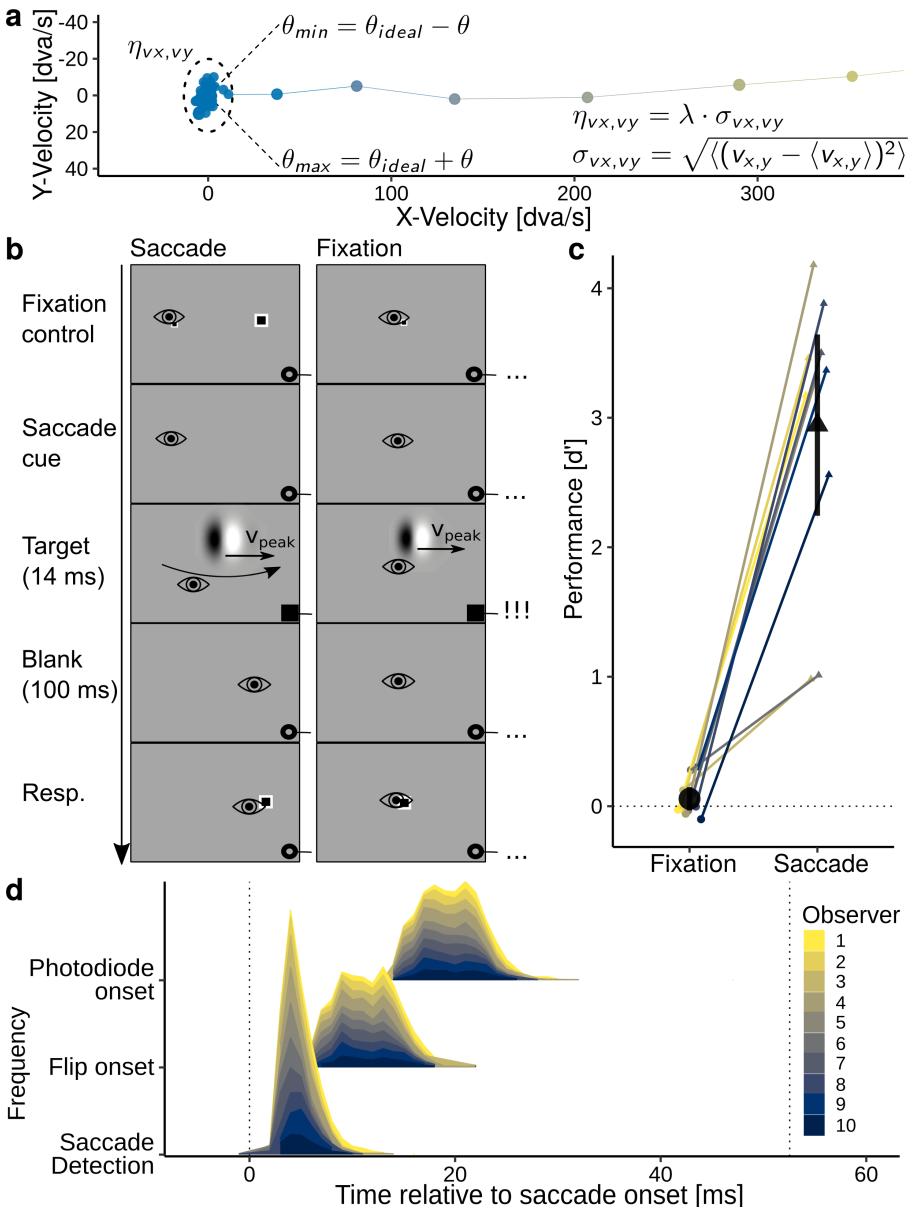

Figure 2.2: Subjective and objective tests for strictly intra-saccadic stimulus presentations.
a Illustration of the proposed online saccade detection algorithm. Two-dimensional velocity thresholds $\eta_{vx,vy}$ (short-dashed ellipse) are computed by multiplying the median-based standard deviation of preceding velocity samples $\sigma_{vx,vy}$ with the free scaling parameter λ. An optional direction criterion limits directions of detected saccades to a range between directions from θ_{min} to θ_{max} (long-dashed lines) around the instructed saccade direction θ_{ideal}.
b Experimental paradigm used for subjective and objective tests. In the saccade condition, a vertical Gabor patch, rapidly drifting at a speed similar to the observer's average saccadic peak velocity, was displayed upon saccade detection for 13.9 ms. Stimulus contrast was either 100% or 0%. The same stimulus was displayed to the fixating eye. Observers indicated whether the stimulus was present or not. During stimulus presentation, black squares were presented to trigger a photodiode.
c Subjective test. Gabor patches drifting at high speeds were undetectable during fixation. If presented gaze-contingently during saccades, the Gabors were detectable, as the reduction of their retinal velocity rendered them visible. This is proof that presentations must have happened strictly during saccades.
d Objective test. Saccades were detected online on average 5 ms after their physical onset, graphics card refreshes occurred around 6 ms later. Photodiode measurements confirmed stimulus onsets 20 ms after saccade onset. Saccade onset and offset are shown as vertical dotted lines.

algorithm detected saccades as early or even earlier than absolute-velocity thresholds, which detected saccades on average 10 ms earlier than boundary techniques. Indeed, given a reasonable parameter choice, detection latencies of only 3 ms could be reached while FA rates remained below 1%. Crucially, the proposed algorithm was also found to be more accurate than absolute-velocity thresholds, even when the latter evaluated more than one velocity sample. To further evaluate performance in noisy or low-precision tracking conditions, we injected random noise into gaze position samples. These analyses revealed that when Gaussian noise with a standard deviation of only 1.5 arcmin was added to data sampled at 1000 Hz, FA rates of absolute-velocity techniques were increased to virtually 100%, rendering this technique useless. In contrast, the proposed algorithm's detection accuracy did not decrease, as detection thresholds were dynamically adjusted.

In addition to simulations, we developed both objective and subjective experimental tests to show that strictly intra-saccadic presentations were feasible. In this test, we presented vertically oriented 0.5-cpd Gabor patches of 100% or 0% contrast (stimulus present or absent, respectively) for 13.9 ms to ten observers, either gaze-contingently during saccades (Figure 2.2b, left column) or during fixation (Figure 2.2b, right column). Crucially, using a Propixx DLP projector (Vpixx Technologies, Saint-Bruno, QC, Canada) running at a temporal resolution of 1440 fps, Gabor patches drifted within their Gaussian aperture (SD = 0.5 dva) at speeds similar to each observer's saccadic peak velocity ($\overline{v}_{peak}$ = 419 dva/s). These high speeds effectively rendered stimuli undetectable during fixation (Figure 2.2c). When presented gaze-contingently during saccades, however, the same stimuli were readily detectable, as retinal velocities were greatly reduced by saccades (Castet & Masson, 2000; Deubel et al., 1987; García-Pérez & Peli, 2001), thus demonstrating that presentations must have happened while the saccade and the drifting stimulus moved in the same direction with similar velocities. This subjective test can be used by vision scientists to determine whether their stimulus presentations really occur during saccades: If gaze-contingently presented gratings flickering in counterphase at 60 Hz or above can be detected by observers, then these presentations must have occurred intra-saccadicly. To objectively measure the physical onset during saccades, we also visually stimulated a photodiode attached to the lower right corner of the presentation screen. Photodiode responses confirmed not only that the drifting Gabor was – including all system delays – physically present 20 ms after saccade onset, but also that the video delay (from the flip of the graphics card's front and back buffer to effective presentation) of the Propixx projection system was equal to the duration of one refresh cycle, i.e., 8.3 ms (Figure 2.2d). Online saccade detection at a sampling rate of 2000 Hz occurred on average around 5 ms after physical saccade onset. Taking into account the 2.7-ms end-to-end delay of the Eyelink 1000+ eye tracking system (SR-Research, 2013), detection latency amounted to 2.3 ms with FA rates of less than 1%.

To conclude, these experimental results demonstrate that the proposed online saccade detection algorithm convincingly enabled early and reliable saccade-triggered stimulus presentations using the 1440-fps Propixx projection system. In addition, extensive simulations not only provided evidence

that this novel approach outperformed traditional approaches, but also elaborated on optimal parameter spaces for various tracking conditions. These insights are highly relevant for a wide range of studies applying gaze-contingent intra-saccadic stimulus manipulations, for which the described algorithm might become a useful tool.

2.3 Study III. Motion streaks as cues to linking object locations across saccades

Reference

Schweitzer, R., & Rolfs, M. (2020). Intra-saccadic motion streaks as cues to linking object locations across saccades. *Journal of Vision*, 20(4):17, 1–24.
doi: 10.1167/jov.20.4.17

Summary

When making a saccade to an object of the visual scene, the object's retinal projection travels rapidly from a peripheral to a foveal location. Given a stable visual environment, the velocity of the retinal translation is always equal to the high velocity of the saccade, and should therefore produce smeared traces, which can be described as motion streaks (subsection 1.3.1). Even though these saccade-induced motion streaks are subject to saccadic omission under natural viewing conditions, they can be readily perceived, e.g., in low-luminance conditions or in the absence of pre- and post-saccadic masking (section 1.3).

In study III (see publication in subsection 5.1.3) we investigated the question whether intra-saccadic motion streaks could, in principle, be used to link object locations that changed during saccades. Using the 1440-fps projection system together with the online saccade detection algorithm evaluated in study II, we displayed rapid, continuous object motion of a target stimulus (as opposed to apparent object motion of a distractor) strictly during saccades, which was the definitive cue to linking the original pre-saccadic and post-saccadic object locations. More specifically, in the saccade session (Figure 2.3a, left column), fifteen observers per experiment made horizontal 14.6-dva saccades to the target, i.e., a 50%-contrast noise patch stimulus, bandpass-filtered to either low SFs (0.28–1.12 cpd) or high SFs (1.12–4.5 cpd). As soon as the saccade was detected, the target moved rapidly upwards or downwards, traveling a distance of 3.6 dva at varying movement durations ranging from 4 ms to 17 ms, thus yielding speeds from 213 dva/s up to 853 dva/s. When the target reached its final vertical position, an identical distractor stimulus was presented at the opposite vertical location. Landing between these two identical stimuli, it was the observers' task to identify the original pre-saccadic target. In a subsequent replay session (Figure 2.3a, right column), we resampled observers' own eye movement trajectories and, combining them with stimulus trajectories, simulated each trial's retinal trajectory during fixation. Crucially, unlike in other paradigms (e.g., Brooks et al., 1980; Wexler & Collins, 2014), simple displacement information could not be

relied on, as target and distractor displacements were always equal and therefore fully predictable. Instead, in both saccade and replay sessions, the only key to solving this trans-saccadic matching task was the continuous motion streak produced by the vertical motion of the target (Figure 2.3b).

In total, four experiments were conducted. As shown in Figure 2.3c, Experiment 1 revealed that task performance was significantly lower during saccades than during fixation. On the one hand, high-SF stimuli were indiscriminable in both saccade and replay conditions, most likely due to unresolvable TFs induced by high-speed motion (Burr & Ross, 1982; Castet et al., 2002). On the other hand, low-SF stimuli allowed for above-chance target identification in both conditions, but to a much larger extent during replay. To test whether the impairment observed during saccades occurred due to post-saccadic masking, we introduced a post-motion blanking period of 250 ms (Deubel, Schneider, & Bridgeman, 1996) in Experiment 2, as previous studies had shown that prolonged post-saccadic target presence greatly reduced perceived smear (Balsdon et al., 2018; Bedell & Yang, 2001; Duyck et al., 2016; Matin et al., 1972). Indeed, blanking caused performance during saccades to fully recover to a level well comparable to perception during fixation (Figure 2.3c, lower row), giving rise to motion streaks that were phenomenologically easily accessible. In addition, even performance for high-SF stimuli was significantly above chance level during saccades, an effect attributable to pre-saccadic attention shifts (Deubel & Schneider, 1996; Kowler, Anderson, Dosher, & Blaser, 1995) that have been shown to specifically enhance high-SF information (Li, Barbot, & Carrasco, 2016). Experiment 2 thus provided an upper bound for task performance, showing that motion streaks were not simply removed from visual processing.

Both Experiments 1 and 2 suggested that motion streaks were most effective when noise patches contained low SFs and moved at lower retinal velocities, yet not providing definitive evidence for the role of motion streaks. We therefore hypothesized that more distinct motion streaks should be produced when a target's orientation was parallel to its retinal motion trajectory, optimally activating orientation-selective motion-streak subunits (Geisler, 1999; Geisler et al., 2001). In contrast, orientations orthogonal to the retinal motion trajectory should lead to high-frequency alternations between low and high luminances on the retina, thus not allowing for effective summation. Three relative orientations, i.e., orientations parallel, oblique, or orthogonal to the stimulus' motion direction, are illustrated in Figure 2.3d. Experiments 3 and 4 therefore used Gabor patches of certain SFs (0.56, 1.12, and 2.25 cpd) and orientations (45° clockwise, 45° counter-clockwise, vertical, and horizontal) instead of noise patches that contained a range of SFs and all possible orientations. Depending on saccade direction, as well as the target's motion direction and orientation, we investigated the effect of relative orientation on task performance. As expected, results of Experiment 3, which was in all respects similar to Experiment 1, showed large impairments of task performance during saccades. Importantly, the data also showed that only targets with parallel relative orientations could be discriminated with above-chance accuracy, given the target contained low-SF information (Figure 2.3d, upper row). Experiment 4 was devised to explore whether – even with post-saccadic masking intact – task performance increased when motion streaks were more prominent. To this end, we

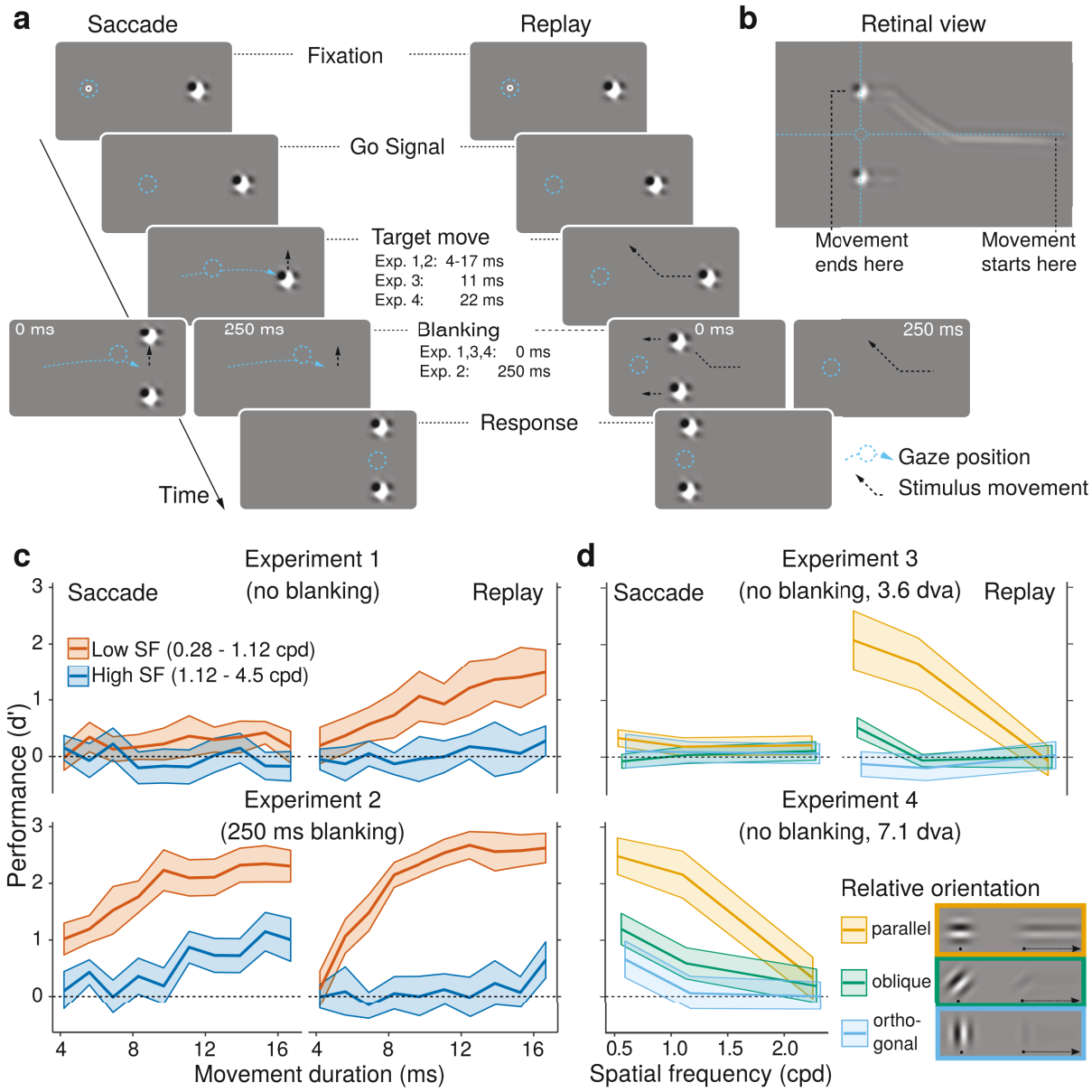

Figure 2.3: Matching pre- and post-saccadic objects based on intra-saccadic motion streaks.
a Experimental paradigm. Observers made 14.6-dva saccades to the target, i.e., a bandpass-filtered noise patch, which rapidly moved upwards or downwards at varying movement durations, strictly during saccades. Upon movement offset (or after a blanking interval), an identical distractor was displayed at the opposite vertical position. Observers' task was to identify the original pre-saccadic target from these two post-saccadic objects. In the replay condition (right column), the each trial's retinal target and distractor trajectories were simulated during fixation at a frame rate of 1440 Hz.
b During both saccades and fixation, the crucial cue to identifying the original was the continuous motion streak produced by the vertical target motion, but not by the distractor.
c Task performance (d') across observers (N=15) in Experiment 1 (upper row) and Experiment 2 (lower row) as a function of movement duration and SF in saccade (left column) and replay (right column) conditions. Note that, in the saccade condition of Experiment 1, low-SF targets were discriminated with above-chance performance ($d' = 0.24$, $t(14) = 4.4$, $p < .001$).
d Mean task performance in Experiment 3 (upper row) and Experiment 4 (lower row) as a function of SF and relative orientation. All error bars represent ± 2 within-subject SEM.

doubled the target's movement duration to 22 ms and movement distance to 7.1 dva (thus leaving stimulus velocity unchanged) and increased stimulus contrast to 100%. Compared to Experiment 3, performance increased remarkably in Experiment 4, demonstrating that effective motion streaks – optimally created by low SFs and orientations parallel to retinal motion trajectories – enabled the identification of the original pre-saccadic target from two identical post-saccadic objects.

To conclude, these results provide a proof of concept that observers were capable of linking pre- and post-saccadic object locations based on continuous, "streaky" motion occurring strictly during saccades. The extent to which this was possible was determined by the distinctiveness of the induced motion streak, as visual factors like SF, contrast, retinal velocity and relative orientation all contributed to task performance. It is yet unclear to what extent these principles hold under more natural viewing conditions (for an example, see subsection 1.3.2), but the current results invite the intriguing hypothesis that motion streaks may contribute to establishing object correspondence across saccades, which will be further investigated in study IV.

2.4 Study IV. Intra-saccadic motion streaks facilitate gaze correction

Reference

Schweitzer, R., & Rolfs, M. (2020). Intra-saccadic motion streaks jump-start gaze correction. *bioRxiv*, 2020.04.30.070094.
doi: 10.1101/2020.04.30.070094

Summary

Among the various questions relating to visual stability (Bridgeman et al., 1994; Cavanagh et al., 2010; MacKay, 1973; Rolfs, 2015; Wurtz, 2008, 2018), the question of object correspondence is a crucial one: How does the visual system determine whether a pre-saccadic peripheral object is the same as a post-saccadic foveal object? Which mechanisms are applied to bridge the "gap in perceptual input" (Richard, Luck, & Hollingworth, 2008, p. 66) during saccades? Whereas object-file theory states that objects are referenced via spatiotemporal factors (Kahneman, Treisman, & Gibbs, 1992; Mitroff & Alvarez, 2007), more recent studies using saccades suggest that object surface features (e.g., color, object identity) encoded in VSTM drive the trans-saccadic matching of objects (Hollingworth, Richard, & Luck, 2008; Richard et al., 2008). Based on previous findings (section 2.3) suggesting that motion streaks could in principle be used to perceptually link pre- and post-saccadic objects, study IV (see subsection 5.1.4 for full manuscript) further examined the possibility that intra-saccadic motion streaks could constitute a source of trans-saccadic object correspondence – either due to smooth spatiotemporal continuity or earlier availability of object features. Based on a classic gaze correction paradigm used to probe object correspondence (Hollingworth et al., 2008), we developed a task that could evaluate this proposal by simultaneously measuring the effects of both availability of surface features and intra-saccadic continuous, "streaky" (as opposed to apparent, step-wise) motion.

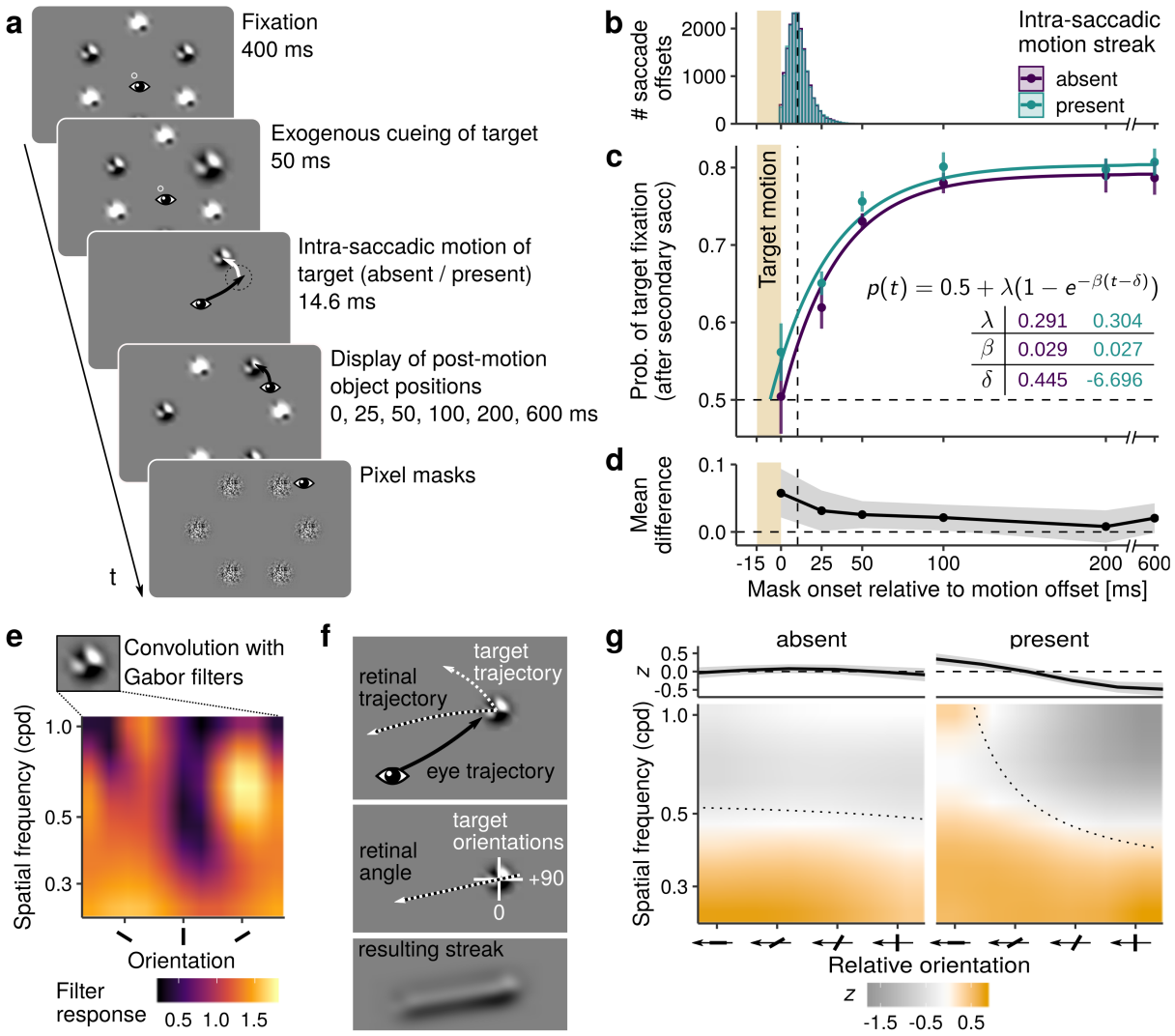

Figure 2.4: The effect of surface features and intra-saccadic motion streaks on gaze correction.
a Task procedure. Observers made saccades to a cued target in a circular array of six objects, consisting of two types of noise patches. During saccades, the target shifted in a CW or CCW manner, so that saccades landed between two objects, prompting a secondary saccade to either of them. Crucially, continuous motion during those shifts was either present (21 equidistant steps along the circular trajectory) or absent (blank screen between first and final stimulus positions). To limit the availability of post-motion surface features, pixel noise masks were displayed after a varying mask onset delay (0–600 ms).
b Distribution of saccade offset relative to motion offset. In both motion conditions, saccades ended on average 10.7 ms after motion offset ($t(9) = 1.24$, $p = .243$).
c Average proportions of secondary saccades to the pre-saccadic target as a function of surface feature duration and presence of continuous intra-saccadic motion. The time course was modeled using an exponential approach to limit, estimated separately for both motion conditions in a mixed-effects approach.
d Average differences between motion-present and -absent conditions (shaded area: 95% CI).
e Orientation-SF energy map produced by convolving the above noise patch with a bank of Gabor filters.
f Illustration of the estimation of relative orientation. The retinal trajectory (i.e., the vector sum of target and eye trajectories) is represented by the retinal angle, encoding retinal motion direction. Relative orientations are defined as the angular distance between orientations and the retinal angle.
g Results of reverse regression analyses, fitted by a multivariate GAM. Z-scores (orange) encode how well filter responses in a given Orientation-SF component predict secondary saccades to the target in motion-absent (left) and motion-present (right) conditions. Dotted lines represent the transition lines from negative to positive Z-scores assuming linear effects of SF and orientation.

Ten observers made 10-dva saccades to an exogenously cued target, that is one of six noise patches (bandpass-filtered to SFs ranging from 0.25–1 cpd) arranged in a circular array (Figure 2.4a). Two types of noise patches were generated on each trial and shown in alternating order. In two thirds of all trials, the target was moved along a circular trajectory for 14.6 ms over a distance of 5.2 dva, consistent with a 30-degree clockwise or counter-clockwise rotation of the entire circular array, whereas in one third of all trials the target remained stationary. When intra-saccadic rotations occurred, observers landed between the originally cued target and a non-cued distractor, thus prompting them to perform gaze correction by making a secondary saccade to the target or the distractor (Deubel, Wolf, & Hauske, 1982; Hallett & Lightstone, 1976b; Hollingworth et al., 2008). To investigate the effect of object features, we occluded all post-motion object locations with pixel noise masks at varying onset delays (0, 25, 50, 100, 200, or 600 ms), thus limiting the availability of surface features for gaze correction and allowing us to study the time course of post-displacement information accumulation. Importantly, to investigate the additional effect of intra-saccadic motion streaks, both continuous (21 frames of a constant velocity of 360 dva/s along the circular trajectory) and apparent (only first and last positions along the trajectory) motion were used, while only continuous motion produced spatiotemporal continuity via motion streaks. Several outcomes were conceivable: Intra-saccadic motion could be fully ignored for gaze correction, play a limited role (e.g., when surface features are only briefly available), or additively improve gaze-correction accuracy regardless of surface-feature availability.

To ensure the validity of the procedure, we made sure that in all trials that entered analyses, displacements occurred intra-saccadicly (Figure 2.4b). In compliance with the theory that surface features encoded in VSTM drive gaze correction (Hollingworth et al., 2008; Hollingworth & Franconeri, 2009; Richard et al., 2008), we found that the likelihood of making a secondary saccade to the original target increased with increasing surface-feature durations. On average, the accumulation of surface feature information reached an asymptote at around 100 ms after motion offset (Figure 2.4c). Crucially to our hypothesis, in virtually all levels of surface-feature duration intra-saccadic motion led to an increased likelihood of directing the secondary saccade towards the pre-saccadic target, even though this effect was clearly strongest when no post-motion surface features were available (Figure 2.4d). In an exploratory analysis, the data of the motion-present and motion-absent conditions were fitted with an exponential growth model (previously applied to describe speed-accuracy trade-offs by Carrasco & McElree, 2001), using a mixed-effects approach (Comets, Lavenu, & Lavielle, 2017), so that group comparisons on the population level could be performed. These revealed that neither asymptotes (λ) nor slopes (β) differed significantly between groups, suggesting that no increase of gain or accumulation rate was caused by intra-saccadic motion. Instead, the effect of intra-saccadic motion was compatible with an earlier onset of information accumulation (δ: $t(9) = 3.45$, $p = .007$) already during target motion. This result received further support by significant reductions of secondary saccade latency (to the target) when intra-saccadic motion was present (see Figure 3 and 4 of the full manuscript in subsection 5.1.4).

To explore whether intra-saccadic motion streaks were responsible for the increased secondary saccade rate to the target, a three-step reverse regression analysis was performed. As study III had already provided evidence that a distinct motion streak could be induced if a moving target's orientation was parallel to its retinal motion trajectory, we hypothesized that secondary saccades to the target would be more likely if the target's orientation incidentally matched the retinal trajectory. First, each trial's target stimulus was convolved with Gabor filters of varying orientation and SF, resulting in a two-dimensional map of filter energy (Figure 2.4e). Second, orientation components were subsequently normalized based on the target's retinal angle, i.e., the direction of the vector sum of the target's and the eyes' trajectories (for an illustration, see Figure 2.4f), thereby estimating relative orientation. Third, logistic mixed-effects regressions were used to estimate how well filter energy in a given relative-orientation–SF component predicted secondary saccades to the target. The significance of the regression weights (z-scores shown in Figure 2.4g) indicated that low-SF content was beneficial for gaze correction in both motion-absent and motion-present conditions, most likely because low SFs allowed for easier discrimination of the target's and distractor's high- or low-luminance surface features. Only when intra-saccadic motion was present, higher SFs could be used for gaze correction, provided that their orientations were close to parallel to their retinal trajectories. In contrast, orientations orthogonal to the retinal trajectory were detrimental to accurate gaze correction. Importantly, this effect of relative orientation could only be found when continuous motion was present, suggesting a role of effective temporal summation that was very similar to the evidence provided by study III.

To conclude, study IV found that intra-saccadic "streaky" motion information could be used rather efficiently to inform gaze correction, one of the oculomotor system's "everyday tasks" (Becker, 1989). Results showed increases of secondary saccade rates to the target along with reductions of secondary saccade latencies, even when little or no post-saccadic surface-feature information was available. Although it remains yet unclear whether the specific benefit could stem from the spatiotemporal continuity provided by motion streaks (as suggested by object-file theory, see Kahneman et al., 1992; Mitroff & Alvarez, 2007) or the earlier availability of surface features (such as luminance or color, see Hollingworth et al., 2008; Richard et al., 2008) encoded in the induced motion streak, these results strongly suggest that there is no gap in visual input during saccades. In contrast to study III, conscious detection of, or attention to motion streaks was unnecessary in this gaze correction task. Although conscious awareness of continuous motion was not assessed, the applied motion velocity, duration, and traveled distance were similar to study III, where intra-saccadic motion streaks were discriminated at only slightly above-chance performance when post-saccadic masking was intact (see also Balsdon et al., 2018). In fact, when asked after the completion of the experiment, all observers stated that they had not noticed any continuous motion. Thus, intra-saccadic motion must have been processed even when motion percepts were largely omitted from conscious awareness.

2.5 Study V. The reference frame of intra-saccadic perception

Reference

Schweitzer, R., Watson, T., Balsdon, T., & Rolfs, M. (in preparation). The reference frame of intra-saccadic vision.

Summary

Evidence from studies III and IV suggested that motion streaks emanated from effective temporal summation in retinal coordinates, especially when inducing targets were oriented parallel to their retinal motion direction. Yet, as most previous studies investigated intra-saccadic motion streaks using static light sources transiently illuminated during saccades (for examples, see section 1.3), it remains an open question how intra-saccadic motion streaks are phenomenologically perceived. In fact, it seems to come naturally to human observers to localize objects in space (i.e., in world-centered coordinates) even though most visual processing occurs in retinal coordinates. This, along with other arguments (see Wurtz, 2008, 2018), is why the retinal signal is thought to be combined with a (most likely extra-retinal) eye position signal (Mittelstaedt, 1990).

Inspired by findings suggesting that intra-saccadic motion streaks can be readily detected when post-saccadic masking is alleviated (Study III; Brooks et al., 1981; Duyck et al., 2016; Matin et al., 1972), in study V (subsection 5.1.5) we gaze-contingently presented rapid target motion during horizontal saccades and then asked observers to report location and appearance of the resulting motion streak, using a standard computer mouse (Figure 2.5a). More specifically, targets could move in 12 different directions, have up to three motion amplitudes/durations (i.e., 2.65 dva / 12.5 ms, 4.0 dva / 18.75 ms, and 5.35 dva / 25.0 ms, thus keeping motion speed constant), and start at one of up to nine position on the screen, thereby making the world-centered motion trajectory of the stimulus impossible to predict. Crucially, by quantifying to what extent (if at all) observers were able to locate the target's intra-saccadic trajectory in space (i.e., on the screen), we could make assumptions about the underlying eye position signal: If the eye position signal were a perfect representation of the eyes' physical position, then observers would be able to report world-centered trajectories, resulting in the shape of a 12-pointed asterisk centered around the true motion onset position. If little or no eye position information were available, we assumed that reports would greatly resemble the retinal trajectories of the target, spatially elongated and strongly shifted in the opposite direction of the saccade.

Three experiments were conducted, whose results are shown in Figure 2.5b, top row. They suggest that observers reported neither retinal nor world-centered trajectories, but that perceived trajectories were in between. Two aspects of these results were especially remarkable. First, in all three experiments the perceived pattern appeared to be significantly modulated by motion amplitudes/durations: The longer the presented motion trajectory was in space and time, the more similar

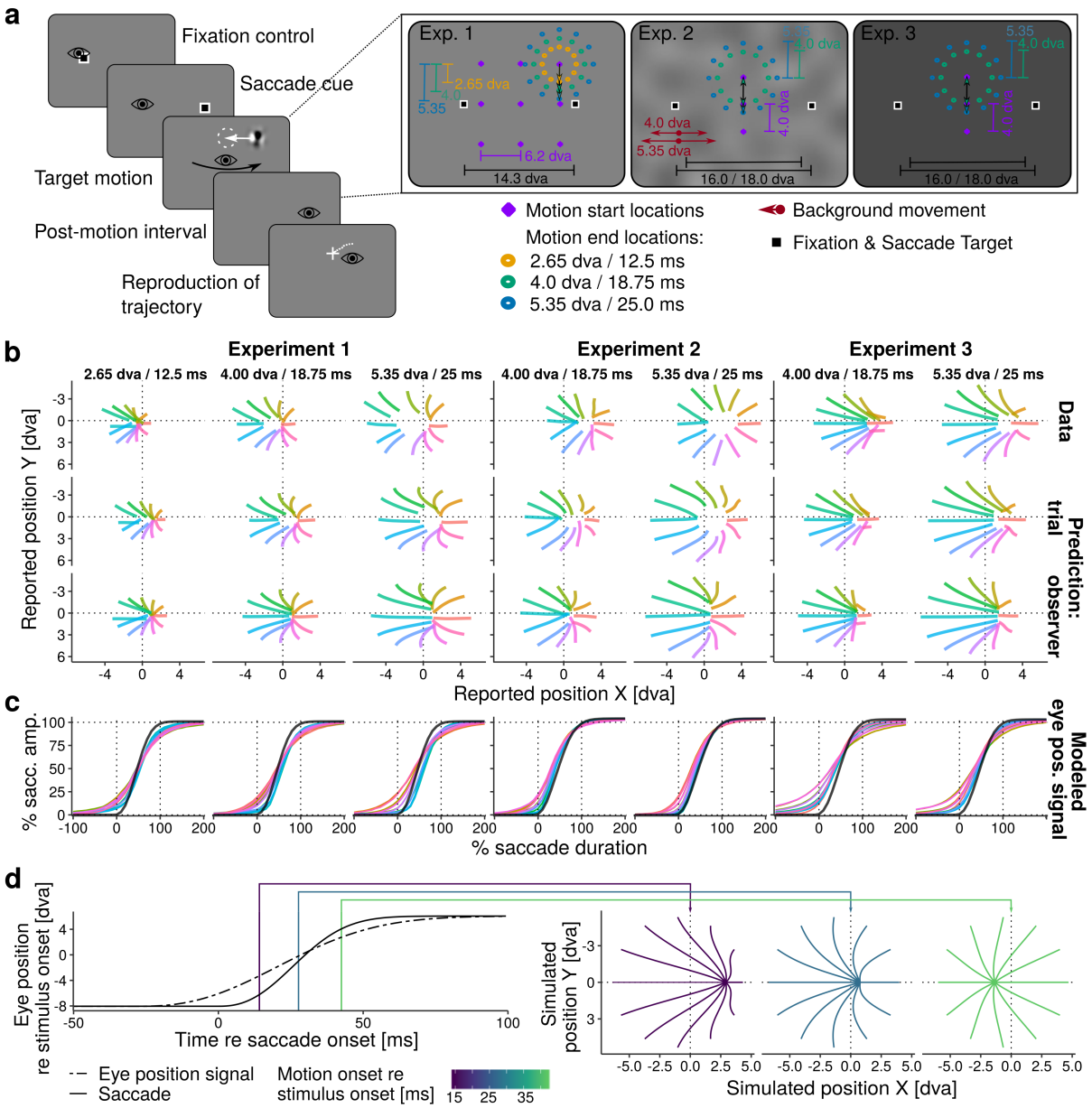

Figure 2.5: Probing the representation of eye position during saccades by studying the subjective appearance and localization of intra-saccadic motion streaks.
a Task procedure. In three experiments, observers made horizontal saccades, during which rapid and unpredictable target motion (12 motion directions, 3 motion amplitudes/durations, and up to 9 motion onset positions were randomly interleaved) was presented, thus producing a motion streak. After a short blank interval, observers reported its perceived trajectory using a computer mouse.
b Average reported results and model predictions. Observers reported neither retinal nor world-centered motion streak trajectories (top row), but trajectories were well approximated by a model assuming that retinal information is combined with a damped eye position signal (center row). The eye position model could not account for the motion-induced offset in motion streak localization (bottom row).
c Eye position signals (averaged across observers) fitted separately for different motion directions relative to the time course of the saccade (black solid line).
d Simulation results elucidating the effect of presentation onset (colored vertical lines) relative to the onset of the saccade on localization and appearance of intra-saccadic motion streaks. Whereas the solid line indicates the saccade-related physical eye position change, the dot-dashed line represents the assumed internal representation of the latter.

were reports to world-centered trajectories. Second, the amount of similarity to world-centered trajectories differed strongly between experiments: Whereas in Experiment 1 and, especially, Experiment 2 observers reported sometimes strikingly world-centered trajectories, this effect fully broke down in Experiment 3. How could this response pattern be explained?

To investigate the underlying eye position signal that could be used to produce perceptual responses, we assumed that positions perceived in world-centered coordinates could be computed by combining retinal input with an internal representation about eye position, captured by the eye position model: $pos_{x,y}(t) = retinal_{x,y}(t) + eye_{x,y}(t)$. Given that both retinal target positions over time and perceived trajectories were known, the eye position signal could be approximated using an extended compressed exponential model, previously used to fit saccade trajectories (Han, Saunders, Woods, & Luo, 2013). As shown in Figure 2.5c, estimated eye position signals were a dampened representation of the saccade trajectory, occurring with an early onset and changing at a slower pace than the saccade, a result that fits well with results from peri-saccadic flash localization studies (Dassonville, Schlag, & Schlag-Rey, 1992; Honda, 1991; Mateeff, 1978) and simulations (Pola, 2004, 2011).

We further used estimated eye position signals to predict perceptual reports. As eye position signals were fitted separately for each observer and motion condition in a mixed-effects framework (Comets et al., 2017), two types of predictions could be made, i.e., trial-level and observer-level model predictions. In Experiments 1 and 3, the trial-level prediction (Figure 2.5b, middle row) matched observers' responses well by reproducing their conspicuous curvature, as well as their length in Experiment 3. This match could be strong evidence that world-centered representation of motion streaks were produced as a consequence of the different time courses of eye position signal and saccade-contingent retinal input: Early target positions were mislocalized in the direction of the saccade because the early-onset eye position signal would encode an eye position not yet reached by the eye, whereas for later target positions this effect would be reversed (see also Figure 2.5d). This explanation very well fits previous experiments which used continuous stimuli (e.g., Honda, 2006; Kennard, Hartmann, Kraft, & Glaser, 1971; Mateeff, 1978). Crucially, as indicated by results shown in Figure 2.5c, estimated eye position signals were subject to a quite consistent ordering, suggesting different time courses for different motion directions. This effect reflected mislocalization of motion onset positions in the direction of target motion, reminiscent of the Fröhlich effect (Fröhlich, 1929), stating that the initial position of a sudden-onset moving object is perceived as shifted in its motion direction. The elimination of motion direction from the model prediction (observer level in Figure 2.5b, bottom row) caused a deterioration of the fit, suggesting that, even during saccades, motion could bias position estimates (Whitney, 2002).

Finally, how could differences between experiments be explained? The hypothesis could be proposed that targets of increased contrast were processed with reduced latencies (Mansfield & Daugman, 1978; Reich, Mechler, & Victor, 2001; Williams & Lit, 1983), thus causing the presented

target to be mislocalized as occurring earlier in time. As elucidated in Figure 2.5d, earlier presentation onsets could cause intra-saccadic motion streaks both to appear more elongated and to be mislocalized in the direction of the saccade. Notably, the same effect was observed after having increased the target's Weber contrast to a value of 10 in Experiment 3. The visual system may thus have an accurate representation about the ongoing saccade (Smalianchuk, Jagadisan, & Gandhi, 2018; Seideman, 2020), yet it may be its latency-dependent synchronization with visual input that causes perceptual mislocalization.

To conclude, in study V we presented evidence that the appearance and localization of intra-saccadic motion streaks could in principle be well explained by the hypothesis that retinal information is combined with an early-onset, slowly changing eye position signal. In addition, response patterns were shown to be largely unaltered by varying visual field positions (Experiment 1), background luminance and structure (Experiment 3), and even additional intra-saccadic large-field motion (Experiment 2). Modeling results suggested that localization of motion streaks could be biased by motion direction and that target contrast played a significant role, a hypothesis that remains to be systematically evaluated in a fourth experiment. Finally, our results provide additional evidence (together with studies III and IV) that intra-saccadic motion streaks are induced in retinal coordinates, but can be – with the help of a damped eye position representation – imperfectly localized in world-centered coordinates, which are readily reported by observers.

3

General Discussion

Even among vision scientists, it is a surprisingly common assumption that vision during saccades is impeded by dedicated brain mechanisms to ”avoid the disturbing consequences of saccadic image motion which would follow if it were left intact” (Burr & Ross, 1982, p. 483). Therefore, much research has investigated the mechanisms of perceptual omission, heavily focusing on the effect of saccadic suppression – that is, the reduction of contrast sensitivity around saccades – even though, as already noted by Volkmann (1962), ”it is doubtful whether central inhibition alone can account for the phenomenal ’continued clear vision’ which occurs under a wide variety of circumstances” (p. 578). In other words, up to this day it remains a highly debated issue whether saccadic suppression (in the sense of central inhibition) even has a role in realizing saccadic omission. In fact, recent studies suggested that it may be an artifact of the specific control dynamics of the oculomotor system (Crevecoeur & Kording, 2017) or of retinal-level circuits responding to image motion (Idrees et al., 2020). One may still perceive a certain separation of the vision science community, each camp favoring either active and extra-retinal or passive and purely visual accounts of saccadic omission.

The starting point of the investigations presented here in this thesis was to choose to leave aside this specific and well-studied question of saccadic omission, and to assume that visual processing during saccades may still occur even though one is not consciously aware of it. As proposed by Watson and Krekelberg (2009), saccadic omission could be conceptualized not as a removal from processing (as captured by the idea of suppression), but as (only) a removal from conscious awareness, most likely achieved by pre- and post-saccadic masking processes (Breitmeyer & Ganz, 1976; Castet, 2010; Matin, 1974; Volkmann, 1986). Following this line of thought, one may ask a whole variety of novel questions, regarding not only the extent of intra-saccadic vision (e.g., what types of visual information can be extracted from intra-saccadic visual input despite high-speed retinal motion?), but also its potential function (e.g., which visual and motor processes could this information contribute to?).

Among the large range of possible experimental paradigms, studies III, IV, and V chose to apply a specific stimulus class, that is, motion streaks induced by rapid retinal translation of single stimuli. Clearly, intra-saccadic motion smear induced by full-field natural scenes is arguably more complex

and therefore also more difficult to study in controlled experimental paradigms. Using controlled visual stimuli, such as Gabor patches and bandpass-filtered noise patches (still more complex than stimuli produced by LEDs or oscilloscopes, e.g., Bedell & Yang, 2001; Brooks et al., 1980), the impact of low-level visual features on motion streak generation and efficiency were investigated, principles that could later be applied to more complex natural scenes (see subsection 1.3.2).

Note that, in order to perform these studies, the availability of a projection system of both high spatial and temporal resolution was a necessary prerequisite. Retinal shifts of objects induced by real-world object motion or one's own eye movements are continuous, whereas common artificial motion displays (using monitors of up to 150 fps) are inherently discontinuous. The retinal consequences of making saccades across bright light sources flickering at 200 Hz or more are widely known as the "phantom array" (Hershberger & Jordan, 1998), i.e., a spatial pattern (best described as a dotted or dashed motion streak) induced by intermittently illuminated stimulus locations as they travel across the retina. As recent studies argue that flicker could be very accurately detected during saccades even at a frequency of 1000 Hz (Roberts & Wilkins, 2013), even higher temporal frequencies would be needed to appropriately emulate the continuous retinal shifts that occur during natural vision. In studies II – V, we achieved this feat using the 1440-fps Propixx DLP projection system (Vpixx Technologies, Saint-Bruno, QC, Canada), whereas in study I, a custom LED setup with a similar refresh rate was built. The former setup thus not only enabled rapid and continuous object motion that inevitably led to the blurring of the motion trajectory, but also allowed us to accurately replay those intra-saccadic retinal target trajectories during fixation (study III) to compare motion streaks induced by both eye and stimulus movement to those induced by stimulus movement only.

3.1 The extent of intra-saccadic vision

To this day, many potential contributions to saccadic omission have been investigated, ranging from reduction of SNR due to large-field image motion (Dorr & Bex, 2013; Idrees et al., 2020; MacKay, 1970; Richards, 1968), over retinal motion smearing (Mitrani & Yakimoff, 1970, 1971), forward and backward masking by structure (Brooks et al., 1981; Campbell & Wurtz, 1978; Castet et al., 2002; Chekaluk & Llewellyn, 1990; Duyck et al., 2018), para- and meta-contrast masking (Breitmeyer & Ganz, 1976; Duyck et al., 2016; Matin et al., 1972; Matin, 1974), and shearing forces (Richards, 1969), to central inhibition (Volkmann, 1986; Burr et al., 1982; Riggs et al., 1974; Riggs & Manning, 1982; Ross et al., 2001a). More recent studies further suggest a role of attentional distraction (Balsdon et al., 2018) and sensorimotor contingencies (Rolfs, Ohl, Schweitzer, Castet, & Watson, 2017; Zimmermann, 2020). In short, as extensively reviewed in section 1.2 and section 1.3, many good reasons exist why one should *not* be aware of the visual consequences of one's own saccades. This first part of the Discussion shall thus try to discuss the extent of intra-saccadic vision from the opposite viewpoint: What can we learn from the presented studies about the circumstances and

pre-conditions under which we can study, or even experience intra-saccadic vision, especially in the case of motion streaks?

3.1.1 What makes a good motion streak?

Burr and Ross (1982) found that contrast sensitivity to drifting gratings and moving bars was impaired when their velocities approached the velocities of saccades. Unlike Kelly (1979), who tested a considerably smaller range of SFs, the authors found that motion sensitivity is not necessarily a function of velocity, but of temporal frequency: While moving a high-SF grating (2 cpd) at a high motion velocity (400 dva/s) induces a high TF (800 Hz), moving a low-SF grating (0.2 cpd) at the same velocity would reduce the induced TF (80 Hz). Based on the results of Burr and Ross (1982), the application of fast horizontal motion of 100 dva/s, as occurring routinely during saccades, would already be sufficient to explain the omission of vertical sinusoidal bars with a width 1 dva, as motion detectors seemed to be unable to resolve TFs above 50 Hz (Burr & Ross, 1982; Castet et al., 2002). Clearly, to achieve this effect, saccades are not necessary, but the retinal speeds induced by them. For instance, in study II, we briefly presented 0.5-cpd gratings drifting at velocities around each observer's saccadic peak velocity and found that these gratings were undetectable during fixation. Similarly, in Experiment 3 of study III (Figure 2.3d), when the retinal trajectories of gratings oriented orthogonal to their trajectories were replayed during fixation, they transiently disappeared along their movement path, thus omitting any motion signal regardless of their SF. Crucially, this is only valid for motion detection described by classic motion models, such as the Reichhardt detector which detects orientations orthogonal to a given direction over time (Adelson & Bergen, 1985; Reichardt, 1987), but not necessarily for motion streaks: When grating orientations were parallel to their motion path, the target's motion remained readily discriminable at SFs below 2 cpd. At SFs of 2.25 cpd even parallel gratings became undetectable, most likely because the target's orientation could never be perfectly matched to its (to some degree) unpredictable retinal trajectory, which was influenced by saccade metrics and presentation onset time. The importance of this finding has to be emphasized: Although high-speed or saccadic motion of targets containing medium or high SFs cannot be resolved strictly using contrast and motion detection, motion streak detectors – which are also sensitive to orientations parallel to motion direction (Geisler, 1999) – might potentially remain the only way to visually represent these targets during the saccade. As some neurons in V1 were shown to be direction-selective to parallel motion (Geisler et al., 2001) and, as reviewed in subsection 1.3.1, orientation-implicated motion interacted with known motion mechanisms and shared much of the neuronal architecture used for motion processing, it might well be that motion streaks have an important role in representing high-speed intra-saccadic object motion.

Motion streaks would be especially prominent if moving objects contained orientation information parallel to their retinal motion trajectory. In this case, they might even allow for the representation of a certain range of SFs that would otherwise be omitted due to high velocities. Preliminary evidence for this view is provided by study IV: Motion streaks enabled the usage of higher-SF surface features

which were otherwise not beneficial for gaze correction (Figure 2.4g). Moreover, in natural scenes, parallel-oriented high-SF scene content was associated with improved post-saccadic discrimination of the intra-saccadic scene (Figure 1.3f). Given that under normal viewing conditions visual scenes are largely static across saccades, a match between stimulus orientations and saccade direction would promote intra-saccadic motion streaks. This case is actually quite likely to occur, as statistics of both natural scene orientations and saccade directions are dominated by cardinal directions (Najemnik & Geisler, 2008; Otero-Millan, Macknik, Langston, & Martinez-Conde, 2013; Coppola, Purves, McCoy, & Purves, 1998).

That said, natural scene statistics also have higher power in the low-SF domain. As shown by study III, task performance (when matching pre- and post-saccadic targets based on the induced motion streak) were also increased when moving targets contained lower SFs. Even though saccadic suppression was shown to be most effective at low SFs (Burr et al., 1982, 1994; Volkmann, 1986), our finding could still be in line with this result for two reasons. First, low-SF cutoffs in classic saccadic suppression studies were much (i.e., by up to a factor of ten) lower than in study III. Indeed, unless tested at high luminance levels (e.g., 400 cd/m^2), saccadic-to-fixation contrast thresholds were only significantly altered at SFs below 0.3 cpd (Burr et al., 1982). Second, the H-H paradigm relied on flashed presentations of full-field gratings, whereas in most of our studies bandpass-filtered noise patches or Gabor gratings were enveloped in (by comparison) very small Gaussian apertures. Crucially, if noise patches consisting of increasingly low SFs were to be presented in small apertures, then their appearance would at some point resemble Gaussian blobs, which would – like single light sources – always produce motion streaks when moving at saccadic velocities (Geisler, 1999). Even though we chose aperture sizes that could always fit one full sinusoidal cycle, this could not necessarily be guaranteed when using noise patches. Thus, it is likely that at least a part of the streak-promoting effect of low-SF content was a result of reduced variation of luminance within the aperture that allowed for more effective temporal summation.

Yet, should extremely low SFs in natural scenes also produce motion streaks? Clearly, to remain resolvable at high velocities, these low SFs do not need to be aligned parallel to the saccade's trajectory. Still, results from tachistoscopically presented natural scenes (subsection 1.3.2) suggested that, even at SFs below 0.1 cpd, natural scenes with orientations parallel to saccade direction were associated with higher discrimination performance. Due to the size of such extremely low SFs (in fact, RF sizes of 7 dva for 0.01-cpd gratings were estimated by Anderson & Burr, 1987), it is however unlikely that they should produce informative motion streaks. For instance, during a 8-dva saccade, a 1-dva target would be shifted by eight times its width, whereas a 8-dva target would only be shifted by one time its width. As streak efficiency has been shown to be not a function of absolute velocity, but of velocity relative to target size (measured by stimulus widths per second; Geisler et al., 2001), the 8-dva target would need an unrealistic 64-dva saccade to produce a comparable motion streak response within the given time interval. Following this line of thought, motion streaks may thus be most beneficial for small or high-SF stimuli. One the one hand, these stimuli would be rendered

invisible at saccadic speeds, if motion streaks did not occur. On the other hand, due to their small size, they could easily exceed the critical speed of 10 spot widths per second (Geisler et al., 2001) and produce efficient motion streaks, even during saccades of very short amplitudes. It may also be for that reason that most studies up to this point have investigated motion streaks by using small light sources (e.g., Bedell & Yang, 2001; Brooks et al., 1980; Matin et al., 1972; Duyck et al., 2016).

3.1.2 Motion streaks versus large-field smear

One may wonder how studies on motion streaks, not only those reported here, but also studies having used simple stimuli generated with LEDs or oscilloscopes, generalize to large-field smear that should occur in natural vision. Natural vision differs from psychophysical experiments not only due to the type of stimulus, i.e., the natural scene, but also because the entire retina is stimulated, whereas in laboratory conditions – unless a Ganzfeld or complete darkness is applied – the relevant spatial range of stimulation is reduced to the presentation screen. Note that only the famous study by Campbell and Wurtz (1978) has so far investigated large-field natural motion smear by briefly illuminating the entire laboratory room around and during observers' saccades, a setup that did not allow for much controlled stimulus manipulation otherwise. At this point in time, one can only speculate whether motion streaks induced by objects as parts of natural scenes are similar to those induced by one single object.

In study V, we found that irrelevant backgrounds did not alter the appearance or localization of intra-saccadic motion streaks. These structured backgrounds did not have natural field statistics, but were bandpass-filtered to very low SFs. Even though they introduced object-like patterns (which should have even remained resolvable at high retinal speeds; Burr & Ross, 1982) and were scaled to Michelson contrast ranges similar to those of natural scenes (Tadmor & Tolhurst, 2000), they did not seem to interact with the strictly intra-saccadic motion streak. In addition, study I provided evidence that motion streaks can be induced by a high number of adjacent light sources which, when combined, produced spatially extended, highly complex patterns of smear. It might thus be reasonable to conceptualize large-field motion smear as the sum of motion streaks induced by all objects present in the scene. The example also shows that neither metacontrast masking by stimulation of adjacent retinal locations over time (Breitmeyer & Ganz, 1976; Matin, 1974) nor attentional distraction due to sudden on- or offset-transients (Balsdon et al., 2018) could prevent perception of smeared light patterns. As outlined in subsection 1.3.2, we specifically studied the properties of large-field smear induced by natural scenes tachistoscopically presented during saccades. Even though, unlike experiments by Campbell and Wurtz (1978), natural scenes were restricted to the presentation screen which subtended 52 $\times$ 30 dva, these stimuli were clearly more complex and cluttered, containing a much larger range of SF-orientation content, as well as color. Still, it was possible to fully recover the effect of relative orientation which was previously found with simple Gabor patches and noise patches, i.e., that scenes with high power in orientations incidentally parallel to the saccade were discriminated more accurately. This suggests that the same features that promoted motion streaks

were also beneficial in large-field smear. During debriefing, observers also reported that in some cases they were able to match scenes based on highly salient objects, such as a bright red car in a parking lot, which became identifiable as intra-saccadic motion streaks and could therefore be segregated from the smeared scene due to color or high luminance or contrast. It may thus well be that salient objects in natural scenes routinely induce intra-saccadic motion streaks, as luminance and contrast were shown to be largely statistically independent in natural scenes (Mante, Frazor, Bonin, Geisler, & Carandini, 2005) and Weber contrasts around and above 1 could well occur in photographs of visual scenes (Tadmor & Tolhurst, 2000).

Assuming that even natural scenes could induce efficient motion streaks inevitably poses the question why one does not become aware of them. How could the visual system account for the unpredictable patterns of smear that might emanate from complex visual scenes? A parsimonious solution may again be masking. First, Matin et al. (1972) first showed that the time course of post-saccadic metacontrast masking depended on the luminance of the target. Even though, when presented strictly during saccades, all target luminances produced comparable streak lengths, high-luminance targets were subject to a much quicker reduction of perceived streak length, when presentation durations exceeded saccade durations. In natural vision, motion streaks induced by high-contrast targets would thus be counteracted by stronger mask energy provided by the post-saccadic presence of the very same target (Breitmeyer, 1978; Breitmeyer & Öğmen, 2000; Matin, 1974). Moreover, masking – more specifically, critical bandwidth masking – could also explain why certain image properties that would promote intra-saccadic smear, such as low SFs or orientations parallel to saccade direction, are omitted as well as others. For instance, it was shown that the direction of motion streaks could be efficiently masking by gratings of the same orientation (Apthorp et al., 2009, 2010, 2011; Burr & Ross, 2002). In addition, Stromeyer and Julesz (1972) found that gratings were best masked by SFs around the grating's SF with bandwidths of up to one octave, a finding that has also been documented using visual adaptation (Blakemore & Campbell, 1969). Even though these experiments were performed with spatially overlapping gratings and noise, thus leaving open the possibility that processes of metacontrast masking are different (see Growney, 1978), it is well possible that similar mechanisms could apply to pre- and post-saccadic masking: The same features of visual objects, that produce distinctive motion smear during the saccade, could cause more efficient bandwidth-specific masking of the latter after saccade offset. Preliminary evidence for this view was provided by the saccadic suppression literature. First, Brooks and Fuchs (1975) found that detection thresholds for pointed and diffuse targets (achieved by neutral density filters) were differently affected by varying backgrounds: On uniform backgrounds, diffuse targets were harder to detect, whereas detection for pointed targets was impaired on structured backgrounds. Second, Idrees et al. (2020) showed that, even though there was no spatial overlap between target and background, low-SF backgrounds strongly impaired the detection for low-SF targets, whereas high-SF backgrounds had a similar effect on high-SF targets. In sum, it may well be that studying

motion streaks in the context of large-field smear will yield different results than studying single motion streaks against a uniform background, as even features of the scene in the retinal periphery (e.g., when using an artificial screen border with a diameter of 20 dva; Idrees et al., 2020) could affect the processing of peri-saccadic targets. As these findings relate to the simple detection of a target, it is well possible that critical-bandwidth masking has contributed to its removal from conscious awareness. Crucially, to further elaborate on this hypothesis with respect to natural vision, a follow-up study is planned that shall investigate the post-saccadic masking time courses of different types of natural scene images.

3.1.3 Omission of intra-saccadic motion streaks

It is simple to experience intra-saccadic motion streaks when making saccades across a single light source in an otherwise dark room. It is also simple to experience that under natural viewing conditions this is very clearly not the case, which does not mean that it is in principle impossible. In study I, for instance, anorthoscopic presentations took place in a standard office under normal illumination conditions, yet intra-saccadic text and images remained readily discriminable. Naturally, the introduction of a black cloth background for the inducing LED strips or the reduction of ambient luminance enhanced the effect – most likely due to increased contrast and prolonged visual persistence – but were not necessary for it to occur. Even though natural large-field smearing of the entire visual scene should have been present at the time of the saccade, only the intended intra-saccadic presentation (and not the co-occurring smear) was rendered visible. An easy explanation would be that the intensity of the mask, which was provided by the static post-saccadic scene, may have been sufficient to remove large-field motion smear from conscious awareness, but not the concurrent high-luminance intra-saccadic stimulation (Ibbotson & Cloherty, 2009; Kahneman, 1968). In this case, a more powerful post-saccadic mask, such as the brief illumination of the entire scene using a flash tube, should be able to break visual persistence and achieve this effect.

Yet, the phenomenon may be more complex than that. In study III, for instance, observers noted that, on a phenomenological level, the replay condition grossly deviated from the preceding saccade condition. Instead of the target's retinal trajectory (shown in Figure 2.3b), a close to vertical, but curved trajectory was perceived that was quite similar to reports in study V (Figure 2.5b). It thus seems that the part of the motion streak induced by both eye and stimulus movement was reported, whereas the part of the motion streak induced by only the static target was omitted from conscious perception. It is unlikely that masking could account for this phenomenon, as it occurred even when the target was present before and after the saccade. As shown by introducing a 250-ms blanking interval in study III, continuous post-saccadic presence of the target impaired the detectability of intra-saccadic motion streaks, but did not change the fact that only motion streaks induced by intra-saccadic target motion were perceived (see also Balsdon et al., 2018). In a way, this observation parallels the finding that static visual targets, unlike flashed targets, were rarely mislocalized in

space around the time of saccades (Schlag & Schlag-Rey, 2002). For instance, Schlag and Schlag-Rey (1995) found that if two target stimuli were flashed in the same position, the first long before the saccade and the second around saccade offset, then the second presentation was mislocalized in the direction of the saccade. Surprisingly, however, veridical localization was found if the first target remained continuously presented until the time of the second target. Several explanations were proposed for this phenomenon. For one, assuming that visual processing should be optimized for largely static and continuous real-world objects, Teichert, Klingenhoefer, Wachtler, and Bremmer (2010) propose that – via recurrent calibration – the visual system is capable of a near-perfect prediction of the changing retinal position of continuously presented targets, and that peri-saccadic mislocalization occurs as a consequence of reconciling this prediction with the sluggish temporal processing dynamics of flashed targets. Schlag and Schlag-Rey (1995) suggest that the visual localization center places an attentional gate on the eye position signal, treating any visual stimulus as stable (e.g., by assuming a simple 'bias for stability' in the face of uncertainty or impoverished vision; Born, 2019), unless a visual event occurs. Yet, it remains unclear what counts as a visual event. As suggested by virtually all peri-saccadic flash localization studies, the onset of a stimulus does, but less so its offset. Following this line of argument, the onset of intra-saccadic target motion would also qualify as such a visual event that requires the renewed estimation of spatial position. For instance, it has been shown that the perception of vertical stimulus motion around the time of saccades is extremely vulnerable to distortions of the motion path (Kennard et al., 1971; Honda, 2006; Mateeff, 1978), suggesting that each newly sampled position along the trajectory is re-evaluated in terms of spatial position. This notion is supported by study V, even for motion parallel to the saccade. Finally, returning to the initial observation, the omission of parts of the motion streak not manipulated by moving the intra-saccadic target (horizontal components of the streaky trajectory illustrated in Figure 2.3b) could be explained by the idea that stimuli positions assumed stable did not undergo visual localization, and could therefore subsequently removed from conscious awareness.

Let us further explore this idea. The observation described above, as well as the finding that continuously present stimuli were not mislocalized even though their offset occurred during saccades (Schlag & Schlag-Rey, 1995), suggest that it must be possible to separate saccade-induced from stimulus-induced changes in retinal position, even during saccades. Put differently, unless the visual system had an approximate prediction about the visual input that the ongoing saccade could generate, it would be difficult to selectively render intra-saccadic changes in target position consciously visible with such temporal and spatial precision. In addition, instead of preemptively attenuating or even shutting down visual processing when a saccade is impending, it appears more likely that saccade-induced input is to some degree monitored to be able to readily signal eventual visual changes that deviate from the expected visual consequences of the saccade. Applying the terminology of the predictive coding framework, top-down predictions, likely produced by sensorimotor contingencies (O'Regan & Noë, 2001), might be able to compensate for bottom-up sensory input and prevent saccade-induced visual changes from reaching conscious awareness. These sensorimotor

contingencies may in turn be learned based on bottom-up sensory input, slowly changing the profile of what information is omitted. Evidence for this view has recently been provided by Zimmermann (2020) by showing that habituation to saccade-contingent vertical displacements in simple saccade trials raised detection thresholds for the same displacements in subsequent test trials. Thus, when a prediction about the sensory outcome of a saccade is violated, for instance when the saccade target suddenly undergoes rapid upward motion or a bright target is flashed in complete darkness, the visual change can be consciously represented, provided that the visual change has enough intensity to be in principle detected. First, whether it can be detected – especially given the noisiness of intra-saccadic visual input – heavily depends on the salience of the visual change. For this reason, target motion orthogonal to the saccade was presented in study III, as it was detected by observers with higher accuracy than target displacements parallel to saccade direction (Wexler & Collins, 2014) and yielded similar performance during saccades and fixation (Brooks et al., 1980). In contrast, small target displacements parallel to the saccade are rarely noticed (Bridgeman et al., 1975), unless the target is re-illuminated after a brief blanking period (Deubel et al., 1996), suggesting that another visual event was needed to re-evaluate the target's position, which would otherwise be considered stable. One could further speculate that the displacement of the target along the saccade trajectory was not noticed, as it was directly masked by the motion streak which it induced while traveling from the periphery towards the fovea. Second, while piloting study III, we found that selective attention to the intra-saccadic motion streak (e.g., by means of prior exposure) greatly enhanced performance. Even in Experiment 1, showing barely above-chance performance in naive observers (Figure 2.3c), trained pilot observers were able to reach performance levels close to those found during the replay session. That post-saccadic onset and offset transients of distant distractor stimuli impaired the detection of intra-saccadic target motion (Balsdon et al., 2018), can be interpreted as evidence that attentional distraction caused by post-saccadic input might play a role in saccadic omission. One may speculate that this role lies in drawing attention away from intra-saccadic visual changes (which may frequently, but incidentally occur given the noisiness of the input) to facilitate the processing of novel post-saccadic information.

To conclude, a type of reafference using learned sensorimotor contingencies might explain not only why – especially given the natural condition of a largely static world – human observer usually do not become aware of the visual consequences of their own saccades, but also why sufficiently salient or velocity-wise optimized intra-saccadic stimulation is readily available. The reafference principle (Von Holst & Mittelstaedt, 1950) has been criticized in the context of visual stability (e.g., Bridgeman et al., 1994; MacKay, 1973), as it seemed unlikely that the spatial and temporal accuracy of any eye position reference (whether in terms of motor efference, proprioception, or visual references) would be high enough to counteract rapid intra-saccadic signal changes in an online fashion. This may however not even be necessary to achieve saccadic omission. Instead, a simple (on average accurate) prediction about the visual consequences of a saccade of a certain amplitude and direction might be sufficient. Due to the inherent retinal velocities and the large amount of smear

occurring during saccades, it may be unlikely that small prediction errors, such as those occurring due to motor and visual noise, would even be noticed. A good example for this situation would be saccadic suppression of displacement (Born, 2019; Bridgeman et al., 1975; Bridgeman & Macknik, 1995). Considerable prediction errors, such as above-threshold visual transients introduced by most experimental manipulations, would more likely reach awareness and, as shown by study V, could even be readily localized in world-centered coordinates. Given the results by Zimmermann (2020), it might well be that visual predictions are constantly refined to best approximate saccade-induced consequences and thereby provide optimal omission. This 'calibration' solution, even though predominantly an explanation for space constancy, has already been proposed in a slightly different fashion by Bridgeman et al. (1994): Eye position is computed by combining information from inflow, outflow, and visual references. With every new fixation, these sources of information are successively mapped to retinal input, thus refining the position estimate, while saccadic suppression of displacement acts as the mechanism that avoids that eventual mismatches reach conscious awareness. However, extreme mismatches between predicted and actual visual input can be perceived as displacement of the perceived visual world or jumping motion during saccades, for instance if the proper execution of eye movements is hindered by paralysis (Stevens et al., 1976). This principle may be equally applied for intra-saccadic vision, given that precise information about saccades' velocity profiles should be in principle available to the visual system (Smalianchuk et al., 2018; Seideman, 2020). Note that, intra-saccadic motion streaks have so far been studied using single light sources in dimly lit or even completely dark environments (e.g., Bedell & Yang, 2001; Brooks et al., 1980; Duyck et al., 2016; Matin et al., 1972), whereas experiments reported here always contained at least one reliable visual reference, i.e., the illuminated presentation screen. As sensorimotor contingencies are most likely established in natural visual environments, which are (unlike laboratory environments) rich in various visual landmarks (Deubel, 2004), it might be an interesting avenue for future experiments to investigate the potential role of visual references in the perception and omission of motion streaks.

3.2 The potential function of intra-saccadic vision

As pointed out in the beginning of this chapter, the question, to what extent we become aware of intra-saccadic visual information, might be orthogonal to the question whether the latter might be useful to active vision in general or, more specifically, to processes of trans-saccadic perception. Clearly, the perceptual and motor consequences of saccades (Aagten-Murphy & Bays, 2019; Becker, 1989; Melcher & Colby, 2008; Robinson, 1981), microsaccades (Collewijn & Kowler, 2008; Martinez-Conde, Macknik, Troncoso, & Hubel, 2009; Rolfs, 2009), fixational eye movements (Martinez-Conde et al., 2004), or smooth pursuit eye movements (Lisberger, Morris, & Tychsen, 1987) have been thoroughly studied. Yet, very little is known about whether strictly intra-saccadic perception (which is in principle well possible despite the well-known effects of saccadic suppression Binda &

Morrone, 2018; Castet, 2010; Ibbotson et al., 2008; Matin et al., 1972; Ross et al., 2001a; Volkmann et al., 1978) is largely a laboratory phenomenon, or whether it could have a functional role.

3.2.1 Spatiotemporal visual consequences of saccades

Recently, Rucci, Ahissar, and Burr (2018) proposed what might be an important general function of intra-saccadic vision, namely the modulation of the spatiotemporal power distribution in the retinal image. The authors emphasize that, in addition to spatial coding which describes the classic view of coding visual information in terms of the spatial layout of the retina and subsequent processing hierarchies, the visual system is in grave need of temporal and spatiotemporal coding. Indeed, temporal transients are needed to optimally stimulate RFs along the visual processing hierarchies (Cleland et al., 1971; Croner & Kaplan, 1995; Hubel & Wiesel, 1968; Nagano, 1980), prevent fading (Ditchburn & Ginsborg, 1952; Riggs & Ratliff, 1952; Stevens et al., 1976), and detect motion (Adelson & Bergen, 1985; Burr & Ross, 1982; Burr & Thompson, 2011; Kelly, 1979). They therefore propose that the primary function of eye movements, both saccades and fixational eye movements, is to transform the (in principle) static image of the world, essentially consisting of an infinite range of SFs and orientations at 0 Hz, into a complex SF–TF pattern that effectively drives neural responses (Rucci et al., 2018). Naturally, what TFs could be induced by a certain SF depends on the amplitude and velocity of each eye movement: Whereas saccades strongly induce visual transients in the low-SF domain (as shown by the finding that intra-saccadic motion can only be induced by low SFs; Castet et al., 2002), fixational eye movements almost exclusively modulate high-SF content, thus enhancing those SFs that have, a priori, lower power in natural scenes. Fixational eye movements could thereby help to resolve extremely high SFs well beyond the density of photoreceptors, thus allowing for high-acuity vision (Intoy & Rucci, 2020). Assuming a delayed temporal response function, it follows that low SFs will be enhanced during early fixation (reproducing the SF power distribution in natural scenes), whereas during late fixation, processing will be dominated by high SFs, which are enhanced by ocular drift. Indeed, Boi, Poletti, Victor, and Rucci (2017) found that detection of high-SF gratings improved with longer presentation durations (after fixation onset), whereas detection of low-SF gratings did not. Similarly, retinal stabilization impaired the detection of high-SF, but not low-SF gratings. What is crucial with respect to the function of intra-saccadic vision, is a third experiment showing that observers were more likely to detect a post-saccadic low-SF (but not a high-SF) stimulus if its onset occurred during the saccade, compared to if it was presented upon fixation onset using a contrast ramp. As effective presentation duration was accounted for, the authors argued that the visual transient, induced by the saccade by shifting the low-SF grating across the retina, led to a facilitation of low-SF information processing during early fixation. Even though this last experiment could not rule out potential alternative explanations, Boi et al. (2017) provide good evidence that eye movements reshape spatiotemporal power, thereby providing necessary visual transients that facilitate post-saccadic processing by enhancing contrast sensitivity across a wide range of SFs (see also Casile, Victor, & Rucci, 2019).

The results reviewed above have interesting implications for the field of active vision and furthermore suggest a slight paradigm change in understanding trans-saccadic vision: Whereas the transients produced by low-SF image content (which remain largely resolvable at saccadic velocities; Burr & Ross, 1982) were often considered harmful to effective trans-saccadic perception, they may now facilitate the coarse-to-fine processing strategies employed by the visual system (Rucci et al., 2018). These two assumptions are of course not mutually exclusive, considering that peri-saccadic visual signals need not reach conscious awareness to be processed and to thereby influence post-saccadic perception (Watson & Krekelberg, 2009).

In this respect, the results presented by Boi et al. (2017) share interesting similarities with study IV. For one, we found that prolonged presence of the target at its final location prior to saccade offset facilitated gaze correction. Even though we specifically investigated the influence of continuous target motion, as opposed to apparent motion, intra-saccadic visual transients occurred in both conditions, either due to the onset of target motion or due to the appearance of the target at its final location. In fact, as predicted by the exponential model shown in Figure 2.4c, proportions of target fixations would already be above-chance around saccade offset, even in the absence of intra-saccadic motion, which may suggest a general benefit of intra-saccadic transients compared to post-saccadic transients. In addition, to explain the greater benefit of intra-saccadic motion, more diverse spatiotemporal power might have been generated, as target motion induced both additional retinal velocities and possibly (due to the alteration of the retinal trajectory) a separate, direction-dependent range of TFs. This interesting hypothesis would also predict that these benefits would be specific to the low-SF range. As all objects on the screen had largely similar SF content, the effect might therefore have been equally effective for both target and distractor, thus enhancing the sensitivity to discriminate the two objects. Indeed, irrespective of whether intra-saccadic motion was present, low SFs were most beneficial for gaze correction (Figure 2.4g), suggesting that in this task mostly features from the low-SF domain were used to determine object identities. In addition, given that mask onset delays were on average quite short (thus corresponding largely to the simulated time course of visual responses during early fixation; Boi et al., 2017), spatiotemporal power would have been highest at low SFs, thus optimizing visual processing for more coarse than fine object features. Yet, the effect of relative orientation, which was only found at higher (yet by comparison low) SFs and when intra-saccadic motion was presented during the trial, could not be readily explained within the framework of spatiotemporal modulation. Instead, this benefit is best explained either in terms of spatiotemporal continuity or earlier availability of relevant object feature information.

To conclude, recent evidence suggests that saccades may serve the purpose of effectively modulating the spatiotemporal power spectrum according to the statistics of the observed visual scene, especially enhancing low-SF information during early fixation (Boi et al., 2017; Rucci et al., 2018). In fact, in order to reach peak-sensitivity TFs of 10 Hz (Burr & Ross, 1982) with very low SFs, saccadic speeds would be absolutely necessary. Given the high power of these low SFs in natural scenes, as well as the result that the very same SF range was found to be the most prominent feature

in saccade-induced smear (subsection 1.3.2), an important function of intra-saccadic vision might well be the preparation and facilitation of subsequent visual processing of coarse visual information, especially on the level of M-cells and along the low-latency magnocellular pathway (Casile et al., 2019). As proposed by Ibbotson and Cloherty (2009), an enhancement of post-saccadic information could aid post-saccadic masking to more efficiently perform saccadic omission. If this facilitation were driven by visual transients produced by low SFs during saccades, then this mechanism could present itself as a parsimonious new explanation not only for the selectivity of saccadic suppression to low-SF gratings (Burr et al., 1982, 1994; Volkmann et al., 1978), but also as to why intra-saccadic low-SF information – despite being readily resolvable at high retinal speeds – is so well omitted from conscious awareness.

3.2.2 Object correspondence based on motion streaks

While the modulation of the retinal spatiotemporal power distribution constitutes a more general potential function of intra-saccadic vision, we also proposed a potential function of visual processing of intra-saccadic motion streaks in particular: In studies III and IV we put forward the hypothesis that the continuous retinal translation of objects during saccades – which inevitably leads to motion smear – could be used as a visual cue to establish object correspondence across saccades. The issue of object correspondence can be considered a core problem of visual stability and has to this date been thoroughly researched both using saccades and object tracking during fixation (for reviews, see Aagten-Murphy & Bays, 2019; Flombaum, Scholl, & Santos, 2009; Melcher & Colby, 2008; Higgins & Rayner, 2015; Prime, Vesia, & Crawford, 2011). Experimental evidence converged to two possible basic solutions for object correspondence, namely via spatiotemporal continuity (Kahneman et al., 1992; Mitroff & Alvarez, 2007) and encoding of object surface features in VSTM (Hollingworth et al., 2008), or most likely both (Hollingworth & Franconeri, 2009; Richard et al., 2008). In the context of saccades, spatiotemporal continuity was manipulated by varying pre- and post-saccadic object positions (Richard et al., 2008), whereas during fixation, continuity was established by presenting smooth object motion (Mitroff & Alvarez, 2007; Hollingworth & Franconeri, 2009). For instance, Flombaum and Scholl (2006) found that change detection improved in tunnel effect conditions, i.e., a smoothly moving object disappears behind an occluder and briefly afterwards reemerges with a slight change in its features. When spatial or temporal gaps inconsistent with smooth motion were introduced, then change detection rates plummeted. The authors thus proposed the principle of spatiotemporal priority for objects represented in VSTM: If object correspondence can be established via spatiotemporal continuity, then only one representation has to be checked and potentially updated, which is more efficient than comparing it with other distinct object representations (Flombaum et al., 2009). Inspired by the fact that under normal circumstances the change in retinal object positions is deterministically related to the size of the executed eye movement (and is therefore to some degree predictable), it might well be that smooth motion during saccades serves a similar purpose. In fact, in normal visual environments, motion streaks are a necessary consequence of high-speed

motion and may even remain resolvable when motion detection mechanisms fail. Thus, they may be strong candidate for the trans-saccadic problem. Indeed, with respect to their potential role Burr and Thompson (2011, p. 1441) acknowledge that "If nothing else, the studies on motion streaks have illustrated the resourcefulness of the visual motion system, to use all available information – even a cue that might normally be thought of as a hindrance to motion perception rather than a feature – to help it uncover the direction of moving objects and solve the aperture problem."

To explain the effect of continuous intra-saccadic motion found in study IV, one could at least propose three mechanisms. First, motion streaks may have simply provided directional cues to object motion, thus biasing the secondary saccade (Kosovicheva, Wolfe, & Whitney, 2014). Second, the motion streak encoded object features, such as high or low luminance, so that it allowed for comparison of features in VSTM at an earlier point during the saccade (Hollingworth et al., 2008). Third, spatiotemporal continuity created spatiotemporal priority, facilitating the updating of the target object's representation in short-term memory (Flombaum & Scholl, 2006; Flombaum et al., 2009). At this point, it is impossible to rule out either of the three hypotheses, especially as they are not mutually exclusive. Yet, it is possible to make suggestions how to specify the contribution of the motion streak. First, to determine whether the benefit lies in earlier availability of object features or spatiotemporal continuity, a version of the experiment should be tested in which presentation duration is accounted for. In other words, whereas in the motion-present condition the target is continuously present while it is moving, even in the motion-absent condition the target should be continuously present throughout the saccade, i.e., displayed at its post-saccadic target location. If performance in both conditions were similar, then a facilitation via earlier availability of object features would be likely. If performance in the duration-controlled motion-absent condition were however similar to performance in the present motion-absent condition in study IV, then a special role of spatiotemporal continuity via motion streaks would be likely. Second, in order to investigate whether intra-saccadic motion simply biases secondary saccades to one object or the other, incongruent conditions could be introduced, for instance by displaying continuous target motion opposite to the actual array rotation. In congruent trials, in which motion direction reveals the post-saccadic target position, one would again expect a benefit for target stimuli relative to the motion-absent condition. In incongruent trials, in which motion points to the post-saccadic location of the distractor, two outcomes are conceivable. On the one hand, secondary saccades to the distractor could occur more prevalently, suggesting that object motion biases gaze correction towards one or the other object. On the other hand, these incongruent motion streaks could simply not elicit any behavioral benefit, suggesting that pre- and post-saccadic object features would still undergo matching in VSTM, which ultimately drives the secondary saccade. Indeed, the idea of spatiotemporal priority (Flombaum et al., 2009) would predict that the induction of false continuity would impair or at least slow down the matching process in VSTM, provided that post-saccadic object features are available. Some preliminary evidence in favor of this view is provided by the finding that continuous target motion sped up

target-bound saccades, but did not slow down distractor-bound saccades. Regardless of the specific underlying mechanism – which shall be scrutinized in future experiments – we have provided evidence that continuous target motion mattered for gaze correction, and could have provided a cue for establishing object correspondence, which is parsimoniously in line with previous investigations (e.g., Flombaum & Scholl, 2006; Kahneman et al., 1992; Mitroff & Alvarez, 2007).

Whereas study III found that motion streaks were able to reveal post-saccadic object identities in a perceptual task, providing proof of concept that motion streaks could in principle link object locations, study IV showed that such benefit could also occur in a motor task that required neither explicit instruction nor knowledge about streaky object motion. Interestingly, none of the observers became aware of motion-present and motion-absent conditions throughout the course of the experiment, as motion presentations were not only extremely brief and rapid, but also well masked by the presence of post-saccadic objects (Bedell & Yang, 2001; Duyck et al., 2016; Matin et al., 1972). In addition, that in both motion conditions six objects were displayed with a sudden onset transient, could have enhanced this masking effect (see previous section) or caused attentional distraction (Balsdon et al., 2018). The presence of many (potentially redundant) objects is also a feature of cluttered scenes, suggesting that similar effects may occur in more natural vision. It is indeed a fascinating hypothesis that the benefit of intra-saccadic motion was present, even though observers were not aware of the latter. Unfortunately, we did not assess perceptual performance in detecting these motion streaks, but it may be possible to approximate the latter based on the results of study III, where sensitivity in Experiment 1 at a motion duration of 14 ms was at approximately $d' = 0.25$. The improvement caused by increased contrast and motion duration in Experiment 4 relative to Experiment 3 would set the upper bound of sensitivity to $d' = 1$. Note that, whereas in study III it was crucial to the task to detect object motion, observers in study IV were tasked to pay attention and respond to post-saccadic object features (given the time-limiting effect of masking) without being informed about the potential occurrence of streaky motion. Yet, it is a possibility that gaze correction depended on at least the conscious detection of object displacement (or even continuous motion) during a saccade. Hollingworth et al. (2008) explicitly tested this assumption by instructing observers to fixate an outer ring whenever they detected a trans-saccadic displacement of the target. The authors found that in a quarter of all displacement trials observers fixated the pre-saccadic target with near-ceiling accuracy regardless of the instruction, even though this suggests that they did not detect any displacement. In addition, after they made a voluntary secondary saccade to the outer ring, they performed a tertiary saccade to the pre-saccadic target in more than half of all trials. Crucially, all these instruction-defying saccades were made at normal latencies, very similar to those found in study IV. This evidence suggests that gaze correction is to a large degree an automatic process, for which conscious awareness was neither required nor present, and that the same was the case in our task, as shown by low saccadic latencies. At a larger scale, this may parallel the findings by Võ, Aizenman, and Wolfe (2016) and Kok, Aizenman, Võ, and Wolfe (2017), suggesting that human observers have little conscious access to their own saccade patterns.

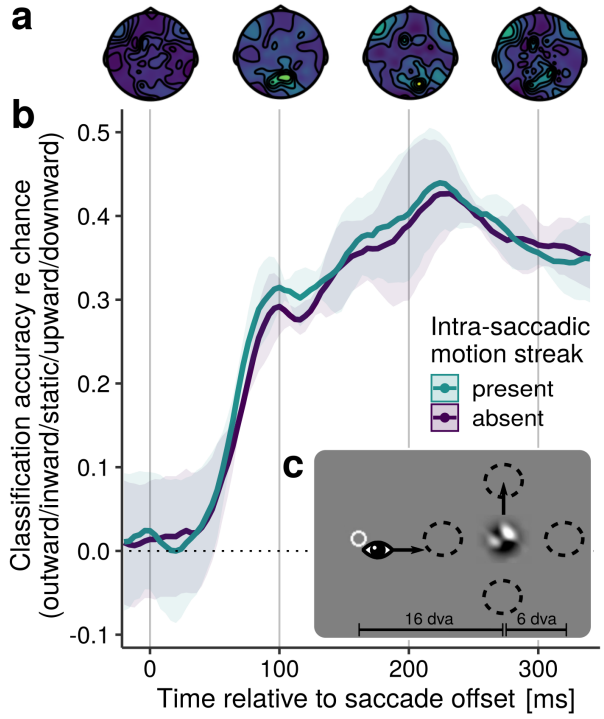

Figure 3.1: Preliminary results (n=3) of the motion-streak decoding experiment. Post-saccadic target position in each trial was decoded, separately for motion-present and motion-absent conditions, from 64-channel EEG data (largely cleaned of oculomotor artifacts by an optimized ICA procedure proposed by Dimigen, 2020) at each 4-ms time bin using linear support vector machines (Fan et al., 2008) trained on n-1 corresponding trials.
a Topography plots show the distribution of absolute SVM classifier weights at 0, 100, 200, and 300 milliseconds after saccade offset, respectively.
b Time course of above-chance classification accuracy of post-saccadic position relative to saccade offset.
c Observers made 16-dva saccades to a noise patch target (0.25–1 cpd, 0.5 Gaussian aperture SD) which could be intra-saccadicly moved to four different locations at 6 dva eccentricity (dashed circles) or remain static. Target motion was either continuous or apparent (36 frames, 25 ms) and observers were tasked to make a secondary saccade to the post-saccadic target. The experiment's pre-registration can be found at OSF: `https://osf.io/qm5ca/?view_only=0ba60417ece04006a96a53994db3cee6`

Even though at this point it remains unclear whether a putative mechanism of trans-saccadic object correspondence via the monitoring of motion streaks could operate in the absence of conscious awareness, which would clearly be a prerequisite for its usefulness in real-world scenarios, at least some evidence in favor of this hypothesis is provided by study IV: Significant reductions of secondary saccade latencies even up to the duration of presented motion were found regardless of whether surface features were available or not. These small reductions resembled the object-specific preview benefits found by Mitroff and Alvarez (2007) and would unlikely be caused by engagement of recurrent conscious processing (Lamme, 2003). To more closely study the time course of visual processing of intra-saccadic motion streaks, an EEG-eye tracking experiment was set up. The task greatly resembled previous study IV (Figure 3.1c), but this time only featured a single target, which observers made saccades to. During saccades, the target could be displaced to four different screen locations or remain static, moving either continuously, thus producing a motion streak, or in a step-wise fashion. Observers had no perceptual task, but were instructed to made a secondary saccade to the post-saccadic target, if it moved. Employing a multivariate pattern analysis technique (Crouzet, Busch, & Ohla, 2015; G. Edwards, VanRullen, & Cavanagh, 2018), the target's post-saccadic location was decoded from co-registered EEG data. If motion streaks had direct relevance for tracking object locations across saccades, then earlier or more accurate classification of post-saccadic object location would be expected. Although this is not (yet) convincingly evident in the preliminary results displayed in Figure 3.1b, target locations could be decoded as early as 100 ms after saccade offset (around the time of the lambda response; Dimigen et al., 2011) with a clear occipital topography (Figure 3.1a).

This suggests an early visual processing of motion streaks that preceded the execution of secondary saccades. These occurred between 150 and 200 ms after primary saccade offset and are already reflected in the frontal topographies at 200 ms and 300 ms (Figure 3.1a), suggesting that at later time points the classifier used actual eye position data (most likely residuals of the corneoretinal dipole) to determine post-saccadic object location. The finding that these secondary saccade latencies were lower than those found in study IV parallels previous results suggesting latency-increasing effects of distractor presence (e.g., Walker, Deubel, Schneider, & Findlay, 1997). Note that the decoding of brief and high-speed visual stimulation presented strictly during saccades has not yet been attempted, so it has to be emphasized that these are preliminary results. Yet, they provide some evidence that intra-saccadic motion-streak information is processed early on, potentially modulating the novel visual input registered upon fixation onset.

It has been shown that human performance in detecting object changes across saccades is actually quite poor and often results in change blindness (Simons & Levin, 1997). For instance, Henderson and Hollingworth (2003b) found that global reversals of entire visual scenes overlaid with vertical bars were detected at near-zero rates. Similarly, the replacement of features of an object – or even the entire object – during a saccade was rarely noticed, and if so, then predominantly whenever replacements took place around the saccade target, or when short saccades below 5 dva were made (Henderson & Hollingworth, 2003a). These findings are largely in line with the still quite influential "saccade target theory of visual stability" (McConkie & Currie, 1996), which suggests that only local, not global information around the saccade goal is processed to compute object correspondence across saccades. More specifically, the theory suggests that, as a pre-saccadic step, not only the location, but also the features of an arbitrary target object (so-called locating information) in the retinal periphery are encoded in memory. Upon saccade landing, the saccade target locating process is initiated to find the initial pre-saccadic target with the help of the previously encoded locating information. Once the object is found, a bi-directional mapping between pre- and post-saccadic retinal locations can be created, giving rise to the percept of a locally (but not necessarily globally) stable world. If, however, the pre-saccadicly encoded saccade target could not be found within local search region, for instance due to motor errors or object displacements, then the error signal would give rise to change detection and eventual gaze correction. In this framework, motion streaks could contribute at various stages. First, especially when saccades are made to targets at greater eccentricities, the extraction of locating information will certainly be less efficient and related with greater uncertainty (Hess & Field, 1993; Michel & Geisler, 2011; Zhang, Morvan, & Maloney, 2010). In addition, visual acuity to form and color decreases in the retinal periphery (Kleitman & Blier, 1928). Especially in cluttered scenes, it may thus be difficult to perform visual search based on coarse information, which would in part also explain why change detection performance decreased at greater saccade amplitudes (Henderson & Hollingworth, 2003a; McConkie & Currie, 1996). Some of these issues could most likely be alleviated by the allocation of pre-saccadic attention at the saccade target (Deubel & Schneider, 1996; Kowler et al., 1995; Li et al., 2016; Rolfs et al., 2011),

but intra-saccadic motion streaks could additionally facilitate this search by invoking the principle of spatiotemporal priority (Flombaum et al., 2009). Second, motion streaks may provide an additional search benefit when objects within the saccade target search region have similar features or even the same identity. This situation is illustrated in Figure 1 of study IV: In principle, even without extra-retinal information about saccade amplitude and direction, the motion streak traces the target object directly from its (uncertain) peripheral location into the fovea, thus revealing which of the two targets was foveated. By occluding the intra-saccadic motion streak in the figure, one can visibly experience increased uncertainty about object identity. Indeed, that distinctive motion streaks allow for this kind of matching, even if objects are completely identical, was thoroughly tested in study III. Third, the saccade target theory would also predict the effect of primary saccade landing found in study IV (see also Hollingworth et al., 2008): As the saccade target search region is determined by the saccade's landing position, objects that incidentally fall into the search region may (sometimes erroneously) be identified as the pre-saccadic target, whereas other, potentially more suitable candidates are not taken into account. As model comparisons suggested that this effect of landing position was orthogonal to the effect of intra-saccadic motion, they may be separate mechanisms: Whereas the saccade determines the size of the search area, spatiotemporal priority may be granted to these objects when represented in VSTM. Fourth, the idea that stability across saccades is computed locally may also explain why task-irrelevant background manipulations, such as the intra-saccadic large-field motion induced in study V, were neither noticed nor effective. Unless the streak-inducing targets were also saccade targets and thus within saccade-target search range, which was the case in both studies III and IV, spatiotemporal priority could not affect the linking of pre- and post-saccadic object representations. This proposal is compatible with the finding that object manipulations taking place at the saccade starting point were rarely noticed (Henderson & Hollingworth, 2003a). This effect, although it was most likely confounded with the eccentricity of the target during presentation, was also found in study V, where motion streaks were rarely detected when presented around the fixation target. Even though results from study IV suggest that the benefit of intra-saccadic motion is specific to the saccade target, it is still an open and interesting question whether even target-independent motion signals could provide a similar, more global benefit.

Finally, it is interesting to note that the saccade target theory, as well as its enhancements by taking into account the potential role of motion streaks, is not in need of classic ideas of reafference to explain stability (Von Holst & Mittelstaedt, 1950; Mittelstaedt, 1990), as object correspondence is purely based on retinal locations and features encoded in VSTM. Importantly, the theory does not make any predictions about how stability should be achieved in the absence of discriminable objects, such as when observers make sequential saccades to the remembered locations of two (at that point extinguished) targets in the double-step paradigm (Hallett & Lightstone, 1976a, 1976b). Arguably, the successful execution of the second saccade would depend on a successful spatial updating mechanism based on an internal representation of the first saccade (Sommer & Wurtz, 2008; Wurtz, 2008, 2018). Indeed, Ostendorf, Liebermann, and Ploner (2010) showed that a patient

with an unilateral lesion in MD was impaired in such a task, while being able to perform visually guided saccades with normal accuracy. This result suggests that (at least in the absence of visual objects) efference copies are needed to update gaze direction. Interestingly, the impairment in the extinguished double-step task was not complete, suggesting that other sources of information, such as the highly salient screen borders (Deubel, 2004) or even proprioceptive signals (Bridgeman & Stark, 1991; Gauthier et al., 1990; Zhang et al., 2010), were able to compensate for the error to some degree. It is thus likely that any potential role of intra-saccadic motion streaks is (at most) additional – and not an alternative – to established mechanisms of visual stability.

3.3 Methodological considerations and limitations

As an online saccade detection algorithm was implemented in study II that allowed for the registration of saccade onsets as early as 2.3 ms after their physical onset (not taking into account the eye tracking system's end-to-end latency) with a very low FA rate, studies III to V (and Balsdon et al., 2018) used convenient gaze-contingently triggered intra-saccadic presentation regimes. On the one hand, the advantage of this approach is that, compared to previous experiments scheduling presentations around each observer's average saccade latency (e.g., Castet et al., 2002; Diamond et al., 2000), the overall number of trials can be greatly reduced and more strictly intra-saccadic experimental conditions can be tested. On the other hand, potentially interesting saccade-contingent time courses of responses (e.g., Honda, 1991, 2006; Morrone, Ross, & Burr, 1997; Ross, Morrone, & Burr, 1997) cannot be made visible and fixation conditions have to be tested separately. Note that, due to inevitable refresh and video latencies, physical presentation onsets often occurred only up to 16.7 ms later. Such latencies could be reduced by technologies like G-sync (Poth et al., 2018), but can never be fully avoided. An interesting alternative are tachistoscopic presentation techniques, such as those described in subsection 1.3.2, as stimuli can be drawn to screen in advance and gaze-contingently presented at latencies below 1 ms. Related to the issue of presentations contingent upon saccade onset is the potential issue of confounding effects of stimulus duration with largely unpredictable saccade metrics during intra-saccadic presentation (but see also Han et al., 2013). Put differently, higher performance at longer stimulus durations may be the consequence of both longer retinal exposure with the stimulus and, for instance, the lower retinal velocities occurring in the deceleration stage of the saccade, or even further extended motion streaks around the saccadic peak velocity. This problem is present in both studies III and V, and could not be remedied. An alternative would be the manipulation of motion velocity at constant duration, resulting however in motion amplitudes that could not be kept constant. In any case, this confounding factor was not crucial to the conclusions drawn from studies III and V, but should be controlled for in future studies by additional post-hoc analyses.

Stimulus presentations contingent upon saccade onset have the additional conceptual and practical disadvantage that there will always be a lag between the onset of saccade-induced and stimulus-

induced visual changes. In other words, whereas in natural vision the visual transient produced by the onset of retinal large-field motion occurs instantly, eventual manipulations of the latter would necessarily produce a second disruption. Even though this disruption may not, or only rarely be noted by the observer (as in study V), it is incongruent with natural saccade-induced stimulation. Provided that the visual system has even a moderately accurate prediction of a saccade's visual consequences, the delayed onset of an intra-saccadic manipulation will not concur with typical stimulation and may therefore not have any effect. Although the results presented by Zimmermann (2020) suggest that the visual system may even habituate to highly unnatural visual displacements orthogonal to the saccade direction, these manipulations have clearly little ecological validity. Similarly, the usage of sudden-onset, strictly intra-saccadic rapid motion is an event that will rarely be induced in natural environments, neither by moving objects nor by sudden changes in the saccade's trajectory. It will thus be a more realistic research avenue to manipulate motion smear parallel to the saccade direction by using static targets, or targets moving in parallel to the saccade. Manipulations of motion streak length, which routinely occur due to natural variations in saccade amplitudes, could be studied with this approach. An ideal experimental setup would involve a low-latency presentation system with high temporal resolution that avoids gaze-contingent delays, potentially even allowing for retinal stabilization during saccades (e.g., Mateeff, 1978). That way, it would be possible to study the effects of visual stimuli present throughout the entire saccade by applying motion proportional to the change in eye position at any given point in time.

Finally, when testing participants in intra-saccadic tasks like the ones reported here, an interesting general observation can be made, which most likely has a strong impact on most studies on intra-saccadic perception. If observers are tasked not only to make saccades of large amplitudes, such as those instructed in studies III and V, but also to detect an intra-saccadic target at the same time, then they tend to make saccades that do not reach the saccade target, or even make a sequence of 2, 3, or 4 saccades to reach the saccade target. As a consequence, a large proportion of trials had to be excluded or repeated. Note that observers were practically never aware of this tendency, which is why in such a case an automatic feedback was triggered which displayed observers' actual saccade trajectories on the screen. Although this feedback helped to some extent, some study participants could not, despite trying hard, alter or counteract these saccade patterns, and perceived the feedback as grossly contradicting their phenomenal experience. Funnily, one observer was convinced that the study was not about intra-saccadic vision, but about assessing a person's frustration tolerance. At this point, it is unclear why this tendency emerged. For instance, there might have been a tradeoff between planning an accurate saccade to the instructed target and attending to the brief intra-saccadic presentation. Alternatively, the saccade might have been biased towards the predicted spatial location of the intra-saccadic target (Walker et al., 1997). Finally, intra-saccadic flashes, when presented in the later stages of the saccade, could have induced saccadic adaptation (Panouillères et al., 2016). Taking into account the processing latencies occurring in the visual system (Lichtenstein & White, 1961; Mansfield & Daugman, 1978; Reich et al.,

2001), as well as the latencies involved in saccade programming (Becker, 1989; Robinson, 1981), it is however highly implausible that the changes in saccade trajectory were an instant response to the intra-saccadic stimulus. Regardless of the underlying mechanism, this observation has important methodological implications for all experimental paradigms using intra-saccadic manipulations, especially when stimulus detection is required: By disrupting the visual flow typically occurring during saccades, one does not simply change visual experience, but also alters the very motor process that determines this experience.

3.4 Future directions

The studies reported up to this point contributed to building a methodological and conceptual framework for studying the perceptual and motor consequences of intra-saccadic vision. On a methodological level, novel presentation techniques and algorithms were conceived – not only to demonstrate the general possibility of efficient intra-saccadic perception (study I), but also to improve gaze-contingent experimental paradigms that could study the latter, as well as to evaluate the usage of cutting-edge high-speed projection systems (study II). On a conceptual level, experimental evidence suggested that rapid smeared object motion during saccades matters: Motion streaks were able to perceptually reveal rapid trans-saccadic object transitions (study III), facilitated gaze correction in accuracy and speed (study IV), and could even be readily (though imperfectly) localized in spatiotopic coordinates (study V). Even if these results may seem to contradict common intuitions about one's subjective blindness during saccades (Dodge, 1900), they are largely (if not fully) compatible with most prior investigations on both saccadic omission (section 1.2) and motion smear (section 1.3). Thus, more than answering long-standing questions, these studies motivate future research on the potential role of self-induced sensory consequences for visual stability.

First, does saccade-induced motion smear in natural-scene and free-viewing settings make a difference? As visual scene and saccade statistics have similarities (Najemnik & Geisler, 2008; Otero-Millan et al., 2013; Coppola et al., 1998), this coincidence may produce distinctive patterns of motion smear that could be used as cues to saccade amplitude and direction. For instance, when replaying previously collected saccade patterns during fixation at 1440 fps, thus replicating the actual saccadic velocities, smear is rarely noticed, yet a sense of motion direction and spatial distance is conveyed. By systematically removing, counteracting, or amplifying visual motion during saccades, it may be possible to study whether these large-scale motion signals play a role in scene viewing, for instance when localizing specific visual objects.

Second, do intra-saccadic motion signals contribute to saccadic omission, beyond the established noise-inducing effects related to saccadic suppression (Brooks & Fuchs, 1975; Idrees et al., 2020; MacKay, 1970; Richards, 1969)? Phenomenal observations discussed above, as well as recent evidence (Rolfs et al., 2017; Zimmermann, 2020), invite the hypothesis that the visual system may employ predictions regarding the sensory consequences of its own saccades to efficiently omit

conforming visual signals. How are these predictions, most likely based on sensorimotor contingencies (O'Regan & Noë, 2001), generated and could they be re-evaluated by training? How precise do these predictions need to be to perform omission and what error margins do they tolerate? How closely are they related to individual saccade metrics? By further developing gaze-contingent presentation techniques, it may be possible to manipulate visual feedback during saccades and investigate these questions.

Third, what is the extent and function of more natural intra-saccadic vision, which is usually omitted from conscious perception? Although study IV has provided some evidence that motion streaks could contribute to processes like gaze correction, which do not necessarily require conscious awareness, it remains unclear how to explain this specific contribution mechanistically. In addition, virtually all studies at this point – both previous and those reported here – used detectable visual transients, such as sudden motion onsets or flashes, to probe vision during saccades. These stimuli are of course reliable tools for assessing visual function, but are, at least for the intra-saccadic interval, not the type of visual input the system would have most experience with. Instead, processing may be optimized for continuous stimulation (for similar arguments, see Schlag & Schlag-Rey, 1995; Teichert et al., 2010) which can be – maybe precisely for this reason – effectively omitted from conscious awareness. Future studies should therefore specifically investigate the type of input that goes unnoticed during saccades to incrementally uncover the mechanisms responsible for real-world intra-saccadic vision, that is, the one we do not experience.

Finally, it is a fascinating possibility that intra-saccadic motion smear may be more than a threat to visual stability which must be kept out of the system to maintain a representation of the world that remains unaffected by recurrent disruptions due to saccades. Self-induced motion signals may in the end be useless for trans-saccadic continuity, but at this point there is as much evidence against this assumption as there this in favor of it, as only very few steps have been taken to critically investigate the alternative hypothesis. It is without question that, whether they are useful or not, several intriguing visual and non-visual mechanisms may be readily available to omit these signals from conscious awareness, so that they do not disturb us during critical visual tasks. What might be even more intriguing, however, is the perspective (although it may be stated in a slightly hyperbolic way) that "there is no need to postulate mechanisms that compensate for the smear that is created by eye saccades, because this smear is part of what it is to see. If the retinal receptors did not signal a global smear during saccades, then the brain would have to assume that the observer was not seeing, and that he or she was perhaps hallucinating or dreaming." (O'Regan & Noë, 2001, p. 950).

4

References

Aagten-Murphy, D., & Bays, P. M. (2019). Functions of memory across saccadic eye movements. In *Processes of visuospatial attention and working memory* (pp. 155–183). Springer International Publishing.

Adams, W. J., Elder, J. H., Graf, E. W., Leyland, J., Lugtigheid, A. J., & Muryy, A. (2016). The Southampton-York natural scenes (SYNS) dataset: Statistics of surface attitude. *Scientific reports*, *6*, 35805.

Adelson, E. H., & Bergen, J. R. (1985, February). Spatiotemporal energy models for the perception of motion. *J. Opt. Soc. Am. A*, *2*(2), 284–299.

Alais, D., Apthorp, D., Karmann, A., & Cass, J. (2011). Temporal integration of movement: the time-course of motion streaks revealed by masking. *PloS one*, *6*(12).

Anderson, S. J., & Burr, D. C. (1987). Receptive field size of human motion detection units. *Vision research*, *27*(4), 621–635.

Anstis, S. M., & Atkinson, J. (1967). Distortions in moving figures viewed through a stationary slit. *The American Journal of Psychology*.

Apthorp, D., & Alais, D. (2009). Tilt aftereffects and tilt illusions induced by fast translational motion: Evidence for motion streaks. *Journal of Vision*, *9*(1), 27–27.

Apthorp, D., Cass, J., & Alais, D. (2010). Orientation tuning of contrast masking caused by motion streaks. *Journal of Vision*, *10*(10), 11.

Apthorp, D., Cass, J., & Alais, D. (2011). The spatial tuning of ”motion streak” mechanisms revealed by masking and adaptation. *Journal of Vision*, *11*(7), 17.

Apthorp, D., Schwarzkopf, D. S., Kaul, C., Bahrami, B., Alais, D., & Rees, G. (2013). Direct evidence for encoding of motion streaks in human visual cortex. *Proceedings of the Royal Society B: Biological Sciences*, *280*(1752), 20122339.

Apthorp, D., Wenderoth, P., & Alais, D. (2009). Motion streaks in fast motion rivalry cause orientation-selective suppression. *Journal of Vision*, *9*(5), 10.

Bahill, A. T., Clark, M. R., & Stark, L. (1975, January). The main sequence, a tool for studying human eye movements. *Mathematical Biosciences*, *24*(3), 191–204.

Balsdon, T., Schweitzer, R., Watson, T., & Rolfs, M. (2018). All is not lost: Post-saccadic contributions to the perceptual omission of intra-saccadic streaks. *Consciousness and cognition*, *64*, 19-31.

Barlow, H. B. (1958). Temporal and spatial summation in human vision at different background intensities. *The Journal of physiology*, *141*(2), 337–350.

Becker, W. (1989). The neurobiology of saccadic eye movements. metrics. *Reviews of oculomotor research*, *3*, 13.

Bedell, H. E., Tong, J., & Aydin, M. (2010). The perception of motion smear during eye and head movements. *Vision research*, *50*(24), 2692–2701.

Bedell, H. E., & Yang, J. (2001). The attenuation of perceived image smear during saccades. *Vision Research*, *41*(4), 521–528.

Binda, P., & Morrone, M. C. (2018). Vision during saccadic eye movements. *Annual review of vision science*, *4*, 193–213.

Blakemore, C., & Campbell, F. W. (1969). On the existence of neurones in the human visual system selectively sensitive to the orientation and size of retinal images. *The Journal of physiology*, *203*(1), 237–260.

Boi, M., Poletti, M., Victor, J. D., & Rucci, M. (2017). Consequences of the oculomotor cycle for the dynamics of perception. *Current Biology*, *27*(9), 1268–1277.

Born, S. (2019). Saccadic suppression of displacement does not reflect a saccade-specific bias to assume stability. *Vision*, *3*(4), 49.

Braun, D. I., Schütz, A. C., & Gegenfurtner, K. R. (2017, July). Visual sensitivity for luminance and chromatic stimuli during the execution of smooth pursuit and saccadic eye movements. *Vision Research*, *136*, 57–69.

Breitmeyer, B. G. (1978). Metacontrast masking as a function of mask energy. *Bulletin of the Psychonomic Society*, *12*(1), 50–52.

Breitmeyer, B. G., & Ganz, L. (1976). Implications of sustained and transient channels for theories of visual pattern masking, saccadic suppression, and information processing. *Psychological review*, *83*(1), 1-36.

Breitmeyer, B. G., & Öğmen, H. (2000). Recent models and findings in visual backward masking: A comparison, review, and update. *Perception & psychophysics*, *62*(8), 1572–1595.

Bremmer, F., Kubischik, M., Hoffmann, K.-P., & Krekelberg, B. (2009). Neural dynamics of saccadic suppression. *Journal of Neuroscience*, *29*(40), 12374–12383. doi: 10.1523/JNEUROSCI.2908-09.2009

Bridgeman, B. (2007). Efference copy and its limitations. *Computers in biology and medicine*, *37*(7), 924–929.

Bridgeman, B., Hendry, D., & Stark, L. (1975). Failure to detect displacement of the visual world during saccadic eye movements. *Vision research*, *15*(6), 719–722.

Bridgeman, B., & Macknik, S. (1995). Saccadic suppression relies on luminance information. *Psychological research*, *58*(3), 163–168.

Bridgeman, B., & Stark, L. (1991). Ocular proprioception and efference copy in registering visual direction. *Vision research*, *31*(11), 1903–1913.

Bridgeman, B., Van der Heijden, A. H. C., & Velichkovsky, B. M. (1994). A theory of visual stability across saccadic eye movements. *Behavioral and Brain Sciences*, *17*(2), 247–258.

Brooks, B. A., & Fuchs, A. F. (1975). Influence of stimulus parameters on visual sensitivity during saccadic eye movement. *Vision Research*, *15*(12), 1389–1398.

Brooks, B. A., Impelman, D., & Lum, J. (1981). Backward and forward masking associated with saccadic eye movement. *Perception & Psychophysics*, *30*(1), 62–70.

Brooks, B. A., Yates, J., & Coleman, R. (1980). Perception of images moving at saccadic velocities during saccades and during fixation. *Experimental Brain Research*, *40*(1), 71–78.

Burr, D. (1980). Motion smear. *Nature*, *284*(5752), 164–165.

Burr, D. (1981). Temporal summation of moving images by the human visual system. *Proc. R. Soc. Lond. B*, *211*(1184), 321–339.

Burr, D., Holt, J., Johnstone, J., & Ross, J. (1982). Selective depression of motion sensitivity during saccades. *The Journal of physiology*, *333*(1), 1–15.

Burr, D., & Morgan, M. J. (1997). Motion deblurring in human vision. *Proceedings of the Royal Society of London. Series B: Biological Sciences*, *264*(1380), 431–436.

Burr, D., & Morrone, C. (1996). Temporal impulse response functions for luminance and colour during saccades. *Vision research*, *36*(14), 2069–2078.

Burr, D., Morrone, M., & Ross, J. (1994). Selective suppression of the magnocellular visual pathway during saccadic eye movements. *Nature*, *371*(6497), 511–513.

Burr, D., & Ross, J. (1982). Contrast sensitivity at high velocities. *Vision research*, *22*(4), 479–484.

Burr, D., & Ross, J. (2002). Direct evidence that ”speedlines” influence motion mechanisms. *Journal of Neuroscience*, *22*(19), 8661–8664.

Burr, D., & Thompson, P. (2011). Motion psychophysics: 1985-2010. *Vision research*, *51*(13), 1431–1456.

Campbell, F., & Wurtz, R. (1978). Saccadic omission: why we do not see a grey-out during a saccadic eye movement. *Vision research*, *18*(10), 1297–1303.

Carrasco, M., & McElree, B. (2001). Covert attention accelerates the rate of visual information processing. *Proceedings of the National Academy of Sciences*, *98*(9), 5363–5367.

Casile, A., Victor, J. D., & Rucci, M. (2019). Contrast sensitivity reveals an oculomotor strategy for temporally encoding space. *Elife*, *8*, e40924.

Castet, E. (2010). Perception of intra-saccadic motion. In *Dynamics of visual motion processing, chapter 10* (pp. 213–238). Springer.

Castet, E., Jeanjean, S., & Masson, G. S. (2001). "Saccadic suppression" - no need for an active extra-retinal mechanism. *Trends in Neurosciences*, *24*(6), 316–317.

Castet, E., Jeanjean, S., & Masson, G. S. (2002). Motion perception of saccade-induced retinal translation. *Proceedings of the National Academy of Sciences*, *99*(23), 15159–15163.

Castet, E., & Masson, G. (2000). Motion perception during saccadic eye movements. *Nature Neuroscience*, *2*, 177–183.

Cavanagh, P., Hunt, A. R., Afraz, A., & Rolfs, M. (2010, April). Visual stability based on remapping of attention pointers. *Trends in Cognitive Sciences*, *14*(4), 147–153.

Chahine, G., & Krekelberg, B. (2009). Cortical contributions to saccadic suppression. *PloS one*, *4*(9).

Chekaluk, E., & Llewellyn, K. R. (1990). Visual stimulus input, saccadic suppression, and detection of information from the postsaccade scene. *Perception & Psychophysics*, *48*(2), 135–142.

Chen, S., Bedell, H. E., & Öğmen, H. (1995). A target in real motion appears blurred in the absence of other proximal moving targets. *Vision research*, *35*(16), 2315–2328.

Cleland, B. G., Dubin, M. W., & Levick, W. R. (1971). Sustained and transient neurones in the cat's retina and lateral geniculate nucleus. *The Journal of physiology*, *217*(2), 473–496.

Collewijn, H., & Kowler, E. (2008). The significance of microsaccades for vision and oculomotor control. *Journal of Vision*, *8*(14), 20–20.

Collins, T., Rolfs, M., Deubel, H., & Cavanagh, P. (2009). Post-saccadic location judgments reveal remapping of saccade targets to non-foveal locations. *Journal of vision*, *9*(5), 29.

Collins, T., & Wallman, J. (2012, June). The relative importance of retinal error and prediction in saccadic adaptation. *Journal of Neurophysiology*, *107*(12), 3342–3348.

Comets, E., Lavenu, A., & Lavielle, M. (2017). Parameter estimation in nonlinear mixed effect models using saemix, an R implementation of the SAEM algorithm. *Journal of Statistical Software*, *80*(3), 1–41. doi: 10.18637/jss.v080.i03

Coppola, D. M., Purves, H. R., McCoy, A. N., & Purves, D. (1998). The distribution of oriented contours in the real world. *Proceedings of the National Academy of Sciences*, *95*(7), 4002–4006.

Crevecoeur, F., & Kording, K. (2017). Saccadic suppression as a perceptual consequence of efficient sensorimotor estimation. *eLife*, *6*, e25073.

Croner, L. J., & Kaplan, E. (1995). Receptive fields of p and m ganglion cells across the primate retina. *Vision research*, *35*(1), 7–24.

Crouzet, S. M., Busch, N. A., & Ohla, K. (2015). Taste quality decoding parallels taste sensations. *Current Biology*, *25*(7), 890–896.

Dassonville, P., Schlag, J., & Schlag-Rey, M. (1992). Oculomotor localization relies on a damped representation of saccadic eye displacement in human and nonhuman primates. *Visual neuroscience*, *9*(3-4), 261–269.

Deubel, H. (2004). Localization of targets across saccades: Role of landmark objects. *Visual Cognition*, *11*(2-3), 173–202.

Deubel, H., Elsner, T., & Hauske, G. (1987). Saccadic eye movements and the detection of fast-moving gratings. *Biological cybernetics*, *57*(1-2), 37–45.

Deubel, H., Schneider, W., & Bridgeman, B. (1996). Postsaccadic target blanking prevents saccadic suppression of image displacement. *Vision research*, *36*(7), 985–996.

Deubel, H., & Schneider, W. X. (1996). Saccade target selection and object recognition: Evidence for a common attentional mechanism. *Vision research*, *36*(12), 1827–1838.

Deubel, H., Wolf, W., & Hauske, G. (1982). Corrective saccades: Effect of shifting the saccade goal. *Vision research*, *22*(3), 353–364.

Diamond, M., Ross, J., & Morrone, M. (2000). Extraretinal control of saccadic suppression. *Journal of Neuroscience*, *20*(9), 3449–3455.

Dimigen, O. (2020). Optimizing the ICA-based removal of ocular EEG artifacts from free viewing experiments. *Neuroimage*, *207*, 116117.

Dimigen, O., Sommer, W., Hohlfeld, A., Jacobs, A. M., & Kliegl, R. (2011). Coregistration of eye movements and EEG in natural reading: analyses and review. *Journal of Experimental Psychology: General*, *140*(4), 552.

Ditchburn, R. W., & Ginsborg, B. L. (1952). Vision with a stabilized retinal image. *Nature*, *170*(4314), 36–37.

Dodge, R. (1900). Visual perception during eye movement. *Psychological Review*, *7*(5), 454.

Dorr, M., & Bex, P. J. (2013). Peri-saccadic natural vision. *The Journal of Neuroscience*, *33*(3), 1211–1217.

Duffy, F. H., & Lombroso, C. T. (1968). Electrophysiological evidence for visual suppression prior to the onset of a voluntary saccadic eye movement. *Nature*, *218*(5146), 1074-1075.

Duyck, M., Collins, T., & Wexler, M. (2016). Masking the saccadic smear. *Journal of vision*, *16*(10), 1.

Duyck, M., Wexler, M., Castet, E., & Collins, T. (2018). Motion masking by stationary objects: a study of simulated saccades. *i-Perception*, *9*(3), 2041669518773111.

Edwards, G., VanRullen, R., & Cavanagh, P. (2018). Decoding trans-saccadic memory. *Journal of Neuroscience*, *38*(5), 1114–1123.

Edwards, M., & Crane, M. (2007). Motion streaks improve motion detection. *Vision research*, *47*(6), 828–833.

Engbert, R., & Kliegl, R. (2003). Microsaccades uncover the orientation of covert attention. *Vision research*, *43*(9), 1035–1045.

Engbert, R., & Mergenthaler, K. (2006). Microsaccades are triggered by low retinal image slip. *Proceedings of the National Academy of Sciences*, *103*(18), 7192-7197.

Enroth-Cugell, C., & Robson, J. G. (1966). The contrast sensitivity of retinal ganglion cells of the cat. *The Journal of physiology*, *187*(3), 517–552.

Erdmann, B., & Dodge, R. (1898). *Psychologische Untersuchungen über das Lesen auf experimenteller Grundlage*. Halle, Niemeier.

Fan, R.-E., Chang, K.-W., Hsieh, C.-J., Wang, X.-R., & Lin, C.-J. (2008). Liblinear: A library for large linear classification. *Journal of machine learning research*, *9*(Aug), 1871–1874.

Flombaum, J. I., & Scholl, B. J. (2006). A temporal same-object advantage in the tunnel effect: facilitated change detection for persisting objects. *Journal of Experimental Psychology: Human Perception and Performance*, *32*(4), 840.

Flombaum, J. I., Scholl, B. J., & Santos, L. R. (2009). Spatiotemporal priority as a fundamental principle of object persistence. In B. M. Hood & L. R. Santos (Eds.), *The origins of object knowledge* (pp. 135–164). Oxford Scholarship Online. doi: 10.1093/acprof:oso/9780199216895.001.0001

Fröhlich, F. W. (1929). *Die empfindungszeit: ein beitrag zur lehre von der zeit-, raum-und bewegungsempfindung*. G. Fischer.

García-Pérez, M. A., & Peli, E. (2001). Intrasaccadic perception. *Journal of Neuroscience*, *21*(18), 7313–7322.

García-Pérez, M. A., & Peli, E. (2011). Visual contrast processing is largely unaltered during saccades. *Frontiers in Psychology*, *2*, –. doi: 10.3389/fpsyg.2011.00247

Gauthier, G., Nommay, D., & Vercher, J. (1990, December). Ocular muscle proprioception and visual localization of targets in man. *Brain*, *113*(6), 1857–1871.

Geisler, W. S. (1999). Motion streaks provide a spatial code for motion direction. *Nature*, *400*(6739), 65-69.

Geisler, W. S., Albrecht, D. G., Crane, A. M., & Stern, L. (2001). Motion direction signals in the primary visual cortex of cat and monkey. *Visual neuroscience*, *18*(4), 501–516.

Gibson, J. J. (1966). *The senses considered as perceptual systems* (L. Carmichael, Ed.). George Allen & Unwin Ltd, London.

Gibson, J. J., & Radner, M. (1937). Adaptation, after-effect and contrast in the perception of tilted lines. i. quantitative studies. *Journal of experimental psychology*, *20*(5), 453.

Glass, L. (1969). Moire effect from random dots. *Nature*, *223*(5206), 578–580.

Glass, L., & Smith, M. A. (2011). Glass patterns. *Scholarpedia*, *6*(8), 9594. (revision #137324) doi: 10.4249/scholarpedia.9594

Gross, E. G., Vaughan, H. G., & Valenstein, E. (1967). Inhibition of visual evoked responses to patterned stimuli during voluntary eye movements. *Electroencephalography and clinical Neurophysiology*, *22*(3), 204–209.

Growney, R. (1978, January). Metacontrast as a function of the spatial frequency composition of the target and mask. *Vision Research*, *18*(9), 1117–1123.

Grüsser, O.-J., Krizic, A., & Weiss, L.-R. (1987). Afterimage movement during saccades in the dark. *Vision Research*, *27*(2), 215–226.

Guthrie, B. L., Porter, J. D., & Sparks, D. L. (1983). Corollary discharge provides accurate eye position information to the oculomotor system. *Science*, *221*(4616), 1193–1195.

Hallett, P. E., & Lightstone, A. D. (1976a). Saccadic eye movements to flashed targets. *Vision research*, *16*(1), 107–114.

Hallett, P. E., & Lightstone, A. D. (1976b). Saccadic eye movements towards stimuli triggered by prior saccades. *Vision research*, *16*(1), 99–106.

Han, P., Saunders, D. R., Woods, R. L., & Luo, G. (2013). Trajectory prediction of saccadic eye movements using a compressed exponential model. *Journal of Vision*, *13(8)*(27).

Helmholtz, H. v. (1866). *Handbuch der Physiologischen Optik*. Leipzig: Voss.

Henderson, J. M., & Hollingworth, A. (2003a). Eye movements and visual memory: Detecting changes to saccade targets in scenes. *Perception & psychophysics*, *65*(1), 58–71.

Henderson, J. M., & Hollingworth, A. (2003b). Global transsaccadic change blindness during scene perception. *Psychological science*, *14*(5), 493–497.

Hershberger, W. A., & Jordan, J. S. (1998, January). The phantom array: A perisaccadic illusion of visual direction. *The Psychological Record*, *48*(1), 21–32.

Hess, R. F., & Field, D. (1993). Is the increased spatial uncertainty in the normal periphery due to spatial undersampling or uncalibrated disarray? *Vision Research*, *33*(18), 2663–2670.

Higgins, E., & Rayner, K. (2015). Transsaccadic processing: stability, integration, and the potential role of remapping. *Attention, Perception, & Psychophysics*, *77*(1), 3–27.

Hildreth, E. C. (1984). The computation of the velocity field. *Proceedings of the Royal society of London. Series B. Biological sciences*, *221*(1223), 189–220.

Hollingworth, A., & Franconeri, S. L. (2009). Object correspondence across brief occlusion is established on the basis of both spatiotemporal and surface feature cues. *Cognition*, *113*(2), 150–166.

Hollingworth, A., Richard, A. M., & Luck, S. J. (2008, February). Understanding the function of visual short-term memory: transsaccadic memory, object correspondence, and gaze correction. *Journal of experimental psychology. General*, *137*(1), 163–181.

Honda, H. (1991). The time courses of visual mislocalization and of extraretinal eye position signals at the time of vertical saccades. *Vision research*, *31*(11), 1915–1921.

Honda, H. (2006). Achievement of transsaccadic visual stability using presaccadic and postsaccadic visual information. *Vision Research*, *46*(20), 3483–3493.

Hubel, D. H., & Wiesel, T. N. (1968). Receptive fields and functional architecture of monkey striate cortex. *The Journal of physiology*, *195*(1), 215–243.

Ibbotson, M. R., & Cloherty, S. L. (2009, June). Visual perception: Saccadic omission - suppression or temporal masking? *Current Biology*, *19*(12), 493–496.

Ibbotson, M. R., Crowder, N. A., Cloherty, S. L., Price, N. S. C., & Mustari, M. J. (2008). Saccadic modulation of neural responses: Possible roles in saccadic suppression, enhancement, and time compression. *The Journal of Neuroscience*, *28*(43), 10952–10960. doi: 10.1523/JNEUROSCI.3950-08.2008

Idrees, S., Baumann, M. P., Franke, F., Münch, T. A., & Hafed, Z. M. (2020). Perceptual saccadic suppression starts in the retina. *Nature Communications*, *11*(1), 1–19.

Intoy, J., & Rucci, M. (2020). Finely tuned eye movements enhance visual acuity. *Nature communications*, *11*(1), 1–11.

Kahneman, D. (1968). Method, findings, and theory in studies of visual masking. *Psychological Bulletin*, *70*(6p1), 404.

Kahneman, D., Treisman, A., & Gibbs, B. (1992). The reviewing of object files: Object-specific integration of information. *Cognitive Psychology*, *265*, 175-219.

Kelly, D. H. (1979). Motion and vision. ii. stabilized spatio-temporal threshold surface. *J. Opt. Soc. Am.*, *69*(10), 1340–1349.

Kennard, D. W., Hartmann, R. W., Kraft, D. P., & Glaser, G. H. (1971). Brief conceptual (nonreal) events during eye movement. *Biological psychiatry*, *3*(3), 205.

Kleitman, N., & Blier, Z. A. (1928). Color and form discrimination in the periphery of the retina. *American Journal of Physiology-Legacy Content*, *85*(2), 178–190.

Knöll, J., Binda, P., Morrone, M. C., & Bremmer, F. (2011). Spatiotemporal profile of peri-saccadic contrast sensitivity. *Journal of vision*, *11*(14), 15.

Kok, E. M., Aizenman, A. M., Võ, M. L.-H., & Wolfe, J. M. (2017). Even if i showed you where you looked, remembering where you just looked is hard. *Journal of Vision*, *17*(12), 2–2.

Kosovicheva, A. A., Wolfe, B. A., & Whitney, D. (2014). Visual motion shifts saccade targets. *Attention, Perception, & Psychophysics*, *76*(6), 1778–1788.

Kowler, E., Anderson, E., Dosher, B., & Blaser, E. (1995). The role of attention in the programming of saccades. *Vision research*, *35*(13), 1897–1916.

Krekelberg, B., Dannenberg, S., Hoffmann, K.-P., Bremmer, F., & Ross, J. (2003). Neural correlates of implied motion. *Nature*, *424*(6949), 674–677.

Krekelberg, B., Vatakis, A., & Kourtzi, Z. (2005). Implied motion from form in the human visual cortex. *Journal of neurophysiology*, *94*(6), 4373–4386.

Lamme, V. A. F. (2003). Why visual attention and awareness are different. *Trends in cognitive sciences*, *7*(1), 12–18.

Latour, P. L. (1962). Visual threshold during eye movements. *Vision Research*, *2*(3), 261–262.

Laubrock, J., Cajar, A., & Engbert, R. (2013). Control of fixation duration during scene viewing by interaction of foveal and peripheral processing. *Journal of Vision*, *13*(12), 11–11.

Lewis, R., Zee, D., Hayman, M., & Tamargo, R. (2001). Oculomotor function in the rhesus monkey after deafferentation of the extraocular muscles. *Experimental Brain Research*, *141*(3), 349–358.

Li, H., Barbot, A., & Carrasco, M. (2016). Saccade preparation reshapes sensory tuning. *Current Biology*, *26*(12), 1564-1570.

Lichtenstein, M., & White, C. T. (1961). Relative visual latency as a function of retinal locus. *JOSA*, *51*(9), 1033–1034.

Lisberger, S. G., Morris, E. J., & Tychsen, L. (1987). Visual motion processing and sensory-motor integration for smooth pursuit eye movements. *Annual review of neuroscience*.

MacKay, D. M. (1970). Elevation of visual threshold by displacement of retinal image. *Nature*, *225*(5227), 90–92.

MacKay, D. M. (1973). Visual stability and voluntary eye movements. In *Central processing of visual information a: integrative functions and comparative data* (pp. 307–331). Springer.

Mansfield, R. J. W., & Daugman, J. G. (1978). Retinal mechanisms of visual latency. *Vision Research*, *18*(9), 1247–1260.

Mante, V., Frazor, R. A., Bonin, V., Geisler, W. S., & Carandini, M. (2005, December). Independence of luminance and contrast in natural scenes and in the early visual system. *Nature Neuroscience*, *8*(12), 1690–1697.

Martinez-Conde, S., Macknik, S. L., & Hubel, D. H. (2004, March). The role of fixational eye movements in visual perception. *Nature Reviews Neuroscience*, *5*(3), 229–240.

Martinez-Conde, S., Macknik, S. L., Troncoso, X. G., & Hubel, D. H. (2009). Microsaccades: a neurophysiological analysis. *Trends in neurosciences*, *32*(9), 463–475.

Mateeff, S. (1978). Saccadic eye movements and localization of visual stimuli. *Perception & Psychophysics*, *24*(3), 215–224.

Mathôt, S., Melmi, J., & Castet, E. (2015). Intrasaccadic perception triggers pupillary constriction. *PeerJ*, *3*, e1150.

Matin, E. (1974). Saccadic suppression: a review and an analysis. *Psychological bulletin*, *81*(12), 899.

Matin, E., Clymer, A., & Matin, L. (1972). Metacontrast and saccadic suppression. *Science*, *178*(4057), 179–182.

McConkie, G. W., & Currie, C. B. (1996). Visual stability across saccades while viewing complex pictures. *Journal of Experimental Psychology: Human Perception and Performance*, *22*(3), 563.

McLaughlin, S. (1967). Parametric adjustment in saccadic eye movements. *Perception & Psychophysics*, *2*, 359–362.

Melcher, D., & Colby, C. L. (2008). Trans-saccadic perception. *Trends in cognitive sciences*, *12*(12), 466–473.

Michel, M., & Geisler, W. S. (2011). Intrinsic position uncertainty explains detection and localization performance in peripheral vision. *Journal of Vision*, *11*(1), 18–18.

Mitrani, L., & Yakimoff, N. (1970). Smearing of the retinal image during voluntary saccadic eye

movements. *Vision Research*, *10*(5), 405–409.

Mitrani, L., & Yakimoff, N. (1971). Is saccadic suppression really saccadic? *Vision Research*, *11*(10), 1157–1161.

Mitroff, S. R., & Alvarez, G. A. (2007). Space and time, not surface features, guide object persistence. *Psychonomic Bulletin & Review*, *14*(6), 1199–1204.

Mittelstaedt, H. (1990). Basic solutions to the problem of head-centric visual localization. In R. Warren & A. H. Wertheim (Eds.), *Perception and control of self-motion* (pp. 267–287). Erlbaum Hillsdale, NJ.

Morris, A. P., & Krekelberg, B. (2019). A stable visual world in primate primary visual cortex. *Current Biology*, *29*(9), 1471–1480.

Morrone, M. C., Ross, J., & Burr, D. (1997). Apparent position of visual targets during real and simulated saccadic eye movements. *J. Neurosci.*, *17*(20), 7941.

Nagano, T. (1980). Temporal sensitivity of the human visual system to sinusoidal gratings. *JOSA*, *70*(6), 711–716.

Najemnik, J., & Geisler, W. S. (2008). Eye movement statistics in humans are consistent with an optimal search strategy. *Journal of Vision*, *8*(3), 4. doi: 10.1167/8.3.4

Odom, J. V., Bach, M., Brigell, M., Holder, G. E., McCulloch, D. L., Tormene, A. P., & Vaegan. (2010, February). ISCEV standard for clinical visual evoked potentials (2009 update). *Documenta Ophthalmologica*, *120*(1), 111–119.

O'Regan, J. K., & Noë, A. (2001). A sensorimotor account of vision and visual consciousness. *Behavioral and brain sciences*, *24*(5), 939.

Ostendorf, F., Liebermann, D., & Ploner, C. J. (2010). Human thalamus contributes to perceptual stability across eye movements. *Proceedings of the National Academy of Sciences*, *107*(3), 1229–1234.

Otero-Millan, J., Macknik, S. L., Langston, R. E., & Martinez-Conde, S. (2013). An oculomotor continuum from exploration to fixation. *Proceedings of the National Academy of Sciences*, *110*(15), 6175–6180. doi: 10.1073/pnas.1222715110

Panouillères, M. T. N., Gaveau, V., Debatisse, J., Jacquin, P., LeBlond, M., & Pélisson, D. (2016). Oculomotor adaptation elicited by intra-saccadic visual stimulation: Time-course of efficient visual target perturbation. *Frontiers in human neuroscience*, *10*, 91.

Pola, J. (2004). Models of the mechanism underlying perceived location of a perisaccadic flash. *Vision research*, *44*(24), 2799–2813.

Pola, J. (2011). An explanation of perisaccadic compression of visual space. *Vision research*, *51*(4), 424–434.

Poth, C. H., Foerster, R. M., Behler, C., Schwanecke, U., Schneider, W. X., & Botsch, M. (2018). Ultrahigh temporal resolution of visual presentation using gaming monitors and G-sync. *Behavior research methods*, *50*(1), 26–38.

Prime, S. L., Vesia, M., & Crawford, J. D. (2011). Cortical mechanisms for trans-saccadic memory and integration of multiple object features. *Philosophical Transactions of the Royal Society of London B: Biological Sciences*, *366*(1564), 540–553.

Purves, D., Augustine, G. J., Fitzpatrick, D., Hall, W. C., LaMantia, A.-S., McNamara, J. O., & White, L. E. (2011). *Neuroscience. fifth edition*. MA: Sinauer Associates.

Reich, D. S., Mechler, F., & Victor, J. D. (2001). Temporal coding of contrast in primary visual cortex: when, what, and why. *Journal of neurophysiology*, *85*(3), 1039–1050.

Reichardt, W. (1987). Evaluation of optical motion information by movement detectors. *Journal of Comparative Physiology A*, *161*(4), 533–547.

Richard, A., Luck, S., & Hollingworth, A. (2008). Establishing object correspondence across eye movements: Flexible use of spatiotemporal and surface feature information. *Cognition*, *109*(1), 66–88.

Richards, W. (1968). Visual suppression during passive eye movement. *J. Opt. Soc. Am.*, *58*(8), 1159–1160.

Richards, W. (1969). Saccadic suppression. *Journal of the Optical Society of America*, *59*(5), 617–623.

Riggs, L. A., & Manning, K. A. (1982, July). Saccadic suppression under conditions of whiteout. *Invest. Ophthalmol. Vis. Sci.*, *23*(1), 138–143.

Riggs, L. A., Merton, P. A., & Morton, H. B. (1974). Suppression of visual phosphenes during saccadic eye movements. *Vision research*, *14*(10), 997–1011.

Riggs, L. A., & Ratliff, F. (1952). The effects of counteracting the normal movements of the eye. *Journal of the Optical Society of America*, *42*(11), 872–873.

Roberts, J. E., & Wilkins, A. J. (2013). Flicker can be perceived during saccades at frequencies in excess of 1 khz. *Lighting Research & Technology*, *45*(1), 124–132.

Robinson, D. A. (1981). Control of eye movements. In *Handbook of physiology, section I: The nervous system, 2.* American Physiological Society: Bethesda, MD.

Rock, I. (1981). Anorthoscopic perception. *Scientific American*, *244*(3), 145–153.

Rock, I., Halper, F., DiVita, J., & Wheeler, D. (1987). Eye movement as a cue to figure motion in anorthoscopic perception. *Journal of Experimental Psychology: Human Perception and Performance*, *13*(3), 344.

Rolfs, M. (2009). Microsaccades: small steps on a long way. *Vision research*, *49*(20), 2415–2441.

Rolfs, M. (2015). Attention in active vision: A perspective on perceptual continuity across saccades. *Perception*, *44*, 900–919.

Rolfs, M., Jonikaitis, D., Deubel, H., & Cavanagh, P. (2011). Predictive remapping of attention across eye movements. *Nature neuroscience*, *14*(2), 252-258.

Rolfs, M., Ohl, S., Schweitzer, R., Castet, E., & Watson, T. (2017). Object motion thresholds are amplitude-contingent and tuned to specifically eliminate retinal motion produced by saccades [abstract]. *Journal of Vision*, *17*(10), 1274–1274. (Talk at VSS 2017)

Ross, J., Badcock, D. R., & Hayes, A. (2000). Coherent global motion in the absence of coherent velocity signals. *Current Biology*, *10*(11), 679–682.

Ross, J., Morrone, M., Goldberg, M., & Burr, D. (2001a). Changes in visual perception at the time of saccades. *Trends in neurosciences*, *24*(2), 113–121.

Ross, J., Morrone, M., Goldberg, M. E., & Burr, D. C. (2001b). Response: "Saccadic suppression" - no need for an active extra-retinal mechanism. *Trends in Neurosciences*, *24*(6), 317–318. doi: 10.1016/S0166-2236(00)01827-0

Ross, J., Morrone, M. C., & Burr, D. C. (1997). Compression of visual space before saccades. *Nature*, *386*(6625), 598–601.

Rucci, M., Ahissar, E., & Burr, D. (2018). Temporal coding of visual space. *Trends in cognitive sciences*, *22*(10), 883–895.

Schlag, J., & Schlag-Rey, M. (1995). Illusory localization of stimuli flashed in the dark before saccades. *Vision research*, *35*(16), 2347–2357.

Schlag, J., & Schlag-Rey, M. (2002). Through the eye, slowly; delays and localization errors in the visual system. *Nature Reviews Neuroscience*, *3*(3), 191–191.

Schweitzer, R., & Rolfs, M. (2020). An adaptive algorithm for fast and reliable online saccade detection. *Behavior research methods*, *52*(3), 1122-1139. doi: 10.3758/s13428-019-01304-3

Schweitzer, R., Watson, T., Watson, J., & Rolfs, M. (2019). The joy of retinal painting: A build-it-yourself device for intrasaccadic presentations. *Perception*, *48*(10), 1020–1025. doi: 10.1177/0301006619867868

Seideman, J. A. (2020). A dynamic, imperturbable link between midbrain activity and saccade velocity. *Journal of Neurophysiology*, *123*(2), 451–453.

Simons, D. J., & Levin, D. T. (1997). Change blindness. *Trends in cognitive sciences*, *1*(7), 261–267.

Smalianchuk, I., Jagadisan, U. K., & Gandhi, N. J. (2018). Instantaneous midbrain control of saccade velocity. *Journal of Neuroscience*, *38*(47), 10156–10167.

Sommer, M. A., & Wurtz, R. H. (2008). Brain circuits for the internal monitoring of movements. *Annu. Rev. Neurosci.*, *31*, 317–338.

Sperry, R. W. (1950). Neural basis of the spontaneous optokinetic response produced by visual inversion. *Journal of comparative and physiological psychology*, *43*(6), 482.

SR-Research. (2013). *Eyelink 1000 plus user manual, version 1.0.12.* SR Research Ltd Mississauga, Ontario.

Stevens, J. K., Emerson, R. C., Gerstein, G. L., Kallos, T., Neufeld, G. R., Nichols, C. W., & Rosenquist, A. C. (1976). Paralysis of the awake human: visual perceptions. *Vision research*, *16*(1), 93–98.

Stromeyer, C. F., & Julesz, B. (1972). Spatial-frequency masking in vision: Critical bands and spread of masking. *JOSA*, *62*(10), 1221–1232.

Sylvester, R., Haynes, J., & Rees, G. (2005). Saccades differentially modulate human lgn and v1 responses in the presence and absence of visual stimulation. *Current Biology*, *15*(1), 37–41.

Tadmor, Y., & Tolhurst, D. J. (2000, October). Calculating the contrasts that retinal ganglion cells and lgn neurones encounter in natural scenes. *Vision Research*, *40*(22), 3145–3157.

Teichert, T., Klingenhoefer, S., Wachtler, T., & Bremmer, F. (2010). Perisaccadic mislocalization as optimal percept. *Journal of vision*, *10*(8), 19.

Thiele, A., Henning, P., Kubischik, M., & Hoffmann, K.-P. (2002). Neural mechanisms of saccadic suppression. *Science*, *295*(5564), 2460–2462.

Thilo, K. V., Santoro, L., Walsh, V., & Blakemore, C. (2004). The site of saccadic suppression. *Nature neuroscience*, *7*(1), 13–14.

Võ, M. L.-H., Aizenman, A. M., & Wolfe, J. M. (2016). You think you know where you looked? you better look again. *Journal of Experimental Psychology: Human Perception and Performance*, *42*(10), 1477.

Volkmann, F. C. (1962, May). Vision during voluntary saccadic eye movements. *J. Opt. Soc. Am.*, *52*(5), 571–578.

Volkmann, F. C. (1986). Human visual suppression. *Vision research*, *26*(9), 1401–1416.

Volkmann, F. C., Riggs, L., White, K., & Moore, R. (1978). Contrast sensitivity during saccadic eye movements. *Vision research*, *18*(9), 1193–1199.

Von Holst, E., & Mittelstaedt, H. (1950). Das Reafferenzprinzip [the principle of reafference]. *Naturwissenschaften*, *37*(20), 464–476.

Walker, R., Deubel, H., Schneider, W. X., & Findlay, J. M. (1997). Effect of remote distractors on saccade programming: evidence for an extended fixation zone. *Journal of neurophysiology*, *78*(2), 1108–1119.

Wang, X., Zhang, M., Cohen, I. S., & Goldberg, M. E. (2007). The proprioceptive representation of eye position in monkey primary somatosensory cortex. *Nature neuroscience*, *10*(5), 640–646.

Watson, T., & Krekelberg, B. (2009). The relationship between saccadic suppression and perceptual stability. *Current Biology*, *19*(12), 1040–1043.

Watson, T., & Krekelberg, B. (2011). An equivalent noise investigation of saccadic suppression. *Journal of Neuroscience*, *31*(17), 6535–6541.

Westheimer, G. (2008). Directional sensitivity of the retina: 75 years of Stiles-Crawford effect. *Proceedings of the Royal Society B: Biological Sciences*, *275*(1653), 2777–2786.

Wexler, M., & Collins, T. (2014). Orthogonal steps relieve saccadic suppression. *Journal of Vision*, *14*(2), 13.

Whitney, D. (2002). The influence of visual motion on perceived position. *Trends in cognitive sciences*, *6*(5), 211–216.

Williams, J. M., & Lit, A. (1983). Luminance-dependent visual latency for the hess effect, the pulfrich effect, and simple reaction time. *Vision research*, *23*(2), 171–179.

Wurtz, R. H. (2008). Neuronal mechanisms of visual stability. *Vision research*, *48*(20), 2070–2089.

Wurtz, R. H. (2018). Corollary discharge contributions to perceptual continuity across saccades. *Annu. Rev. Vis. Sci.*, *4*(1), 215–237. doi: 10.1146/annurev-vision-102016-061207

Zhang, H., Morvan, C., & Maloney, L. T. (2010). Gambling in the visual periphery: a conjoint-measurement analysis of human ability to judge visual uncertainty. *PLoS Comput Biol*, *6*(12), e1001023.

Zimmermann, E. (2020). Saccade suppression depends on context. *Elife*, *9*, e49700.

5

Appendix

5.1 Original articles

5.1.1 Study I

Publication:

Schweitzer, R., Watson, T., Watson, J., & Rolfs, M. (2019). The joy of retinal painting: A build-it-yourself device for intrasaccadic presentations. *Perception*, 48(10), 1020–1025. doi: 10.1177/0301006619867868

Conference presentations:

Schweitzer, R., Watson, T., Watson, J., & Rolfs, M. (May, 2019). The joy of intra-saccadic retinal painting. Demo night presentation at the *19th Annual Meeting of the Vision Sciences Society*, St. Petersburg (FL), USA.

Schweitzer, R., Watson, T., & Rolfs, M. (August, 2017). Intra-saccadic persistence of vision. Demo night presentation at the *40th European Conference on Visual Perception*, Berlin, Germany.

Featured code:

Demo code: `https://github.com/richardschweitzer/IntrasaccadicRetinalPainting`

Re-use permissions:

"You may use the Final Published PDF [...] in your dissertation or thesis, including where the dissertation or thesis will be posted in any electronic Institutional Repository or database"

Source: `https://uk.sagepub.com/en-gb/eur/journal-author-archiving-policies-and-re-use` (accessed on July 20 2020)

Short and Sweet

PERCEPTION

Perception
2019, Vol. 48(10) 1020–1025

DOI: 10.1177/0301006619867868
journals.sagepub.com/home/pec
SAGE

The Joy of Retinal Painting: A Build-It-Yourself Device for Intrasaccadic Presentations

Richard Schweitzer
Department of Psychology, Humboldt-Universität zu Berlin, Berlin, Germany; Bernstein Center for Computational Neuroscience Berlin, Berlin, Germany; Berlin School of Mind and Brain, Humboldt-Universität zu Berlin, Berlin, Germany

Tamara Watson
School of Social Sciences and Psychology, Western Sydney University, Sydney, Australia

John Watson
Independent Researcher, North Gosford, New South Wales, Australia

Martin Rolfs
Department of Psychology, Humboldt-Universität zu Berlin, Berlin, Germany; Bernstein Center for Computational Neuroscience Berlin, Berlin, Germany; Berlin School of Mind and Brain, Humboldt-Universität zu Berlin, Berlin, Germany

Abstract

As the eyes move, they incessantly impose motion blur on the retinal image, yet our perception of the world remains undisturbed. In fact, it is often assumed that intrasaccadic visual signals are largely eliminated from processing by a dedicated suppression mechanism. Here, we describe an easy-to-build presentation device that produces a stimulus that is highly salient and well resolvable during saccades: Using LED strips with high temporal resolution, any type of text and image stimulus can be presented in an anorthoscopic fashion—as if seen through and travelling behind a narrow slit—at very short durations. Whereas these stimuli appear as a brief flash during fixation, saccades spread them across the retina, producing spatially extended and well-resolved retinal images. In fact, retinally painted images induced by saccades across a series of anorthoscopic image presentations were correctly identified by observers in 90% of all cases. So why should we suppress intrasaccadic perception if it enables us to experience the joy of retinal painting?

Corresponding author:
Richard Schweitzer, Humboldt-Universität zu Berlin, Unter den Linden 6, Berlin 10099, Germany.
Email: richard.schweitzer@hu-berlin.de

Keywords
eye movements, anorthoscopic presentation, intrasaccadic perception, visual persistence, retinal painting

Date Received: 24 April 2019; accepted: 15 July 2019

A large body of literature in the field of active vision suggests that vision is suppressed around and during rapid eye movements, the so-called *saccades* (e.g., Castet, 2009; Volkmann, 1976). Indeed, unless saccades are made in a dark room with only a few small light sources present, human observers rarely perceive the massive amount of motion blur (also known as intrasaccadic smear) that saccades should induce as they sweep the whole visual scene across their retinae at dazzling velocities. The fact that the retinal consequences of our own saccades are omitted from visual perception is often thought to be realized by an active, extraretinal suppression mechanism—commonly known as saccadic suppression—that eliminates certain types of intrasaccadic visual input from further processing (Burr, Morrone, & Ross, 1994; Ross, Morrone, Goldberg, & Burr, 2001; Thiele, Henning, Kubischik, & Hoffmann, 2002). As a consequence, approximately one eighth of the visual information received while actively exploring the visual world should be discarded. This amounts to 2 hours on a day with a decent amount of sleep. Would it not be great to be able to utilize this significant amount of time? Here, we present a simple device that produces a salient, highly resolvable intrasaccadic stimulus by applying the principle of retinal painting. But before we get to this point, we must introduce two important facts.

First, visual processing is not shut down during saccades. For example, in a unique setup, Campbell and Wurtz (1978) showed that when a room was illuminated just during a saccade, so that the brief intrasaccadic scene was not masked by pre- and postsaccadic retinal images (Castet, Jeanjean, & Masson, 2002; Duyck, Collins, & Wexler, 2016; Matin, Clymer, & Matin, 1972), observers readily perceived a smeared and greyed-out scene. When they further reduced the duration of illumination to 5 ms or less, observers even reported a relatively clear image of the room (Campbell & Wurtz, 1978). The authors concluded that the effect of saccadic suppression—that is, the elevation of perisaccadic contrast thresholds by around 0.5 log units (Volkmann, 1986)—does not prevent intrasaccadic perception.

Second, to match the high velocities and brief durations of saccades, one would need costly stimulus presentation devices capable of high temporal resolution, as well as gaze-contingent control (e.g., Balsdon, Schweitzer, Watson, & Rolfs, 2018). Here, we utilize a different method, almost tailored for intrasaccadic purposes: *anorthoscopic presentation*. Anorthoscopic presentation is based on displaying small parts of visual objects in a sequential manner, one section at a time, as if seen through a narrow slit. The finding that observers were capable of anorthoscopic perception, that is, resolving the form and identity of figures from this kind of piecewise presentation despite the fact that the stimulus only covered a tiny part of the retina, has already fascinated researchers in the 19th century. To explain the phenomenon, Helmholtz (1867) proposed a retinal painting hypothesis that is quite relevant for our application: He suggested that (unconscious) eye movements across the slit might spread those sequential stimulations across the retina, thereby allowing visual persistence to create a spatially distinct pattern (Rock, 1981; Rock, Halper, DiVita, & Wheeler, 1987). Although this explanation does not hold for the more general phenomenon of anorthoscopic perception (Anstis & Atkinson, 1967; Fendrich, Rieger, & Heinze, 2005;

Rieger, Grüschow, Heinze, & Fendrich, 2007; Rock & Halper, 1969), it certainly is valid for the intrasaccadic case, where presentations are extremely brief and high eye velocities induce a considerable amount of spread across the retina.

Although anorthoscopes were traditionally built using two axially mounted disks—one showing the stimulus and the other moving the slit—we applied four Adafruit DotStar LED strips (Adafruit Industries, New York City, NY, USA) for presentation (see Figure 1 for schematic). Each had a length of 1 m and featured 144 5×5 mm RGB pixels that were controlled by a Raspberry Pi 3B (Raspberry Pi Foundation, Cambridge, UK) using the supplied DotStar Pi Painter Libraries (Burgess, 2015). In this LED-based anorthoscopic presentation, any kind of picture stimulus can be presented: After being rescaled to a vertical resolution corresponding to the number of LED pixels, the image is presented column-wise from left to right. During visual fixation, this kind of presentation will look like a brief flash (Figure 2, left). If the same presentation happens to occur during a saccade, the presented columns will fall on different parts of the retina, creating a spatially distributed pattern, easily perceivable by the observer (Figure 2, right).

To put the presentation device to the test, we presented nine stimulus sets, each consisting of four different images or words (e.g., *enjoy*, *your*, *beer*, *mate*, each with a constant presentation duration of 25 ms, amounting to approximately 35 frames in our setup), to 10 observers. For each set, they had 1 minute of time to name the word on each strip. No further instructions were given, except the information that moving the eyes would be necessary. To our surprise, observers did extremely well: On average, 89% ($SD = 10\%$) of all words and 95% ($SD = 6\%$) of all pictures were correctly identified well below the time limit.

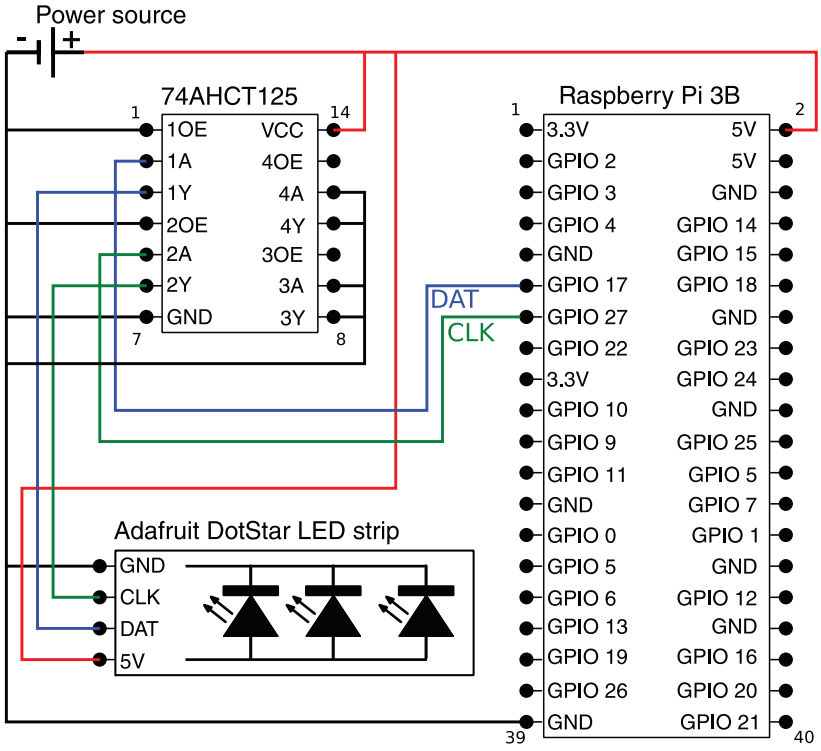

Figure 1. Minimal schematic for building the anorthoscopic presentation device. An Adafruit DotStar LED strip is controlled by a Raspberry Pi 3B via a 74AHCT125 level shifter. In addition, it would be advisable to use a 1000 μF capacitor to decouple the 5 V power supply.
Note: Please refer to the online version of the article to view the figures in colour.

Figure 2. Photographs of the anorthoscopic presentation using four Adafruit DotStar LED strips behind standard diffusors under static conditions (*left panel*) and when swiftly manually turning the camera to the right (*right panel*). Whereas brief vertical flashes are perceived during fixation, complex patterns, such as text become well visible during saccades. Photos were taken by Julius Krumbiegel, using a a Sony ILCE-7RM2 digital camera mounted on a revolvable tripod with a prolonged exposure time of 1/3 seconds to match the speed of the hand movement.
Note: Please refer to the online version of the article to view the figures in colour.

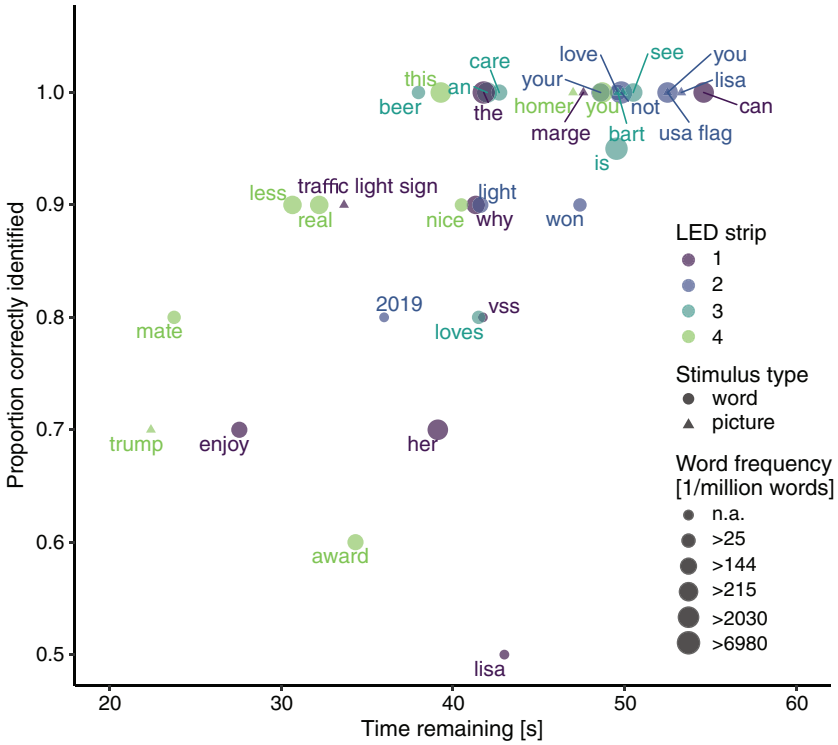

Figure 3. Mean proportion of correct stimulus identifications and corresponding time remaining (of each trial's 60-second deadline) across 10 observers. Seven trials involved word stimuli (circles), and in two trials, pictures were displayed (triangles). Word frequencies were based on the British National Corpus (Leech & Rayson, 2014).
Note: Please refer to the online version of the article to view the figures in colour.

It took participants a mean time of 29 seconds ($SD = 16$ seconds) to identify all four stimuli correctly. They identified pictures as well as short and frequent words with greater accuracy and speed (Figure 3). In incorrect trials, stimuli were rarely misidentified (<17% of incorrect trials, e.g., *night* instead of *light*, *now* instead of *won*), but could simply not be resolved. Participants' (spontaneous) strategies involved short, horizontal saccades at a high rate, often combined with rapid head movements. Notably, those observers strongly relying on combined head–eye movements did not exhibit any considerable increase in performance ($M_{\text{head+eye}} = 0.94$, $SD_{\text{head+eye}} = 0.07$; $M_{\text{eye}} = 0.91$, $SD_{\text{eye}} = 0.1$). Many also reported that stimuli suddenly clearly appeared as a result of an involuntary saccade, even while they were not actively attending to the LED strips.

This anorthoscopic presentation device demonstrates in visually striking manner that the inherent high velocities of human saccades can be utilized to efficiently paint text or images on the retina that are visible exclusively during saccades. The device is not only cost-effective (i.e., less than 200€ for a minimal setup with one LED strip) and easy to build (see schematics, Figure 1), but a list of components, as well as all code necessary to run the demo, including several test stimuli, can also be found online at https://github.com/richardschweitzer/IntrasaccadicRetinalPainting, empowering everybody to enjoy intrasaccadic retinal painting in the snugness of one's own living room.

Acknowledgements

The authors acknowledge the significant contribution of Phillip Burgess's Pi Painter libraries (https://github.com/adafruit/Adafruit_DotStar_Pi) and well-documented tutorial at https://learn.adafruit.com/dotstar-pi-painter. Finally, the authors thank Julius Krumbiegel for his excellent photos.

Author Contributions

T. W. initiated the project. J. W. designed and built the first prototype of the device and provided instructions. R. S. built the reported setup with four LED strips, implemented the presentation interface, and collected and analyzed reported data. R. S., M. R. and T. W. wrote and edited the manuscript.

Declaration of Conflicting Interests

The author(s) declared no potential conflicts of interest with respect to the research, authorship, and/or publication of this article.

Funding

The author(s) disclosed receipt of the following financial support for the research, authorship, and/or publication of this article: R. S. was supported by the Studienstiftung des deutschen Volkes and the Berlin School of Mind and Brain. M. R. was supported by the Deutsche Forschungsgemeinschaft (DFG, grants RO3579/2–1, RO3579/8–1 and RO3579/10–1). T. W. was supported by the Australian Research Council (ARC, grants DP150100516 and DP170101537).

ORCID iD

Richard Schweitzer https://orcid.org/0000-0002-1781-572X

References

Anstis, S. M., & Atkinson, J. (1967). Distortions in moving figures viewed through a stationary slit. *The American Journal of Psychology*, *80*, 572–585.

Balsdon, T., Schweitzer, R., Watson, T. L., & Rolfs, M. (2018). All is not lost: Post-saccadic contributions to the perceptual omission of intra-saccadic streaks. *Consciousness and Cognition*, *64*, 19–31.

Burgess, P. (2015). *DotStar pi painter*. Retrieved from https://learn.adafruit.com/dotstar-pi-painter

Burr, D. C., Morrone, M. C., & Ross, J. (1994). Selective suppression of the magnocellular visual pathway during saccadic eye movements. *Nature*, *371*, 511–513.

Campbell, F. W., & Wurtz, R. H. (1978). Saccadic omission: Why we do not see a grey-out during a saccadic eye movement. *Vision Research*, *18*, 1297–1303.

Castet, E. (2009). Perception of intra-saccadic motion. In *Dynamics of visual motion processing* (pp. 213–238). Boston, MA: Springer.

Castet, E., Jeanjean, S., & Masson, G. S. (2002). Motion perception of saccade-induced retinal translation. *Proceedings of the National Academy of Sciences*, *99*, 15159–15163.

Duyck, M., Collins, T., & Wexler, M. (2016). Masking the saccadic smear. *Journal of Vision*, *16*, 1.

Fendrich, R., Rieger, J. W., & Heinze, H.-J. (2005). The effect of retinal stabilization on anorthoscopic percepts under free-viewing conditions. *Vision Research*, *45*, 567–582.

Helmholtz, H. L. (1867). *Handbuch der physiologischen optik [Manual of physiological optics]*. Leipzig, Germany: L. Voss.

Leech, G., & Rayson, P. (2014). Word frequencies in written and spoken English: Based on the British national corpus. Abingdon, England: Routledge.

Matin, E., Clymer, A. B., & Matin, L. (1972). Metacontrast and saccadic suppression. *Science*, *178*, 179–182.

Rieger, J. W., Grüschow, M., Heinze, H.-J., & Fendrich, R. (2007). The appearance of figures seen through a narrow aperture under free viewing conditions: Effects of spontaneous eye motions. *Journal of Vision*, *7*, 10.

Rock, I. (1981). Anorthoscopic perception. *Scientific American*, *244*, 145–153.

Rock, I., & Halper, F. (1969). Form perception without a retinal image. *The American Journal of Psychology*, *82*, 425–440.

Rock, I., Halper, F., DiVita, J., & Wheeler, D. (1987). Eye movement as a cue to figure motion in anorthoscopic perception. *Journal of Experimental Psychology: Human Perception and Performance*, *13*, 344–352.

Ross, J., Morrone, M. C., Goldberg, M. E., & Burr, D. C. (2001). Changes in visual perception at the time of saccades. *Trends in Neurosciences*, *24*, 113–121.

Thiele, A., Henning, P., Kubischik, M., & Hoffmann, K. P. (2002). Neural mechanisms of saccadic suppression. *Science*, *295*, 2460–2462.

Volkmann, F. C. (1976). Saccadic suppression: A brief review. In R. A. Monty & J. W. Senders (Eds.), *Eye movements and psychological processes* (pp. 73–83). Hillsdale, NJ: Erlbaum.

Volkmann, F. C. (1986). Human visual suppression. *Vision Research*, *26*, 1401–1416.

5.1.2 Study II

Publication:

Schweitzer, R., & Rolfs, M. (2020). An adaptive algorithm for fast and reliable online saccade detection. *Behavior research methods*, *52*(3), 1122-1139. doi: 10.3758/s13428-019-01304-3

Pre-print:

Schweitzer, R., & Rolfs, M. (2019). An adaptive algorithm for fast and reliable online saccade detection. *bioRxiv*, 693309. doi: 10.1101/693309

Conference presentations:

Schweitzer, R., & Rolfs, M. (May, 2019). Rapid and robust online saccade detection. Poster at the *19th Annual Meeting of the Vision Sciences Society*, St. Petersburg (FL), USA.

Data, analyses, code for experiment:

`https://osf.io/3pck5/`

Featured code:

Detection algorithm: `https://github.com/richardschweitzer/OnlineSaccadeDetection`

Re-use permissions:

"Author(s) retain the following non-exclusive rights for the published version provided that, when reproducing the Article or extracts from it, the Author(s) acknowledge and reference first publication in the Journal: [...] c. to reproduce, or to allow a third party Assignee to reproduce the Article in whole or in part in any printed volume (book or thesis) written by the Author(s)."

Source: Springer Copyright Transfer Statement (received via Email on September 6 2019)

Behavior Research Methods
https://doi.org/10.3758/s13428-019-01304-3

An adaptive algorithm for fast and reliable online saccade detection

Richard Schweitzer [1,2,3] · Martin Rolfs [1,2]

Abstract
To investigate visual perception around the time of eye movements, vision scientists manipulate stimuli contingent upon the onset of a saccade. For these experimental paradigms, timing is especially crucial, because saccade offset imposes a deadline on the display change. Although efficient online saccade detection can greatly improve timing, most algorithms rely on spatial-boundary techniques or absolute-velocity thresholds, which both suffer from weaknesses: late detections and false alarms, respectively. We propose an adaptive, velocity-based algorithm for online saccade detection that surpasses both standard techniques in speed and accuracy and allows the user to freely define the detection criteria. Inspired by the Engbert–Kliegl algorithm for microsaccade detection, our algorithm computes two-dimensional velocity thresholds from variance in the preceding fixation samples, while compensating for noisy or missing data samples. An optional direction criterion limits detection to the instructed saccade direction, further increasing robustness. We validated the algorithm by simulating its performance on a large saccade dataset and found that high detection accuracy (false-alarm rates of < 1%) could be achieved with detection latencies of only 3 ms. High accuracy was maintained even under simulated high-noise conditions. To demonstrate that purely intrasaccadic presentations are technically feasible, we devised an experimental test in which a Gabor patch drifted at saccadic peak velocities. Whereas this stimulus was invisible when presented during fixation, observers reliably detected it during saccades. Photodiode measurements verified that—including all system delays—the stimuli were physically displayed on average 20 ms after saccade onset. Thus, the proposed algorithm provides a valuable tool for gaze-contingent paradigms.

Keywords Saccade detection · Eye movements · Intrasaccadic perception · Gaze-contingent presentation

In the field of active vision, most eyetracking experiments study visual perception around goal-directed rapid eye movements, so-called saccades. Specifically, when investigating trans-saccadic or intrasaccadic perception, an experimental paradigm has to be implemented in a way that a stimulus or the configuration of stimuli is manipulated online (i.e., in real time) and gaze-contingently, starting with the onset of a saccade (Higgins & Rayner, 2015; Hollingworth, Richard, & Luck, 2008; Melcher & Colby, 2008; Prime, Vesia, & Crawford, 2011; Wolf & Schütz, 2015). Because saccades are rapid and brief events, often with a skewed velocity profile (Figs. 1a and 1b), this is not always as trivial as it may sound. Every computational step between an eye movement and a change in the display adds undesired delays, and every shortcut (e.g., through rough approximations) may lead to false alarms—that is, the detection of a saccade when none has happened. Here we will discuss an algorithm that realizes early online saccade detection without sacrificing reliability, and is thus able to greatly reduce the overall delay between saccade onset and display change.

To elucidate the challenge that gaze-contingent paradigms pose with regard to timing, let us consider a typical trans-saccadic experimental scenario: Participants are instructed to make a saccade toward a colored patch at a 10-deg of visual angle (dva) eccentricity, resulting in saccades with average peak velocities of 300 dva per second (dva/s) and durations of 40 ms (Collewijn, Erkelens, & Steinman, 1988). When trying to manipulate the color of the patch during the saccade, so that upon landing an updated stimulus with a new color is displayed to the observer, we as experimenters have to consider at least four additive sources of latency in our experimental setups (Fig. 2) in order to make the presentation deadline of each saccade offset.

✉ Richard Schweitzer
richard.schweitzer@hu-berlin.de

[1] Department of Psychology, Humboldt-Universität zu Berlin, Berlin, Germany

[2] Bernstein Center for Computational Neuroscience Berlin, Berlin, Germany

[3] Berlin School of Mind and Brain, Humboldt-Universität zu Berlin, Berlin, Germany

Published online: 08 November 2019

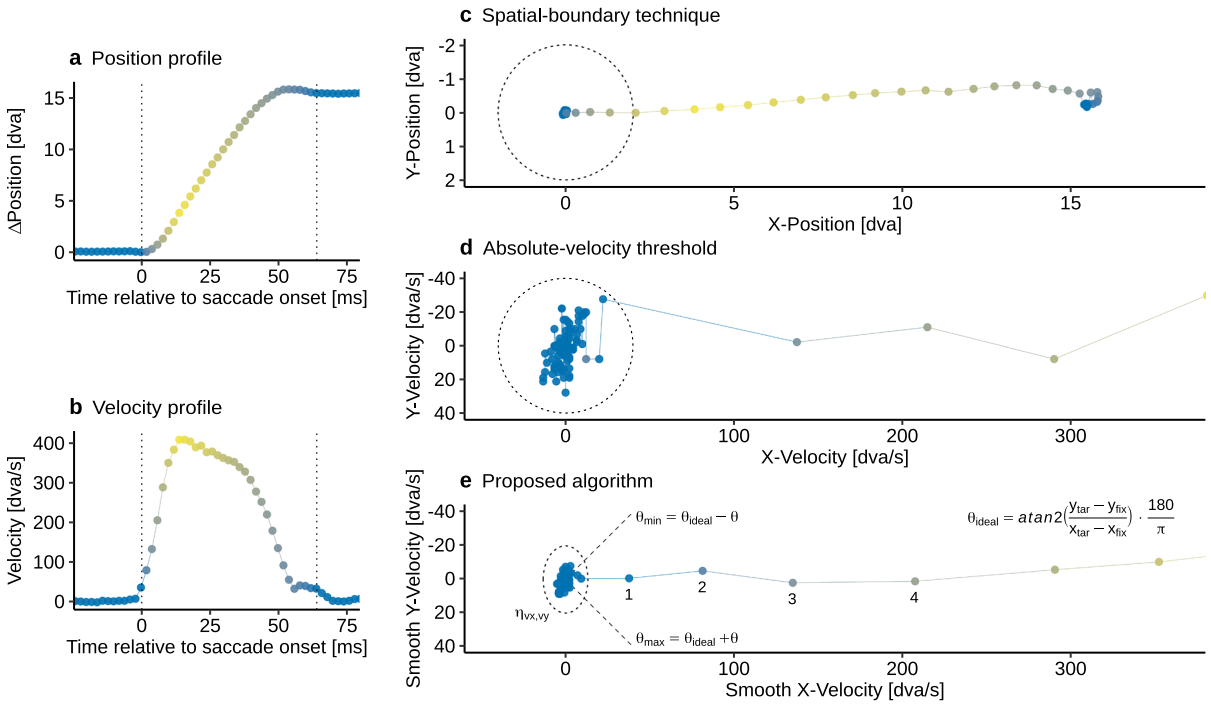

Fig. 1 Illustration of different saccade detection techniques, based on an exemplary saccade. (a–b) Plots of position and velocity profiles of a horizontal, rightward 15-dva saccade, sampled uniformly at 500 Hz. Color represents the sample-to-sample velocity (yellow = peak velocity). (c) Illustration of saccade detection using a spatial-boundary technique. Saccades are detected once gaze position reaches past the spatial boundary, defined by a 2-dva radius (dotted circle) around the instructed fixation position. (d) Illustration of an absolute-velocity threshold. Gaze position data are transformed into two-dimensional velocity space, and a saccade is detected once velocities exceed a predefined value—for example, 40 dva/s in this example. (e) Illustration of the proposed algorithm. Gaze position data are resampled to a uniform sampling rate, transformed into two-dimensional velocity space, which is smoothed by a five-point running-average filter. Median-based standard deviations are computed separately for the horizontal and vertical dimensions, forming an elliptic velocity threshold $\eta_{vx,vy}$. An optional direction criterion θ (here, 45°) can restrict detection to a range around the instructed saccade direction θ_{ideal} (e.g., computed via the fixation and saccade landing positions xy_{fix} and xy_{tar}), with θ_{max} and θ_{min} as the upper and lower boundaries. Moreover, the user may specify, in order to detect a saccade, how many samples are needed that satisfy both the velocity and direction criteria. In this example, we have numbered the first four samples for which this is the case.

First, the online access to gaze position data is delayed. This *end-to-end sample delay* includes not only the time taken for a physical event to be registered, processed, and made available online by the eyetracking system (e.g., capturing

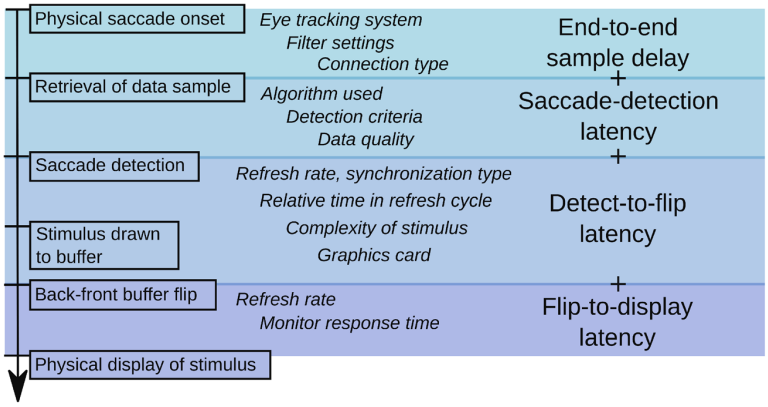

Fig. 2 Schematic illustrating four categories of latencies in a temporal sequence (top to bottom) occurring when display changes are locked to saccade onset. Factors influencing the magnitude of the delays are shown in italics.

an image of the eye, fitting the pupil and corneal reflection, and extrapolating gaze position), but also the time needed to retrieve the data via Ethernet, USB, or analog ports. Although the retrieval time is usually negligible (i.e., on the order of microseconds), the total end-to-end sample delay can be considerable. According to manufacturer manuals, it may range from 1.8 to 3 ms in the EyeLink 1000 (SR Research, 2010), from 1.7 to 1.95 ms in the Trackpixx3 (VPixx Technologies, 2017), from 3 to 14 ms in the EyeLink II (SR Research, 2005), and up to 33 ms in the Tobii TX Series (Tobii Technology AB, 2010).

Second, as we need a reliable, and thus often a more conservative, criterion to decide whether a saccade has actually been initiated, the onset of the saccade detected online usually lags behind the onset of the saccade detected offline. Henceforth, this delay will be referred to as the *saccade detection latency*. Techniques to detect saccades during experiments often involve an invisible spatial boundary (Fig. 1c) at some distance from the initial fixation point that the gaze position has to cross (Rayner, 1975). This widely used technique (e.g., Collins, Rolfs, Deubel, & Cavanagh, 2009; Kalogeropoulou & Rolfs, 2017; Szinte & Cavanagh, 2011) usually provides reliable but late saccade detection (~ 15 ms after the actual saccade onset at a sampling rate of 500 Hz for a boundary 2 dva from fixation; see Fig. 5a in the Results). An alternative to the boundary technique is based on velocity thresholds (Fig. 1d): The measured speed of the eye must exceed a certain value, such as 30 dva/s (Deubel, Schneider, & Bridgeman, 1996; Han, Saunders, Woods, & Luo, 2013; Panouillères et al., 2016), 40 dva/s (Castet, Jeanjean, & Masson, 2002), or even 100 dva/s (Arabadzhiyska, Tursun, Myszkowski, Seidel, & Didyk, 2017), so saccades can be detected much earlier, but they often suffer from increased false alarm rates.

Third, once we have detected a saccade in the data retrieved online, the stimulus has to be drawn to the graphics card's back-buffer and the flip with the front-buffer has to be synchronized with the display's vertical retrace (Kleiner, Brainard, & Pelli, 2007). This *detect-to-flip latency* is determined by the refresh rate of the monitor and depends on the time of detection within the refresh cycle. Novel technologies such as G-Sync are able to reduce this latency to the submillisecond range by allowing flips as soon as rendering is complete, without having to wait for the screen refresh (Poth et al., 2018).

Fourth, there is the *flip-to-display latency*—that is, the time from the execution of the flip until the physical stimulus presentation on the screen. Whereas the transfer of the entire video signal takes up to one frame duration, the display's reaction time can additionally increase the flip-to-display latency, as well as introduce temporal jitter.

Taking into account all sources of delay (e.g., a 5-ms end-to-end sample delay using an EyeLink II at 500 Hz with normal link filtering + 15-ms detection latency using a boundary technique + 5-ms mean detect-to-flip latency with a 120-Hz monitor + 8.3-ms flip-to-display latency), the physical change will occur in the last quarter of the 40-ms saccade. Because both gaze-contingent displays and saccade profiles can be subject to considerable variance, we thus increase the risk of achieving a postsaccadic instead of the intended intrasaccadic display change. Failure to acknowledge or control these latencies may thus lead to erroneous results and unwarranted conclusions.

Although most of the latencies mentioned above largely depend on the specific hardware used, we can optimize the saccade detection latency to achieve low-latency gaze-contingent presentations. Crucially, the choice of the saccade detection criterion determines both the timing and the reliability of the experimental paradigm: Whereas a conservative detection criterion (e.g., a spatial boundary) may provide reliable but late detection, a liberal detection criterion (e.g., a low absolute-velocity threshold) may lead to early detection at the cost of increased false alarm rates. This may become especially relevant when detecting saccades based on velocity using high sampling frequencies, as any error in gaze position divided by a shorter sampling interval will lead to amplified velocity estimates (Han, Saunders, Woods, & Luo, 2013). To achieve reliable online detection, velocity thresholds would therefore have to be manually adjusted to the precision and sampling frequency of the eyetracker, as well as to the situation- and participant-dependent noise levels (see also Engbert & Mergenthaler, 2006). To date, no algorithm provides both fast and early online saccade detection while at the same time remaining reliable in noisier conditions.

Here we present a velocity-based online saccade detection algorithm that adaptively estimates noise levels on the basis of preceding fixation data to provide robust results in the presence of random sample-to-sample noise, dropped samples, blinks, and fixational eye movements, while allowing its user to flexibly adjust the detection criterion to the specific experimental situation. We tested the performance of the algorithm and the impact of various parameter combinations and noise levels in a large-scale simulation with more than 34,000 saccades, and compared the algorithm to boundary techniques and absolute-velocity thresholds. We then present an objective and perceptual test for reliable, gaze-contingent, and strictly intrasaccadic presentations that underlines the algorithm's usefulness in real-time experimental scenarios.

The proposed algorithm

Online saccade detection relies on the continuous sampling of gaze position data (x, y) and the corresponding timestamps (t) throughout each trial of the experiment. Gaze position data collected during fixation is used to establish a threshold to

demarcate the transition from fixation to saccade. Following Engbert and Kliegl's widely used algorithm for microsaccade detection (Engbert & Kliegl, 2003; Engbert & Mergenthaler, 2006), the algorithm thus detects the onset of a saccade based on an elliptical, two-dimensional velocity threshold $\eta_{vx,vy}$ (dotted line, Fig. 1d), as defined by the product of the median-based standard deviation of horizontal and vertical gaze position dimensions (σ_{vx}, σ_{vy}) and a free scaling parameter λ to adjust the velocity criterion.

$$\eta_{vx,vy} = \lambda \cdot \sigma_{vx,vy}$$

In addition, the user may provide a parameter k specifying how many of the most recent of all velocity samples must exceed the defined threshold. That way, robustness against false alarms due to noise-related velocity peaks is increased. In case the user intends to limit detection of saccades to an instructed saccade direction (θ_{ideal}), which is often the case in controlled experimental paradigms, the algorithm allows for specification of an additional direction criterion θ that determines the direction range around the ideal saccade direction that individual velocity samples are allowed in (dashed lines, Fig. 1d). This direction criterion can be used to avoid false detections of the instructed saccade as a consequence of other eye movements events that may satisfy the velocity criterion, such as blinks or microsaccades.

To make the algorithm suitable for online applications, two important features were implemented. First, owing to the fact that during online experiments it is rarely possible to retrieve every single data sample, missing position samples are linearly interpolated, either to a sampling rate specified by the user or to a sampling rate computed on the basis of the number of samples retrieved in a given time. Second, two-point velocity samples are computed (to avoid edge velocities of zero) and then smoothed by a five-point running average to reduce the impact of high frequency noise (Engbert & Mergenthaler, 2006). To not overestimate the first and most recent velocity samples, the vector edges are padded with repetitions of the first and the most recent samples, respectively. Subsequently, based on smoothed velocity samples, the median velocities (in most cases equaling zero) and the median-based standard deviations (σ_{vx}, σ_{vy}) are computed as described by Engbert and colleagues (Engbert & Kliegl, 2003; Engbert & Mergenthaler, 2006; Engbert, Rothkegel, Backhaus, & Trukenbrod, 2016):

$$\sigma_{vx,vy} = \sqrt{\left\langle \left(v_{x,y} - \langle v_{x,y} \rangle\right)^2 \right\rangle}$$

The brackets $\langle . \rangle$ stand for the median estimator. To optimize processing speed, we use the quick select algorithm for median selection (Press, Teukolsky, Vetterling, & Flannery, 2007).

To determine whether a saccade is ongoing, only the most recently retrieved k samples (k has to be defined by the user beforehand) are tested whether eye velocity exceeds the specified threshold, which is computed on the basis of all preceding $n–k$ samples. An ongoing saccade is detected only if all k samples pass this velocity test criterion *vel*:

$$vel(i) = \left(\left(\frac{v_{x,n-k+i}}{\eta_{vx}} \right)^2 + \left(\frac{v_{y,n-k+i}}{\eta_{vy}} \right)^2 \right) > 1$$

As we mentioned above, in case of the application of an additional direction criterion *dir*, the direction of the same samples must also fall within a direction range specified by the user.

$$dir(i) = \theta_{max} > \left(atan2\left(v_{y,n-k+i}, v_{x,n-k+i}\right) \cdot \frac{180}{\pi} \right) > \theta_{min}$$

On the basis of this equation, the ideal saccade direction can be conveniently computed using the instructed fixation and saccade target regions (θ_{ideal}, Fig. 1e).

The algorithm automatically returns the used velocity thresholds, as well as (optionally) interpolated position data, and—if a saccade has been detected—the timestamp and computed eye velocity at detection. Since online saccade detection by definition occurs after saccade onset, and lower detection threshold are more susceptible to noise, the algorithm also provides an estimate for the actual saccade onset by tracing back in time one sample that falls below another velocity threshold—that is, the product of a user-defined threshold parameter λ_{onset} (not necessarily the same as the λ used for saccade detection) and the computed median-based standard deviation $\sigma_{vx,vy}$. This two-step procedure (Arabadzhiyska et al., 2017; Dorr, Martinetz, Gegenfurtner, & Barth, 2010) allows the user to get real-time access to a reliable timestamp of saccade onset, for instance to provide feedback on saccade latency in a certain trial, to trigger a display change at a predefined time relative to saccade onset, or to fit ongoing saccade trajectories (Han et al., 2013).

To code is openly available online at https://github.com/richardschweitzer/OnlineSaccadeDetection. It uses standard C libraries and can thus be used across platforms. We provide a module in Python, as well as an implementation to be compiled as a mex-function in Matlab (The Mathworks, Natick, MA, USA).

Materials and method

Simulation

Data

For validation of the algorithm, we compiled a dataset consisting of a total of 34,183 saccades, measured from participants' dominant eye. The data was collected from two past

experiments (i.e., Schweitzer & Rolfs, 2017; Watson, Schweitzer, Castet, Ohl, & Rolfs, 2017), as well as from one pilot study. Using an EyeLink II at a sampling rate of 500 Hz, a number of 17,090 horizontal (left- and rightward) saccades with an instructed amplitude of 14.6 dva, as well as a number of 10,809 saccades in eight different directions (cardinal and intercardinal directions) and of 10 dva amplitude, entered analysis. Furthermore, collected with an EyeLink 1000+ at a sampling rate of 1000 Hz, we included 6,284 additional saccades in the same eight directions, but of 8-dva amplitude.

Pre-processing of the data used for the validation (offline data analysis) involved three steps. First, trial data was reduced to those samples between the onset of successful fixation (preceding the saccade go signal) and 100 ms after the participant's gaze first reached the target area (boundary with 2-dva radius around saccade target). Second, the onset and offset of the saccade—defined as the ground truth in all analyses—was detected using the Engbert–Kliegl algorithm (Engbert & Kliegl, 2003; Engbert & Mergenthaler, 2006) with a threshold parameter of $\lambda = 5$ and a minimum duration of 16 ms (eight samples at 500 Hz and 16 samples at 1000 Hz). Trials, in which saccades could not be detected or in which more than one saccade occurred within the chosen time interval were excluded. Third, eye movement data was transformed from the setup-specific pixel values to degrees of visual angle. Subsequently, position data and timestamps were normalized relative to the detected onset of the saccade to allow for comparisons between saccades of different amplitudes and durations. Saccade data and code used for simulations are available on the Open Science Framework: https://osf.io/3pck5/.

Procedure

To simulate the performance of the online detection algorithm, we divided the data of each trial in saccade absent (i.e., prior to saccade onset as detected offline) and saccade present (i.e., after saccade onset as detected offline) segments. The algorithm was then run sequentially on each data sample (ordered by time stamps) in the respective segment, taking into account all previous samples for threshold estimation. That way, we simulated its usage during an experimental trial in which new data samples are retrieved cumulatively. If saccades were detected while iterating through absent segments, we registered a false alarm (FA), if not, the trial counted as a correct rejection (CR). Similarly, if saccades were detected after offline-detected saccade onset, we registered a correct detection (hit), if not, the trial counted as a miss. To evaluate the performance of the boundary technique (2 dva) and absolute-velocity threshold (40 dva/s), we used the same procedure.

To explore the behavior of the algorithm in a larger parameter space, online saccade detection was tested in both absent and present segments for every available parameter combination—that is, threshold parameter λ (levels: 5, 10, 15, 20), samples above threshold needed k (levels: 1, 2, 3, 4), and direction criterion θ (levels: none, 45°, 30°, 15°). In addition, we convoluted all data samples with Gaussian noise (*SD*s: 0, 0.025, 0.05, 0.1 dva) on both horizontal and vertical dimension and randomly removed a proportion of all samples (levels: 0, 10, 20, 30%), to simulate eyetracker noise and sample loss, respectively. This test setup resulted in a total of 1,024 within-saccade conditions. To achieve a fair comparison between the proposed algorithm and the two traditional techniques, we also tested the performance of the boundary and absolute-velocity techniques for varying numbers of samples (levels: 1, 2, 3, 4).

For each within-saccade condition and additionally for each available sampling rate and saccade direction, we computed detection sensitivity index d' and summary statistics for detection latency (saccade present segments only) of the three detection methods—that is, boundary techniques, absolute-velocity thresholds, and the described online detection algorithm. In addition, we computed an efficiency score (ES)—that is, the proportion of correct rejections divided by the mean detection latency relative to the actual saccade onset (Townsend & Ashby, 1983).

Analysis

As a first step, we computed summary statistics (mean, standard deviation, standard error) for detection latency (separately for each online detection technique and within-saccade condition), and median-based standard deviation of velocity samples. For detection accuracy, we computed d', proportion of hits and false alarms for each online detection technique and condition, and estimated their standard error using nonparametric bootstrapping with 2,000 repetitions.

To understand the individual effects of the algorithm's parameters on the dependent variables d' and detection latency (in milliseconds), we applied multiple regression to the aggregated data. Sampling rate was included as an effect-coded factor (– 0.5 = 500 Hz; + 0.5 = 1000 Hz), while the threshold factor λ and samples above threshold k were included as continuous predictors centered around their mean. Direction restriction was also included as a continuous predictor (in degrees: 180, 45, 30, 15).

To analyze the online detection algorithms' robustness against noise, we ran a second multiple regression on detection accuracy (d') and detection latency (in milliseconds), including five factors and their interactions: sampling rate (effect-coded: – 0.5 = 500 Hz; + 0.5 = 1000 Hz), Gaussian noise standard deviation (continuous; 0, 1.5, 3, 6 arcmin), percentage of samples dropped (continuous; 0%, 10%, 20%, 30%), detection technique used (dummy-coded: boundary, absolute velocity, algorithm [$\lambda = 5$], algorithm [$\lambda = 10$], algorithm [$\lambda = 15$], algorithm [$\lambda = 20$]), and the respective number of samples

needed above criteria (centered, effect-coded: – 1.5 = one sample; – 0.5 = two samples; 0.5 = three samples; 1.5 = four samples).

Experimental test

Participants

Ten observers (including the first author) participated in the experiment. All observers (four female; age range: 22–35 years old) had normal or corrected-to-normal vision. The study was conducted in agreement with the Declaration of Helsinki (2008), approved by the Ethics Committee of the German Society for Psychology, and all observers provided written informed consent before participation. We tracked participants' dominant eye (eight of ten observers with right ocular dominance) for one session with an average duration of 30 min for 480 trials in total.

Apparatus

The experiment took place in a dimly lit, sound-attenuated cabin. A Propixx DLP Projector (Vpixx Technologies, Saint-Bruno, QC, Canada) running at a temporal resolution of 1,440 frames per second and a spatial resolution of 960 × 540 pixels projected into the cabin onto a 200 × 113 cm screen (Celexon HomeCinema, Tharston, Norwich, UK). The projector was connected to the experimental host-PC via a Datapixx3 (Vpixx Technologies, Saint-Bruno, QC, Canada). Observers were seated at a distance of 180 cm away from the projection screen with their head supported by a chin rest. Stimulus display was controlled using the PsychProPixx function from PsychToolbox (Kleiner et al., 2007; Pelli, 1997), running in Matlab 2016b (Mathworks, Natick, MA, USA) on a custom-built desktop computer with an Intel i7-2700K eight-core processor, 8 GB working memory, and an Nvidia GTX 1070 Ti graphics card, running Ubuntu 18.04.1 (64-bit) as the operating system. The setup is illustrated in Fig. 3. Eyetracking was performed using an EyeLink 1000+ desktop base system, tracking participants' dominant eye at a sampling rate of 2000 Hz. Tracking was controlled during the experiment using the EyeLink Toolbox (Cornelissen, Peters, & Palmer, 2002). Moreover, we collected data from a photodiode connected to an actiChamp electroencephalographic (EEG) amplifier (Brain Products, Gilching, Germany), which was attached to the lower right corner of the projection screen (i.e., at approximately 36-dva eccentricity relative to central fixation), again at a sampling rate of 2000 Hz. To synchronize the eyetracking and photo sensor data, we applied a DB-25 Y-splitter cable to simultaneously send triggers of 1-ms duration to the EyeLink host computer and EEG host computer. During pre-processing of the data, we used the EYE-EEG Toolbox (Dimigen, Sommer, Hohlfeld, Jacobs, & Kliegl, 2011) in EEGLAB (Delorme & Makeig, 2004) to temporally align both recordings. For all triggers across recordings, we found a mean absolute misalignment error of 0.38 ms—that is, below one sample.

Stimuli

The stimuli were Gabor patches of vertical orientation enveloped in a Gaussian window with a standard deviation of 0.5 dva, presented on a uniform gray background (luminance of 30 cd/m^2). All Gabor patches had a spatial frequency of 0.5 cycles per degree of visual angle (cpd) and a contrast of 100% (0% in stimulus-absent conditions).

In both saccade and fixation trials (see below and Fig. 4), the stimulus presentation duration amounted to 20 frames at a frame rate of 1440 Hz—that is, 13.9 ms. To reduce the transient elicited by a sudden stimulus onset, the first four and last four presentation frames, respectively, were used to linearly ramp up and down stimulus contrast. Presentation locations were randomly chosen in each trial: Relative to the screen center, stimuli could appear at an eccentricity of up to 8 dva within a range of 360 deg. Because we aimed to present stimuli at largely the same retinal eccentricities both during saccade and fixation trials, we estimated that intrasaccadic presentations would be realized in the first half of the saccade and would therefore be effective when the saccade crossed the screen's center vertical midline. In fact, across all participants the gaze position at stimulus onset was 1.24 dva (SD = 0.92 dva) left of the vertical midline for rightward saccades, and 1.31 dva (SD = 1.0 dva) right of it for leftward saccades.

Throughout their presentation, the Gabor patches were drifting at a constant speed equivalent to the saccadic peak velocity, which was automatically computed during the experiment. That is, after each saccade trial, gaze position data collected during the trial were resampled to 500 Hz and cropped to the relevant time interval between cue onset and 30 ms after reaching the target region. Second, we used the Engbert–Kliegl saccade detection algorithm (Engbert & Kliegl, 2003; Engbert & Mergenthaler, 2006), with a minimum duration of eight samples and λ = 10, to extract the saccade latency and saccadic peak velocity. Third, we computed the median saccadic peak velocity based on the 30 most recent saccade trials. Fourth, to investigate the effect of stimulus drift velocity relative to saccade velocity, we defined the stimulus drift velocity as the resulting median or added or subtracted 50 dva/s, on the basis of which we then computed the Gabor's phase change per frame. This procedure resulted in three conditions and distributions of stimulus drift velocities (M_{-50} = 366 dva/s, M_0 = 416 dva/s, M_{+50} = 466 dva/s), matching the mean saccadic peak velocity of 419 dva/s. Although in both conditions drift velocity was computed on the basis of the most recent saccadic peak velocities, given the fact that fixation and saccade trials were presented in an

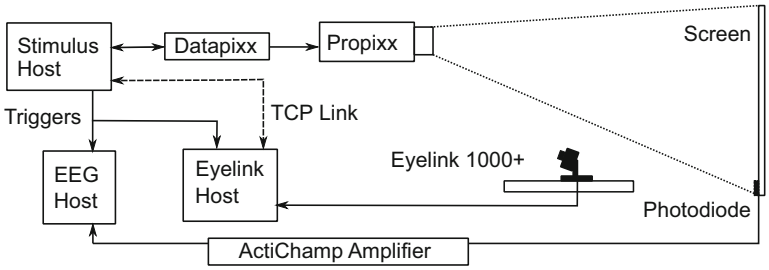

Fig. 3 Setup used to co-register the gaze position and photodiode data. The stimulus host computer performed online monitoring of gaze position via the TCP link, stimulus presentation using a ProPixx DLP projector with a frame rate of 1440 Hz, as well as synchronized triggering of the electroencephalographic (EEG) and EyeLink host computers, recording photodiode and gaze position, respectively.

interleaved manner, the presented drift velocities might have differed between conditions. This, however, was not the case [$t_{-50}(9) = -0.28$, $p_{-50} = .80$; $t_0(9) = -1.8$, $p_0 = .10$; $t_{+50}(9) = -0.43$, $p_{+50} = .68$]. To achieve visibility during saccades, the Gabor patches always drifted in the direction of the saccade (Castet & Masson, 2000; Deubel, Elsner, & Hauske, 1987).

The instructed fixation location was marked using a full-contrast black rectangular dot with a white outline and size of 0.4 dva. For the saccade target location, a similar stimulus was applied, only of twice the size—that is, 0.8 dva.

Procedure

Each participant performed a total of 480 trials, consisting of 240 saccade trials and 240 fixation trials. For each trial type, there were 120 stimulus-absent and 120 stimulus-present

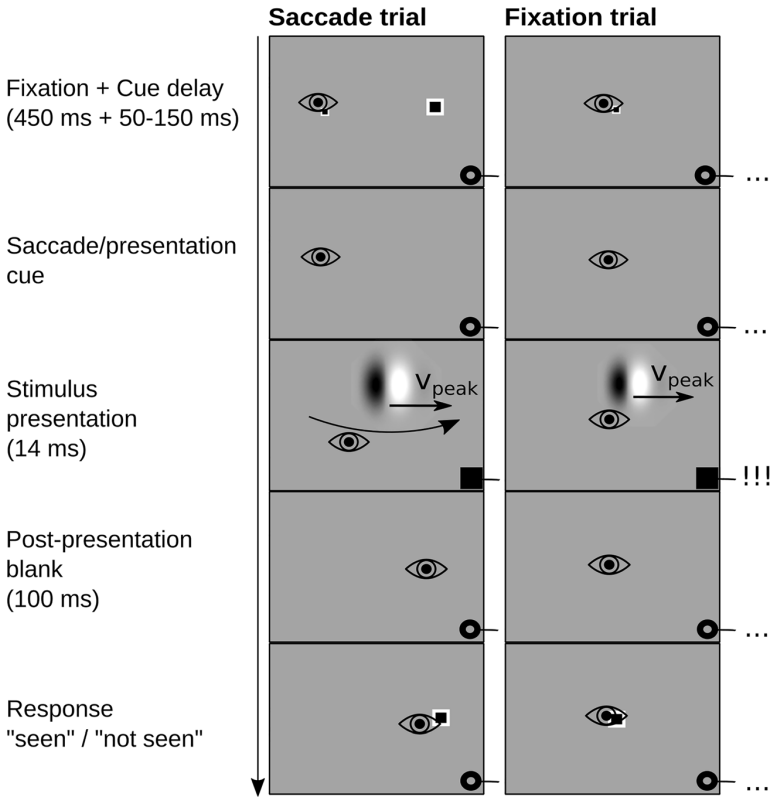

Fig. 4 Experimental procedures used in saccade and fixation trials. In saccade trials, observers made a 16-dva saccade, whereas in fixation trials, observers maintained central fixation. In saccade trials, as soon as a saccade was detected online, and in fixation trials, after the observer's median saccade latency, a Gabor patch (vertical orientation, 0.5 cpd) enveloped in a Gaussian window with a standard deviation of 0.5 dva and drifting at the saccadic peak velocity (the median peak velocity of the 30 most recent saccade trials) was presented for 13.9 ms. During stimulus presentation, a black square was projected onto a photodiode located in the lower right corner of the screen, generating a signal change in the photodiode.

trials, which then contained three stimulus velocity conditions (sum of the median peak velocity and either – 50, 0, or +50 dva/s) and two stimulus drift directions (leftward vs. rightward, in saccade trials according to the saccade direction). All trials were presented in interleaved and randomized order.

Saccade trials Each saccade trial (Fig. 4, left sequence) began with the display of two dots (see the Stimuli section), of which the smaller one represented the fixation location and the larger one the saccade target. Both dots had a horizontal eccentricity of 8 dva relative to the screen center. After successful fixation within a 2-dva radius around the fixation dot for 450 ms, followed by a random delay of 50 to 150 ms, both dots disappeared from the screen—that is, the saccade cue. Participants were instructed to make a saccade (16 dva) toward the remembered target location right after the disappearance of the dots. Saccades were detected online within a window of 10 s (mean saccade latency was 275 ms, SD = 135 ms) after the onset of the saccade cue using the algorithm described in this article (parameters: $\lambda = 10$, $k = 3$, $\theta = 30°$). As soon as a saccade in the instructed direction was detected, we triggered the presentation of a Gabor patch drifting at saccadic peak velocities. In stimulus-present trials, the patch occurred intrasaccadically for 13.9 ms within a radius of 8 dva around the screen center with 100% contrast, whereas in stimulus-absent trials, the patch had zero contrast. Stimulus-absent and -present trials were present in an interleaved manner and were equally probable. Regardless of whether a stimulus was present or absent in a given trial, the presentation was always accompanied by a black dot with a size of 4 dva that was displayed (for the same time as the stimulus) at the location of the photodiode attached to the lower right corner of the screen. Then, 100 ms after stimulus offset (i.e., on average, 82 ms after saccade offset), the saccade target dot would reappear, to give participants feedback on the accuracy of their saccade and prompt their response. Participants were instructed to respond with the right arrow if they had detected a stimulus, and the left arrow if they had not. They did not receive feedback on their detection performance but were shown their own saccade trajectory on the screen whenever they did not reach the saccade-target area (2-dva radius) or made more than one saccade before reaching the latter. Trials with these insufficient saccades were not repeated.

Fixation trials Fixation trials (Fig. 4, right sequence) were initiated with the display of a small dot (0.4 dva) representing the center of a fixation area with 2-dva radius. Just like during saccade trials, gaze had to stay within this area for 450 ms to initiate the presentation sequence (plus random delay of 50 to 150 ms), until the dot disappeared. Prior to stimulus presentation, a delay with the duration of the participant's median saccade latency (based on the 30 most recent saccade trials) was added to imitate the saccade trials and to increase temporal predictability. For the presentation of the rapidly drifting Gabor patch and the photodiode dot under fixation, the same parameters were applied as during saccade trials (see the Stimuli and Saccade Trials sections above). Again, 100 ms after stimulus offset, a larger dot (0.8 dva) appeared, prompting the participant's response (right arrow = "seen," left arrow = "not seen"). Participants were instructed to maintain fixation until the appearance of the response cue and received feedback whenever their gaze left the fixation area.

Analysis

We collected a total of 480 trials (240 saccade trials and 240 fixation trials in interleaved and randomized order) per participant plus one additional set of 305 trials from one participant owing to an aborted session. Due to insufficient fixation or early responses, 9.2% of all fixation trials had to be excluded. In saccade trials, 17.1% were excluded due to unsuccessful initial fixations, not reaching the target area with only one saccade or responding before having reached the target area. Although the Gabor stimuli should be invisible during fixation due to their high drift velocity (Castet & Masson, 2000; Deubel et al., 1987; García-Pérez & Peli, 2011; Watson et al., 2017), 1% of the remaining saccade trials were still excluded because the saccade offset preceded the stimulus offset (as measured by the photodiode). Finally, 0.4% of all trials were removed because of dropped frames. On average, 222 (SD = 13) of the initial 240 fixation trials and 201 (SD = 23) of the initial 240 saccade trials were included for analysis.

Photodiode data and eye movement data were merged using the EYE-EEG Toolbox (Dimigen et al., 2011) and downsampled to 1000 Hz. Saccades were detected using Engbert–Kliegl algorithm (Engbert & Kliegl, 2003; Engbert & Mergenthaler, 2006) with a threshold of $\lambda = 5$ and a minimum saccade duration of 16 samples, constituting the ground truth for the analyses on latency. In addition, messages on saccades and fixations generated by the EyeLink system were imported to validate the saccade detection results from the Engbert–Kliegl algorithm. Unfiltered photodiode voltage time series data was transformed to standard z-scores separately for each experimental session, so that the standard luminance of the screen produced values around 0 and the reduction in photodiode response due to the brief presentation of the black dot during stimulus presentation resulted in values well below – 4. To determine whether the stimulus was on the screen we thus selected those values below the cutoff of – 3. In both saccade and fixation trials, we computed retinal velocity of the stimulus during its presentation by estimating eye velocity (using a five-point running mean) from those gaze samples collected during stimulus presence as determined by the photodiode, and subtracting it from the drift velocity of the stimulus.

To analyze the influence of retinal velocity on task performance on a trial-by-trial basis, we used a logistic mixed-effect regression with random intercepts and slopes for observers (Bates, Mächler, Bolker, & Walker, 2015) to predict correct responses from retinal velocity (continuous predictor, *z*-scores computed separately for fixation and saccade conditions) and condition (effect-coded; – 0.5 = fixation, + 0.5 = saccade). Confidence intervals for log odds weights were determined via parametric bootstrapping with 10,000 repetitions. Hierarchical model comparisons were performed using the likelihood ratio test.

We furthermore used *t* tests to determine whether task performance (*d′*) was different from chance levels and a univariate repeated measures analysis of variance (ANOVA) to compare task performance in the fixation and saccade conditions.

Results

Simulation results

Here we simulated a situation similar to most experimental paradigms: Once an observer receives a cue to make a saccade, we continuously retrieve data samples from the eyetracker to determine whether at any point in time the observer has initiated a saccade or not. In this setup, detection performance has two main aspects, namely accuracy (i.e., detection after saccade onset and not before that) and latency (i.e., when is a saccade detected relative to the actual saccade onset, as determined offline). In this simulation, we asked two main questions: (1) How is the performance of the proposed algorithm impacted by the choice of parameters, and (2) how does its performance compare to classic techniques, such as spatial boundaries and absolute-velocity thresholds, especially under conditions of additional noise and data loss?

As is shown in Fig. 5a, online saccade detection is a trade-off between speed and accuracy. At a sampling rate of 500 Hz, given that only one retrieved data sample is sufficient for detection, boundary techniques (red squares) have a very high accuracy [p(FA) = 0.4%, SD = 0.3%; mean d' = 6.3, SD = 0.74] but long saccade detection latencies (M = 15 ms, SD = 1.1 ms), whereas absolute-velocity thresholds (green squares) have shorter detection latencies (M = 4.4 ms, SD = 0.23 ms), but with lower accuracy [p(FA) = 11.6%, SD = 3%; mean d' = 4.6, SD = 0.34]. Importantly, the type of eyetracking system and the sampling frequency of the eyetracker are major moderators of the performance of both techniques. At low sampling rates, samples become less frequently available, whereas at high sampling rates, sample-to-sample noise impacts the velocity estimates to a larger extent (Han et al., 2013). For comparison, at a sampling rate of 1000 Hz, the saccade detection latencies of both techniques decrease as compared to 500 Hz (boundary: M = 11.2 ms, SD = 0.96 ms; absolute velocity: M = 1.4 ms, SD = 0.08 ms), whereas false alarm rates increase drastically for absolute-velocity thresholds [p(FA) = 63%, SD = 6%; mean d' = 2.8, SD = 0.16].

Even though these traditional online saccade detection methods are often used on only one data sample, they are naturally not restricted to this definition. To enable a fair comparison to the proposed algorithm that evaluates a number of samples defined by the user (here, one to four samples), we tested whether the performance of the traditional techniques can be improved when more than one sample is taken into account (Fig. 5). Indeed, for absolute-velocity thresholds applied to two or more samples, detection accuracy increased remarkably [500 Hz: p(FA) = 2%, SD = 1%; mean d' = 5.5, SD = 0.5; 1000 Hz: p(FA) = 0.5%, SD = 0.3; mean d' = 5.9, SD = 0.25], but at the cost of an increase in saccade detection latencies (500 Hz: M = 8.6 ms, SD = 1.7 ms; 1000 Hz: M = 4.3 ms; SD = 0.53 ms). Boundary techniques, on the other hand, benefited very little from additional test samples [500 Hz: p(FA) = 0.3%, SD = 0.2%, mean d' = 6.4, SD = 0.7; 1000 Hz: p(FA) = 0.1%, SD = 0.7%, mean d' = 6.2, SD = 0.2], as their accuracy was already at ceiling for one sample, and their detection latencies only increased further (500 Hz: M = 18.9 ms, SD = 1.18 ms; 1000 Hz: 13.3 ms, SD = 0.95 ms).

Detection accuracy of the proposed algorithm (shapes in shades of violet in Figs. 5 and 6) remained largely unaltered across sampling frequencies [averaged across the entire tested parameter space, for 500 Hz: mean p(FA) = 11.7%, SD = 2.5%; d' = 5.1, SD = 1.0; 1000 Hz: mean p(FA) = 14.6%, SD = 3.2%; d' = 5.1, SD = 1.5; β = – 0.01, t(128) = – 0.06, p = .95], due to the adaptive adjustment of the noise level, while detection latencies decreased [500 Hz: M = 5.5 ms, SD = 2.1 ms; 1000 Hz: M = 3.7 ms, SD = 1.9 ms; β = – 1.5, t(128) = – 6.1, p < .0001].

Saccade-detection accuracy (Fig. 5b) and latency (Fig. 5c), however, strongly depended on the choice of the necessary parameters k, λ, and θ. First, increasing the number of samples needed above threshold k improved accuracy (d') by 0.48 per sample [β = 0.48, t(128) = 8.2, p < .0001], but also increased latency by 1.27 ms per sample [β = 1.27, t(128) = 11.6, p < .0001]. Note that a similar effect was found above for absolute-velocity thresholds (see also Fig. 5a). Second, a higher threshold parameter λ similarly increased both accuracy [β = 0.125, t(128) = 10.6, p < .0001] and latency [β = 0.14, t(128) = 6.3, p < .0001]. Third, accepting a wider range of saccade directions (in degrees) led to a decrease of accuracy [β = – 0.004, t(128) = – 5.9, p < .0001] and latency [β = – 0.01, t(128) = – 6.9, p < .0001]. Although for saccade detection latencies all three parameters had additive effects (Fig. 5c), interactions were present for detection accuracy: The benefit of increasing the number of samples above thresholds k [β = – 0.07, t(128) = – 6.6, p < .0001] or restricting directions θ was smaller at higher thresholds [β = 0.0004, t(128) = 3.2, p = .002], because detection accuracy would reach ceiling (Fig.

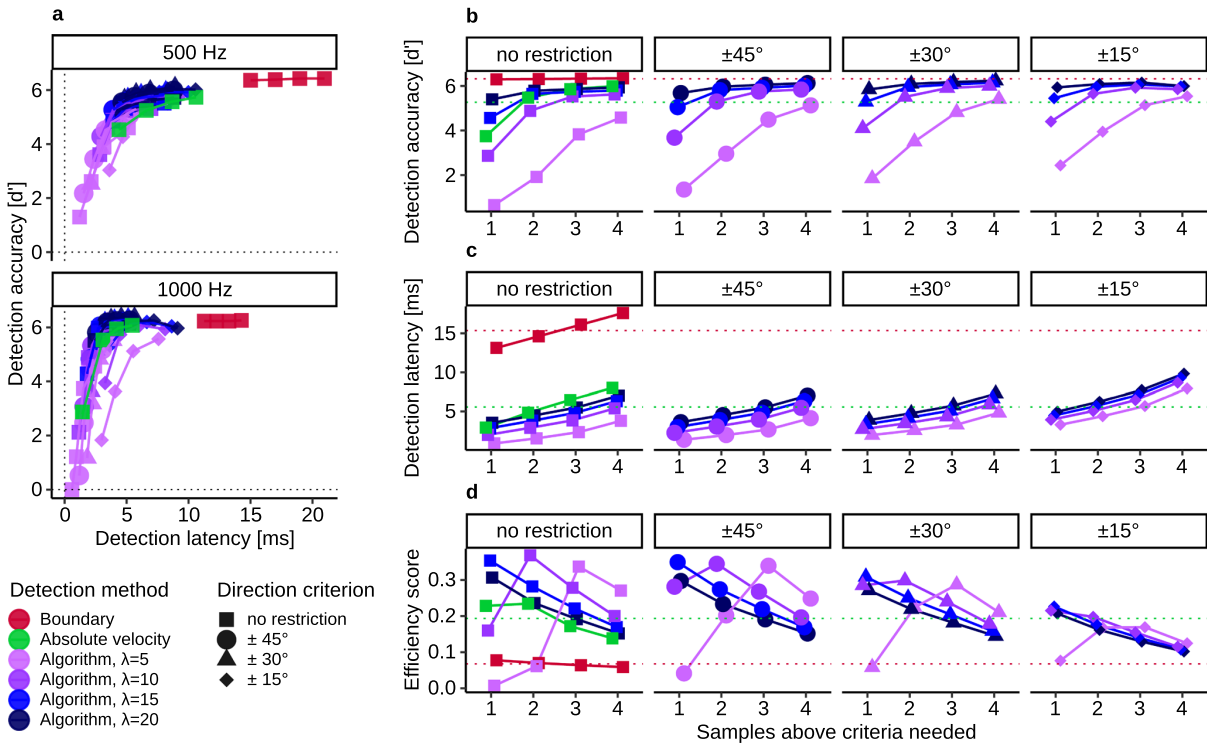

Fig. 5 Grand averages of detection performance and latency, as determined by simulation. (a) The trade-off of detection accuracy and detection latency for each sampling rate. Every dot represents the mean across all trials, including all eight tested saccade directions, with color indicating the type of detection method (and threshold factor λ) used and shape indicating the direction criterion (θ) used. The four connected values indicate the number of samples above threshold (k) needed for detection in each condition (always increasing from left to right). (b–d) Mean detection accuracy, latency, and efficiency, respectively, averaged across sampling rates for different parameter combinations (λ, θ, k). The green and red dotted reference lines indicate the average results (across samples above criteria, k) for the absolute-velocity thresholds and boundary techniques, respectively.

5b). Accordingly, direction restriction was more effective at low λ and low k [$\beta = 0.001$, $t(128) = 2.1$, $p = .043$].

To improve the understanding of this speed–accuracy trade-off, we introduced an efficiency score (Townsend & Ashby, 1978), based on the ratio of correct rejection rate and detection latency (Fig. 5d). Importantly, it becomes evident that for optimal parameter choice, the efficiency of the proposed algorithm is well above the efficiency of both the boundary and absolute-velocity techniques, even when these techniques evaluated more than one sample. With extremely conservative settings (see Figs. 5b–5d, rightmost panels), however, detection latency will be increased to a large degree, so that some saccades might not be detected in time. With regard to the optimal choice of parameters, it is important to consider the noise levels and sampling rate of the eyetracker. For our simulation, we chose two eyetrackers with similar spatial precision (RMS = 0.01 dva; SR Research, 2005, 2010), but varying sampling rates. We found that the positive effects of detection threshold λ and number of samples above threshold k on detection accuracy were slightly stronger when tracking at higher than at lower sampling rates [λ: $\beta = 0.047$, $t(128) = 1.99$, $p = .049$; k: $\beta = 0.24$, $t(128) = 2.01$, $p = .038$]. This suggests that a more conservative parameter choice is more beneficial at higher sampling rates, where increased velocity due to tracker noise is more likely to occur (see also Fig. 6, bottom row).

How do online saccade detection techniques cope with conditions in which noise is drastically increased or in which several samples are dropped? We simulated these situations by adding uncorrelated, Gaussian noise (standard deviations of up to 6 arcmin) to the data and by randomly removing data samples (up to 30%). As is shown in Fig. 6 (top row), absolute-velocity thresholds (green lines) are strongly impacted by noise [$\beta = -0.75$, $t(672) = -6.1$, $p < .0001$], as the false alarm rate reached almost 100% after adding Gaussian noise of 1.5 arcmin *SD* at 1000 Hz, reducing this technique's efficiency to virtually zero—that is, 0.0005 (*SD* = 0.0004). As predicted, at 500 Hz the impact of noise was smaller, but still an efficiency of virtually zero was reached at a Gaussian noise *SD* of 3.0 arcmin (mean efficiency = 0.001, *SD* = 0.0008). The detection accuracy of the proposed algorithm (500 Hz: mean efficiency = 0.11, *SD* = 0.012; 1000 Hz: mean efficiency =

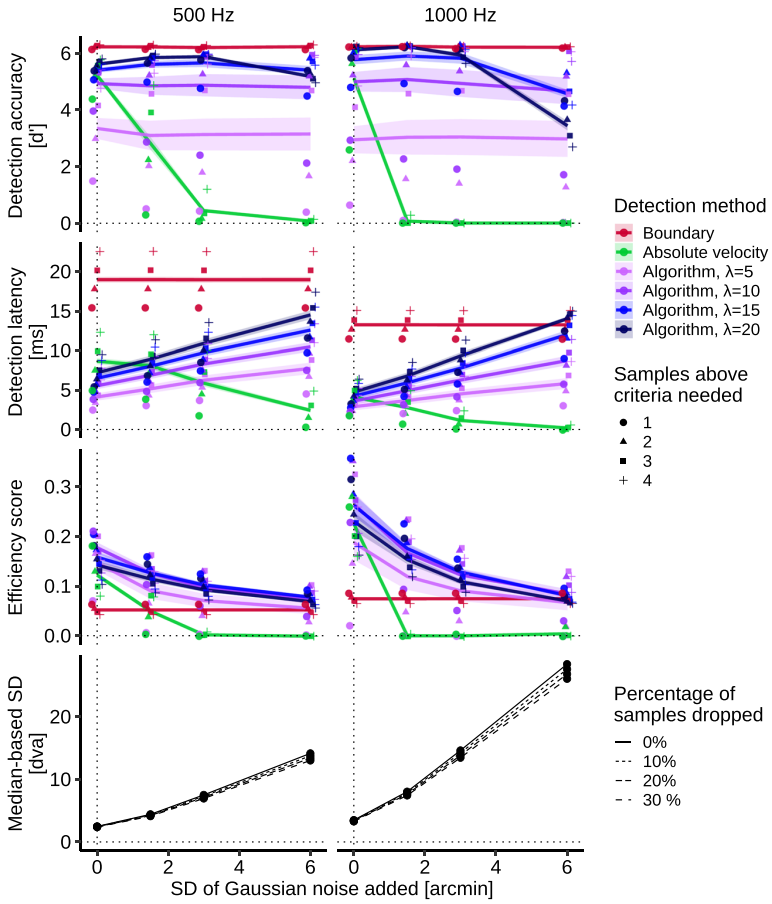

Fig. 6 *Top three rows:* Mean detection accuracy, latency, and efficiency of the three online saccade detection techniques for different noise levels (*SD* of Gaussian noise added to both sample dimensions, *x* and *y*) and sampling rates (left column = 500 Hz, right column = 1000 Hz), averaged across all levels of percentage of samples dropped. The lines represent averages across the entire tested parameter space, and symbols represent the number of samples above threshold needed to detect a saccade (*k*). Shaded areas indicate 95% confidence intervals. *Bottom row:* Median-based standard deviations of absolute velocity estimates used to compute velocity thresholds. Different line types represent the percentage of samples dropped.

0.15, *SD* = 0.021), on the other hand, was largely unimpaired by noise [$\lambda = 5$: $\beta = -0.03$, $t(672) = -0.4$, $p = .68$; $\lambda = 10$: $\beta = -0.04$, $t(672) = -0.6$, $p = .53$; $\lambda = 15$: $\beta = -0.12$, $t(672) = -1.7$, $p = .08$]. At a threshold factor of $\lambda = 20$, however, detection accuracy decreased starting at Gaussian noise *SD*s of 6 arcmin [$\beta = -0.3$, $t(672) = -4.1$, $p = .0004$], since the velocity thresholds were simply too high: If median-based velocity *SD*s such as 26 dva/s (Fig. 6, bottom row, right panel) were multiplied by a factor of 20, we would achieve unreasonable velocity thresholds as high as 520 dva/s, and thus miss most ongoing saccades. Furthermore, in the presence of noise and when working with lower velocity thresholds, it was beneficial to increase the number of samples that should be evaluated by the algorithm, to improve accuracy [absolute velocity: $\beta = 0.69$, $t(672) = 3.1$, $p = .002$; algorithm [$\lambda = 5$]: $\beta = 1.5$, $t(672) = 6.6$, $p < .0001$; algorithm [$\lambda = 10$]: $\beta = 0.78$, $t(672) = 3.5$, $p = .0004$].

Because the velocity threshold is estimated on the basis of the current noise level, to preserve robustness across trials and participants, higher velocity thresholds due to increased noise levels should be accompanied by increased detection latencies. Indeed, for every threshold factor λ, the saccade detection latency of the algorithm increased with noise level [$\lambda = 5$: $\beta = 0.55$, $t(672) = 19.7$, $p < .0001$; $\lambda = 10$: $\beta = 0.85$, $t(672) = 30.7$, $p < .0001$; $\lambda = 15$: $\beta = 1.19$, $t(672) = 43.1$, $p < .0001$; $\lambda = 20$: $\beta = 1.42$, $t(672) = 51.2$, $p < .0001$]. Naturally, increasing the number of samples above the criteria needed to detect the saccade also increased latency across all tested algorithms [$\beta = 1.47$, $t(672) = 24.5$, $p < .0001$].

With respect to dropped samples, boundary techniques and absolute-velocity thresholds suffered from longer detection latencies due to dropped samples [boundary: $\beta = 0.05$, $t(672) = 14.8$, $p < .0001$; absolute velocity relative to boundary: $\beta = 0.015$, $t(672) = 3.0$, $p = .003$], especially when more

samples were evaluated [boundary: $\beta = 0.02$, $t(672) = 6.7$, $p < .0001$; absolute velocity relative to boundary: $\beta = 0.007$, $t(672) = 0.7$, $p = .46$]. The latency of the proposed algorithm was less affected by dropped samples than were the two traditional techniques [$\lambda = 5$: $\beta = -0.03$, $t(672) = -6.9$, $p < .0001$; $\lambda = 10$: $\beta = -0.03$, $t(672) = -6.4$, $p < .0001$; $\lambda = 15$: $\beta = -0.03$, $t(672) = -6.4$, $p < .0001$; $\lambda = 20$: $\beta = -0.03$, $t(672) = -6.7$, $p < .0001$], a result that is likely related to the interpolation of missing data samples that the algorithm performs prior to smoothing and threshold estimation. In fact, median-based standard deviations depended strongly on the noise level, but hardly on the percentage of dropped samples in the data (Fig. 6, bottom row). Although latency increased, all tested algorithms maintained their accuracy when samples were dropped [boundary: $\beta = -0.007$, $t(672) = -0.8$, $p = .44$; absolute velocity: $\beta = 0.005$, $t(672) = 0.35$, $p = .73$; algorithm [$\lambda = 5$]: $\beta = -0.01$, $t(672) = -1.0$, $p = .31$; algorithm [$\lambda = 10$]: $\beta = -0.007$, $t(672) = -0.49$, $p = .62$; algorithm [$\lambda = 15$]: $\beta = -0.003$, $t(672) = -0.24$, $p = .81$; algorithm [$\lambda = 20$]: $\beta = -0.001$, $t(672) = -0.01$, $p = .92$].

As is shown in Fig. 6 (third row), efficiency scores remained constant for the boundary technique [$\beta = -0.0003$, $t(672) = 0.001$, $p = .99$] and decreased with increasing noise levels for all velocity-based algorithms [absolute velocity: $\beta = -0.027$, $t(672) = -7.6$, $p < .0001$; algorithm [$\lambda = 5$]: $\beta = -0.017$, $t(672) = -4.9$, $p < .0001$; algorithm [$\lambda = 10$]: $\beta = -0.024$, $t(672) = -6.9$, $p < .0001$; algorithm [$\lambda = 15$]: $\beta = -0.022$, $t(672) = -6.5$, $p < .0001$; algorithm [$\lambda = 20$]: $\beta = -0.02$, $t(672) = -5.7$, $p < .0001$], but the least square means of the computed linear model revealed a considerable difference between the absolute efficiency of the tested algorithms: Across sampling rates and for the means of noise level (i.e., 2.62 arcmin), percentage of dropped samples (i.e., 15% dropped samples), and number of samples above threshold (i.e., 2.5 samples), the proposed algorithm outperformed both boundary techniques ($M = 0.065$, 95% CI [0.058, 0.071]) and absolute-velocity thresholds ($M = 0.052$, 95% CI [0.045, 0.058]) on all threshold factor levels ($\lambda = 5$: $M = 0.105$, 95% CI [0.098, 0.11]; $\lambda = 10$: $M = 0.14$, 95% CI [0.134, 0.147]; $\lambda = 15$: $M = 0.14$, 95% CI [0.134, 0.147]; $\lambda = 20$: $M = 0.12$, 95% CI [0.117, 0.13]).

Finally, in a separate simulation, we also found that the algorithm's running time (i.e., the time elapsed from invocation to return of the `mex` function in Matlab 2016b on a Dell Optiplex 3020 with an Intel i5-4590 processor running Kubuntu 18.04) on data collected for 2 s was on average 0.051 ms at a sampling rate of 500 Hz ($SD = 0.005$ ms, $N = 30{,}000$), 0.097 ms at 1000 Hz ($SD = 0.009$ ms, $N = 30{,}000$), and 0.187 ms at 2000 Hz ($SD = 0.011$ ms, $N = 30{,}000$). The algorithm's time average complexity is thus linear (and quadratic, in the worst case).

Experimental results

To present an example of application of the algorithm and to show that its application makes strictly intrasaccadic presentations well possible, we developed an objective and a perceptual test. Since our setup allowed for the co-registration of stimulus events, EEG recordings, and eyetracking at a high temporal resolution, the objective test used a photodiode to measure physical stimulus onset and offset during the saccade, in which the saccade was detected online with the proposed algorithm (see Fig. 3 for the Apparatus). In addition, as a perceptual test, we presented a Gabor patch (vertical orientation, 0.5 cpd spatial frequency, 0.5 dva *SD* Gaussian aperture) that—due to its high drift velocity (on average, 420 dva/s)—would be invisible during fixation but become detectable only if the eye was moving at a similar velocity in the same direction (Castet & Masson, 2000; Watson et al., 2017). Observers were instructed to indicate whether they perceived a Gabor patch that could be presented anywhere within a range of 8 dva around screen center and was present in 50% of all saccade and fixation trials (Fig. 4).

Online saccade detection in saccade trials worked well. Only 1% of valid trials had to be excluded due to too early or too late detection. The mean detection latency amounted to 5 ms ($SD = 2.06$ ms). Unlike the results from the simulation, however, this latency estimate still included system delays, most crucially the end-to-end sample delay of the eyetracker: According to the manufacturer, the EyeLink 1000+ with normal filter settings at a sampling rate of 2000 Hz is expected to have an average delay of 2.7 ms ($SD = 0.2$ ms; SR Research, 2013). Correcting for these delays, the mean detection latency would be around 2.3 ms. As a comparison, the mean detection latency (determined by our simulation) with the same parameters and eyetracking system, but tracking at 1000 Hz, amounted to 3.4 ms ($SD = 0.66$ ms), while remaining at a high accuracy level [p(FA) = 0.3%, $SD = 0.06$%; mean $d' = 6.1$, $SD = 0.4$]. The second crucial latency for gaze-contingent displays is the flip latency (i.e., the time when the flip occurs relative to saccade onset; see Fig. 7b), which depends on the hardware, the display frame rate used, as well as the time within the refresh cycle. In this experiment, the flip latency was on average 11 ms ($SD = 3.1$ ms), as a mean detect-to-flip delay of 6 ms ($SD = 2.46$ ms) incurred. Finally, the flip-to-display latency should be deterministic, as the ProPixx DLP projector updates its entire display with microsecond precision as soon as all video data are transferred. Indeed, the flip-to-display latency amounted to an average of 8.15 ms ($SD = 0.35$ ms), which is in line with the graphic card's refresh rate of 120 Hz. The addition of all system delays resulted in a physical stimulus onset around 19.6 ms ($SD = 3.1$ ms) after saccade onset (photodiode onset in Fig. 7b), leading to the intended intrasaccadic display right when the eye was in midflight (Fig. 7a).

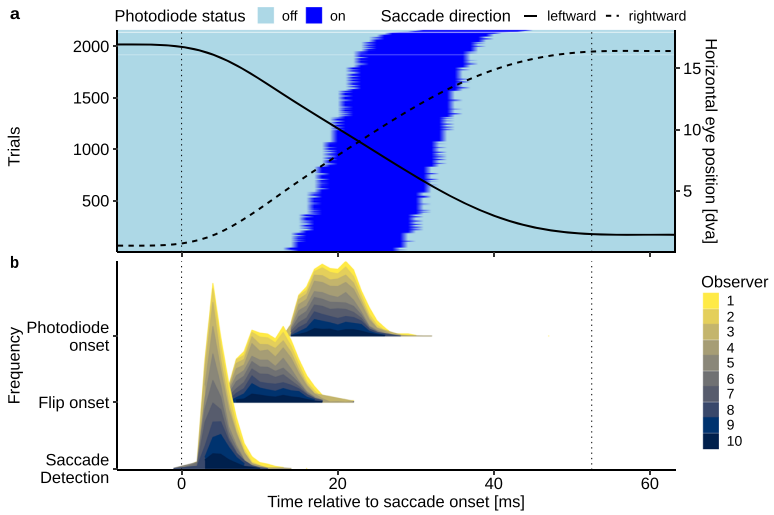

Fig. 7 Timing events in the experimental test. (a) "On" times of the photodiode (dark blue) of all saccade trials, displayed and sorted according to their time relative to the onset and offset of the saccade (dotted vertical lines). The solid and dashed lines represent the mean horizontal saccade trajectories of leftward and rightward saccades over time (smoothed by a univariate general additive model). (b) Distributions of detection, flip, and photodiode onset times relative to the onset of the saccade. Shadings indicate data from different observers.

If the intrasaccadic stimulus presentation was indeed successful, then observers should have been able to detect the rapidly drifting Gabor during saccades and not during fixation, as only an ongoing eye movement could decrease the (relative) velocity of the stimulus on the retina to the point where it would become perceivable. When observers were fixating, their detection performance was not significantly different from chance level [mean $d' = 0.06$, $SD = 0.14$; $t(9) = 1.28$, $p = .23$], suggesting that the Gabor stimulus drifting at an average velocity of 419 dva/s ($SD = 61.4$ dva/s) was indeed invisible when the eye was not moving (Fig. 8a). In contrast, we found that the stimuli were readily detected during saccades, as performance drastically improved relative to the fixation condition [mean $d' = 2.94$, $SD = 1.1$; $F(1, 9) = 59.6$, $\eta^2 = .79$, $p < .0001$].

To further explore the potential effect of retinal velocity on detection performance, we computed each trial's mean retinal velocity during stimulus presentation (see the Analysis section). We found that the retinal velocity was on average 416 dva/s ($SD = 45$ dva/s) during fixation, whereas it was reduced to 68 dva/s ($SD = 68.8$ dva/s) during saccades. Note that the mean retinal velocity during saccades was in most cases positive, because presentation of the stimulus extended into the deceleration phase of the saccadic velocity profile (Fig. 7a).

A logistic mixed-effect regression (Bates et al., 2015) revealed not only a large increase of correct responses in the saccade condition ($\beta = 3.0$, $t = 5.7$, 95% CI [2.13, 4.13]), but also a significant negative effect of retinal velocity ($\beta = -0.12$, $t = -2.41$, 95% CI [– 0.23, – 0.016]), suggesting that, across both conditions, higher retinal velocity was associated with lower task performance. An interaction between condition and retinal velocity was also significant ($\beta = -0.20$, $t = -2.06$, 95% CI [– 0.4, – 0.01]). Because overall performance was much lower in the fixation condition, this interaction suggests that the effect of retinal velocity was exclusive to the saccade condition (Fig. 8b). To check whether the difference between the fixation and saccade conditions was mediated by a difference in retinal eccentricity at the time of stimulus presentation, we also computed the mean retinal position of the stimulus. In the saccade condition, stimuli had an average 1-dva offset of horizontal eccentricity against the saccade direction ($M_{x,\text{sac,left}} = 1.31$ dva, $SD_{x,\text{sac,left}} = 1.1$ dva; $M_{x,\text{sac,right}} = -1.15$ dva, $SD_{x,\text{sac,right}} = 1.2$ dva) relative to the fixation condition ($M_{x,\text{fix,left}} = 0.30$ dva, $SD_{x,\text{fix,left}} = 0.54$ dva; $M_{x,\text{fix,right}} = -0.37$ dva, $SD_{x,\text{fix,right}} = 0.62$ dva), which can be explained by the fact that stimulus presentation extended into the second half of the saccade in most cases—that is, when the eye had already passed the screen center (the mean horizontal presentation location). To determine whether this slight difference in eccentricity had any effect on task performance, we added absolute horizontal and vertical eccentricity to the logistic mixed-effect regression. We found an increase in log-likelihood that was not significant [$\Delta LL = +8.8$, $\chi^2(21) = 17.51$, $p = .68$], suggesting that retinal eccentricity played, if any, a subordinate role in our task.

Discussion

Timing is crucial when studying visual perception around the time of saccades, especially when manipulating stimulus configurations gaze-contingently with the onset of a saccade. In

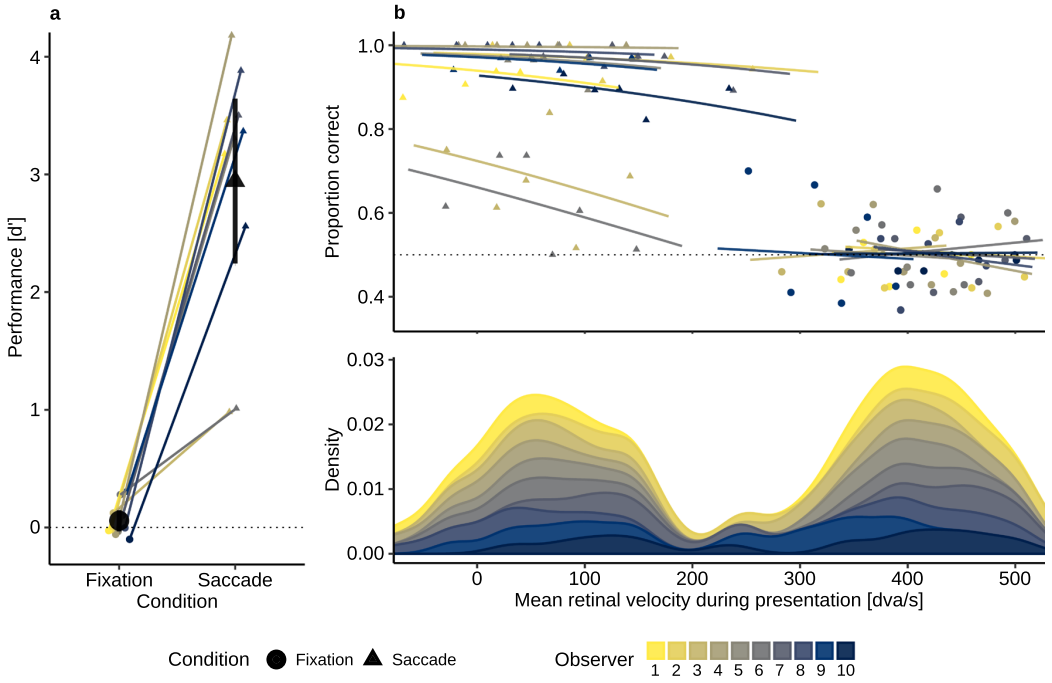

Fig. 8 Behavioral results from the perceptual test. (a) Stimulus detection performance (*d'*) in the fixation and saccade conditions for individual observers. The large black circles and triangles represent group means for the fixation and saccade conditions. Error bars indicate 95% confidence intervals, based on ± 2 *SEM*s. (b) *Upper panel:* Model fits from the logistic mixed-effect regression with random intercepts and slopes for observers. The points indicate mean proportions correct in six equal-sized bins of retinal velocity (i.e., mean eye velocity during stimulus presentation subtracted from stimulus velocity) per condition per observer. *Lower panel:* Distribution of retinal velocities for each observer for the fixation (right peak) and saccade (left peak) conditions.

gaze-contingent experimental paradigms, various sources of latency have to be considered, ranging from eyetracker delays, saccade detection latencies, graphic card refreshes, video delays, and monitor reaction time. Whereas most of these latencies can be reduced by enhancing hardware capabilities, a more efficient online saccade detection algorithm improves timing performance independently of the experimental setup. Unfortunately, the most commonly used online detection techniques—that is, the spatial boundary technique and the absolute-velocity threshold—have significant shortcomings: The former provides reliable but late saccade detection, whereas the latter is fast but struggles with reliability, especially at higher sampling rates or slightly increased noise levels. Inspired by a widely used algorithm for (micro)saccade detection (Engbert & Kliegl, 2003; Engbert & Mergenthaler, 2006), we developed a velocity-based online saccade detection algorithm that incorporates both algorithms' strong points: It allows for rapid saccade detection due to low velocity thresholds, it is robust against noise by applying smoothing, adaptive adjustment of velocity thresholds, and an optional direction criterion, and it allows the user to flexibly specify more liberal or more conservative detection criteria. Across various gaze-contingent experimental paradigms, as well as in non-scientific applications, this open-source algorithm could help create comparable and reproducible results by (1) avoiding timing problems (due to its early saccade detection) and (2) increasing stability (due to its increased robustness against noise).

We validated the algorithm, as well as the boundary and the absolute-velocity technique, in a large-scale simulation (> 30,000 saccades). We found that the algorithm provided considerably earlier saccade detection than boundary techniques (up to 10 ms or more, depending on sampling rate), which was more similar to (although in most cases slightly slower than) the latency of the absolute-velocity technique. Crucially, the algorithm's accuracy in online saccade detection was on par with the boundary technique and significantly larger than that of the absolute-velocity technique, especially at high sampling rates and even when the number of evaluated samples was accounted for. Moreover, when corrupting the collected data with noise, absolute-velocity techniques suffered from a drastic increase in false alarms, whereas the proposed algorithm maintained its detection accuracy by updating its velocity threshold and exhibited significantly larger efficiency scores than both traditional techniques. This is an important result and prerequisite for the use during eyetracking experiments, because many factors that vary throughout the experiment or on a trial-by-trial basis, such as pupil diameter, time since last

calibration, head movements, gaze eccentricity, or marker visibility, may influence accuracy and precision of recordings (Nyström, Andersson, Holmqvist, & Van De Weijer, 2013) and thus alter the noise level. Since the algorithm updates velocity thresholds with every new incoming data sample, various negative influences on detection accuracy can be accounted for. For instance, even small drifts in measured gaze positions, such as those occurring during fixation when head-mounted eyetrackers shift their position slightly relative to the participant's eyes (which can lead to erroneous saccade detections when using boundary techniques), would simply lead to elevated velocity thresholds that preserve detection accuracy. At the same time, the incentive to achieve high data quality remains, as increased noise levels may still have a negative impact on detection latency. The idea of employing adaptive thresholds for online saccade detection to reduce susceptibility to noise is not entirely new. For example, in their PyGaze toolbox, Dalmaijer, Mathôt, and Van der Stigchel (2014) have used an additional root-mean-square (RMS) criterion along with user-defined thresholds for velocity and acceleration. Unlike that approach, our proposed algorithm depends neither on absolute threshold definitions nor on a calibration of RMS, because thresholds are computed on the basis of all preceding samples collected during a trial and thus efficiently capture trial-to-trial variance. Moreover, its nonblocking implementation in the programming language C allows for flexible, multi-platform usage (e.g., Python, Matlab, Octave), and yields high speed: Running the algorithm in real time is feasible because a large number of collected samples, such as those collected from eyetrackers sampling at 2000 Hz, can be processed within microseconds. However, due to its linear time complexity, it cannot be guaranteed that the algorithm will finish prior to any given deadline. For example, if the algorithm were run on an unnecessarily large number of samples, such as 4,000,000, then it would take ~187 ms (based on the results of our simulation), exceeding by far the duration of a saccade.

We found that the detection criterion and subsequent performance of the algorithm strongly depends on the parameters supplied: More conservative settings (i.e., higher threshold factor, more samples above threshold, a tighter range of accepted directions) will improve detection accuracy to a maximum, but will come at the cost of increased detection latency, and in the worst case—as is shown by the high-noise conditions—may lead to abnormally high velocity thresholds that will make saccade detection impossible. We thus suggest a careful weighting of parameters depending on the experimental setup and paradigm used. For example, when using a threshold factor of $\lambda = 5$, it makes sense to have at least three samples above threshold to detect a saccade. Indeed, if the algorithm were used to detect microsaccades during an experiment, low thresholds should be used, as eye velocities during microsaccades are not as high as those during saccades, whereas three or more samples should be evaluated (for a successful application with a different implementation, see Yuval-Greenberg, Merriam, & Heeger, 2014). If, however, a threshold factor of $\lambda = 20$ were used, one sample above threshold might often be enough to reliably detect a saccade without adding significant additional delay. In pilot work with the TrackPixx3 (VPixx Technologies, 2017), we also found that binocular online saccade detection (running the detection algorithm on each eye separately) allows for lower threshold factors, as the probability that velocity thresholds are exceeded simply due to noise in both eyes simultaneously is smaller than for one eye only. The choice of threshold also depends on the noise level and sampling rate of the eyetracker in use, as a higher sampling rate can inflate velocity estimates (Han et al., 2013). In some systems, such as the EyeLink 1000+ (SR Research, 2013), these two variables are not independent: With deactivated heuristic filters, RMS noise amounts to 0.02 dva at 1000 Hz and to 0.03 dva (monocular tracking) and 0.04 dva (binocular tracking) at 2000 Hz. Additional filter levels supplied by the manufacturer can reduce these noise levels, but introduce additional end-to-end sample delay (also depending on sampling rate). It is thus important to understand that the parameter choice for optimal online saccade detection performance is intrinsically dependent on both the recording settings and the nature of the task. For instance, a direction restriction can only be applied in paradigms, in which it is certain or at least very likely that the participant will indeed make a saccade in a given direction. In case of a two-alternative forced choice paradigm, it would be possible to call the algorithm twice, each time with different direction criteria, but it would be impossible to apply a direction criterion in a free viewing context. Ultimately, it remains an advantage that the experimenter is able to fine-tune the detection criterion according to the relative costs for longer detection latencies or for an increased false alarm rate incurring in a specific task.

With the introduction of the objective and perceptual test experiment, we provided a real-world example of a gaze-contingent paradigm in which timing was crucial, in this case for the intrasaccadic presentation to be successful. This test builds on the finding that rapidly drifting or flickering gratings that are invisible during fixation can be rendered visible due to the reduction of retinal velocity occurring when the eye moves across them (Castet & Masson, 2000; Mathôt, Melmi, & Castet, 2015; García-Pérez & Peli, 2011). We used a projection system operating at submillisecond temporal resolution to briefly display a rapidly drifting Gabor patch entirely during the saccade, and we asked observers to detect it. We established that the Gabor patch was indeed largely invisible during fixation. It was absolutely crucial in this task, therefore, that the stimulus was presented while the eye was in midflight to achieve an approximate match of the velocities of stimulus and eye. Both observers' high task performance in the saccade

condition (perceptual test) and recordings from a photodiode (objective test) confirmed that despite all possible system delays strictly intrasaccadic presentations with a physical onset as early as 20 ms after saccade onset were well possible. At the same time, only 1% of all trials had to be removed from analysis because presentations did not happen strictly during the saccade—for example, due to late detections or erroneous detections while fixating (see the Method section). Importantly, the described perceptual test can be a valuable tool to determine whether a presentation is actually intrasaccadic when photodiode measurements are unavailable: If a drifting stimulus that is otherwise undetectable during fixation can be reliably discriminated during a saccade, then its presentation must be (at least partly) intrasaccadic. By examining discrimination performance as a function of time relative to the measured saccade detection, the timing of a gaze-contingent paradigm can be systematically investigated. Note that although we displayed the drifting Gabor patch using a projector with a frame rate of 1440 Hz, other studies have achieved similar presentations using much lower frame rates, such as 122 Hz (García-Pérez & Peli, 2011), 150 Hz (Mathôt et al., 2015), or 160 Hz (Castet & Masson, 2000), suggesting that the perceptual test should work with any gamma-calibrated laboratory monitor running at frame rates of 120 Hz or more.

But the finding is interesting for two other reasons. First, it shows that if a stimulus has high contrast, is optimized for the high velocity of saccades (Castet & Masson, 2000; Deubel et al., 1987; García-Pérez & Peli, 2011; Mathôt et al., 2015; Schweitzer, Watson, Watson, & Rolfs, 2019), and is not affected by pre- and postsaccadic masking (Campbell & Wurtz, 1978; Castet, 2010), then it is readily detectable, if not highly salient. Second, the finding indicates that timing during and around saccades matters. It is widely assumed that visual processing is suppressed during and around the time of saccades (Burr, Holt, Johnstone, & Ross, 1982; Burr, Morrone, & Ross, 1994; Ross, Morrone, Goldberg, & Burr, 2001). This is the reason why many trans-saccadic paradigms relying on gaze-contingent manipulations assume that as long as a display change falls within the window of saccadic suppression—which precedes saccade onset by up to 100 ms and exceeds the saccade duration by up to 50 ms (Diamond, Ross, & Morrone, 2000; Volkmann, 1986; Volkmann, Riggs, White, & Moore, 1978)—it is neither noticed nor processed. There is, however, converging evidence that stimuli undergoing saccadic suppression can shape postsaccadic perception (Watson & Krekelberg, 2009), and that the relative timing of a stimulus relative to saccade offset drastically changes both the appearance of that stimulus and its likelihood of being consciously perceived (Balsdon, Schweitzer, Watson, & Rolfs, 2018; Bedell & Yang, 2001; Campbell & Wurtz, 1978; Duyck, Collins, & Wexler, 2016; Matin, Clymer, & Matin, 1972). There is also evidence that brief intrasaccadic flashes were able to drive saccadic adaptation when presented during the deceleration phase of an ongoing saccade (Panouillères et al., 2016). Although for many experiments and the conclusions drawn from them intrasaccadic display changes may not be absolutely crucial, it is important to be aware of the possibility that an intended intrasaccadic change might in fact be a nonintended postsaccadic change due to insufficient control of timing or hidden latencies in the hardware. Earlier saccade detection can alleviate this risk.

We conclude that implementing efficient gaze-contingent display changes across saccades can be tricky, owing to a range of system latencies that have an impact on a paradigm's timing behavior. We as experimenters need to examine these latencies closely in order to draw the right conclusions from our results. Early online saccade detection can assist greatly in this task, as it saves valuable time for the setup to perform the intended (trans-saccadic) changes, but it comes at the cost of reduced online saccade detection accuracy—especially at higher noise levels—making it ultimately harder to smoothly collect data. The algorithm proposed here outperforms traditional detection methods in speed and accuracy, while adjusting detection thresholds in response to increased noise levels. These properties make it a reliable tool even when collecting data under suboptimal recording circumstances, as well as computationally feasible to use for the online scenario, due to its near real-time processing and linear complexity. Finally, the open-source availability of the code leaves it open for researchers to use and adapt the algorithm to their specific needs, making it a versatile tool for the field of active vision.

Acknowledgements We acknowledge the significant contributions of Ralf Engbert, Konstantin Mergenthaler, Petra Sinn, and Hans Trukenbrod for making the code of their microsaccade detection toolbox publicly available, as well as Nicolas Devillard for the excellent ANSI C implementations and comparisons of different median search algorithms (http://ndevilla.free.fr/median/median/index.html). R.S. was supported by the Studienstiftung des deutschen Volkes and the Berlin School of Mind and Brain. M.R. was supported by the Deutsche Forschungsgemeinschaft (DFG, grants RO3579/2-1, RO3579/8-1, and RO3579/10-1).

Availability Implementations of the proposed algorithm in C, Python, and Matlab are available on Github: https://github.com/richardschweitzer/OnlineSaccadeDetection.

Open practices statement The saccade data and code used for simulations, data collected throughout the experimental test, experimental code, and data analysis scripts are available on the Open Science Framework: https://osf.io/3pck5/. The experimental test was not preregistered.

Author contributions R.S. implemented the algorithm and ran simulations. Validation procedure was conceptualized by R.S. and M.R. The

experimental test was designed, run, and analyzed by R.S. under M.R.'s supervision. R.S. drafted the manuscript, and M.R. provided critical revisions.

References

Arabadzhiyska, E., Tursun, O. T., Myszkowski, K., Seidel, H.-P., & Didyk, P. (2017). Saccade landing position prediction for gaze-contingent rendering. *ACM Transactions on Graphics*, *36*, 50.

Balsdon, T., Schweitzer, R., Watson, T. L., & Rolfs, M. (2018). All is not lost: Post-saccadic contributions to the perceptual omission of intra-saccadic streaks. *Consciousness and Cognition*, *64*, 19–31.

Bates, D., Mächler, M., Bolker, B., & Walker, S. (2015). Fitting linear mixed-effects models using lme4. *Journal of Statistical Software*, *67*, 1–48. doi:https://doi.org/10.18637/jss.v067.i01

Bedell, H. E., & Yang, J. (2001). The attenuation of perceived image smear during saccades. *Vision Research*, *41*, 521–528.

Burr, D. C., Holt, J., Johnstone, J. R., & Ross, J. (1982). Selective depression of motion sensitivity during saccades. *Journal of Physiology*, *333*, 1–15.

Burr, D. C., Morrone, M. C., & Ross, J. (1994). Selective suppression of the magnocellular visual pathway during saccadic eye movements. *Nature*, *371*, 511–513. doi:https://doi.org/10.1038/371511a0

Campbell, F. W., & Wurtz, R. H. (1978). Saccadic omission: Why we do not see a grey-out during a saccadic eye movement. *Vision Research*, *18*, 1297–1303.

Castet, E. (2010). Perception of intra-saccadic motion. In U. J. Ilg & G. S. Masson (Eds.), Dynamics of visual motion processing (pp. 213–238). Berlin, Germany: Springer.

Castet, E., Jeanjean, S., & Masson, G. S. (2002). Motion perception of saccade-induced retinal translation. *Proceedings of the National Academy of Sciences*, *99*, 15159–15163.

Castet, E., & Masson, G. S. (2000). Motion perception during saccadic eye movements. *Nature Neuroscience*, *2*, 177–183.

Collewijn, H., Erkelens, C. J., & Steinman, R. M. (1988). Binocular co-ordination of human horizontal saccadic eye movements. *Journal of Physiology*, *404*, 157–182.

Collins, T., Rolfs, M., Deubel, H., & Cavanagh, P. (2009). Post-saccadic location judgments reveal remapping of saccade targets to non-foveal locations. *Journal of Vision*, *9*(5), 29. doi:https://doi.org/10.1167/9.5.29

Cornelissen, F. W., Peters, E. M., & Palmer, J. (2002). The Eyelink Toolbox: Eye tracking with MATLAB and the Psychophysics Toolbox. *Behavior Research Methods, Instruments, & Computers*, *34*, 613–617. doi:https://doi.org/10.3758/BF03195489

Dalmaijer, E. S., Mathôt, S., & Van der Stigchel, S. (2014). PyGaze: An open-source, cross-platform toolbox for minimal-effort programming of eyetracking experiments. *Behavior Research Methods*, *46*, 913–921. doi:https://doi.org/10.3758/s13428-013-0422-2

Delorme, A., & Makeig, S. (2004). EEGLAB: An open source toolbox for analysis of single-trial EEG dynamics including independent component analysis. *Journal of Neuroscience Methods*, *134*, 9–21. doi:https://doi.org/10.1016/j.jneumeth.2003.10.009

Deubel, H., Elsner, T., & Hauske, G. (1987). Saccadic eye movements and the detection of fast-moving gratings. *Biological Cybernetics*, *57*, 37–45.

Deubel, H., Schneider, W. X., & Bridgeman, B. (1996). Postsaccadic target blanking prevents saccadic suppression of image displacement. *Vision Research*, *36*, 985–996. doi:https://doi.org/10.1016/0042-6989(95)00203-0

Diamond, M. R., Ross, J., & Morrone, M. C. (2000). Extraretinal control of saccadic suppression. *Journal of Neuroscience*, *20*, 3449–3455.

Dimigen, O., Sommer, W., Hohlfeld, A., Jacobs, A. M., & Kliegl, R. (2011). Coregistration of eye movements and EEG in natural reading: Analyses and review. *Journal of Experimental Psychology: General*, *140*, 552–572. doi:https://doi.org/10.1037/a0023885

Dorr, M., Martinetz, T., Gegenfurtner, K. R., & Barth, E. (2010). Variability of eye movements when viewing dynamic natural scenes. *Journal of Vision*, *10*(10), 28. doi:https://doi.org/10.1167/10.10.28

Duyck, M., Collins, T., & Wexler, M. (2016). Masking the saccadic smear. *Journal of Vision*, *16*(10), 1. doi:https://doi.org/10.1167/16.10.1

Engbert, R., & Kliegl, R. (2003). Microsaccades uncover the orientation of covert attention. *Vision Research*, *43*, 1035–1045. doi:https://doi.org/10.1016/S0042-6989(03)00084-1

Engbert, R., & Mergenthaler, K. (2006). Microsaccades are triggered by low retinal image slip. *Proceedings of the National Academy of Sciences*, *103*, 7192–7197.

Engbert, R., Rothkegel, L., Backhaus, D., & Trukenbrod, H. A. (2016). *Evaluation of velocity-based saccade detection in the smi-etg 2W system* [Technical Report]. Retrieved from http://read.psych.uni-potsdam.de/attachments/article/156/TechRep-16-1-Engbert.pdf

García-Pérez, M. A., & Peli, E. (2011). Visual contrast processing is largely unaltered during saccades. *Frontiers in Psychology*, *2*, 247. doi:https://doi.org/10.3389/fpsyg.2011.00247

Han, P., Saunders, D. R., Woods, R. L., & Luo, G. (2013). Trajectory prediction of saccadic eye movements using a compressed exponential model. *Journal of Vision*, *13*(8), 27. doi:https://doi.org/10.1167/17.8.4

Higgins, E., & Rayner, K. (2015). Transsaccadic processing: Stability, integration, and the potential role of remapping. *Attention, Perception, & Psychophysics*, *77*, 3–27. doi:https://doi.org/10.3758/s13414-014-0751-y

Hollingworth, A., Richard, A. M., & Luck, S. J. (2008). Understanding the function of visual short-term memory: Transsaccadic memory, object correspondence, and gaze correction. *Journal of Experimental Psychology. General*, *137*, 163–181. doi:https://doi.org/10.1037/0096-3445.137.1.163

Kalogeropoulou, Z., & Rolfs, M. (2017). Saccadic eye movements do not disrupt the deployment of feature-based attention. *Journal of Vision*, *17*(8), 4. doi:https://doi.org/10.1167/17.8.4

Kleiner, M., Brainard, D., & Pelli, D. (2007). What's new in Psychtoolbox-3? *Perception*, *36*(ECVP Abstract Suppl), 14.

Mathôt, S., Melmi, J., & Castet, E. (2015). Intrasaccadic perception triggers pupillary constriction. *PeerJ*, *3*, e1150.

Matin, E., Clymer, A. B., & Matin, L. (1972). Metacontrast and saccadic suppression. *Science*, *178*, 179–182.

Melcher, D., & Colby, C. L. (2008). Trans-saccadic perception. *Trends in Cognitive Sciences*, *12*, 466–473. doi:https://doi.org/10.1016/j.tics.2008.09.003

Nyström, M., Andersson, R., Holmqvist, K., & Van De Weijer, J. (2013). The influence of calibration method and eye physiology on eyetracking data quality. *Behavior Research Methods*, *45*, 272–288. doi:https://doi.org/10.3758/s13428-012-0247-4

Panouillères, M. T., Gaveau, V., Debatisse, J., Jacquin, P., LeBlond, M., & Pélisson, D. (2016). Oculomotor adaptation elicited by intra-saccadic visual stimulation: Time-course of efficient visual target perturbation. *Frontiers in Human Neuroscience*, *10*, 91. doi:https://doi.org/10.3389/fnhum.2016.00091

Pelli, D. G. (1997). The VideoToolbox software for visual psychophysics: Transforming numbers into movies. *Spatial Vision*, *10*, 437–442. doi:https://doi.org/10.1163/156856897X00366

Poth, C. H., Foerster, R. M., Behler, C., Schwanecke, U., Schneider, W. X., & Botsch, M. (2018). Ultrahigh temporal resolution of visual presentation using gaming monitors and g-sync. *Behavior Research Methods*, *50*, 26–38.

Press, W. H., Teukolsky, S. A., Vetterling, W. T., & Flannery, B. P. (2007). Numerical recipes: The art of scientific computing (3rd ed.). Cambridge, UK: Cambridge University Press.

Prime, S. L., Vesia, M., & Crawford, J. D. (2011). Cortical mechanisms for trans-saccadic memory and integration of multiple object features. *Philosophical Transactions of the Royal Society B*, *366*, 540–553.

Rayner, K. (1975). The perceptual span and peripheral cues in reading. *Cognitive Psychology*, *7*, 65–81.

Ross, J., Morrone, M. C., Goldberg, M. E., & Burr, D. C. (2001). Changes in visual perception at the time of saccades. *Trends in Neurosciences*, *24*, 113–121.

Schweitzer, R., & Rolfs, M. (2017). Intra-saccadic motion streaks as a cue to the localization of objects across eye movements [Abstract]. *Journal of Vision*, *17*(10), 918. doi:https://doi.org/10.1167/17.10.918

Schweitzer, R., Watson, T., Watson, J., & Rolfs, M. (2019). The joy of retinal painting: A build-it-yourself device for intrasaccadic presentations. *Perception*, *48*, 1020–1025. doi:https://doi.org/10.1177/0301006619867868

SR Research. (2005). EyeLink II user manual, version 2.14. Mississauga, ON: SR Research Ltd.

SR Research. (2010). EyeLink 1000 user manual, version 1.5.2. Mississauga, ON: SR Research Ltd.

SR Research. (2013). EyeLink 1000 plus user manual, version 1.0.12. Mississauga, ON: SR Research Ltd.

Szinte, M., & Cavanagh, P. (2011). Spatiotopic apparent motion reveals local variations in space constancy. *Journal of Vision*, *11*(2), 4. doi:https://doi.org/10.1167/11.2.4

Tobii Technology AB. (2010). *Timing guide for Tobii eye trackers and eye tracking software* [Technical Report]. Retrieved from https://www.tobiipro.com/siteassets/tobii-pro/learn-and-support/design/eye-tracker-timing-performance/tobii-eye-tracking-timing.pdf

Townsend, J. T., & Ashby, F. G. (1978). Methods of modeling capacity in simple processing systems. In J. N. J. Castellan & F. Restle (Eds.), Cognitive theory (Vol. 3, pp. 199–239). New York, NY: Erlbaum.

Townsend, J. T., & Ashby, F. G. (1983). *Stochastic modeling of elementary psychological processes*. Cambridge University Press Archive.

Volkmann, F. C. (1986). Human visual suppression. *Vision Research*, *26*, 1401–1416.

Volkmann, F. C., Riggs, L. A., White, K. D., & Moore, R. K. (1978). Contrast sensitivity during saccadic eye movements. *Vision Research*, *18*, 1193–1199.

VPixx Technologies. (2017). TRACKPIXX3 hardware manual version 1.0. Saint-Bruno, QC: VPixx Technologies Inc.

Watson, T. L., & Krekelberg, B. (2009). The relationship between saccadic suppression and perceptual stability. *Current Biology*, *19*, 1040–1043.

Watson, T., Schweitzer, R., Castet, E., Ohl, S., & Rolfs, M. (2017). Intra-saccadic localisation is consistently carried out in world-centered coordinates [Abstract]. *Journal of Vision*, *17*(10), 1276. doi:https://doi.org/10.1167/17.10.1276

Wolf, C., & Schütz, A. C. (2015). Trans-saccadic integration of peripheral and foveal feature information is close to optimal. *Journal of Vision*, *15*(16), 1. doi:https://doi.org/10.1167/15.16.1

Yuval-Greenberg, S., Merriam, E. P., & Heeger, D. J. (2014). Spontaneous microsaccades reflect shifts in covert attention. *Journal of Neuroscience*, *34*, 13693–13700. doi:https://doi.org/10.1523/JNEUROSCI.0582-14.2014

5.1.3 Study III

Publication:

Schweitzer, R., & Rolfs, M. (2020). Intra-saccadic motion streaks as cues to linking object locations across saccades. *Journal of Vision*, 20(4):17, 1–24. doi: 10.1167/jov.20.4.17

Conference presentations:

Schweitzer, R. & Rolfs, M. (March, 2018). Localization of objects across saccades based on intra- saccadic motion streaks. Talk at the *60th TeaP (Tagung experimentell arbeitender Psychologen)*, Marburg, Germany.

Schweitzer, R. & Rolfs, M. (May, 2017). Intra-saccadic motion streaks as a cue to the localization of objects across eye movements. Talk at the *17th Annual Meeting of the Vision Sciences Society*, St. Petersburg (FL), USA.

Pre-registration, data, analyses:

Experiment 1: `https://osf.io/zszd9/`

Experiment 2: `https://osf.io/c95g6/`

Experiment 3: `https://osf.io/7apa8/`

Experiment 4: `https://osf.io/7q9pr/`

Featured code:

Pre-processing tools: `https://github.com/richardschweitzer/EyelinkEDFTools_R`

Re-use permissions:

"Ownership of the copyright shall remain with the Author(s), subject to the rights granted to ARVO in paragraphs 6 and 7. The Author(s) shall retain the non-exclusive right to any use of the Work, so long as the Author(s) provide(s) attribution to the place of original publication."

Source: `http://arvojournals.org/DocumentLibrary/ARVOLicensetoPublish.pdf` (accessed on July 20 2020)

Journal of Vision (2020) 20(4):17, 1–24

Intra-saccadic motion streaks as cues to linking object locations across saccades

Richard Schweitzer

Department of Psychology, Humboldt-Universität zu Berlin, Berlin, Germany
Bernstein Center for Computational Neuroscience Berlin, Berlin, Germany
Berlin School of Mind and Brain, Humboldt-Universität zu Berlin, Berlin, Germany

Martin Rolfs

Department of Psychology, Humboldt-Universität zu Berlin, Berlin, Germany
Bernstein Center for Computational Neuroscience Berlin, Berlin, Germany
Berlin School of Mind and Brain, Humboldt-Universität zu Berlin, Berlin, Germany

When visual objects shift rapidly across the retina, they produce motion blur. Intra-saccadic visual signals, caused incessantly by our own saccades, are thought to be eliminated at early stages of visual processing. Here we investigate whether they are still available to the visual system and could—in principle—be used as cues for localizing objects as they change locations on the retina. Using a high-speed projection system, we developed a trans-saccadic identification task in which brief but continuous intra-saccadic object motion was key to successful performance. Observers made a saccade to a target stimulus that moved rapidly either up or down, strictly during the eye movement. Just as the target reached its final position, an identical distractor stimulus appeared on the opposite side, resulting in a display of two identical stimuli upon saccade landing. Observers had to identify the original target using the only available clue: the target's intra-saccadic movement. In an additional replay condition, we presented the observers' own intra-saccadic retinal stimulus trajectories during fixation. Compared to the replay condition, task performance was impaired during saccades but recovered fully when a post-saccadic blank was introduced. Reverse regression analyses and confirmatory experiments showed that performance increased markedly when targets had long movement durations, low spatial frequencies, and orientations parallel to their retinal trajectory—features that promote intra-saccadic motion streaks. Although the potential functional role of intra-saccadic visual signals is still unclear, our results suggest that they could provide cues to tracking objects that rapidly change locations across saccades.

Introduction

The dystopian science-fiction television series "Black Mirror" featured an episode in which people could record memories through their pupils (Armstrong & Welsh, 2011). Replays of these memories revealed a common but wrong intuition of how our eyes capture the world around us. They showed skillfully crafted videos, with smooth camera movements from one location to the next. In reality, we make several saccadic eye movements every second that rapidly shift the entire image of the visual scene across the retina. Upon each new fixation, each object in the scene is projected onto a new part of the retina and processed by new populations of neurons throughout retinotopic visual cortex. Yet, these jerky displacements are not part of our perceptual experience—the visual world is stable. Whereas this phenomenon has received attention for centuries and has inspired research and theory to this date (Binda & Morrone, 2018; Burr & Morrone, 2011; Cavanagh, Hunt, Afraz, & Rolfs, 2010; Hall & Colby, 2011; Higgins & Rayner, 2015; Marino & Mazer, 2016; Wurtz, 2018; Ziesche & Hamker, 2014), a fundamental question remains unanswered: How does the visual system keep track of an object that is changing locations on the retina as the eyes move (Rolfs, 2015; Wurtz, 2008)? That is, how do we determine a correspondence between two successive views of an object across a saccade?

Here we hypothesized that intra-saccadic information could contribute to object identification across saccades.

Citation: Schweitzer, R. & Rolfs, M. (2020). Intra-saccadic motion streaks as cues to linking object locations across saccades. *Journal of Vision*, *20*(4):17, 1–24, https://doi.org/10.1167/jov.20.4.17.

https://doi.org/10.1167/jov.20.4.17 Received July 13, 2019; published April 25, 2020 ISSN 1534-7362

For example, motion streaks, which occur due to the slow integration of visual signals at early stages of visual processing (Geisler, 1999), are generated each time eye movements cause object movement across the retina (Bedell & Yang, 2001; Brooks, Impelman, & Lum, 1981; Duyck, Collins, & Wexler, 2016; Matin, Clymer, & Matin, 1972). Motion streaks—and intra-saccadic smear in general—imposed by our own eye movements have been widely considered a hindrance to perceptual stability that are counteracted by specialized mechanisms and thus eliminated from perception (for a collection of examples, see Castet, 2010). These mechanisms range from passive accounts, such as shearing forces in the retina that reduce visual sensitivity during saccades (Richards, 1969) and pre- and post-saccadic masking (Castet, 2010; Matin et al., 1972), to active suppression of information in the magnocellular pathway (Burr, Morrone, & Ross, 1994; Ross, Morrone, Goldberg, & Burr, 2001), as well as combinations of these (Volkmann, Riggs, White, & Moore, 1978; Wurtz, 2018). We know, however, that intra-saccadic motion perception is possible if the stimulus has a velocity similar to that of the saccade (Castet & Masson, 2000; Castet, Jeanjean, & Masson, 2002). Similarly, if the visual scene is briefly illuminated during a saccade, observers have a clear impression of a smeared and blurry visual scene (Campbell & Wurtz, 1978). In addition, stimuli undergoing saccadic suppression can still influence post-saccadic judgments, even if the observer is unaware of them (Watson & Krekelberg, 2009). Recently, the hypothesis has been proposed that effectively modulating the spatiotemporal power distribution in the retinal image saccades enhances low spatial frequencies (SFs) and thus facilitates a coarse-to-fine strategy of post-saccadic visual processing (Boi, Poletti, Victor, & Rucci, 2017; Rucci, Ahissar, & Burr, 2018). Indeed, Boi et al. (2017) showed that contrast sensitivity to post-saccadic low SF (but not high SF) information is greater if the stimulus has its onset during the saccade than if the same stimulus is presented with a contrast ramp during fixation. A functional role of visual processing during the saccade might thus be facilitating the processing of coarse information during early fixation. In particular, a potential function role of intra-saccadic visual information, such as motion streaks, remains elusive.

Perception of intra-saccadic motion streaks induced by saccades across a static stimulus (often presented in a dimly lit, uniform background or in complete darkness) has been investigated in past studies. For example, Matin et al. (1972) investigated the perceived length of motion streaks induced by varying on-durations of a single light source, and Brooks et al. (1981) studied the threshold elevation in detecting them independent of pre- and post-saccadic masks during both real and simulated saccades. Bedell and Yang (2001) used a similar paradigm and found that, given similar prolonged post-movement durations of the light source being on, perceived streaks were still significantly longer during fixation than during saccades, suggesting an additional attenuation of smear around saccades. More recently, Duyck et al. (2016) used an objective technique to quantify streak efficiency by tasking their participants with localizing a gap (realized by briefly dimming a light-emitting diode during the saccade) in an intra-saccadic motion streak.

All of the studies showed that the perceived streak was directly related to presentation duration, revealed the location of the inducing light source, and could be attenuated by presenting prolonged post-movement endpoints. Although it is again impossible to conclude from these results whether or not intra-saccadic motion streaks are relevant to the visual system, the hypothesis that they could be is informed by three insights. First, motion and contrast detection during saccades have been shown to be possible, provided that the presented stimulus has been optimized for the direction and velocity of the saccade (Castet & Masson, 2000; Castet et al., 2002; García-Pérez & Peli, 2011; Mathôt, Melmi, & Castet, 2015; Schweitzer & Rolfs, 2019). Second, information undergoing perceptual omission is not eliminated from visual processing (Watson & Krekelberg, 2009). Third, in a static visual environment, self-induced retinal input is related to any ongoing eye movement and could thus provide information about the direction, amplitude, and velocity of eye movements (Matin et al., 1972).

To test the hypothesis whether it is, in principle, possible to use strictly intra-saccadic continuous object motion to link the identities of objects across saccades as they change locations on the retina, we developed a trans-saccadic identification paradigm. Observers (N = 15) made a saccade toward a target stimulus in the visual periphery. Upon saccade landing, the display contained two stimuli—the target stimulus and an identical distractor—one above and one below the target's previous location. Observers had to identify the original target stimulus, which had moved rapidly but continuously to its new location as the eyes were in flight (see Methods section). The distractor stimulus, in turn, merely appeared on the opposite side as soon as the target stimulus had reached its final location. To identify the target stimulus in a two-alternative forced choice task (Figure 1a), therefore, observers could not simply rely on detecting a displacement (Brooks, Yates, & Coleman, 1980; Wexler & Collins, 2014) or use efficient encoding of the pre-saccadic object location in memory (Zimmermann, Morrone, & Burr, 2013), as they would in a classic saccadic suppression of displacement task (Bridgeman, Hendry, & Stark, 1975), because the size of the displacements was always the same for both post-saccadic stimuli and thus entirely predictable across all trials. Instead, in our task intra-saccadic continuous object motion was

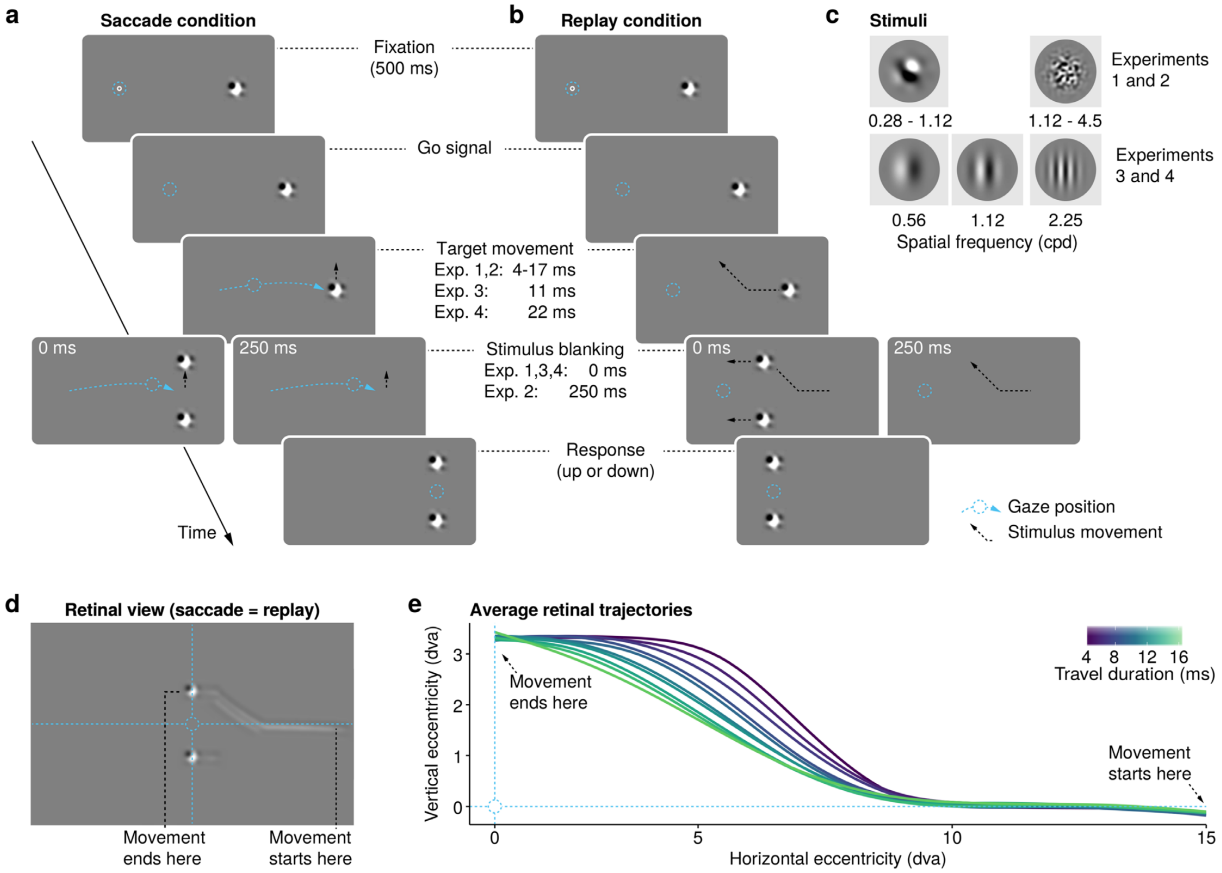

Figure 1. Experimental procedure. (a) Saccade condition, where human observers made horizontal saccades of 14.6 dva to a target stimulus. Upon saccade detection, the target moved either up or down by 3.6 dva with short movement durations (4–17 ms). In Experiments 1, 3, and 4, a second, identical distractor stimulus was presented immediately upon completion of the stimulus movement, at the alternative location, opposite the target stimulus. In Experiment 2, the target stimulus disappeared as soon as it reached its final vertical position and reappeared along with a distractor after a 250-ms blanking period. (b) Replay condition, where, in a fixation condition, we simulated intra-saccadic retinal input by replaying the trajectory of the stimulus according to the observer's own eye movement as recorded in the saccade session. (c) In Experiments 1 and 2, stimuli were 50% contrast noise patches in a Gaussian aperture ($SD = 0.45$ dva), bandpass-filtered to either low SF (0.28–1.12 cpd) or high SF (1.12–4.5 cpd). In Experiments 3 and 4, stimuli were Gabor patches of varying orientations (sigma = 0.45 dva) with SF of 0.56, 1.12, or 2.25 cpd. (d) Illustration of retinal stimulus trajectories in an example trial (rightward saccade and upward stimulus movement). Stimulus movements in both saccade and replay conditions would produce the same retinal trajectories, but only the target stimulus could produce a continuous streak. The shape of that streak depends on both saccade and stimulus speed. (e) Average retinal trajectories for the range of movement durations used (shown again for rightward saccades and upward stimulus movements).

the key to linking the target's pre- and post-saccadic locations.

Presenting precise, continuous object motion during the brief saccadic interval required visual presentation at speeds an order of magnitude faster than standard laboratory screens can display. Using a digital light processing (DLP) projector tailored to this purpose, we updated stimulus positions at submillisecond resolution strictly during the saccade and achieved high velocities of vertical motion ranging from 213 to 853 degrees of visual angle (dva) per second due to extremely short movement durations (4 to 17 ms). To ensure that participants could perform the task in principle and to have a comparison for performance during saccades, we also assessed performance during fixation. To this end, we upsampled participants' eye movement data (recorded at 500 Hz) to the frequency of the projector (updating the display at 1440 Hz) and replayed

the trajectory of the stimulus in a second session (Figure 1b). This procedure simulated the retinal consequences of the saccade task with high temporal fidelity.

Across four experiments, we investigated to what extent the rapid movement of objects across the retina induced by combined stimulus and eye movements informs the identification of the original pre-saccadic object from the two identical post-saccadic objects. We found that performance in this trans-saccadic identification task was influenced by the distinctness of the motion streak as induced by intra-saccadic retinal object movement, as well as by its temporal and spatial extent throughout the saccade. Subtle motion streaks, available for a short period during the saccade, yield only low, yet above-chance, performance (Experiments 1 and 3), unless post-movement blanking interval is introduced (Experiment 2). In contrast, performance increased to a large extent when high-contrast objects with an orientation optimized for the retinal trajectory of the stimulus moved over large portions of the saccade (Experiment 4). Given that static, salient objects in the visual scene generate intra-saccadic visual input throughout the entire duration of the saccade, these results invite the intriguing hypothesis that they might provide a parsimonious visual cue that helps the visual system to keep track of retinal locations of objects across saccades.

Methods

Participants

Fifteen participants per experiment were recruited through word of mouth and campus mailing lists. They had normal or corrected-to-normal vision and gave written informed consent prior to beginning the experiment. Monetary reimbursement was offered for their time. The study was conducted in agreement with the latest version of the Declaration of Helsinki and approved by the Ethics Committee of the German Society for Psychology, and participants provided written informed consent before participation. All experiments reported here were preregistered on the Open Science Framework (see below).

Experiment 1

Two sessions (saccade and replay, each a maximum of 800 trials) were run on separate days. Participants (10 female, 5 male) had a mean age of 25.5 years (range, 19–40) and received 18 Euros for both sessions. Ten of 15 participants had right ocular dominance, and 14 participants were right-handed. Ocular dominance was determined using a variant of the Porta test (Della Porta, 1593). Observers were asked to align both hands relative to a salient vertical line in their environment. By closing one eye or the other in alternation, they reported which eye caused a larger horizontal shift of the world. Pre-registration, data, and participant data can be found on the Center for Open Science website (https://osf.io/zszd9).

Experiment 2

Participants (9 female, 6 male) with a mean age of 22.7 years (range, 18–28) completed two sessions (maximum of 800 trials) on separate days and received 18 Euros for both sessions. Nine participants had right ocular dominance, and 13 participants were right-handed. Pre-registration and data can be found at https://osf.io/c95g6/.

Experiment 3

Thirteen female and three male participants with a mean age of 23.7 years (range, 19–39) completed two sessions (maximum of 768 trials) on separate days and received 16 Euros for both sessions. As in the second experiment, nine participants had right ocular dominance, and 13 participants were right-handed. Pre-registration and data can be found at https://osf.io/7apa8/.

Experiment 4

Nine female and six male participants with a mean age of 25 years (range, 18–31) completed one session (maximum of 768 trials) and received 10 Euros as remuneration. Out of a total of 15 participants, nine had right ocular dominance, and 14 participants were right-handed. Pre-registration and data can be found at https://osf.io/7q9pr/.

Apparatus

Stimuli were projected onto a 200 × 113 cm video-projection screen (Celexon HomeCinema, Tharston, Norwich, UK), using a Propixx DLP Projector (Vpixx Technologies, Saint-Bruno, QC, Canada) running at a temporal resolution of 1440 frames per second and a spatial resolution of 960 × 540 pixels^2. Experiments took place in a dimly lit, sound-attenuated room. The gray background used in all experiments had an average luminance of 30 cd/m^2. Observers sat 270 cm from the projector with their head supported by a chin rest. Eye movements were measured using an Eyelink 2 head-mounted system (SR Research, Osgoode, ON, Canada) with a sampling rate of 500 Hz. Stimulus display was implemented in MATLAB 2015a (MathWorks, Natick, MA, USA), using Psychtoolbox (Brainard, 1997; Kleiner, Brainard, Pelli, Ingling, Murray, & Broussard, 2007) and Eyelink Toolbox (Cornelisen, Peters, & Palmer, 2002) extensions, running on a Dell Precision T7810 Workstation with a Debian 8

operating system (Round Rock, TX, USA). Responses were collected via a standard US-English keyboard.

Stimuli

All stimuli, both noise and Gabor patches, were enveloped in a Gaussian window with a standard deviation of 0.45 dva. The fixation dot used in all experiments and sessions was a white circle of 0.3-dva radius. When fixated, the area within the circle was filled by another white circle of 0.1-dva radius.

Experiments 1 and 2

Stimuli were random noise patches (Gaussian pixel noise) of low or high SFs, bandpass-filtered either from 0.28 to 1.125 cycles per degree of visual angle (cpd) or from 1.125 to 4.5 cpd (see Figure A6 in the Appendix). All noise patches were scaled to an amplitude of 0.5, thus reducing their contrast to 50%.

Experiments 3 and 4

Stimuli were Gabor patches of varying SF (0.56, 1.125, or 2.25 cpd) and orientation (0°, 45°, 90°, or 135°). In Experiment 3 their contrast was 50%, whereas in Experiment 4 a contrast of 100% was used. Phases were 0° or 180°, so that patches were mid-gray at their center.

Procedure

Saccade and replay trials were performed in separate sessions on separate days. All trials within a session were presented in a random and interleaved fashion. There was an equal proportion of rightward and leftward saccades and of upward and downward stimulus movement.

Saccade session

Participants fixated a dot in the left or right half of the screen at 7.4 dva horizontal eccentricity from the screen center. Fixation control was passed after 500 ms of fixation within a 1.3-dva radius around the fixation dot. After 5 seconds without fixation or 25 re-fixations, the trial was aborted and a new calibration requested. The extinction of the fixation dot after successful fixation was the cue to make a saccade to the target stimulus, either to the right or to the left, which was located on the other half of the screen at 14.6-dva horizontal eccentricity. As soon as the saccade was detected (see Online saccade detection section), the target moved vertically upward or downward at high velocities (see below). By pressing either the arrow-up or arrow-down key on the keyboard, participants indicated whether the target stimulus moved up or down. To be able to respond, a participant's gaze position had to first reach the initial target location (i.e., a circular boundary of a 1.8-dva radius around the initial target area).

Experiment 1: Noise patch stimuli traveled a distance of 3.6 dva. The duration and speed of the movement were manipulated via the number of frames displayed between the start and end locations of the target: six to 24 frames in steps of two (0.7-ms frame duration), translating to movement durations of 4 to 17 ms and stimulus velocities of 213 to 853 dva/s. As soon as the target stimulus reached its final position, a similar distractor stimulus was displayed at the mirror location above or below the initial target location, so that after the saccade both identical stimuli were located at a 3.6-dva vertical eccentricity from the initial target location. From each participant (N = 15), we collected 10 trials in each experimental condition: session (2) × saccade direction (2) × stimulus movement direction (2) × stimulus movement duration (10) × stimulus SF (2). In subsequent analyses, we collapsed across saccade and stimulus movement directions, so that each experimental cell (session × stimulus movement duration × stimulus SF) contained up to 40 trials per participant.

Experiment 2: All stimulus and procedure parameters were similar to Experiment 1; however, as soon as the target stimulus reached its final position, a blank screen was introduced for 250 ms before both the target and distractor stimulus reappeared. Similar to Experiment 1, there were 10 trials per experimental condition.

Experiment 3: Gabor patch stimuli traveled a distance of 3.6 dva for a duration of 11 ms (16 frames) at a corresponding velocity of 320 dva/s. There were eight trials per experimental condition: session (2) × saccade direction (2) × stimulus movement direction (2) × stimulus phase (2) × stimulus SF (3) × stimulus orientation (4). As in the two previous experiments, data were collapsed across saccade and stimulus movement directions.

Experiment 4: Gabor patch stimuli traveled a distance of 7.1 dva for a duration of 22 ms (32 frames), thus at a velocity equal to that for Experiment 3 (320 dva/s). Similar to Experiment 3, eight trials were run in each experimental condition.

Replay session

In the replay condition, the fixation dot was at screen center. Just as in the saccade session, fixation control was passed after 500 ms of fixation. Participants were required to remain in the initial fixation area while the target stimulus used in the saccade session moved from the periphery of the screen toward the central fixation point, depending on the direction of the saccade (from the right for leftward saccades or from the left

for rightward saccades). To imitate the movement of the stimulus across the retina during a saccade, eye movement data recorded in each trial of the saccade condition was saved, smoothed using a local regression algorithm (LOWESS) with a span of 13, and resampled to 1440 Hz to be replayed at a screen refresh rate during the replay condition. Thus, the saccadic velocity profile, the stimulus characteristics, and the stimulus movement in a specific trial remained largely the same in both saccade and replay conditions. To reduce the temporal uncertainty in the replay condition, the saccade onset was set to a fixed duration after cue onset which was determined by the observer's median saccade latency minus 100 milliseconds, as recorded in the saccade session. Only trials in which fixation control was passed, no wrong key was pressed, and no early responses occurred were included in the replay sessions.

Online saccade detection

Saccades were detected online using a custom-made velocity-based detection algorithm inspired by the Engbert-Kliegl detection algorithm for microsaccades (Engbert & Mergenthaler, 2006). Eye position was sampled online in all trials. With the onset of the saccade cue, all valid samples collected since the beginning of that fixation period served as input for the algorithm, which was repeatedly executed after every retrieval of a gaze position sample until the saccade was successfully detected. As a first step, eye position data, smoothed by a moving window of a span of five samples, were transformed into a two-dimensional velocity space for x and y coordinates separately. The velocity detection threshold was determined by the median velocity plus the median-based standard deviation multiplied by a factor of 15. To detect a saccade, at least the two most recent samples with a velocity above this threshold had to be registered. As an additional criterion, the direction of eye movement above threshold was computed. A horizontal rightward saccade was only detected when its direction was in the range of 360° ± 25°, whereas a leftward saccade had to be in the range of 180° ± 25°. A more thorough description of the algorithm can be found in Schweitzer and Rolfs (2019).

With a mean online saccade detection latency (online detection relative to saccade onset detected offline) of 12.5 ms (Experiment 1), 12.5 ms (Experiment 2), 12.3 ms (Experiment 3), and 11.4 ms (Experiment 4), we achieved physical stimulus onsets of ∼27 ms after the onset of the saccade (Figures A1 and A2 in the Appendix). This latency already includes a deterministic video latency of the ProPixx projection system used which occurs because the presentation of the ProPixx projector (unlike a CRT monitor) updates only once the entire signal because the refresh of the graphics card is transferred (the duration of one refresh cycle at 120 frames per second; personal communication, Peter April, June 2018; see also Schweitzer & Rolfs, 2019).

Data analysis

Preprocessing

Data preprocessing and all subsequent analyses were implemented in R (R Core Team, 2015). Trials were excluded in which participants did not pass fixation control, pressed a response key before reaching the initial target area, or pressed the wrong response key. Subsequently, saccades were detected offline using the velocity-based saccade detection algorithm by Engbert and Mergenthaler (Engbert & Mergenthaler, 2006), using a minimum duration of eight samples (i.e., 16 ms at a sampling rate of 500 Hz) and a threshold parameter value of 5. We excluded trials in which saccades could not be detected or participants made more than two saccades (between saccade cue onset and reaching the saccade target area). Trials with one or two saccades (e.g., in case of a single corrective saccade) were included for analysis if the amplitude of the primary saccade was within ±3.1 dva around the instructed saccade amplitude of 14.6 dva. This decision was based on the sum of the defined experimental target areas (i.e., a 1.3-dva radius around the fixation location and a 1.8-dva radius around the saccade target). As a next step, trials were excluded in which display frames during stimulus movement were dropped and therefore prolonged stimulus durations. Furthermore, we removed all trials in which online saccade detection did not succeed during the relevant saccade or stimulus movement was not finished before saccade offset.

To compute the physical onset and offset of the stimulus movement, we added the deterministic video latency of the projector of 8.3 ms (mentioned above) to the respective time stamps of the synchronization with the vertical blank (median latency for online saccade detection, 12 ms; median latency for physical stimulus onset relative to online saccade detection, 15 ms; median saccade duration, 62 ms). As it is crucial to determine the exact time of presentation during the saccade, we validated our procedure in a separate experiment using photodiode measurements (Schweitzer & Rolfs, 2019). Averaged across movement durations and participants, stimulus movements finished 24 ms (Experiment 1, $SD = 6.7$ ms), 25 ms (Experiment 2, $SD = 6.6$ ms), 29 ms (Experiment 3, $SD = 6.7$ ms), and 14 ms (Experiment 4, $SD = 5.8$ ms) before saccade offset. Crucially, these timings depended on both the presented movement duration and saccade duration. Because both saccade duration ($M = 62$ ms, $SD = 10$ ms) and physical stimulus onset relative to saccade onset ($M = 27$ ms, $SD = 2.2$ ms) were

largely similar across conditions (Figures A1 and A2), movement duration reliably predicted the time left until saccade offset ($\beta = -0.97$; $t = -9.6$; 95% CI, –1.17 to –0.78). Moreover, we excluded trials in which offline saccade detection produced unreasonable results, such as when saccade durations were longer or saccadic peak velocities were higher than the participant's individual 97.5% quantile (average cutoff at 90-ms saccade duration and 517 dva/s saccadic peak velocity). In addition, in the replay condition, trials were also excluded if a participant's gaze did not stay within 2 dva around the initial fixation zone. As a result, around three-quarters of the initial number of trials remained for analysis (see below and Open Methods at OSF, https://osf.io/7q9pr/). Summary statistics for saccadic peak velocity, saccade amplitude, saccade duration, saccade latency, and stimulus onset relative to the onset of the saccade are shown in Figures A1 and A2 in the Appendix.

Experiment 1: We excluded 26% of all trials in the saccade session and 29% of all trials in the replay session during preprocessing.

Experiment 2: We excluded 24% of trials in the saccade session and 19% of trials in the replay session during preprocessing.

Experiment 3: We excluded 29% of saccade trials and 21% of replay trials.

Experiment 4: In the saccade condition, 28% of trials were excluded.

Task performance

The sensitivity index (d') was computed for every observer and condition. Within-subject *SEM* values were computed based on Cousineau's method (Cousineau, 2005), applying Morey's correction (Morey, 2008). For hypothesis testing, task performance was modeled using linear mixed-effects models (Bates, Mächler, Bolker, & Walker, 2015) in which observers were added as the random factor (intercept only). Additional analyses on performance were conducted using logistic mixed-effects regression on the dichotomous response variable "correct response". To test the significance of fixed factors, we calculated 95% confidence intervals of estimates via bootstrapping (30,000 repetitions) and conducted hierarchical model comparisons using likelihood ratio tests.

Experiments 1 and 2: Target matching performance (expressed as d') was computed for each observer and within-subject conditions session, SF, and movement duration. In the models, movement duration (ms) was included as a continuous variable centered around the median value of the levels (i.e., 10.4 ms), and the factors of session and SF were contrast coded (session, –0.5 = replay, 0.5 = saccade; SF: –0.5 = high, 0.5 = low).

Experiments 3 and 4: Performance (expressed as d') was again computed for each observer and the within-subject conditions of session, SF, and relative orientation. In the models, relative orientation was treated as a dummy-coded ordered factor (reference condition was orthogonal) and SF (in cpd) as a continuous variable centered at its median level (i.e., 1.125 cpd), whereas sessions were again contrast coded (–0.5 = replay, 0.5 = saccade).

Estimating relative orientation

Retinal stimulus positions across time (i.e., stimulus position relative to current gaze position) were computed by subtracting the gaze position data of the participant's dominant eye (resampled to 1440 Hz for the replay session) during stimulus movement from the screen position vector of the stimulus. Subsequently, for each frame of stimulus display, we computed the direction of the moving stimulus across the retina in radians (0, vertical; $-\pi/4$, 45° tilt counter-clockwise; $\pi/4$, 45° tilt clockwise; $\pm\pi/2$, horizontal). The angle of retinal trajectory, as displayed in Figure A3 in the Appendix, was the median of all directions for each trial. Relative orientation was computed by subtracting the orientation of the stimulus from the angle of its retinal movement trajectory (see also Figures 3a–3e). As relative orientation would depend on saccade direction and stimulus movement direction, we normalized the angles in a way that values larger than zero represent retinal trajectories steeper than stimulus orientation.

Reverse regression

In Experiments 1 and 2, a reverse regression analysis was performed to determine which spatial frequencies and orientations drive correct responses. As a first step, similar to previous studies (Li, Barbot, & Carrasco, 2016; Wyart, Nobre, & Summerfield, 2012), we convolved noise patch stimuli with two Gabor filters (in sine phase and cosine phase) of varying orientations (from $-\pi/2$ to $\pi/2$ in 11 equal steps) and SFs (steps 0.28, 0.38, 0.52, 0.71, 0.96, and 1.31 cpd for low-SF noise patches and 1.31, 1.79, 2.43, 3.31, and 4.5 cpd for high-SF noise patches) and extracted the energy of each SF-orientation component (Figure 3a). In doing so, we obtained a two-dimensional energy map for each individual noise patch, which was normalized for each observer and SF condition (Figure 3b). Importantly, to compute correct filter responses to each orientation, Gabor filters were applied not only to orientations from $-\pi/2$ to $\pi/2$, but also to their counterparts from $-\pi/2 + \pi$ to $\pi/2 + \pi$. This was done because the real and imaginary parts of the filters are computed by sine and cosine, respectively; thus, filter responses for one orientation may be different from that orientation + π, although the orientation of the Gabor is the same (Movellan, 2002). As a consequence, the energy of an orientation in a noise patch was the mean of both of

Journal of Vision (2020) 20(4):17, 1–24

these filter responses. To allow a comparison across trials, orientations were subsequently transformed to relative orientations by subtracting orientation steps from the angle of retinal trajectory in the respective trial (Figures 3c–3e; see also the Estimating relative orientation section). Finally, relative orientation steps were organized in 10 bins with a width of $\pi/10$ and a center of 0. As a second step, logistic regressions were applied to predict correct responses from the filter responses (for an example, see Figure A4 in the Appendix). Movement duration was included as an additive continuous predictor to control for its effect on performance. Regressions were run in every experimental condition and component (experiment × session × relative orientation × SF). The log odds estimate of each model served as an indicator of how strongly correct responses were driven by a given component in a given experimental condition.

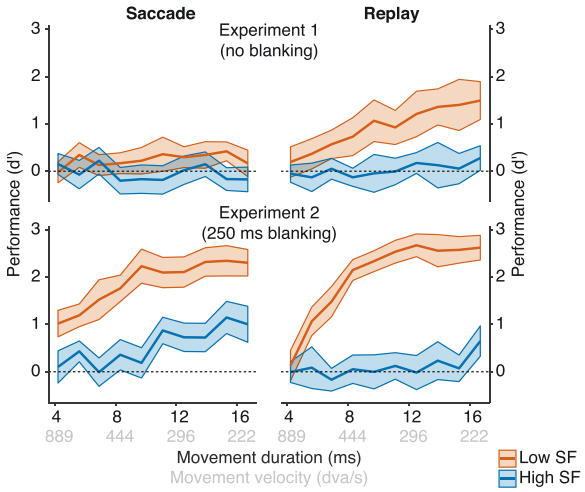

Figure 2. Target identification performance in Experiment 1 (top row) and Experiment 2 (bottom row). Mean performance (expressed as d') across participants (N = 15 in both experiments) as a function of stimulus movement duration in saccade (left column) and replay condition (right column). All error bars represent ±2 within-subject *SEM*. Movement durations translate directly to movement velocity, as the traveled distance was kept constant at 3.6 dva.

Results

In Experiment 1, the target stimulus was a noise patch (Figure 1c), bandpass-filtered to either low or high SF ranges. The target moved either up or down briefly after the onset of the saccade. As soon as the target had reached its final vertical position, we presented a distractor stimulus at the vertical location opposite of the target. Thus, whereas the target stimulus moved continuously, the distractor stimulus appeared when the target stimulus reached its final vertical position, forcing the participant to use intra-saccadic motion streaks (see Figure 1d for a schematic) to pair the post-saccadic target stimulus with the pre-saccadic one.

To quantify an observer's ability to link pre- and post-saccadic object locations in this task, we computed the sensitivity index (d') for each condition and observer. Overall, performance in the saccade condition was low but clearly above chance for low SF, with average $d' = 0.24$, $t(14) = 4.4$, and $P = 0.0006$; for high SF, $d' = -0.04$, $t(14) = -1.1$, and $P = 0.29$. To compare conditions, we fitted linear mixed-effects models (Bates et al., 2015) to these indices and computed confidence intervals for the given estimates using parametric bootstrapping (Table A1 in the Appendix for full model specification and results). Performance between saccade and replay conditions differed significantly when collapsed across SF and movement durations ($\beta = -0.38$; $t = -7.67$; 95% CI, –0.48 to –0.28) (Figure 2, upper row), and performance at longer movement durations was significantly lower in the saccade condition compared to the replay condition ($\beta = -0.064$; $t = -5.1$; 95% CI, –0.09 to –0.04), in particular at low SFs ($\beta = -0.05$; $t = -2.0$; 95% CI, –0.098 to –0.001). Although this finding is compatible with the general notion of saccadic suppression (i.e., the reduction of visual sensitivity before or during a saccade), the origin of poor localization performance remains unclear: Were intra-saccadic motion streaks actively suppressed from visual processing, or did post-saccadic masking limit the brief intra-saccadic input's access to conscious awareness?

We addressed this question in Experiment 2 (Figure 2, bottom row), in which we introduced a blanking period of 250 ms right after the target movement offset to alleviate post-saccadic masking (Campbell & Wurtz, 1978; Deubel, Schneider, & Bridgeman, 1996; Duyck et al., 2016). In the absence of a static post-saccadic retinal image and an immediate distractor stimulus, overall performance in the saccade condition improved drastically as compared to Experiment 1 ($d'_{\mathrm{Exp=1,saccade}} = 0.1$; $d'_{\mathrm{Exp=2,saccade}} = 1.2$; $t(28) = 7.15$; $P < 0.0001$), and was even higher than performance in the corresponding replay condition ($\beta = 0.16$; $t = 3.1$; 95% CI, 0.06–0.27). Although compared to the replay condition performance was again lower for low SF stimuli ($\beta = -0.57$; $t = -5.4$; 95% CI, –0.78 to –0.37), high SF stimuli were more accurately localized during the saccade than during fixation ($d'_{\mathrm{SF=high,replay}} = 0.1$; $d'_{\mathrm{SF=high,saccade}} = 0.55$; $t(14) = 3.3$; $P = 0.005$).

We designed the trans-saccadic identification task specifically such that the target and distractor stimulus

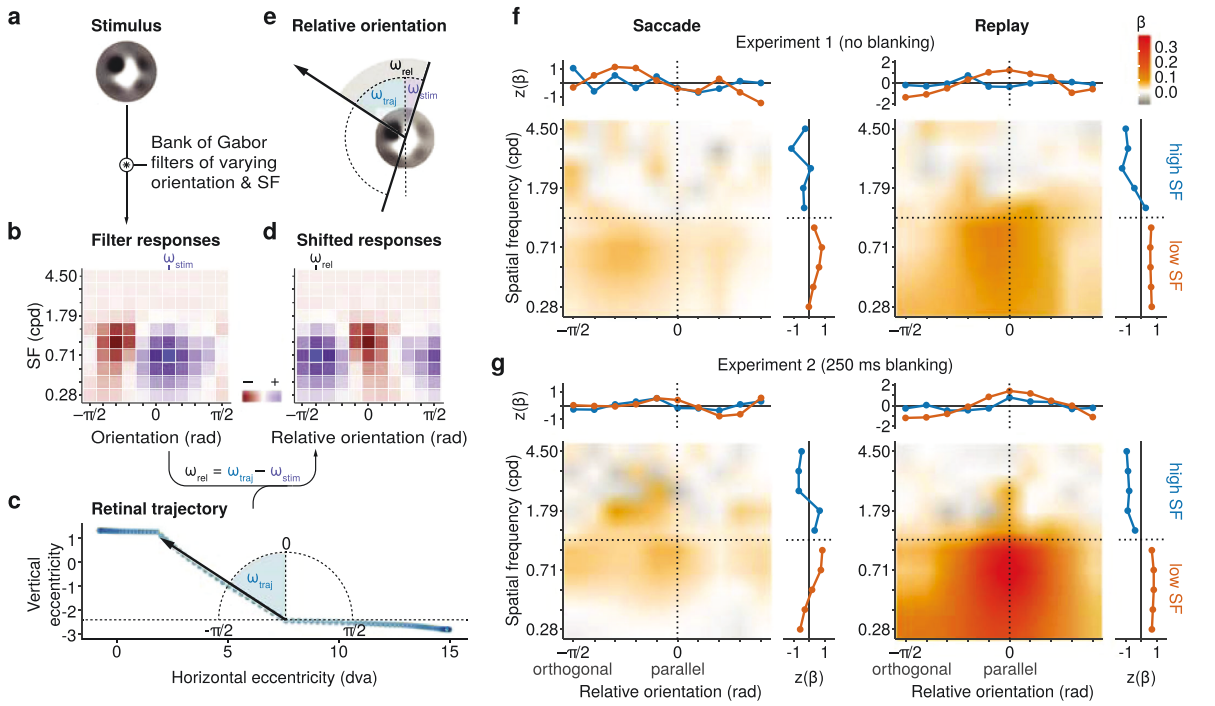

Figure 3. Impact of SF and relative orientation of a target stimulus on performance in Experiments 1 and 2, established using reverse regression. (a) The individual noise patch of each trial was convolved with a bank of Gabor filters of various orientations ($-\pi/2$ to $\pi/2$) and SFs (0.28–4.5 cpd), resulting in filter energy maps. (b) Each position in the array represents the energy of a certain oriented SF component in a stimulus. For example, the presented noise patch responds most strongly to a Gabor filter of 0.71 cpd and a tilt of 0.31 rad; ω_{stim} denotes the orientation component of the stimulus as presented on the screen (0 = vertical). (c) We derived the angle of the retinal trajectory of the target from the eye movement and stimulus movement data for each trial. Here, ω_{traj} represents the angle of the retinal trajectory. (d, e) Relative orientation (ω_{rel}) is computed by subtracting the orientations (ω_{stim}) of the stimulus from the angle of the retinal trajectory (ω_{traj}). Hence, the orientation space of each stimulus is normalized to its retinal movement trajectory (0 = stimulus orientation is parallel to its retinal movement trajectory). (f, g) Results from the reverse regression analysis of Experiment 1 and 2, respectively. Colors indicate the log odds estimate of logistic regressions fitted to predict correct responses from filter responses. High beta values for an oriented SF component indicate that these components drive correct identifications of post- and pre-saccadic stimuli. The marginal normalized means illustrate average relative orientation and SF tuning for low (red) and high (blue) SF subspaces.

could only be distinguished based on the continuous motion streak elicited by the target. More specifically, it is the vertical component of the streak, induced by the movement of the stimulus, that is crucial to correct identification of the target (Figure 1d). Note that, although such intra-saccadic stimulus movements rarely (if ever) occur in natural environments, we chose to use stimuli moving orthogonally to the direction of the saccade to separate the respective contributions of eye and stimulus movement to the generation of the streak. If, indeed, participants used intra-saccadic motion streaks to link object locations across saccades, then their performance in our task must be related to the distinctiveness of that vertical component. This distinctiveness should depend on at least three factors.

First, as the distance the target traveled was kept constant, shorter movement duration should yield less distinct streaks. Our results support this assumption, as longer movement durations (and, thus, lower retinal speeds) led to higher identification performance in both Experiment 1 ($\beta = 0.03$; $t = 5.3$; 95% CI, 0.02–0.045) and Experiment 2 ($\beta = 0.1$; $t = 15.0$; 95% CI, 0.09–0.11).

Second, at high retinal velocities (median saccadic peak velocity of 392 dva/s; see Figures A1 and A2 in the Appendix), low SFs yielded higher performance than high SFs (Burr & Ross, 1982). This, too, was borne out by Experiment 1 ($\beta = 0.59$; $t = 11.9$; 95% CI, 0.49–0.69) and Experiment 2 ($\beta = 1.62$; $t = 30.7$; 95% CI, 1.52–1.72). In addition, performance increased

with movement duration, in particular for low SF as compared to high SF stimuli in both Experiment 1 ($\beta = 0.056$; $t = 4.5$; 95% CI, 0.03–0.08) and Experiment 2 ($\beta = 0.08$; $t = 6.3$; 95% CI, 0.06–0.11), suggesting that low SFs also produced more distinct motion streaks when high retinal velocities were imposed by saccades.

Finally, stimuli with an orientation parallel to their movement trajectory result in lower temporal alternations between high and low luminance on the retina; thus, they should produce more pronounced streaks than stimuli with the orthogonal orientation. To explore the contribution of orientation relative to the retinal movement trajectory (henceforth referred to as relative orientation; see Figure 3 and Figures A3 and A5 in the Appendix), we used a reverse regression approach, implemented as a two-step procedure. First, we convolved the noise patch from every trial (Figure 3a) with Gabor filters of varying orientations and SFs (Li et al., 2016; Wyart et al., 2012). Each stimulus could thus be represented by an array of filter responses quantifying the energy of certain SF-orientation components in a given noise patch (Figure 3b). Stimulus orientations were subsequently converted to levels of relative orientation based on the retinal trajectory of each stimulus in each trial (Figures 3c–3e). In a second step, we used logistic regression to predict correct responses from the filter responses in a given component. Specifically, for each combination of experiment, session, relative orientation, and SF, we computed a beta weight describing to what extent that combination drove target identification performance (Figure A4 in the Appendix).

In the replay condition, this reverse regression analysis revealed a clear tuning around a relative orientation of zero. An orientation parallel to the movement trajectory of the stimulus was associated with higher performance, in particular at low SF (Figures 3f and 3g, right panels). In the saccade condition, tuning could also be observed, but it was less pronounced and shifted slightly toward negative relative orientations. The latter suggests that orientations more vertical than the angle of retinal trajectory were discriminated more accurately (Figures 3f and 3g, left panels). In addition, SFs below 0.5 cpd seemed to relate to correct identification less strongly in the saccade condition than in the replay condition. This is compatible with a reduction of contrast sensitivity around the onset of saccades, which is specific to very low SFs (Burr et al., 1982; Volkmann et al., 1978).

Although the reverse-regression analyses were planned (see pre-registrations), the random nature of noise patches renders this approach quasi-experimental; therefore, we conducted Experiment 3 to test whether the reverse regression results can be confirmed. Experiment 3 was identical to Experiment 1 in all respects, except that we replaced bandpass-filtered noise-patch stimuli with Gabor patches of a fixed number of SFs (0.56, 1.12, and 2.25 cpd) and orientations (horizontal, vertical, 45° clockwise, 45° counterclockwise). Importantly, depending on the horizontal saccade direction and the vertical stimulus movement direction—and given a specified movement duration (11.1 ms) that was optimal for the stimulus orientations used (Figure A3)—these orientations translated directly to a critical set of relative orientations. Stimuli were parallel, oblique, or orthogonal to the retinal trajectory of the stimulus (for an illustration, see Figure A5 in the Appendix). For example, given a rightward saccade, a Gabor with a counterclockwise tilt of 45° would have a parallel relative orientation if it moved upward and an orthogonal relative orientation if it moved downward.

Note that we devised Experiment 3 as a proof of concept (which we built upon in Experiment 4). As in the previous experiments, observers had to rely on short motion streaks generated during very brief periods of vertical motion (about 17% of the total duration of a saccade, in order to achieve strictly intra-saccadic presentations). Based on Experiment 1 and the fact that the stimulus was much less rich in orientation and SF content, we expected performance to be very low in the saccade condition. Indeed, as in Experiment 1, performance was much lower during saccades than during fixation (Figure 4a). Crucially, however, average target identification performance was significantly higher than chance for all SF levels, provided the Gabor orientation was parallel to its retinal motion trajectory, where $d'_{\text{parallel}} = 0.24$, $t(14) = 3.47$, and $P = 0.004$, but it was at chance for other orientations, such that $d'_{\text{not parallel}} = 0.05$, $t(14) = 0.99$, and $P = 0.34$ (Figure 4b). We next fitted linear mixed-effects models across both saccade and replay conditions (see Table A2 in the Appendix for the full model), as well as separately for each condition in a hierarchical model comparison. In the saccade condition, only relative orientation significantly increased log likelihood: $\Delta LL = +4.62$, $\chi^2(2) = 9.24$, and $P = 0.01$; neither SF, where $\Delta LL = +0.06$, $\chi^2(1) = 0.01$, and $P = 0.91$, nor an interaction of both factors, where $\Delta LL = +1.4$, $\chi^2(2) = 2.7$, and $P = .24$, did. In the replay condition, log likelihood increased with relative orientation: $\Delta LL = +30.7$, $\chi^2(2) = 61.4$, and $P < 0.0001$; SF: $\Delta LL = +8.2$, $\chi^2(1) = 16.4$, and $P < 0.0001$; and their interaction: $\Delta LL = +26.34$, $\chi^2(2) = 52.7$, and $P < 0.0001$. This shows that relative orientation mattered in both saccade and replay conditions and confirmed that targets with orientations parallel to the trajectory of the stimulus were identified more accurately. More accurate identification of low SF stimuli was evident only in the replay condition. This could have two explanations. Either performance is indeed independent of SFs during saccades or overall performance was just too low in the saccade condition to uncover any effects of SF.

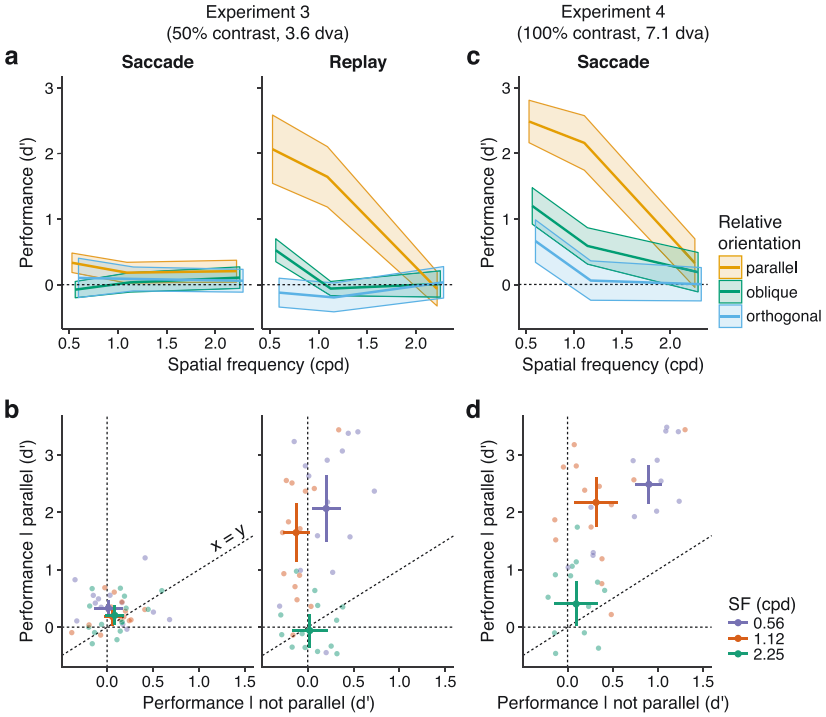

Figure 4. Target identification performance in Experiment 3 and 4. (a) Mean performance across participants (N = 15) as a function of relative orientation in the saccade condition (left column) and in the replay condition (right column) of Experiment 3. (b) Comparison of performance for parallel vs. non-parallel stimulus orientations in Experiment 3. Each dot represents one observer in a SF condition. For all SFs in the saccade condition, targets with orientations parallel to the motion trajectory were identified above chance. (c) Mean performance in Experiment 4 (N = 15) with stimuli at full contrast and twice the movement duration. (d) Comparison of performance for parallel vs. non-parallel stimulus orientations in Experiment 4. Performance was significantly higher for parallel stimulus orientations, in particular at low and medium SFs. All error bars represent ±2 within-subject *SEM*.

In Experiment 4, therefore, we investigated whether performance in the saccade task would improve compared to Experiment 3 if intra-saccadic streaks were more prominent, as they should be during natural vision. To this end, we doubled stimulus movement duration to 22 ms (about 35% of the total duration of a saccade) and increased the traveled distance to 7.1 dva, thus leaving stimulus velocity unaltered. We also increased stimulus contrast to 100%. As a consequence, intra-saccadic motion streaks extended further in time and space while keeping post-saccadic masking intact. Under these conditions, identification performance increased to a level previously found only during fixation or blanking. As in Experiment 3, it was by far the highest when Gabor patches were oriented parallel to their movement trajectory (Figure 4c). Indeed, compared to orthogonal orientations, performance was significantly higher in both oblique ($\beta = 0.46$; $t = 3.6$; 95% CI, 0.21–0.71) and parallel ($\beta = 1.61$; $t = 12.6$; 95% CI, 1.36–1.86) orientations (Table A2 in the Appendix). In addition, performance decreased with higher SFs ($\beta = –0.33$; $t = –2.67$; 95% CI, –0.58 to –0.09). Log-likelihood increased with relative orientation, where $\Delta LL = +40.4$, $\chi^2(2) = 80.8$, and $P < 0.0001$; with SF, where $\Delta LL = +18.0$, $\chi^2(1) = 36.1$, and $P < 0.0001$; and with their interaction, where $\Delta LL = +15.1$, $\chi^2(2) = 30.2$, and $P < 0.0001$. Although stimulus velocity remained unaltered compared to Experiment 3, performance increased markedly with longer streaks and enhanced contrast, demonstrating that relative orientation of a stimulus indeed predicts performance in keeping track of the original stimulus across the saccade by means of intra-saccadic motion streaks.

Discussion

Saccadic eye movements impose motion blur on the retina. Although this intra-saccadic smear has the potential to provide excellent visual feedback

about the movement of the eyes across the visual scene (Watson & Krekelberg, 2009), the resulting intra-saccadic blur is assumed to be suppressed to maintain perceptual stability (Burr et al., 1982; Castet, 2010; Ross et al., 2001). Here we studied intra-saccadic motion streaks induced by single objects moving rapidly across the retina during saccades, as a model example for intra-saccadic smear. We investigated the novel hypothesis that these intra-saccadic signals might serve a purpose in the visual system, facilitating trans-saccadic object localization by linking pre- and post-saccadic retinal object locations.

Visual processing of intra-saccadic motion smear

There is strong evidence that performance in our experiments relies on the detection of motion streaks rather than motion per se or simply luminance contrast. Geisler (1999) suggested that perception of motion streaks is likely grounded in motion detectors with both orientation and directional tuning (for neurophysiological evidence, see Geisler, Albrecht, Crane, & Stern, 2001) and therefore in motion and contrast mechanisms, provided that movement speeds are high enough to induce streaks and stimuli have sufficient contrast to allow the orientation-selective units to resolve the motion streak (Edwards & Crane, 2007). The key difference between previous studies on motion streaks and ours is the speed of the stimuli used. Whereas previous studies presented stimulus speeds of 1 to 24 dva/s (e.g., Apthorp & Alais, 2009; Edwards & Crane, 2007; Geisler, 1999), our stimuli induced retinal speeds (i.e., the vector sum of stimulus and eye movement speed) in the range of 300 to 1000 dva/s in both saccade and replay session.

That these speeds inevitably produce motion streaks is compatible not only with the phenomenological appearance of the stimuli (i.e., a blurred trace that is readily detectable when blanking is applied) but also with previous literature showing that contrast and motion perception alone at these high velocities is difficult or even impossible. Indeed, Burr & Ross (1982) showed that contrast sensitivity to a grating drifting at only 100 dva/s decreased by almost one log unit when its spatial frequency was increased from 0.1 to 0.7 cpd, and that gratings drifting at 800 dva/s could only be detected if their SF was below 0.1 cpd. Moreover, Schweitzer and Rolfs (2019) found that Gabor patches (0.5 cpd and 0.5 dva SD Gaussian aperture) rapidly drifting within their aperture (thus not producing any motion streaks) became impossible to detect during fixation when drift velocities came close to or exceeded saccadic peak velocities (~400 dva/s). Finally, Castet et al. (2002) presented striking evidence that intra-saccadic gratings (with orthogonal orientation to the saccade direction, saccadic peak velocities around 280 dva/s) induced motion percepts if their SFs were 0.04 and 0.18 cpd, but not if their SF was 1.81 cpd, because the latter induced temporal frequencies of ~500 Hz, which cannot be resolved by motion detectors.

Note that the high-SF stimuli applied in Experiments 1 and 2 (on average 2.25 cpd) could thus induce temporal frequencies from 675 to 2250 Hz on the retina when being moved at the speeds we used, which parsimoniously explains low performance in all high-SF conditions (including the replay conditions). Further support is provided by Experiments 3 and 4: If motion detection were the major predictor for performance in our paradigms, then we would expect that task performance would be best for Gabor stimuli (especially at low SF) if their orientation were orthogonal to their motion trajectory, as these orientations would optimally activate motion detectors (Adelson & Bergen, 1985; Reichardt, 1987). However, the contrary was the case. In both saccade and replay conditions, performance for orthogonal stimuli was rarely above chance level; instead, stimuli with orientations matching their retinal movement trajectory led to maximum task performance. These stimuli allowed for effective temporal summation; that is, they generated a streak.

This effect is consistent with the motion streak literature. Masks oriented parallel to the trajectory of a stimulus masked motion direction more efficiently than orthogonal masks (Burr & Ross, 2002; Geisler, 1999), and neurons in monkey V1 showed greater activation parallel to the direction of motion when motion was sufficiently fast to produce a streak (Geisler et al., 2001). These striking similarities suggest a specific role of motion streaks in our study that cannot be accounted for by contrast and motion detection mechanisms alone.

Our findings also demonstrate that intra-saccadic smear is not removed from visual processing but can lead to identification performance comparable to that found during fixation, as demonstrated by the blanking conditions used in Experiment 2. In fact, observers consistently reported a clear and vivid impression of a blurred trajectory, which was likely to drive localization performance in the blanking condition. Blanking is known to relieve saccadic suppression of displacement (Deubel et al., 1996), but given that stimulus motion was orthogonal (and not parallel) to the saccade direction and covered distances of more than 3 dva, observers had no trouble identifying the trans-saccadic stimulus displacements (Wexler & Collins, 2014). Instead, we assume that blanking alleviated post-saccadic masking. This assumption is compatible with results indicating that the prolonged presence of intra-saccadic stimuli beyond the end of the eye movement significantly reduces the amount and length of perceived smear (Balsdon, Schweitzer, Watson, & Rolfs, 2018; Bedell & Yang, 2001; Duyck et al., 2016; Matin et al., 1972).

Although temporal masking is often attributed to stimuli covering the entire display (Castet et al., 2002) or even the entire visual field (Campbell & Wurtz, 1978), it is possible to achieve similar effects with just simple flashes of light without a necessary spatial or retinal overlap, an effect attributed to meta-contrast masking (Matin et al., 1972). Interestingly, this mechanism has been shown to be equally effective both during real and simulated saccades (Brooks et al., 1980; Brooks et al., 1981). The absence of post-saccadic masking, however, is not representative for the circumstances of natural vision, where every intra-saccadic input is followed (and thus masked) by a more reliable and stable retinal image (Castet, 2010). Blanking therefore provided an estimate for an upper bound of identification performance in the saccade condition.

Remarkably, participants also achieved a similarly high level of performance during saccades even when post-saccadic masking was intact; provided the motion streaks extended over a large share of the saccade duration, the inducing stimuli had high contrast and orientations parallel to their retinal trajectory. In particular, using a motion streak duration of 22 ms in Experiment 4—covering just over a third of the saccade duration—performance drastically improved compared to Experiment 3, where stimuli moved across the retina at the same velocity and angle as in Experiment 4 but for only half the time (11 ms). As these experimental conditions are still quite specific and hardly comparable to vision under natural viewing conditions, one can at this point only speculate about whether motion streaks in natural scenes—where input is rich in SF, orientation, and color content, and motion streaks are present throughout the entire saccade—would enable reliable trans-saccadic identification. Further research will be needed to investigate how our results with motion streaks induced by single objects generalize to more complex large-field intra-saccadic smear: By moving entire visual scenes during saccades to increase, reduce, or eliminate induced smear, it would be possible to systematically investigate how intra-saccadic large-field smear impacts trans-saccadic object identification in more natural visual configurations.

Task performance during saccades and during fixation

With medium contrast stimuli, brief movement durations and post-saccadic masking intact (Experiments 1 and 3), target identification performance in the saccade condition was relatively poor compared to the replay condition. This was expected based on the short motion streak distinguishing the target from the distractor stimulus and was consistent with a number of established phenomena. First, the pre- and post-saccadic images might have acted as forward and backward masks, respectively. During real (as opposed to simulated) saccades, the entire visual field moves across the retina, causing the brief, feeble intra-saccadic input to be temporally surrounded by two powerful, high-intensity masks (Castet et al., 2002; Castet, 2010). This view is compatible with the explanation that the prolonged presence of intra-saccadic stimuli after saccade offset might have acted as a meta-contrast mask reducing perceived smear (Breitmeyer & Ganz, 1976; Campbell & Wurtz, 1978; Duyck et al., 2016; Matin et al., 1972).

Although the experiment was conducted in a dimly lit room, the screen border and immediate surroundings may have also contributed to the difference in saccade and replay conditions. For example, false screen borders (i.e., peripheral backgrounds surrounding a uniform presentation area) increased detection thresholds of peri-saccadic stimuli both during saccades and when moved at saccade-like speeds during fixation (Idrees, Baumann, Franke, Muench, & Hafed, 2019). These results suggest that peripheral large-field motion without overlap with the relevant stimulus can decrease visual performance during saccades. In our paradigm, the saccade condition caused such large-field motion, whereas the replay condition did not, even though the stimulus trajectories on the retina were similar. Second, contrast sensitivity decreases around the onset of the saccade, a phenomenon known as saccadic suppression (Burr et al., 1982). Although this effect is widely interpreted as a mechanism of active visual suppression to maintain perceptual stability (Burr et al., 1994; Ross et al., 2001), it was recently argued that this threshold elevation could be explained by signal-dependent noise introduced during saccade execution that subsequently leads to the down-weighting of peri-saccadic visual information (Crevecoeur & Körding, 2017). For example, using a blank screen, previous studies have observed an elevation of contrast threshold during real saccades (up to 50 ms after saccade offset), but not during simulated saccades (Diamond, Ross, & Morrone, 2000).

Alternatively, this effect could also be interpreted in terms of strictly visual factors, as there is evidence that a threshold elevation can occur already on the retinal level, such as in isolated mouse and pig retinae presented with saccade-like image displacements (Idrees et al., 2019). Finally, the sudden onset of the distractor stimulus right after completed target motion might have caused an attentional distraction from the brief intra-saccadic streak (Balsdon et al., 2018). Each of these effects might have also contributed to the difference between saccade and replay conditions. Moreover, saccades lead to other changes, such as attention shifts (Rolfs, Jonikaitis, Deubel, & Cavanagh, 2011) or changes in perceptual tuning (Li et al., 2016; Ohl, Kuper, & Rolfs, 2017), that cannot be controlled for in a simulated saccade condition.

Distinct motion streaks are associated with high task performance

Across all experimental conditions, we found that low SFs were identified more accurately than high SFs. Due to the high retinal velocities resulting from combined rapid eye and stimulus movement, high SF stimuli are rendered invisible, whereas low SFs—which are predominant in smeared visual scenes—remain resolvable (Burr, 1981; Burr & Ross, 1982). One interesting exception was the result that high SFs were more reliably identified during saccades than during fixation when the blanking period was introduced in Experiment 2. We speculate that this result is a consequence of well-established effects: During the preparation of a saccade, visuospatial attention selected the target of the movement (Deubel & Schneider, 1996; Kowler, Anderson, Dosher, & Blaser, 1995; Ohl et al., 2017; Rolfs & Carrasco, 2012), increasing visual sensitivity for high SFs in an obligatory fashion (Li et al., 2016; Li, Pan, & Carrasco, 2019). In the context of our task, this increase in sensitivity at the saccade target could have led to two complementary phenomena. On the one hand, masking of high-SF stimuli may have been more efficient when targets were present upon saccade landing, which was the case in Experiments 1, 3, and 4. On the other hand, performance for high-SF stimuli may have been enhanced when post-saccadic masking was alleviated by the blanking condition. These effects could well explain the enhanced performance for high-SF intra-saccadic stimuli in Experiment 2.

In most conditions, however, correct target identifications were strikingly more prominent for low-SF stimuli. In classic studies of saccadic suppression, however, the strongest reductions in contrast sensitivity were found at low SFs (Burr et al., 1982; Volkmann et al., 1978). This result has been taken to suggest that the visual system selectively removes SF content that dominates intra-saccadic stimulation to preserve visual stability, possibly by raising thresholds specifically in the magnocellular pathway (Burr et al., 1994; Ross et al., 2001). Indeed, it has been suggested that a modulation of visual processing around saccades occurs as early as in the lateral geniculate nucleus (Sylvester, Haynes, & Rees, 2005; Thilo, Santoro, Walsh, & Blakemore, 2004). Although the lowest SFs used in our experiments (0.28 cpd in Experiments 1 and 2; 0.56 cpd in Experiments 3 and 4) were still a tenfold higher than the lowest SFs used in studies of saccadic suppression, (i.e., 0.02–0.04 cpd) (e.g., Burr et al., 1982; Burr et al., 1994; Diamond et al., 2000), we found that low-SF stimuli could be identified most accurately. In contrast to studies of saccadic suppression, however, we presented stimuli at medium to high contrasts rather than at threshold. Indeed, recent evidence shows that saccades reformat the visual input signal to emphasize post-saccadic low-SF information (Boi et al., 2017). Thus, intra-saccadic visual signals are not eliminated from visual processing and could constitute a valuable source for trans-saccadic object identification.

Most previous studies on intra-saccadic motion streaks used oscilloscopes (e.g., Bedell & Yang, 2001; Brooks et al., 1980; Brooks et al., 1981) or light-emitting diodes (e.g., Duyck et al., 2016), allowing for limited control over the stimulus. The application of noise and Gabor patches made it possible to study observers' performance as a function of streak distinctiveness while controlling for contrast, SF, and duration. Exploratory reverse regression suggested an effect of relative orientation; that is, orientations parallel to the retinal motion direction elicit stronger motion streaks, probably due to effective signal summation (Burr, 1981). Experiments 3 and 4 confirmed this hypothesis by showing that Gabor stimuli were identified more accurately when their orientation matched their retinal trajectory. Although this result provides strong evidence that the features of the target (and its resulting intra-saccadic motion streak) drove performance in our task, one might argue that the transient of the distractor onset contributed to observers' decisions. Several points speak against this assumption: First, in the non-blanking experiments, both target and distractor were always displayed at their final locations at the same time, so that temporal offset could not be used as a cue. Second, even if the onset of the distractor did inform responses along with the target, the efficiency of the streak of the target must have nevertheless been processed for it to be used as a contrast in this two-alternative forced-choice task. Third, we have shown previously that transients of irrelevant distractors can impair direction judgments of intra-saccadic stimulus movement (Balsdon et al., 2018), suggesting that if any effect was present then the onset of the distractor in our paradigm would have had a negative effect on task performance.

Ecological validity of the paradigm

Given our setup and the nature of the task, the effect of relative orientation had to be investigated in a sparse and artificial setting that does not necessarily represent visual processes under natural circumstances. We speculate, however, that even in natural vision, where the amount of visual information is undoubtedly denser and more cluttered, motion streaks may play a role when saccade directions match stimulus orientations available in the scene. Indeed, both saccades (Najemnik & Geisler, 2008; Otero-Millan, Macknik, Langston, & Martinez-Conde, 2013) and the distribution of orientations in natural scenes (Coppola, Purves, McCoy, & Purves, 1998; Torralba & Oliva, 2003) have strong biases for the cardinal directions,

and thus might promote intra-saccadic motion streaks during active visual behavior. In the case of cardinal directions, a large proportion of signals would be parallel and orthogonal to the saccade direction. In fact, a possible neuronal sensor for inferring direction from motion streaks was proposed as a combination of an oriented, but not direction-selective, cell that is sensitive to orientation parallel to the saccade direction and a perpendicularly oriented direction-selective cell that is sensitive to motion signals orthogonal to the saccade direction (Geisler, 1999). Future research will have to determine whether our findings from a sparse laboratory environment translate to natural vision.

Crucially, we devised our paradigm as a proof of concept to test whether human observers are, in principle, capable of using high-speed stimulus movement, which induces motion streaks during saccades, to identify the original, pre-saccadic target stimulus. As observers judged motion streaks elicited by combined eye and stimulus movement in a sparse visual display, the paradigm's ecological validity may be limited. For example, rapid object movement strictly during saccades will rarely occur in the natural world, so that motion streaks will almost exclusively be induced by eye movements over stable visual scenes. In fact, unlike the experiments reported here, most previous studies on intra-saccadic motion streaks displayed static sources of light and studied the perceived saccade-dependent smear (e.g., Bedell & Yang, 2001; Brooks et al., 1981; Duyck et al., 2016; Matin et al., 1972) and were therefore unable to critically test the hypothesis whether induced smear could be used as a cue to matching pre- and post-saccadic targets.

Moreover, natural scenes may not always contain demarcated objects like the target stimuli applied here, so intra-saccadic motion streaks in cluttered scenes are likely to be less salient in these cases. Indeed, we showed recently that even onsets and offsets of spatially distant distractor stimuli around the offset of saccades can impair perceptual performance in detecting intra-saccadic target movement (Balsdon et al., 2018). Based on the results presented here, we cannot claim that the role of motion streaks in tracking objects is specific to trans-saccadic vision. Indeed, it would be fascinating if the same visual cues would be used to link object locations both during fixation and across saccades.

Implications for understanding visual stability

When we make saccades to scan a visual scene, objects constantly change locations on the retina and thus produce smear in the process. To achieve visual stability, the visual system must not only keep track of these retinal locations but also deal with the retinal consequences of the eye movement. Processing of intra-saccadic motion streaks could potentially serve both tasks. First, there would be no need for active removal of intra-saccadic smear from visual processing, as long as an elevation of threshold would prevent these signals from reaching conscious awareness (Watson & Krekelberg, 2009), such as, for example, via pre- and post-saccadic masking (Castet, 2010). In the paradigm described here, we did not assess whether observers were aware of a motion streak but instructed them to indicate the original pre-saccadic stimulus. In all experiments, except for experiment 2, observers generally reported low confidence and almost never "seeing" a motion streak, suggesting that conscious awareness might not have been a necessary condition for correct responses in this task. Second, motion streaks might facilitate the establishment of object correspondence in terms of smooth spatiotemporal continuity (Kahneman, Treisman, & Gibbs, 1992; Mitroff & Alvarez, 2007), as well as surface features, such as color (Hollingworth et al., 2008; Richard, Luck, & Hollingworth, 2008), which is thought to be less affected (Burr et al., 1994; Diamond et al., 2000; Knöll, Binda, Morrone, & Bremmer, 2011), albeit not unimpaired by mechanisms of saccadic suppression (Braun, Schütz, & Gegenfurtner, 2017). In addition, it might be an interesting perspective that intra-saccadic motion streaks could contribute to object localization across saccades, when the eyes fail to hit their target (Collins, Rolfs, Deubel, & Cavanagh, 2009). To test whether motion streaks really aid the establishment of object correspondence across saccades in a normal visual environment, future experiments may use implicit measures (e.g., corrective saccades to displaced stimuli) and study objects in more complex visual scenes (e.g., McConkie & Currie, 1996).

We conclude that intra-saccadic motion streaks routinely produced by objects in the visual field are not removed from processing. Although their function (if there is any) in natural vision is still unclear, our results provide a proof of concept that (1) observers can identify objects across saccades based only on image smear and (2) identification performance increased with the distinctness and duration of the resulting motion streaks. Identification of objects based on motion streaks could potentially constitute a previously undiscovered contribution to visual stability, complementing pre- and post-saccadic landmarks (Deubel, 2004), efference copies (Collins et al., 2009), or attentional remapping (Rolfs et al., 2011). High-speed projection systems for accurate stimulus display provide opportunities for future research to investigate the potential contribution of visual feedback during saccades to the perception of stability across these rapid eye movements.

Conclusions

Saccades are the fastest and most frequent human movements. By relocating the fovea (the retina's receptor-packed center), they provide rapid access to high-acuity vision across the entire visual scene. Each saccade, however, shifts objects in the scene to new parts of the retina. How does the brain keep track of these objects to maintain perceptual continuity? Using a novel trans-saccadic identification task, we show that intra-saccadic motion streaks—arising from slow integration of retinal signals—can in principle be used as cues to linking object locations across saccades. These results challenge the long-standing assumption that intra-saccadic motion signals are eliminated from visual processing to reduce saccade-induced blurring of sensory information. We have yet a long way to go in understanding the potential function of intra-saccadic vision. The current results suggest that perception of intra-saccadic object motion could potentially constitute a parsimonious contribution to perceptual continuity in active vision.

Keywords: eye movements, saccades, motion streaks, object correspondence, active vision

Acknowledgments

We thank Jan-Niklas Klanke, Clara Kuper, Polina Arbuzova, Luke Pendergrass, Julius Krumbiegel, and Olga Shurygina for their help with running the experiments, Sven Ohl for his valuable comments on reverse regression and linear mixed-effects modeling, and Patrick Cavanagh for valuable feedback on a draft of the manuscript.

RS was supported by the Studienstiftung des deutschen Volkes and the Berlin School of Mind and Brain. MR was supported by the Deutsche Forschungsgemeinschaft (DFG, grants RO3579/2-1, RO3579/8-1 and RO3579/10-1). The DFG and the Open Access Publication Fund of Humboldt-Universität zu Berlin supported the publication of this work.

Commercial relationships: none.
Corresponding author: Richard Schweitzer.
Email: richard.schweitzer@hu-berlin.de.
Address: Department of Psychology, Humboldt-Universität zu Berlin, Berlin, Germany.

References

Adelson, E. H., & Bergen, J. R. (1985). Spatiotemporal energy models for the perception of motion. *Journal of the Optical Society of America A, 2*(2), 284–299.

Apthorp, D., & Alais, D. (2009). Tilt aftereffects and tilt illusions induced by fast translational motion: Evidence for motion streaks. *Journal of Vision, 9*(1), 27.

Armstrong, J., & Welsh, B. (2011). *Black mirror (television series). Episode 3. The entire history of you*. London: Zeppotron.

Balsdon, T., Schweitzer, R., Watson, T. L., & Rolfs, M. (2018). All is not lost: Post-saccadic contributions to the perceptual omission of intra-saccadic streaks. *Consciousness and Cognition, 64*, 19–31.

Bates, D., Mächler, M., Bolker, B., & Walker, S. (2015). Fitting linear mixed-effects models using lme4. *Journal of Statistical Software, 67*(1), 1–48.

Bedell, H. E., & Yang, J. (2001). The attenuation of perceived image smear during saccades. *Vision Research, 41*(4), 521–528.

Binda, P., & Morrone, M. C. (2018). Vision during saccadic eye movements. *Annual Review of Vision Science, 4*, 193–213.

Boi, M., Poletti, M., Victor, J. D., & Rucci, M. (2017). Consequences of the oculomotor cycle for the dynamics of perception. *Current Biology, 27*(9), 1268–1277.

Brainard, D. H. (1997). The psychophysics toolbox. *Spatial Vision, 10*, 433–436.

Braun, D. I., Schütz, A. C., & Gegenfurtner, K. R. (2017). Visual sensitivity for luminance and chromatic stimuli during the execution of smooth pursuit and saccadic eye movements. *Vision Research, 136*, 57–69.

Breitmeyer, B. G., & Ganz, L. (1976). Implications of sustained and transient channels for theories of visual pattern masking, saccadic suppression, and information processing. *Psychological Review, 83*(1), 1.

Brooks, B. A., Impelman, D. M., & Lum, J. T. (1981). Backward and forward masking associated with saccadic eye movement. *Perception & Psychophysics, 30*(1), 62–70.

Brooks, B. A., Yates, J. T., & Coleman, R. D. (1980). Perception of images moving at saccadic velocities during saccades and during fixation. *Experimental Brain Research, 40*(1), 71–78.

Burr, D.C. (1981). Temporal summation of moving images by the human visual system. *Proceedings of the Royal Society of London B: Biological Sciences, 211*(1184), 321–339.

Burr, D.C., & Morrone, M. C. (2011). Spatiotopic coding and remapping in humans. *Philosophical Transactions of the Royal Society of London B: Biological Sciences, 366*(1564), 504–515.

Burr, D.C., & Ross, J. (1982). Contrast sensitivity at high velocities. *Vision Research, 22*(4), 479–484.

Burr, D.C., & Ross, J. (2002). Direct evidence that "speedlines" influence motion mechanisms. *Journal of Neuroscience, 22*(19), 8661–8664.

Burr, D.C., Holt, J., Johnstone, J. R., & Ross, J. (1982). Selective depression of motion sensitivity during saccades. *The Journal of Physiology, 333*(1), 1–15.

Burr, D.C., Morrone, M. C., & Ross, J. (1994). Selective suppression of the magnocellular visual pathway during saccadic eye movements. *Nature, 371*(6497), 511.

Bridgeman, B., Hendry, D., & Stark, L. (1975). Failure to detect displacement of the visual world during saccadic eye movements. *Vision Research, 15*(6), 719–722.

Campbell, F. W., & Wurtz, R. H. (1978). Saccadic omission: Why we do not see a grey-out during a saccadic eye movement. *Vision Research, 18*(10), 1297–1303.

Castet, E. (2010). Perception of intra-saccadic motion. In G. S. Masson, & U. J. Ilg (Eds.), *Dynamics of visual motion processing: Neuronal, behavioral, and computational approaches* (pp. 213–238). New York: Springer.

Castet, E., & Masson, G. S. (2000). Motion perception during saccadic eye movements. *Nature Neuroscience, 2*, 177–183.

Castet, E., Jeanjean, S., & Masson, G. S. (2002). Motion perception of saccade-induced retinal translation. *Proceedings of the National Academy of Sciences of the United States of America, 99*(23), 15159–15163.

Cavanagh, P., Hunt, A. R., Afraz, A., & Rolfs, M. (2010). Visual stability based on remapping of attention pointers. *Trends in Cognitive Sciences, 14*(4), 147–153.

Collins, T., Rolfs, M., Deubel, H., & Cavanagh, P. (2009). Post-saccadic location judgments reveal remapping of saccade targets to non-foveal locations. *Journal of Vision, 9*(5), 29.1–29.9.

Coppola, D. M., Purves, H. R., McCoy, A. N., & Purves, D. (1998). The distribution of oriented contours in the real world. *Proceedings of the National Academy of Sciences of the United States of America, 95*(7), 4002–4006.

Cornelisen, F. W., Peters, E. M., & Palmer, J. (2002). The eyelink toolbox: Eyetracking with MATLAB and the psychophysics toolbox. *Behaviour Research Methods, 34*(4), 613–617.

Cousineau, D. (2005). Confidence intervals in within-subject designs: A simpler solution to Loftus and Masson's method. *Tutorials in Quantitative Methods for Psychology, 1*(1), 42–45.

Crevecoeur, F., & Körding, K. P. (2017). Saccadic suppression as a perceptual consequence of efficient sensorimotor estimation. *ELife, 6*, 25073.

Della Porta, G. (1593). *De refractione optices parte: libri novem*. Napoli: Ex officina Horatii Salviani, apud Jo. Jacobum Carlinum, & Antonium Pacem.

Deubel, H. (2004). Localization of targets across saccades: Role of landmark objects. *Visual Cognition, 11*(2–3), 173–202.

Deubel, H., & Schneider, W. X. (1996). Saccade target selection and object recognition: Evidence for a common attentional mechanism. *Vision Research, 36*(12), 1827–1837.

Deubel, H., Schneider, W. X., & Bridgeman, B. (1996). Postsaccadic target blanking prevents saccadic suppression of image displacement. *Vision Research, 36*(7), 985–996.

Diamond, M. R., Ross, J., & Morrone, M. C. (2000). Extraretinal control of saccadic suppression. *Journal of Neuroscience, 20*(9), 3449–3455.

Duyck, M., Collins, T., & Wexler, M. (2016). Masking the saccadic smear. *Journal of Vision, 16*(10), 1.

Edwards, M., & Crane, M. F. (2007). Motion streaks improve motion detection. *Vision Research, 47*(6), 828–833.

Engbert, R., & Mergenthaler, K. (2006). Microsaccades are triggered by low retinal image slip. *Proceedings of the National Academy of Sciences of the United States of America, 103*(18), 7192–7197.

García-Pérez, M. A., & Peli, E. (2011). Visual contrast processing is largely unaltered during saccades. *Frontiers in Psychology, 2*, 247.

Geisler, W. S. (1999). Motion streaks provide a spatial code for motion direction. *Nature, 400*(6739), 65.

Geisler, W. S., Albrecht, D. G., Crane, A. M., & Stern, L. (2001). Motion direction signals in the primary visual cortex of cat and monkey. *Visual Neuroscience, 18*(4), 501–516.

Hall, N. J., & Colby, C. L. (2011). Remapping for visual stability. *Philosophical Transactions of the Royal Society of London B: Biological Sciences, 366*(1564), 528–539.

Higgins, E., & Rayner, K. (2015). Transsaccadic processing: Stability, integration, and the potential role of remapping. *Attention, Perception, & Psychophysics, 77*(1), 3–27.

Hollingworth, A., Richard, A. M., & Luck, S. J. (2008). Understanding the function of visual short-term memory: Transsaccadic memory, object correspondence, and gaze correction. *Journal of Experimental Psychology: General, 137*(1), 163.

Idrees, S., Baumann, M.-P., Franke, F., Muench, T. A., & Hafed, Z. M. (2019). Saccadic suppression by way of retinal-circuit image processing. *BioRxiv*, 562595, https://doi.org/10.1101/562595.

Kahneman, D., Treisman, A., & Gibbs, B. J. (1992). The reviewing of object files: Object-specific integration of information. *Cognitive Psychology, 265*, 175–219.

Kleiner, M., Brainard, D., Pelli, D., Ingling, A., Murray, R., & Broussard, C. (2007). What's new in Psychtoolbox-3. *Perception, 36*(14), 1.

Kowler, E., Anderson, E., Dosher, B., & Blaser, E. (1995). The role of attention in the programming of saccades. *Vision Research, 35*(13), 1897–1916.

Knöll, J., Binda, P., Morrone, M. C., & Bremmer, F. (2011). Spatiotemporal profile of peri-saccadic contrast sensitivity. *Journal of Vision, 11*(14), 15.

Li, H. H., Barbot, A., & Carrasco, M. (2016). Saccade preparation reshapes sensory tuning. *Current Biology, 26*(12), 1564–1570.

Li, H. H., Pan, J., & Carrasco, M. (2019). Presaccadic attention improves or impairs performance by enhancing sensitivity to higher spatial frequencies. *Scientific Reports, 9*(1), 2659.

Marino, A. C., & Mazer, J. A. (2016). Perisaccadic updating of visual representations and attentional states: Linking behavior and neurophysiology. *Frontiers in Systems Neuroscience, 10*, 3.

Matin, E., Clymer, A. B., & Matin, L. (1972). Metacontrast and saccadic suppression. *Science, 178*(4057), 179–182.

Mathôt, S., Melmi, J. B., & Castet, E. (2015). Intrasaccadic perception triggers pupillary constriction. *PeerJ, 3*, e1150.

McConkie, G. W., & Currie, C. B. (1996). Visual stability across saccades while viewing complex pictures. *Journal of Experimental Psychology: Human Perception and Performance, 22*(3), 563–581.

Mitroff, S. R., & Alvarez, G. A. (2007). Space and time, not surface features, guide object persistence. *Psychonomic Bulletin & Review, 14*(6), 1199–1204.

Morey, R. D. (2008). Confidence intervals from normalized data: A correction to Cousineau (2005). *Tutorial in Quantitative Methods for Psychology, 4*(2), 61–64.

Movellan, J. R. (2002). Tutorial on Gabor filters. Retrieved from https://pdfs.semanticscholar.org/bae5/bae884633e7da2c1ec75d158f8849d2183d3.pdf.

Najemnik, J., & Geisler, W. S. (2008). Eye movement statistics in humans are consistent with an optimal search strategy. *Journal of Vision, 8*(3), 4.

Ohl, S., Kuper, C., & Rolfs, M. (2017). Selective enhancement of orientation tuning before saccades. *Journal of Vision, 17*(13), 2.

Otero-Millan, J., Macknik, S. L., Langston, R. E., & Martinez-Conde, S. (2013). An oculomotor continuum from exploration to fixation. *Proceedings of the National Academy of Sciences of the United States of America, 110*(15), 6175–6180.

R Core Team. (2015). *R: A language and environment for statistical computing*. Retrieved from http://www.R-project.org/.

Reichardt, W. (1987). Evaluation of optical motion information by movement detectors. *Journal of Comparative Physiology A, 161*(4), 533–547.

Richard, A. M., Luck, S. J., & Hollingworth, A. (2008). Establishing object correspondence across eye movements: Flexible use of spatiotemporal and surface feature information. *Cognition, 109*(1), 66–88.

Richards, W. (1969). Saccadic suppression. *Journal of the Optical Society of America, 59*(5), 617–623.

Rolfs, M. (2015). Attention in active vision: A perspective on perceptual continuity across saccades. *Perception, 44*, 900–919.

Rolfs, M., & Carrasco, M. (2012). Rapid simultaneous enhancement of visual sensitivity and perceived contrast during saccade preparation. *Journal of Neuroscience, 32*(40), 13744–13752a.

Rolfs, M., Jonikaitis, D., Deubel, H., & Cavanagh, P. (2011). Predictive remapping of attention across eye movements. *Nature Neuroscience, 14*(2), 252.

Ross, J., Morrone, M. C., Goldberg, M. E., & Burr, D. C. (2001). Changes in visual perception at the time of saccades. *Trends in Neurosciences, 24*(2), 113–121.

Rucci, M., Ahissar, E., & Burr, D. (2018). Temporal coding of visual space. *Trends in Cognitive Sciences, 22*(10), 883–895.

Schweitzer, R., & Rolfs, M. (2019). An adaptive algorithm for fast and reliable online saccade detection. *Behavior Research Methods*, https://doi.org/10.3758/s13428-019-01304-3.

Sylvester, R., Haynes, J. D., & Rees, G. (2005). Saccades differentially modulate human LGN and V1 responses in the presence and absence of visual stimulation. *Current Biology, 15*(1), 37–41.

Thilo, K. V., Santoro, L., Walsh, V., & Blakemore, C. (2004). The site of saccadic suppression. *Nature Neuroscience, 7*(1), 13.

Torralba, A., & Oliva, A. (2003). Statistics of natural image categories. *Network: Computation in Neural Systems, 14*(3), 391–412.

Volkmann, F. C., Riggs, L. A., White, K. D., & Moore, R. K. (1978). Contrast sensitivity during saccadic eye movements. *Vision Research, 18*(9), 1193–1199.

Watson, T. L., & Krekelberg, B. (2009). The relationship between saccadic suppression and perceptual stability. *Current Biology, 19*(12), 1040–1043.

Wexler, M., & Collins, T. (2014). Orthogonal steps relieve saccadic suppression. *Journal of Vision, 14*(2), 13.

Wurtz, R. H. (2008). Neuronal mechanisms of visual stability. *Vision Research, 48*(20), 2070–2089.

Wurtz, R. H. (2018). Corollary discharge contributions to perceptual continuity across saccades. *Annual Reviews of Visual Science. 4*(1), 215–237.

Wyart, V., Nobre, A. C., & Summerfield, C. (2012). Dissociable prior influences of signal probability and relevance on visual contrast sensitivity. *Proceedings of the National Academy of Sciences of the United States of America, 109*(9), 3593–3598.

Ziesche, A., & Hamker, F. H. (2014). Brain circuits underlying visual stability across eye movements-converging evidence for a neuro-computational model of area LIP. *Frontiers in Computational Neuroscience, 8*, 25.

Zimmermann, E., Morrone, M. C., & Burr, D. C. (2013). Spatial position information accumulates steadily over time. *Journal of Neuroscience, 33*(47), 18396–18401.

Appendix

	Experiment 1 (no blanking)	Experiment 2 (250-ms blanking)
Session (saccade)	–0.381	0.165
95% CI	(–0.478, –0.282)	(0.060, 0.268)
t	–7.674	3.123
SF (low)	0.591	1.622
95% CI	(0.494, 0.689)	(1.518, 1.725)
t	11.905	30.741
Travel duration, ms	0.033	0.099
95% CI	(0.021, 0.045)	(0.086, 0.112)
t	5.310	14.994
Session × SF	–0.614	–0.573
95% CI	(–0.808, –0.420)	(–0.778, –0.367)
t	–6.184	–5.433
Session × duration	–0.064	–0.01
95% CI	(–0.088, –0.040)	(–0.036, 0.016)
t	–5.128	–0.773
SF × duration	0.056	0.083
95% CI	(0.032, 0.081)	(0.057, 0.109)
t	4.512	6.290
Session × SF × duration	–0.05	–0.115
95% CI	(–0.098, –0.001)	(–0.167, –0.064)
t	–2.000	–4.359
Intercept	0.291	1.138
95% CI	(0.199, 0.382)	(0.942, 1.334)
t	6.205	11.385
Observations, N	600	600
Log likelihood	–579.566	–625.641
Akaike information criterion	1179.132	1271.282
Bayesian information criterion	1223.101	1315.251

Table A1. Model summary for linear mixed-effects regressions in Experiments 1 and 2.

	Experiment 3 (50% contrast, 3.6 dva)	Experiment 4 (100% contrast, 7.1 dva)
Session (saccade)	0.202	—
95% CI	(–0.011, 0.414)	—
t	1.872	—
SF, cpd	0.042	–0.334
95% CI	(–0.103, 0.189)	(–0.581, –0.087)
t	0.563	–2.668
Oblique orientation	0.117	0.459
95% CI	(–0.034, 0.266)	(0.210, 0.711)
t	1.536	3.591
Parallel orientation	0.868	1.613
95% CI	(0.715, 1.016)	(1.360, 1.863)
t	11.384	12.607
Session × SF	–0.135	—
95% CI	(–0.428, 0.159)	—
t	–0.906	—
Session × oblique	–0.405	—
95% CI	(–0.699, –0.106)	—
t	–2.654	—
Session × parallel	–1.407	—
95% CI	(–1.709, –1.109)	—
t	–9.228	—
SF × oblique	–0.117	–0.218
95% CI	(-0.327, 0.090)	(–0.567, 0.131)
t	–1.111	–1.234
SF × parallel	–0.725	–0.967
95% CI	(–0.931, –0.518)	(–1.314, –0.624)
t	–6.876	–5.466
Session × SF × oblique	0.491	—
95% CI	(0.075, 0.902)	—
t	2.329	—
Session × SF × parallel	1.378	—
95% CI	(0.959, 1.790)	—
t	6.530	—
Intercept	–0.012	0.299
95% CI	(–0.148, 0.123)	(0.047, 0.551)
t	–0.179	2.322
Observations, N	270	135
Log likelihood	–212.796	–134.723
Akaike information criterion	453.592	285.447
Bayesian information criterion	503.97	308.689

Table A2. Model summary for linear mixed-effects regressions in Experiments 3 and 4.

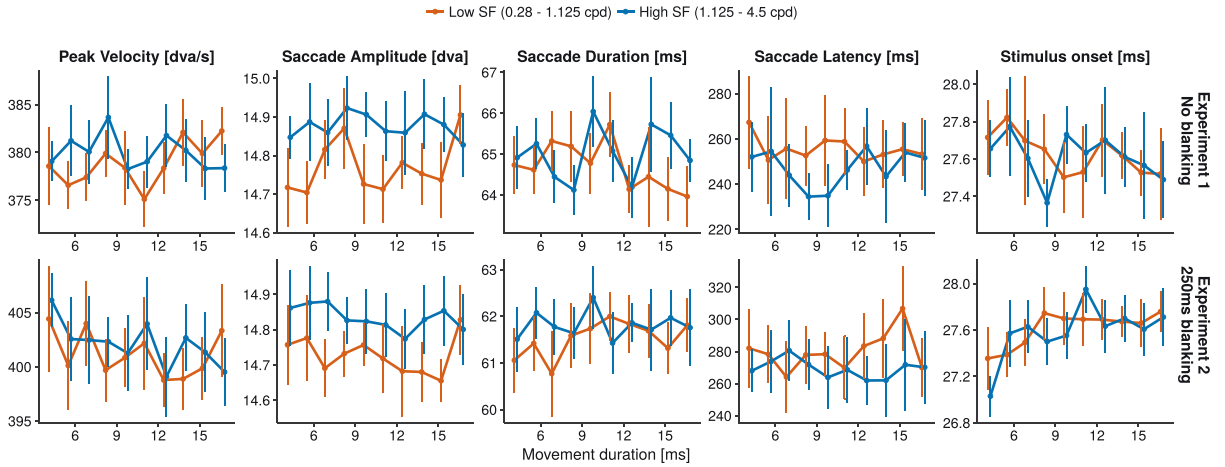

Figure A1. Summary statistics for saccade parameters in Experiments 1 and 2. Each data point represents the average across participants for the experimental conditions of movement duration and SF. All error bars represent ±2 within-subject *SEM*. To check for differences in saccade parameters across conditions, repeated-measures ANOVAs were run for each experiment dependent variable. Significance levels were Bonferroni-corrected for the number of ANOVAs (5 parameters × 4 experiments), resulting in a significance level of 0.0025. Saccade amplitudes were larger for high SF stimuli in both Experiment 1—$F(1,14) = 16.8$, $\eta^2 = 0.019$, and $P = 0.001$—and Experiment 2—$F(1,14) = 21.8$, $\eta^2 = 0.012$, and $P = 0.0004$. Furthermore, stimulus onsets were earlier for the shortest movement duration in Experiment 2: $F(9,126) = 4.55$, $\eta^2 = 0.075$, and $P < 0.0001$. No other effects were significant.

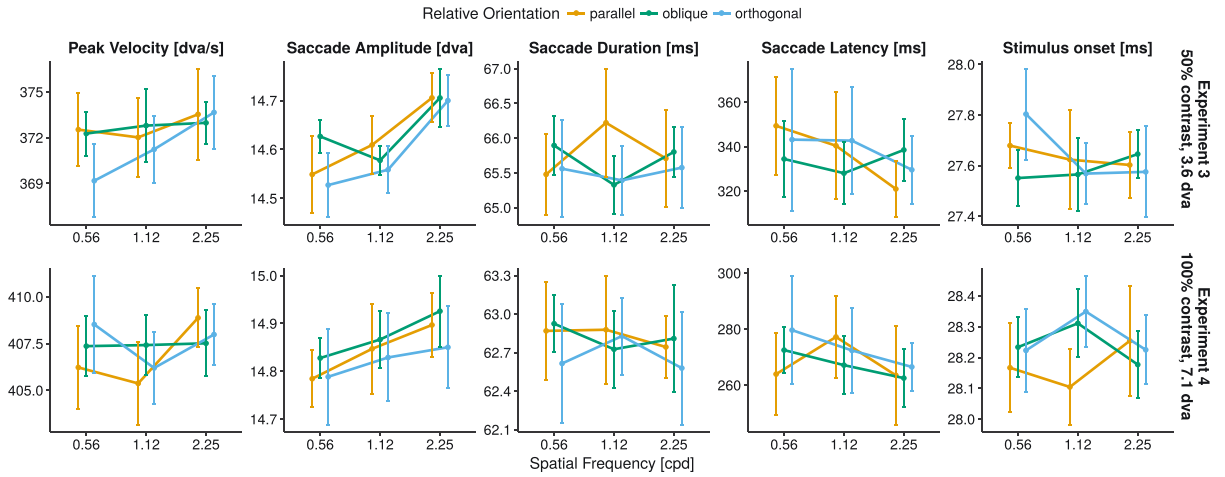

Figure A2. Summary statistics for saccade parameters in Experiments 3 and 4. Each data point represents the average across participants for the experimental conditions of SF and relative orientation. All error bars represent ±2 within-subject *SEM*. Repeated-measures ANOVAs (corrected $\alpha = 0.0025$) revealed that saccade amplitudes were again larger in high SF conditions: $F(2,28) = 16.6$, $\eta^2 = .033$, and $P < 0.0001$. No other effects were significant.

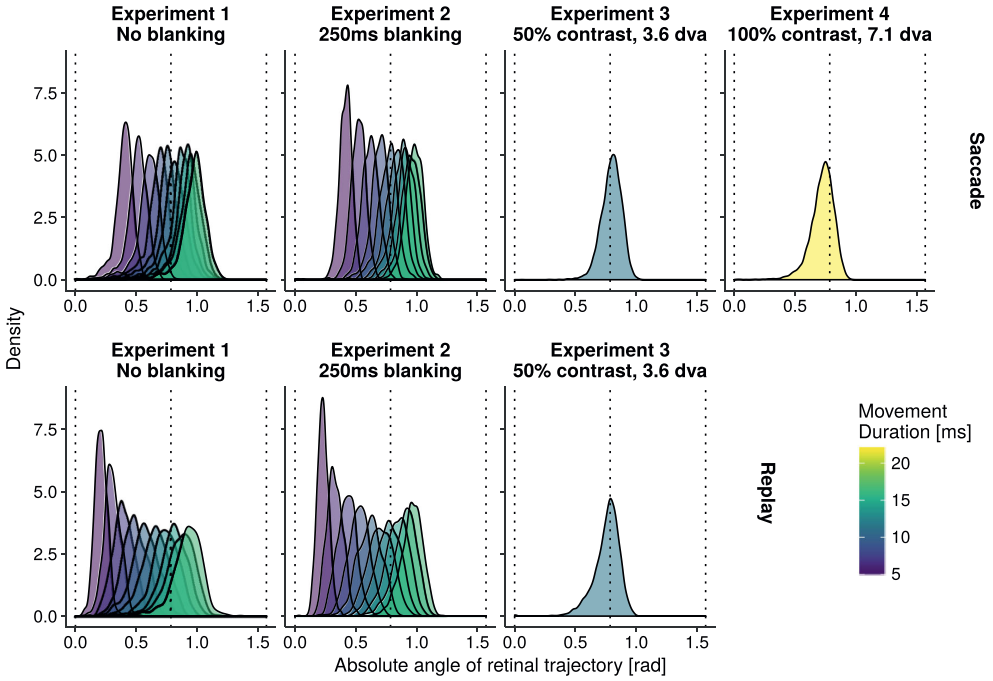

Figure A3. Distributions of absolute angle of retinal trajectory across both sessions of each experiment. Movement durations are coded by color. In Experiments 1 and 2 (left columns), short movement durations and high stimulus velocities led to steeper retinal trajectories (0, vertical trajectory), whereas longer movement durations and lower stimulus speeds resulted in more flat trajectories ($\pm\pi/2$, horizontal trajectory). In Experiment 3 and 4 (right columns), we aimed at producing absolute retinal trajectories around 45° to achieve optimal relative orientations.

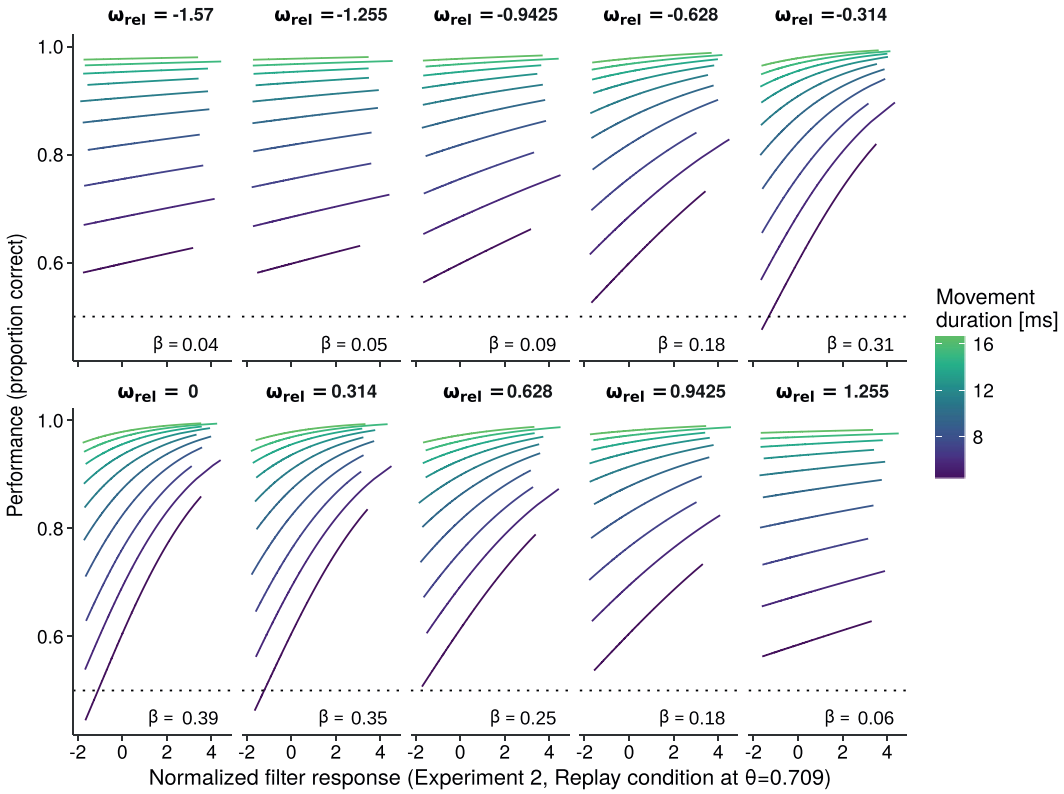

Figure A4. Exemplary results from the reverse regression across relative orientation components in the replay condition of Experiment 2 for one stimulus condition (SF = 0.71).

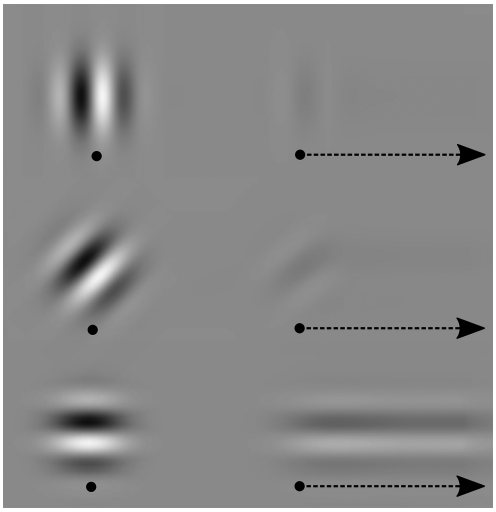

Figure A5. Illustration of distinctiveness of motion streaks for vertical, tilted by 45°, and horizontal Gabor patches (top to bottom, left column). Assuming a rightward horizontal movement trajectory, the relative orientation of the Gabor patches would be orthogonal, oblique, or parallel, respectively. To illustrate retinal smear, an image motion filter with the length of the displayed arrow was used (right column).

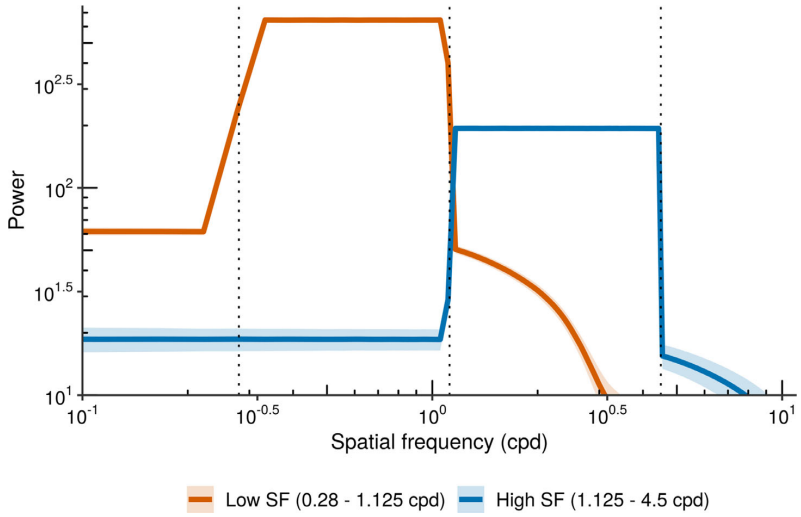

Figure A6. Spatial frequency power spectra of the low-SF (orange) and high-SF (blue) noise patches used in Experiments 1 and 2. A two-dimensional fast Fourier transform was performed on the bandpass-filtered noise, and the radial average of the result was computed. Power dropped steeply around the specified high-pass and low-pass cut-off values of 0.28 and 1.12 cpd for low-SF stimuli and 1.12 and 4.5 cpd for high-SF stimuli (dotted vertical lines).

5.1.4 Study IV

Pre-print:

Schweitzer, R., & Rolfs, M. (2020). Intra-saccadic motion streaks jump-start gaze correction. *bioRxiv*, 2020.04.30.070094. doi: 10.1101/2020.04.30.070094

Pre-registration, data, analyses:

`https://osf.io/aqkzh/`

Featured code:

TrackPixx3 control: `https://github.com/richardschweitzer/TrackPixxToolbox`

Re-use permissions:

Intra-saccadic motion streaks jump-start gaze correction

Richard Schweitzer & Martin Rolfs
Department of Psychology, Humboldt-Universität zu Berlin; Berlin School of Mind and Brain; Bernstein Center for Computational Neuroscience, Berlin

Rapid eye movements (saccades) incessantly shift object locations on the retina. To establish object correspondence across saccades, the visual system is thought to match surface features of objects upon saccade landing. Here we assessed if intra-saccadic visual information about an object's retinal trajectory informs this match-making. Ten human observers made saccades to a cued target in a circular stimulus array. Using a visual projection system with high spatiotemporal fidelity, we swiftly rotated this array as the eyes were in flight, displaying continuous or apparent intra-saccadic target motion for 14.6 ms. Observers' saccades could thus land between the target and a distractor, prompting secondary saccades. We tightly controlled the post-saccadic availability of object features by presenting masks at varying delays. Independently of the availability of object features, target movement increased the rate of gaze-correcting secondary saccades to the original pre-saccadic target with a reduced saccade latency. Intra-saccadic motion was particularly effective in driving gaze correction when the target's stimulus features, in combination with the saccade trajectory, gave rise to efficient motion streaks. These results suggest that intra-saccadic visual information can facilitate the establishment of object correspondence and jump-start gaze correction.

Introduction

Saccadic eye movements are the fastest and most frequent movements of the human body. By placing the fovea at new parts of the visual scene, they provide high-acuity vision across the visual field. At the same time, saccades result in retinal translations that constantly shift the projections of objects onto the retina, and impose large amounts of motion blur on the retinal signal. These consequences, however, do not seem to impair our visual experience, a phenomenon widely known as visual stability (Bridgeman et al., 1994; MacKay, 1973; Wurtz, 2008). A core component of visual stability is the establishment of object correspondence across saccades: How does the visual system determine whether any object located in the periphery prior to a saccade is the same as the object in the foveal region right after that saccade has landed?

There is good evidence that visual short-term memory (VSTM) enables the matching of objects across saccades (Aagten-Murphy & Bays, 2019). For instance, Hollingworth et al. (2008) showed that surface features of visual objects encoded in VSTM, such as color or object identity, can be used for gaze correction when targets were displaced during saccades. To some extent, this result contradicted object-file theory (Kahneman et al., 1992), which supports the notion that objects are referenced via spatiotemporal continuity, not surface features (Mitroff & Alvarez, 2007). Later studies then suggested that both surface features and spatiotemporal continuity could contribute to object cor-

Correspondence concerning this article should be addressed to Richard Schweitzer, Department of Psychology, Humboldt-Universität zu Berlin, Rudower Chaussee 18, 12489 Berlin, Germany. E-mail: richard.schweitzer@hu-berlin.de

respondence, across both brief occlusions while fixating (Hollingworth & Franconeri, 2009) and saccades (Richard et al., 2008).

One potential source of information for object correspondence has been neglected by all studies up to this point: Intra-saccadic object motion across the retina may provide spatiotemporal continuity as well as access to surface features before saccade landing. As illustrated in **Figure 1**, due to temporal integration in the visual system, objects moving at the high velocities of saccades routinely produce smeared traces, so-called motion streaks (Bedell & Yang, 2001; Brooks et al., 1980; Duyck et al., 2016; Geisler, 1999; Matin et al., 1972). Most experiments thus far, in fact, were built on the premise that "vision is suppressed, creating a gap in perceptual input" (Richard et al., 2008, p. 66) and "people are virtually blind" (Hollingworth et al., 2008, p. 163) during saccades. Here, using a high-speed projection system, we adapt a classic gaze correction paradigm (Hollingworth et al., 2008) to investigate the alternative hypothesis that object motion exclusively present during saccades may provide useful information serving object continuity and, hence, gaze correction.

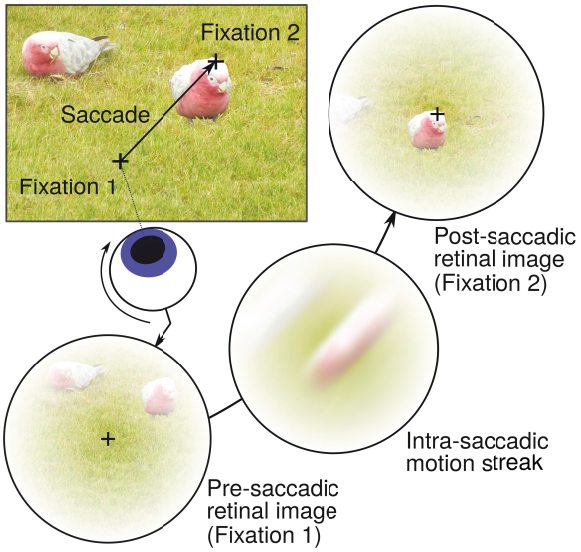

Figure 1. Illustration of intra-saccadic motion streaks. When making a saccade towards the bird on the right, its retinal projection rapidly travels from a pheripheral location (Fixation 1) to a foveal location (Fixation 2), producing a motion streak along its retinal trajectory. Even though intra-saccadic motion streaks are largely omitted from conscious visual perception, likely due to masking by pre- and post-saccadic retinal images (Campbell & Wurtz, 1978; Matin et al., 1972) and attenuation by saccadic suppression (Ross et al., 2001; Volkmann, 1986), could they still inform trans-saccadic processes?

Methods

Apparatus

Stimuli were projected onto a 16:9 (250.2 x 141.0 cm) video-projection screen (Stewart Silver 5D Deluxe, Stewart Filmscreen, Torrance, CA), mounted on a wall 340 cm in front of the participant, using a PROPixx DLP projector (Vpixx Technologies, Saint-Bruno, QC, Canada) running at 1440 Hz refresh rate and a resolution of 960 x 540 pixels. The experimental code was implemented in MATLAB 2016b (Mathworks, Natick, MA, USA) on Ubuntu 18.04, using Psychtoolbox (Kleiner et al., 2007; Pelli, 1997), and was run on a Dell Precision T7810 Workstation supplied with a Nvidia GTX 1070 graphics card. Eye movements of both eyes were recorded via a TRACKPixx3 tabletop system (Vpixx Technologies, Saint-Bruno, QC, Canada) running firmware version 11 and at a sampling rate of 2000 Hz, while participants rested their head on a chin rest. A custom wrapper function toolbox was used to control the eye tracker, which is made publicly available on Github: https://github.com/richardschweitzer/TrackPixxToolbox.

Participants

Ten observers completed three sessions with a duration of approximately 1 hour each on separate days and received 26 Euros as remuneration (plus 2 Euros for every 15 minutes of overtime). We obtained written informed consent from all participants prior to inclusion in the study. The study was conducted in agreement with the latest version of the Declaration of Helsinki (2013) and was approved by the Ethics board of the Department of Psychology at Humboldt-Universität zu Berlin. All observers (5 male, 5 female; mean age: 28; age range: 20 – 37) had normal or corrected-to-normal vision (20/20 ft acuity in the Snellen test;

4 observers wore glasses and 1 observer wore contact lenses). Seven of ten observers had right ocular dominance (established by a variant of the Porta test) and ten observers were right-handed. The experiment was pre-registered at Open Science Framework (OSF). In accordance with pre-registered exclusion criteria, four invited participants had to be replaced because they did not complete all three sessions. Preregistration, data, and analysis scripts can be found at https://osf.io/aqkzh/.

Procedure & Task

A six-stimulus circular array at an eccentricity of 10 degrees of visual angle (dva) was displayed while observers fixated an area with a 1.5 dva radius around a central fixation dot for 400 ms. The stimulus array contained two types of dissimilar noise patches (see Stimuli), in alternating order (**Figure 2a**, top row). Specific stimulus positions were at 0, 60, 120, 180, 240, and 300 (as shown in **Figure 2a**), or alternatively at 30, 90, 150, 210, 270, and 330 degrees relative to the central fixation dot (0 deg: below the fixation point). After successful fixation, an exogenous cue was presented to indicate the saccade target: The target stimulus – one of the six presented stimuli and one of the two types of noise patches – was enlarged linearly up to twice its initial size for 25 ms and then decreased for 25 ms until the initial size was restored. Saccades were detected online using the algorithm described by Schweitzer & Rolfs (2019) with parameters k=2, λ=10, and ϑ=40, on both eyes. As soon as the saccade was detected, the cued stimulus moved 30 deg in a clockwise (CW) or counterclockwise (CCW) direction for 14.6 ms – amounting to a distance traveled of 5.2 dva at a velocity of approximately 360 dva/s – or remained in its pre-saccadic location. Importantly, this 14.6-ms motion was either continuous (motion-present condition), i.e., presenting 21 frames of equally spaced stimulus positions along the circular trajectory (0.25 dva per frame), or apparent (motion-absent condition), i.e., presenting a blank screen between the first and final positions of the stimulus. In both motion conditions, all other noise patches were removed during this short and rapid stimulus motion. As soon as the moving stimulus reached its final position, all stimuli were displayed at their post-motion locations consistent with a 30-deg CW or CCW rotation of the stimulus array. Observers' saccades thus landed between two dissimilar noise patches: One was always the target stimulus which was cued prior to saccade initiation, and the other one – the distractor – was an uncued and therefore irrelevant stimulus. As a consequence, a secondary saccade was made to the target (or erroneously to the distractor) in order to correct for the intra-saccadic displacement which occurred in two thirds of all trials. Crucially, a pixel noise mask (**Figure 2a**, bottom row) occluded the identity of all stimuli presented on the screen with varying delay relative to stimulus motion offset (0, 25, 50, 100, 200, 600 ms), thus limiting observers' time to use stimulus surface features to guide their secondary saccades. This post-motion mask onset delay will henceforth be referred to as of surface-feature duration. 650 ms after stimulus motion offset, each trial was concluded.

Similar to Hollingworth et al. (2008), observers were instructed to make a saccade to the target stimulus upon cue presentation and fixate it. They were informed that the stimulus array could rotate in some trials, in which case they could make a secondary saccade to follow the initial target. If observers' initial central fixation was unsuccessful, or if their primary saccade did not end within a circular region of 2 dva around the pre-saccadic target location, or if more than one saccade was made to reach the pre-saccadic target location, appropriate feedback was provided, and the trial was repeated at the end of the session. No feedback related to observers' secondary saccades was given. To elucidate the trial procedure, a 60-fps video (slowed down by a factor of 24 and using the mouse cursor as a representative of gaze position) can be found at OSF: https://osf.io/f48rm/.

Stimuli

Stimuli were achromatic, random Gaussian noise patches (SD=1) bandpass-filtered to spatial frequencies (SF) from 0.25 to 1 cycles per dva (cpd), displayed on a uniform, grey background. One initial bandpass-

filtered noise matrix was generated on each trial. To maximize the dissimilarity between the two types of noise patches, 75% of a noise SD was added to or substracted from the initial noise matrix, thus increasing or decreasing its luminance (for one example, see **Figure 2a**). This procedure inevitably led to some differences in spatial frequency and orientation for the two types of content in the pairs of noise patches. This effect was intended, as it allowed for both easier discrimination of the two types during trials and for reverse regression analyses involving stimulus features at a later stage (Schweitzer & Rolfs, 2020; Wyart et al., 2012). All noise patches were at full Michelson contrast to maximize their intra-saccadic visibility. Noise patches were enveloped in a Gaussian aperture with a standard deviation of 0.5 dva. Masks displayed at post-motion locations had the same dimensions, but consisted of random black-white pixel noise. Noise masks were identical copies for all stimuli.

The central fixation dot at the beginning of each trial consisted of a white circle of 0.3 dva radius. To indicate that the dot was fixated by the observer, the area within the circle was be filled by another white circle of 0.1 dva radius.

Pre-processing

Observers completed at least 3456 trials, i.e., at least 1152 trials per session. This number of trials resulted from the fully counterbalanced experimental factors: Cued location (6 levels: 1-6 stimuli), initial position of the stimulus array (2 levels: 0, 30 degrees), motion direction (3 levels: CW, CCW, static), presence of continuous intra-saccadic motion (2 levels: absent, present), and delay between the displacement/continuous motion and the masks, i.e., the surface-feature duration (6 levels: 0, 25, 50, 100, 200, 600 ms), thus resulting in a total of 8 trials per experimental cell. Trials were repeated at the end of each session if fixation control was not passed, primary saccades did not reach the pre-saccadic target position, or multiple saccades were made to reachit. On average, observers completed 3705 (SD = 209) trials during all experimental sessions (including repeated and later excluded trials).

Pre-processing involved three major steps. First, 0.5% (SD = 0.4%) of trials were excluded due to unsuccessful fixations (within a central circular boundary of 1.5 dva radius) and dropped frames.

Second, saccades (i.e., primary, secondary, and tertiary saccades in each trial) were detected using the Engbert-Kliegl algorithm (Engbert & Kliegl, 2003; Engbert & Mergenthaler, 2006) with a velocity factor of 10 and a minimal duration of 15 ms. Prior to saccade detection, eye movement data was downsampled to 1000 Hz using bandlimited interpolation. Each trial's data was padded with its first and last samples and shifted prior to downsampling in order to compensate for the edge effects and delays introduced by low-pass filtering. Sections of missing data due to blinks or tracking problems were expanded by 40 samples on each side and linearly interpolated, but only if those samples were not collected during the relevant trial interval, i.e., from the onset of the saccade cue until 450 ms after the offset of the stimulus motion. Saccade detection was performed on both eyes, but only data collected from the observer's dominant eye was analyzed, unless the latter was not available due to missing samples, which occurred in 2.4% (SD = 2.1%) of all trials. In order to achieve a conservative criterion for saccade offset (to remove trials in which stimulus motion was not strictly intra-saccadic), we did not consider above-threshold post-saccadic oscillations (if detected within a window of 50 ms after the first below-threshold sample) to be part of the primary saccade.

Third, on average 10.1% (SD = 7.4%) of the remaining trials were excluded because they failed to satisfy the following criteria: (1) No missing data within the relevant trial interval (see above), (2) detection of one single primary saccade that reached the 2-dva area around the pre-saccadic target location (see Procedure), (3) primary saccade metrics compatible with the instructed 10-dva saccade (i.e., amplitude 6 – 15 dva, peak velocity below 600 dva/s, duration below 75 ms), and (4) strictly intra-saccadic stimulus motion (i.e., motion onset after saccade onset and motion offset before saccade offset, regardless of whether continuous mo-

tion was present or not), taking into account a deterministic 8.3-ms video delay of the PROPixx projection system (see Schweitzer & Rolfs, 2019).

Ultimately, an average of 3397 (SD = 310) trials per observer entered further analyses. Across observers, stimulus motion was physically displayed 17.8 ms (SD = 0.5) after saccade onset and ended 10.7 ms (SD = 3.1) before saccade offset (both for saccades detected offline and including all system latencies, see also **Figure 2b**). Mean primary saccade amplitude amounted to 9.1 dva (SD = 0.3), mean primary saccade duration to 43.8 ms (SD = 3.0), and mean primary saccade peak velocity to 327.1 dva/s (SD = 34.1).

Analysis

Secondary saccades. On average, secondary saccades were made in 88.2% (SD = 14.1, Mdn = 95.1) of CCW-trials, in 88.6% (SD = 14.2, Mdn = 94.8) of CW-trials, and in 32.0% (SD = 26.9, Mdn = 26.8) of static-trials. Mean secondary saccade rates were slightly reduced by two observers who rarely made secondary saccades despite intra-saccadic displacements, i.e., in 54.5% and 73.3% of trials. Note that overall secondary saccade probability was largely constant across surface-feature duration (0 ms: M = 86.7, SD = 13.0; 25 ms: M = 88.3, SD = 13.6; 50 ms: M = 89.0, SD = 14; 100 ms: M = 88.8, SD = 14.8; 200 ms: M = 88.24, SD = 14.9; 600 ms: M = 89.0, SD = 14.3) and motion conditions (absent: M = 88.4, SD = 14.3; present: M = 88.4, SD = 13.8). To determine whether secondary saccades were made to target or distractor stimuli, we determined whether the offset of the secondary saccade landed within a 3-dva window around the center of either stimulus. In fact, in CCW- and CW-trials 94.5% (SD = 5.3) and 94.7% (SD = 5.1) of secondary saccades landed within these regions. In static-trials, which did not enter further analyses, 55.6% (SD = 30.4) of secondary saccades were re-fixations in the region around the target stimulus. Tertiary saccades, i.e., saccades following secondary saccades, were made in only 8.3% (SD = 4.4) of CCW-trials, 8.3% (SD = 4.5) of CW-trials, and 1.8% (SD = 2.4) of static-trials, and were therefore not further analyzed.

To analyze the proportion of secondary saccades to the pre-saccadic target, we used logistic mixed-effects regression analyses (Bates et al., 2015), specifying observers as intercept-only random effects. The factors of intra-saccadic motion (levels: absent, present) and surface-feature duration (levels: 0, 25, 50, 100, 200, 600 ms) were treatment-coded as ordered factors, so that the condition intra-saccadic motion absent at 0 ms mask SOA constituted the intercept of each model. Secondary saccade latency – defined as the time in milliseconds passed between the offset of the primary saccade and the onset of the secondary saccade – was analyzed using linear mixed-effects regressions applying the same random effects and contrast coding. Confidence intervals for slopes were determined via parametric bootstrapping with 2,000 repetitions each. Along with confidence intervals, p-values were computed via Satterthwaite's degrees of freedom method. To test the relevance of experimental manipulations, hierarchical model comparisons were performed using the likelihood ratio test and Bayes factors were computed from two models' respective Bayesian information criteria (Jarosz & Wiley, 2014). While we consistently report the results of model comparisons (pointing out the best model), all reported estimates stem from the full model, not the best model.

To describe the time course of secondary saccade rate to the target, we fitted an exponential growth model with the formula $p(t) = 0.5 + \lambda(1 - e^{-\beta(t-\delta)})$. This model, previously used to describe speed-accuracy tradeoffs (e.g., Carrasco & McElree, 2001), was now used to approximate the proportion of secondary saccades to the target *p(t)* – increasing from a chance level of 0.5 – at any given surface-feature duration *t*. We estimated the three parameters of the model, asymptote (λ), slope (β), and onset (δ), in a mixed-effects approach using the stochastic approximation expectation maximization algorithm (starting parameters: λ=1, β=1, δ=4), implemented in the saemix R package (Comets et al., 2017). This approach allowed each of the parameters to be estimated independently for each observer, separately for absent and present intra-saccadic object motion. Subsequently, paired t-tests were used

to test whether estimated parameters differed between motion conditions. As we conducted independent hypothesis tests on three parameters, significance levels were Bonferroni-corrected, resulting in $\alpha = .016$. All analyses were implemented in R (R Core Team, 2015) and can be found in a markdown document on OSF: https://osf.io/uafsk/. Furthermore, to describe the time course of secondary saccade latencies, mixed-effects generalized additive models (GAMs) were fitted using the mgcv package in R (Wood, 2017). These models, fitted separately for secondary saccades to the target and to the distractor, allowed to capture the nonlinear dynamics of secondary saccades latencies over surface-feature durations, for both experimental conditions of intra-saccadic motion (treatment-coded as ordered factor; reference smooth: absent, difference smooth: present) and for each observer. Thin-plate regression splines (Wood, 2003) were used as smooth functions. **Figure 3** shows the model predictions averaged across observers.

Reverse Regression. As a first step, target noise patches were convolved with Gabor filters (in sine and cosine phase) of varying orientations (from $-\frac{\pi}{2}$ to $+\frac{\pi}{2}$, in steps of $\frac{\pi}{10}$ rad) and spatial frequencies (0.25, 0.29, 0.34, 0.39, 0.46, 0.54, 0.63, 0.73, 0.86, 1 cpd), resulting in one energy map per noise patch, that contained the filter responses for each orientation-SF component (an example is shown in **Figure 5a**, see also Schweitzer & Rolfs, 2020; Wyart et al., 2012).

Second, we estimated the angle of the stimulus' motion trajectory on the retina (for an illustration see **Figure 5b**). In order to compute this retinal trajectory, we subtracted the gaze positions during stimulus presentation (spline-interpolated to match projector refresh rate of 1440 Hz) from the stimulus locations over time. From retinal positions, retinal angles were computed, whose median was subsequently used to normalize each stimulus' orientation components for its respective retinal trajectory. Relative orientation is the angular difference between the retinal angle and the orientations contained in a given noise patch (Schweitzer & Rolfs, 2020). To achieve the equal-sized steps of relative orientations (in the face of retinal angles that naturally varied between trials), the filter responses for the defined orientation and SF levels were interpolated based on a full tensor product smooth (using cubic splines) of each stimulus' energy map. Finally, relative orientation could take any value between 0 (orientation parallel to motion direction) and $\frac{\pi}{2}$ (orientation orthogonal to motion direction).

Finally, we fitted mixed-effects logistic regressions (random intercepts and slopes for observers; Bates et al., 2015) to predict secondary saccades to the target stimulus from standardized filter responses in each combination of relative orientation and SF of the target's energy map. This was done separately for both motion-present and motion-absent conditions (**Figure 5c**), as well as for surface-feature durations. A significant slope for filter responses in a particular relative orientation-SF component indicated that this component drives secondary saccades to the target stimulus. Instead of reporting the log-odds weights of the model, we reported the corresponding z-statistic, i.e., the ratio of the log-odds weight and its standard error, as it allowed for a more straightforward evaluation of significance. We further analyzed the resulting z values with GAMs. Smooth terms for relative orientation (continuous: 0 .. $\frac{\pi}{2}$) and SF (continuous, $\log_{10}$-transformed: -0.6 .. 0), as well as their interactions, were again based on thin-plate regression splines (Wood, 2003) and could include by-variables coding the experimental condition of intra-saccadic motion (treatment-coded as ordered factor; reference smooth: absent, difference smooth: present). Surface-feature duration (reference smooth: 0 ms, difference smooths: 25, 50, 100, 200, 600 ms) was also added in a full model which can be found in the Open Methods (OSF link: https://osf.io/uafsk/). Results shown in **Figure 5c** are averages across all surface-feature durations, thus equally taking into account the effect of object features in both movement-present and movement-absent conditions. For each coefficient of the GAM, a complexity of the smooth term (i.e., estimated degrees of freedom, edf) and the significance of the term were estimated. As these estimates cannot be interpreted directly, we complemented the

GAM with a simple multiple regression (LM) with the same variable coding to report the linear trends within the data.

Results

Efficiency of gaze correction

Post-saccadic surface features and intra-saccadic motion drive gaze correction. Of central interest to our research question was whether in case of intra-saccadic target displacement continuous motion would lead to a higher proportion of gaze correction, that is, secondary saccades to the target stimulus. Crucially, intra-saccadic displacements – whether continuous or apparent – had to occur exclusively during saccades, as extending intra-saccadic stimulus manipulations beyond saccade offset has been shown to drastically alter detection performance and subjective appearance of stimuli (Balsdon et al., 2018; Bedell & Yang, 2001; Castet et al., 2002; Duyck et al., 2016; Matin et al., 1972), despite the finding that the window of saccadic suppression often exceeds the saccade duration (Volkmann, 1986). Having excluded those displacements that were not strictly intra-saccadic (see Preprocessing), presentations finished on average 10.7 ms (SD = 3.1) prior to saccade offset (**Figure 2b**) and there was no difference between motion-absent and motion-present conditions (M_{absent} = 10.68, SD_{absent} = 3.08, $M_{present}$ = 10.75, $SD_{present}$ = 3.08; paired t-test: t(9) = 1.24, p = .243).

We first investigated the time course of stimulus feature processing after the stimulus displacements were concluded. We hypothesized that the more time stimulus features were presented before being occluded by masks (**Figure 2a**), the more likely would observers orient their gaze towards the pre-saccadic target, a behavior that likely reflects object correspondence established by comparing post-saccadic object features with those represented in VSTM (Hollingworth et al., 2008; Richard et al., 2008). Indeed, as shown in **Figure 2c**, in the absence of continuous intra-saccadic motion, proportions of secondary saccades made toward the target stimulus increased rapidly and fairly linearly for surface-feature durations of 0 to 50 ms (25 ms: β = 0.53, z = 6.91, 95% CI [0.39, 0.69], p < .001; 50 ms: β = 1.10, z = 13.77, 95% CI [0.94, 1.26], p < .001), reaching an asymptote at 100 ms after displacements occurred (100 ms: β = 1.47, z = 17.51, 95% CI [1.31, 1.65], p < .001; 200 ms: β = 1.45, z = 17.29, 95% CI [1.30, 1.63], p < .001; 600 ms: β = 1.42, z = 17.02, 95% CI [1.27, 1.59], p < .001). Note that group averages reached this asymptote at a comparably low proportion of 80.1% (SD = 5.3). This result was caused by three observers who selected the initial pre-saccadic target on a proportion of trials that was barely above chance (i.e., 55.2%, 51.2%, and 56.9% at the maximum surface-feature duration of 600 ms). There was however no reason or pre-registered criterion for their exclusion.

When the intra-saccadic motion was absent and the surface features were masked right after displacement, the proportion of secondary saccades to the target was at chance level (β_0 = 0.03, z = 0.12, 95% CI [-0.39, 0.44], p = .905), as no information was available to perform gaze correction. Crucially, when continuous intra-saccadic motion was present, whereas post-motion surface features were unavailable, secondary saccades were made to the target in 56.1% of trials (SEM = 3.4).This data suggests that gaze correction was accurate significantly above chance (β = 0.25, z = 3.37, 95% CI [0.12, 0.41], p < .001). Although this effect slightly diminished with increasing surface-feature duration (**Figure 2d**), we found no significant interactions for any longer surface-feature duration (25 ms: β = -0.11, z = -1.04, 95% CI [-0.32, 0.10], p = .298; 50 ms: β = -0.06, z = -0.52, 95% CI [-0.29, 0.15], p = .602; 100 ms: β = -0.19, z = -1.61, 95% CI [-0.42, 0.03], p = .106; 200 ms: β = -0.20, z = -1.70, 95% CI [-0.44, 0.03], p = .09; 600 ms: β = -0.04, z = -0.37, 95% CI [-0.29, 0.18], p = .710). Thus, the effect of intra-saccadic motion was largely additive to the effect of surface-feature duration. Hierarchical model comparisons provided further evidence for this view: Adding the factor intra-saccadic motion to a model involving only surface-feature duration (i.e., an additive model) improved the fit to a significant degree (BF_{01} = 1130.04, ΔLL = +11.00, $\chi^2(1)$ = 22.02, p < .001), whereas the full model (including also

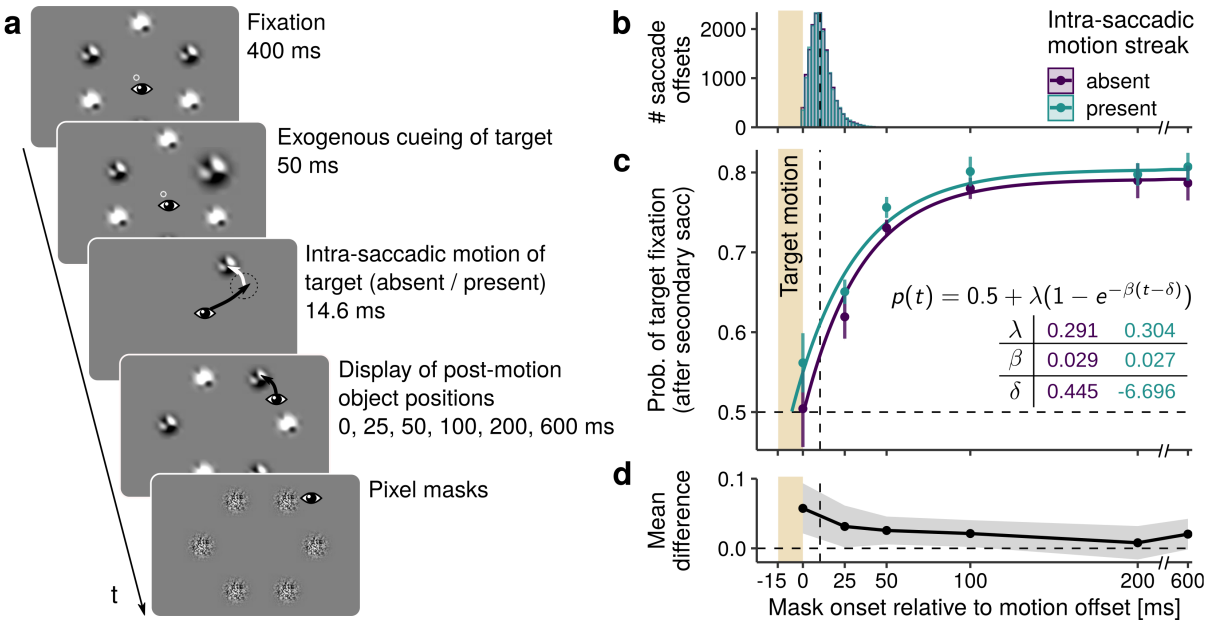

Figure 2. Probing the role of post-saccadic surface features and intra-saccadic motion in gaze correction. **a** Observers made a primary saccade to an exogenously cued target noise patch stimulus (one of two types). Strictly during the saccade, the target rapidly shifted positions, consistent with a 30-degree clockwise or counterclockwise rotation of the entire stimulus array, so that primary saccades always landed between the initially cued stimulus (the target) and the other-type stimulus (the distractor). The intra-saccadic stimulus motion was displayed for 14.6 ms and was either continuous (i.e., 21 equidistant steps along its circular trajectory) or absent (blank screen between first and final stimulus position). After the stimulus' motion, pixel masks were displayed with a varying delay (surface-feature durations: 0, 25, 50, 100, 200, or 600 ms), thus occluding the identity of post-saccadic objects and limiting the observers' ability to establish trans-saccadic correspondence using object features. **b** Stimulus motion was presented strictly during saccades, finishing on average 10.7 ms prior to saccade offset. **c** Likelihood of observers making a secondary saccade towards the initial pre-saccadic target was a function of surface-feature duration, as well as the presence of intra-saccadic motion (purple vs green points, respectively; error bars indicate $\pm SEM$). The beige area illustrates the temporal interval in which intra-saccadic motion took place. Solid lines show predictions of the mixed-effects exponential growth model describing the increase of proportions with increasing surface-feature duration. Average parameter estimates are shown in the table below the model formula. **d** Mean differences between motion conditions for each surface-feature duration with corresponding 95% confidence intervals (gray-shaded area).

the interaction term) was not preferred to the more parsimonious additive model (BF_{01} < 0.001, ΔLL = +2.3, $\chi^2(5) = 4.61$, p = .464).

Taken together, these results suggest that continuous intra-saccadic object motion increased the probability of making a secondary saccade to the cued target. Although the difference between present and absent conditions decreased with increasing surface-feature durations (**Figure 2d**), the performed model comparisons favored a global benefit across surface-feature durations.

Intra-saccadic motion results in early onset of information accumulation for gaze correction. What is the nature of the effect of intra-saccadic object motion in the gaze correction paradigm? To find out, we performed an exploratory analysis: We fitted an exponential model (see Analysis) to the probability of making a secondary saccade to the target (**Figure 2c**). Following this procedure, we estimated three parameters of the time course, i.e., asymptote (λ), slope (β), and onset (δ), for motion-absent vs motion-present conditions. We adopted a mixed-effects approach that allowed the three parameters to vary independently for each ob-

server (Comets et al., 2017), so that paired hypothesis tests could be performed. Mean estimates are shown in the table embedded in **Figure 2c**.

Several hypotheses about the benefit of intra-saccadic motion could thus be addressed. First, intra-saccadic motion may result in a gain increase for post-saccadic object features. In this case, it would be expected that performance in the motion-present condition has the same time of onset, but then reaches a higher asymptote. Indeed, estimated λ were slightly larger in the motion-present condition ($\lambda_{present}$ = 0.304, $SE_{present}$ = 0.058) than in the motion-absent condition (λ_{absent} = 0.291, SE_{absent} = 0.061), but this difference did not reach significance (t(9) = -1.34, p = .214). Second, intra-saccadic motion may lead to an increase of the rate with which post-saccadic information is accumulated, as indicated by the slope of the exponential model. Estimates of β, however, did also not differ between conditions ($\beta_{present}$ = 0.027, $SE_{present}$ = 0.003, β_{absent} = 0.029, SE_{absent} = 0.003, t(9) = 0.49, p = .634), providing no evidence for such rate increase. Third, despite the fact that all object displacements were finished strictly while the eye was still in flight, continuous intra-saccadic object motion may have revealed the post-saccadic location of the target at an earlier stage, thus allowing the onset of information accumulation to occur already during the ongoing motion. Indeed, estimates of the onset parameter δ revealed a significant difference between the two conditions ($\delta_{present}$ = -6.969, $SE_{present}$ = 2.076, δ_{absent} = 0.446, SE_{absent} = 0.053, t(9) = 3.45, p = .007). The results of this analysis suggest that the observed benefit is mainly caused by an earlier availability of object location, which is revealed during intra-saccadic object motion.

Post-saccadic surface features and intra-saccadic motion reduce the latency of gaze correction. Given that the presence of intra-saccadic motion increased the likelihood of secondary saccades to the pre-saccadic target in a way consistent with an earlier onset of post-saccadic target localization, we next analyzed the latency of secondary saccades (**Figure 3**). We expected a facilitation of secondary saccade latencies when directed towards the target, but not when directed towards the distractor. On average, secondary saccades to target stimuli were initiated slightly, but insignificantly faster after primary saccade offset (M = 252.3, SD = 37.4; paired t-test: t(9) = 1.35, p = .210) than secondary saccades to distractor stimuli (M = 259.9 ms, SD = 47.6). Average saccade latencies (**Figure 4c**) were well consistent with those found in previous studies using similar paradigms (cf. Hollingworth et al., 2008). We ran linear mixed-effects regression models separately for secondary saccades to the

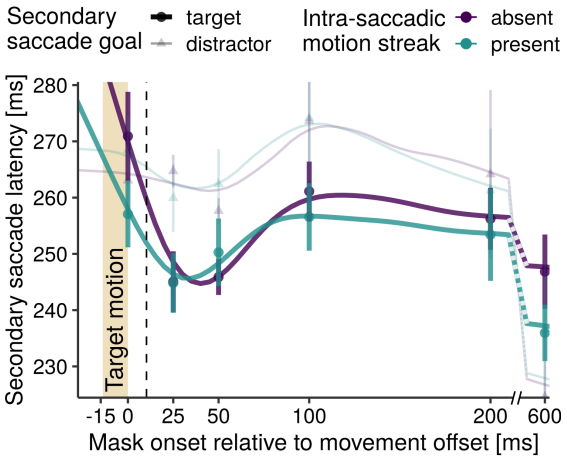

Figure 3. Secondary saccade latency across observers when making secondary saccades to either the initial pre-saccadic target (thick lines and circles) or the distractor (thin, transparent lines and triangles), depending on surface-feature duration and presence of intra-saccadic motion (purple vs green points and lines; error bars indicate $\pm SEM$). The beige area indicates the temporal interval of target motion, the vertical dashed line shows the average time of saccade offset after motion offset. Solid lines are predictions of two mixed-effects generalized additive models that describe the time course of observers' secondary saccade latencies as a function of increasing surface-feature duration. Parametric coefficients of the models indicated an overall significant reduction of secondary saccade latency in the motion-present condition when saccades were directed to the target (Estimate = -5.99, t = -2.21, p = .028), but not when they were directed to the distractor (Estimate = 2.38, t = 0.49, p = .624). The models' difference smooth terms further suggested a time course modulation due to intra-saccadic motion for target-bound secondary saccades (edf = 9.91, F = 2.99, p = .001), but again not for distractor-bound secondary saccades (edf = 1.01, F = 0.04, p = .836).

target and distractor to further explore the effects of our experimental design variables onto secondary saccade latency. For secondary saccades made to the target stimulus, and relative to the intercept of the model (no continuous intra-saccadic motion, no surface features), we found significant latency reductions for increasing surface-feature durations (25 ms: β = -26.60, t = -4.87, 95% CI [-37.55, -15.74], p < .001; 50 ms: β = -28.25, t = -5.20, 95% CI [-39.11, -17.60], p < .001; 100 ms: β = -12.89, t = -2.39, 95% CI [-23.07, -2.21], p = .017; 200 ms: β = -19.18, t = -3.54, 95% CI [-30.02, -8.59], p < .001; 600 ms: β = -29.19, t = -5.39, 95% CI [-40.72, -18.31], p < .001), but these latency reductions did not have a linear time course (**Figure 3**). For secondary saccades made to the distractor, we observed no such dependence (25 ms: β = -0.82, t = -0.127, 95% CI [-13.91, 11.08], p = .898; 50 ms: β = -6.92, t = -1.02, 95% CI [-20.88, 6.72], p = .309; 100 ms: β = 5.87, t = 0.80, 95% CI [-8.40, 19.96], p = .421; 200 ms: β = -3.00, t = -0.40, 95% CI [-18.20, 12.31], p = .690; 600 ms, as an exception: β = -24.75, t = -3.33, 95% CI [-39.45, -10.71], p < .001). Critically, in the absence of surface features, presence of intra-saccadic motion significantly reduced secondary saccade latency to the target (β = -14.27, t = -2.59, 95% CI [-25.43, -3.38], p = .001), but not to the distractor (β = 2.93, t = 0.46, 95% CI [-10.58, 15.41], p = .644). This result was corroborated by model comparisons of models including only surface-feature duration and additive models also including the factor intra-saccadic motion: The additive model was slightly better at explaining latencies of secondary saccades to the target (BF_{01} = 1.72, ΔLL = +3.00, $\chi^2(1)$ = 5.6, p = .018), but not to the distractor (BF_{01} = 0.03, ΔLL = +0.01, $\chi^2(1)$ = 0.03, p = .856). Moreover, adding the interaction term improved neither the target model (BF_{01} < 0.001, ΔLL = +4.0, $\chi^2(5)$ = 7.46, p = .189), nor the distractor model (BF_{01} < 0.001, ΔLL = +0.9, $\chi^2(5)$ = 1.81, p = .874), suggesting that the effect of intra-saccadic stimulus motion on secondary saccade latency was additive. In fact, for both target and distractor models, none of the interactions between intra-saccadic motion and suface-feature duration reached significance, except when making secondary saccades to the target at a surface-feature duration of 50 ms (β = 18.01, t = 2.39, 95% CI [3.20, 32.45], p = .017), in which the effect of the motion streak is reversed with respect to the 0 ms condition (see **Figures 3** and **4d**).

Taken together, the presence of intra-saccadic stimulus motion thus not only increased the proportion of secondary saccades to the initial pre-saccadic target, but also reduced their latency. A notable detail of the latter result is that the estimated reduction of 14.27 ms (95% CI [25.43, 3.38]) in secondary saccade latency (when no surface features were available) is remarkably similar to the duration of intra-saccadic motion, i.e., 14.6 ms.

Primary saccade landing positions influence gaze correction

If more than one candidate object for post-saccadic gaze correction is available, a secondary saccade often goes to the closer one (Hollingworth et al., 2008). To investigate a potential interaction of this effect with our observed influence of surface-feature duration and intra-saccadic object motion, we conducted the following analysis. For each trial, we computed the Euklidean distance from the landing position of the primary saccade to the center of the target and to the center of the distractor (**Figure 4a**). Positive values of the difference between these distances (d_{diff}) denote landing positions closer to the target than to the distractor. Subsequently, we used d_{diff} in linear mixed-effects regressions to predict saccades to the target as opposed to the distractor (logistic regression; **Figure 4b**) and secondary saccade latency to the target (linear regression; **Figure 4d**).

In predicting secondary saccades to the target, d_{diff} drastically improved the model fit (compared to a model assuming only surface-feature duration) as an additive predictor ($BF_{01} > 10^{50}$, ΔLL = +576.7, $\chi^2(1)$ = 1153.26, p < .001), but only marginally in its interaction with surface-feature duration (BF_{01} < 0.001, ΔLL = +5.2, $\chi^2(5)$ = 10.55, p = .061). When neither surface features nor intra-saccadic motion were available (0 ms, absent condition), landing 1 dva closer to the target increased

the probability of making a secondary saccade to the target by a factor of 1.75 (β = 0.56, z = 12.22, 95% CI [0.47, 0.65], p < .001). As shown in **Figure 4b**, this slope decreased slightly when surface features were available upon landing. This decrease was negligible at shorter (25 ms: β = -0.08, z = -1.20, 95% CI [-0.20, 0.05], p = .229; 50 ms: β = -0.07, z = -1.07, 95% CI [-0.21, 0.06], p = .284; 100 ms: β = -0.03, z = -0.47, 95% CI [-0.17, 0.11], p = .636), but significant at longer surface-feature durations (200 ms: β = -0.21, z = -3.01, 95% CI [-0.36, -0.07], p = .003; 600 ms: β = -0.19, z = -2.78, 95% CI [-0.33, -0.06], p = .006). The presence of intra-saccadic target motion significantly increased the probability of secondary saccades to the target when no surface features were available after the displacement (β = 0.34, z = 3.91, 95% CI [0.17, 0.51], p < .001), an effect that was reduced in strength only at 100 ms (β = -0.28, z = -2.16, 95% CI [-0.54, -0.02], p = .031) and 200 ms (β = -0.30, z = -2.28, 95% CI [-0.56, -0.04], p = .023), but not at other surface-feature durations (25 ms: β = -0.16, z = -1.31, 95% CI [-0.40, 0.08], p = .188; 50 ms: β = -0.15, z = -1.22, 95% CI [-0.40, 0.09], p = .223; 600 ms: β = -0.12, z = -0.95, 95% CI [-0.38, 0.13], p = .342). Again, model comparisons suggested that the effects of the two factors were largely additive; including the presence of intra-saccadic motion improved the fit (BF_{01} = 849.46, ΔLL = +12.3, $\chi^2(1)$ = 23.29, p < .001); its interaction with d_{diff} or surface-feature duration did not (BF_{01} < 0.001, ΔLL = +7.3, $\chi^2(11)$ = 16.75, p = .116).

The same analyses were conducted examining linear mixed-effects models predicting secondary saccade latency, provided that these saccades were made to the target. A distribution of all secondary saccade latencies (M_{absent} = 254.6, SD_{absent} = 39.5, $M_{present}$ = 250.4, $SD_{present}$ = 36.4), stacked across observers, is shown in **Figure 4c**. Again, d_{diff} very well predicted saccade latency, but more so as an additive predictor (BF_{01} > 10^{50}, ΔLL = +121.0, $\chi^2(1)$ = 243.85, p < .001) than combined with its interaction with surface-feature duration (BF_{01} < 0.001, ΔLL = +8.1, $\chi^2(5)$ = 14.41, p = .013). When neither surface features nor intra-saccadic motion were available (0 ms, absent condition), landing 1 dva closer to the target reduced secondary saccade latency by 8.4 ms (β = -8.40, t = -4.25, 95% CI [-12.29, -4.53], p < .001). This effect was unaltered by surface-feature duration (25 ms: β = -0.58, t = -0.22, 95% CI [-5.78, 4.59], p = .825; 50 ms: β = 3.02, t = 1.21, 95% CI [-1.97, 7.95], p = .226; 100 ms: β = 2.23, t = 0.89, 95% CI [-2.73, 7.16], p = .372; 200 ms: β = -1.55, t = -0.62, 95% CI [-6.51, 3.33], p = .533; 600 ms: β = 1.61, t = 0.64, 95% CI [-3.24, 6.53], p = .519). When intra-saccadic motion was present, secondary saccade latencies to the target were reduced by 12.4 ms (0 ms: β = -12.36, t = -2.93, 95% CI [-20.71, -4.15], p = .003). This effect was not reduced significantly for any surface feature duration (25 ms: β = 10.79, t = 1.93, 95% CI [-0.15, 21.83], p = .054, 100 ms: β = 4.65, t = 0.89, 95% CI [-5.62, 15.14], p = .374, 200 ms: β = 5.56, t = 1.06, 95% CI [-4.68, 15.93], p = .287, 600 ms: β = 7.25, t = 1.39, 95% CI [-2.95, 17.40], p = .165), except at 50 ms (β = 15.83, t = 2.98, 95% CI [5.26, 26.35], p = .003). Moreover, there was neither an interaction between intra-saccadic motion and d_{diff} (β = -0.45, t = -0.17, 95% CI [-5.78, 4.85], p = .868) nor any higher-level interaction (for full results, see Open Methods at OSF). Even in the grand means, collapsing over any other variables, we found a small, but significant difference between observers' secondary saccade latencies in the present vs absent conditions ($M_{absent\text{-}present}$= 4.17, SEM = 1.68; paired t-test: t(9) = 2.48, p = .035). Indeed, model comparisons revealed that a model including the presence of intra-saccadic motion as an additive factor should be preferred to a model including only d_{diff} and surface-feature duration (BF_{01}= 7.76, ΔLL = +6.1, $\chi^2(1)$ = 13.57, p < .001). The full model only marginally improved the fit of the model over the additive model (BF_{01}< 0.001, ΔLL = +10.0, $\chi^2(11)$ = 18.67, p = .067).

Efficient motion streaks facilitate gaze correction

Finally, to establish which stimulus features drive secondary saccades to the target stimulus, we performed a pre-registered large-scale reverse regression analysis (see Methods). Both contrast sensitivity for

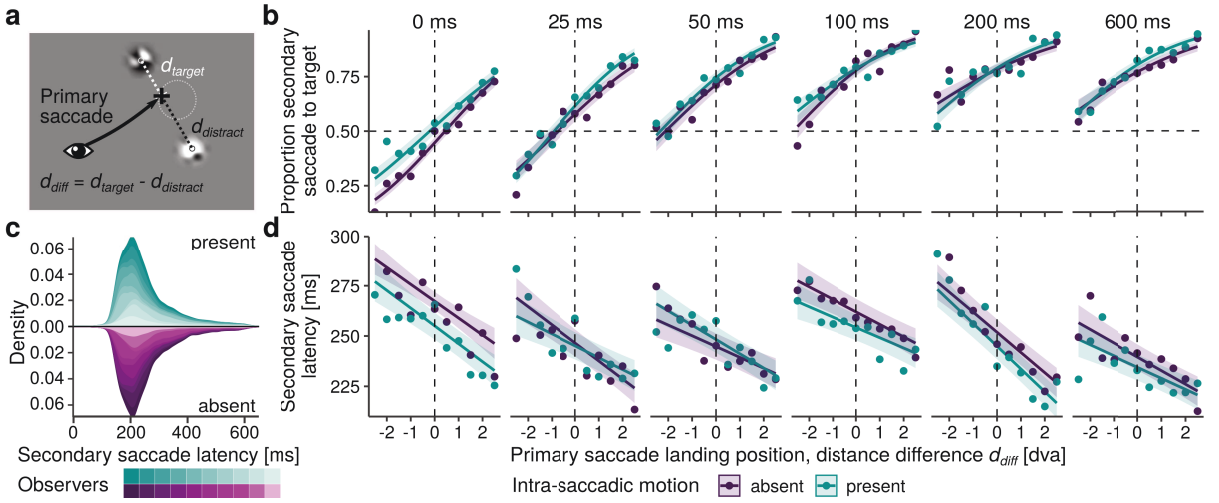

Figure 4. Primary saccade landing positions influence gaze correction. **a** d_{diff} was defined as the difference between the distance from primary saccade landing to the target and the distance to the distractor. Positive values denote that saccades landed closer to the target than to the distractor. **b** Logistic fits modeling the relationship between d_{diff} and the proportion of making a secondary saccade to the target for motion-absent (purple) and motion-present (green) conditions. Panels show results for each surface-feature duration separately. Points indicate group means per 0.5-dva bin. Shaded error bars indicate 95% confidence intervals determined by parametric bootstrapping. **c** Distributions of secondary saccade latencies for each observer. Upper and lower densities represent the motion-absent and motion-present condition, respectively. **d** Linear fits predicting secondary saccade latency to the target stimulus based on d_{diff}, surface-feature duration, and presence of intra-saccadic motion.

moving stimuli and motion perception – especially of high-SF stimuli – are known to dissipate at saccadic velocities (e.g., Burr & Ross, 1982; Castet et al., 2002; Schweitzer & Rolfs, 2019). We hypothesized, therefore, that the rapid movement of the target across the retina produced intra-saccadic motion streaks (Bedell & Yang, 2001; Brooks et al., 1980; Duyck et al., 2016; Geisler, 1999; Matin et al., 1972). In this case, secondary saccades to the target should be facilitated if stimulus features (incidentally) produced a distinctive streak, for instance if the orientation of a stimulus is parallel to its trajectory on the retina (Schweitzer & Rolfs, 2020).

As the noise patches used in this task could potentially contain all possible orientations, as well as SFs from 0.25 to 1 cpd, it was possible to describe each noise patch – both target and distractor – in terms of energy per SF-orientation component (see Methods for details). In brief, for each trial (regardless of whether intra-saccadic target motion was absent or present), we obtained a filter response map for target stimulus by convolving the noise patch with a bank of Gabor filters (**Figure 5a**). Next, we extracted the angle of the target's trajectory across the retina, which was determined by the target trajectory presented on the screen and the gaze trajectory during presentation (for an illustration, see **Figure 5b**). We then normalized stimulus orientations using this retinal angle, resulting in a measure of relative orientation. As a consequence, stimulus orientations parallel to the retinal angle would result in relative orientations of 0 degrees, whereas stimulus orientations orthogonal to the retinal angle would result in relative orientations of 90 degrees. Finally, we ran mixed-effects logistic regressions to predict secondary saccades to the target (as opposed to the distractor) from the filter responses present in all available target stimuli. Note that a positive relationship between filter responses in a SF-orientation component and secondary saccades to the target implies that this component is beneficial for gaze correction to the target.

When intra-saccadic motion was absent (**Figure 5c**, left panel), low SFs predicted secondary saccades to the stimulus better than high SFs (GAM: edf = 4.02, F =

15.38, p < .001; LM: β = -2.48, t = -5.13, 95% CI [-3.43, -1.53], p < .001), whereas relative orientation did not have any impact on gaze correction (GAM: edf = 1.00, F = 0.16, p = .689; LM: β = 0.19, t = 1.02, 95% CI [-0.17, 0.54], p = .306). By contrast, when intra-saccadic motion was present, saccades to target stimuli were driven by smaller relative orientations (GAM: edf = 1.00, F = 15.43, p < .001; LM: β = -1.53, t = -5.97, 95% CI [-2.04, -1.03], p < .001), peaking at relative orientations close to zero (i.e., orientations parallel to the retinal trajectory; **Figure 5c**, middle panel). Moreover, although low SFs were still most relevant, the difference between low and high SFs was reduced (GAM: edf = 2.14, F = 5.01, p = .005; LM: β = 1.43, t = 2.09, 95% CI [0.08, 2.77], p = .036), suggesting that high SFs played a larger role when intra-saccadic motion was available. Crucially, a significant interaction between SFs and relative orientation in the motion-present condition suggested that high SFs were not simply globally more influential, but gained relevance at relative orientations close to zero (GAM: edf = 1.01, F = 21.97, p < .001; LM: β = -3.33, t = -4.63, 95% CI [-4.74, -1.91], p < .001), that is, when (high-SF) stimulus orientations were parallel to the stimulus' retinal trajectory. This interaction was not present in the movement-absent condition (GAM: edf = 1.0, F = 2.24, p = .134; LM: β = 0.75, t = 1.47, 95% CI [-0.25, 1.74], p = .143).

Finally, the right panel of **Figure 5c** shows the difference surface of GAM fits for the two experimental conditions. Both conditions were similar with respect to the high predictive value for low-SF components, suggesting that mainly low spatial frequencies served as cues to initiate secondary saccades to target and distractor stimuli. This result seems plausible, not only because post-saccadic stimulus locations were in the visual periphery, but also because filter responses to low SFs were more dissimilar between distractor and target than to high SFs (due to the way luminance was added or subtracted to make the noise patches dissimilar; see Methods), and therefore allowed for better discrimination between the two stimuli. For instance, filter responses to the target and filter responses to the distractor were positively correlated at a SF of 1 cpd (Pearson correlation coefficient, r(19176) = 0.235, 95% CI [0.222, 0.249], p < .001), but strongly negatively correlated at a SF of 0.25 cpd (r(19176) = -0.655, 95% CI [-0.663, -0.647], p < .001). However, low SFs were beneficial in both movement conditions. Close inspection of the difference surface suggests that (relatively) high-SF information drove saccades to the target only when intra-saccadic motion was presented and orientations were close to parallel to the target's retinal trajectory.

Discussion

With each saccade we make, visual objects move rapidly across our retinae, producing transient blurred motion trajectories lawfully related to the ongoing movement. In this study, we emulated these trajectories using a projection system capable of displaying continuous object motion (as opposed to apparent motion from a simple displacement) strictly during saccades with high spatiotemporal fidelity. This technique allowed us to investigate the novel hypothesis that intra-saccadic information about the changing position of saccade targets might facilitate post-saccadic gaze correction to these targets. We tightly controlled the post-saccadic availability of surface features which have been shown to play a crucial role in gaze correction tasks (Hollingworth et al., 2008; Richard et al., 2008), by presenting pixel masks at varying delays. This manipulation allowed us to assess the impact of intra-saccadic motion on the proportion of secondary saccades to the target and secondary saccade latencies, in addition to the time course of the processing of object features.

Even when little or no post-saccadic object information was available, the presence of intra-saccadic target motion increased the rate of secondary saccades to the original pre-saccadic target and reduced their initiation latency. These results are central to our hypothesis, as they suggest that intra-saccadic information was not suppressed or otherwise omitted – as widely assumed (for a review, see Castet, 2010) – but instrumental for timely gaze correction.

The magnitudes of these effects may seem small at first, but they were consistent with what was to be

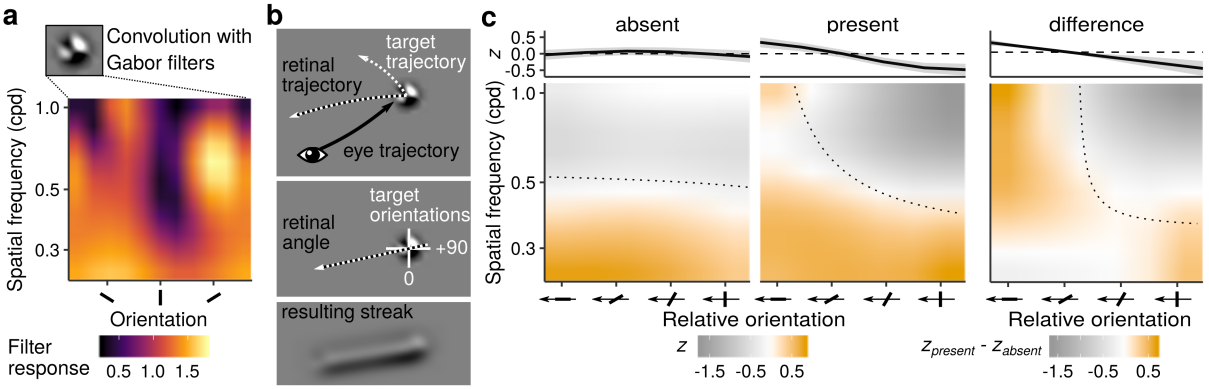

Figure 5. Efficient motion streaks facilitate gaze correction. **a** Example of a filter energy map computed by convolving the noise patch stimulus with a bank of Gabor filters. **b** The retinal trajectory of the target stimulus is the vector sum of the stimulus' trajectory presented on the screen and the eye position vector during presentation. We computed relative orientation by normalizing the stimulus' orientation components using the angle of the retinal trajectory. As illustrated by motion filtering applied to the noise patch, orientations parallel to the stimulus' motion trajectory on the retina should lead to distinctive motion streaks. **c** Results from the reverse regression analyses, fitted by the multivariate GAM, averaged across all surface-feature durations. High z-scores (orange) imply that filter responses in a given SF-orientation component predict the occurrence of a secondary saccade to the target when intra-saccadic motion was present (middle panel) and absent (left panel). Dotted lines represent the transition from negative to positive z-scores estimated by the linear model corresponding to the GAM. Upper marginal means show the effect of relative orientation averaged across all spatial frequency components. The surface difference (right panel) clearly indicates that secondary saccades to the target (and not to the distractor) were mostly driven by stimulus orientations parallel to the stimulus' retinal trajectory, suggesting a role of temporal integration of fast-moving stimuli, i.e., motion streaks.

expected from a 14.6-ms intra-saccadic motion duration: Information about post-displacement object features was accumulated in a exponential fashion right upon motion onset. A comparison of the parameters of these exponential functions suggests that facilitation caused by intra-saccadic motion was not due to an increase of gain or acculumation rate when processing object features and locations, but due to their earlier availability of these, starting with the intra-saccadic target motion. Notably, even when continuous object motion was absent, the models predicted that at saccade offset (on average 10 ms after object motion offset) secondary saccade rates to the target would be already above chance, suggesting that the processing starts before saccade landing. Consistent with this view, the estimated secondary saccade latency reduction was again of the same magnitude as the motion duration both when surface features were unavailable and when they were available for the entire 600 ms. Note that, in this task, the motion duration was barely a third of the mean saccade duration. In natural vision, any visual object could produce motion smear across the entire duration of the saccade, possibly supporting short-latency corrective saccades upon saccade landing.

Furthermore, we not only showed that the effect of intra-saccadic object motion is orthogonal to the effect of primary saccade landing positions (cf. Hollingworth et al., 2008), but also provided evidence for the benefit of effective temporal integration when stimulus orientations were aligned with their retinal motion trajectories – a typical signature of motion streaks (Schweitzer & Rolfs, 2020). In other words, the more effectively the combined movement of eye and target in a given trial generated a motion streak, the more often did a secondary saccade go to the target. Although it has been shown that motion perception during saccades is possible (Castet et al., 2002), contrast sensitivity to gratings orthogonally oriented to their motion trajectories is drastically reduced at saccadic velocities (Burr & Ross, 1982; Mitrani & Yakimoff, 1970). In contrast, motion streaks often remain well resolved even at saccadic speeds (Bedell & Yang, 2001; Brooks et al., 1980;

Duyck et al., 2016; Matin et al., 1972), partly due to visual persistence. This invites the intruiging hypothesis that they might be able to link objects across saccades via spatiotemporal continuity. Our results show that even when objects were displaced while the eyes were in mid-flight, a continuous presence of the target throughout the saccade – as opposed to a very brief disruption of this continuity – facilitated gaze correction, regardless of how long feature information was available after the displacement. Although this facilitation was clearly strongest shortly after motion offset, interactions between surface-feature duration and presence of intra-saccadic motion were rarely significant and all model comparisons performed on both secondary saccade rate and latency data favoured the additive model over the full model. These consistent results suggest that post-saccadic object features and spatiotemporal continuity – established by intra-saccadic continuous object motion – contributed rather independently to gaze correction performance. This conclusion is well in line with the predictions of the object-file theory (Kahneman et al., 1992; Mitroff & Alvarez, 2007), which suggests that objects are bound to spatial indexes. It is also consistent with the view that surface features are functional for the establishment of object correspondence (Hollingworth et al., 2008; Hollingworth & Franconeri, 2009; Richard et al., 2008): Intra-saccadic motion streaks may not only be indicators of amplitude and direction of continuous shifts of objects across saccades, but to some extent also maintain the object's surface features, such as color, which has been shown to be largely unaltered by saccadic suppression (Burr et al., 1994; Bridgeman & Macknik, 1995; Knöll et al., 2011), throughout the saccade.

To conclude, our results support the idea that saccades do not cause gaps in visual processing, as even motion smear induced by high-velocity, brief, unpredictable, and strictly intra-saccadic object motion was taken into account when performing gaze correction. Depending on the efficiency of intra-saccadic vision especially in real-world visual environments, the visual consequences induced by our very own saccades may constitute an unexpected contribution to achieving object continuity and, through it, visual stability.

Acknowledgments

R.S. was supported by the Studienstiftung des deutschen Volkes and the Berlin School of Mind and Brain. M.R. was supported by the Deutsche Forschungsgemeinschaft (DFG, grants RO3579/8-1 and RO3579/10-1).

We thank Emilia Maria Rehse for her indispensable work in data collection, as well as Lisa Kröll, Greta Häberle, Frederik Geweke, and Bryce Yahn for their support in the initial stages of the project.

Author contributions

R.S. and M.R. conceived, designed, and preregistered the study. R.S. implemented and conducted the experiment. R.S. analyzed data under M.R.'s supervision. R.S. drafted the manuscript, and M.R. provided critical revisions.

References

Aagten-Murphy, D., & Bays, P. M. (2019). Functions of memory across saccadic eye movements. In *Processes of visuospatial attention and working memory* (pp. 155–183). Springer International Publishing.

Balsdon, T., Schweitzer, R., Watson, T., & Rolfs, M. (2018). All is not lost: Post-saccadic contributions to the perceptual omission of intra-saccadic streaks. *Consciousness and cognition*, *64*, 19-31.

Bates, D., Mächler, M., Bolker, B., & Walker, S. (2015). Fitting linear mixed-effects models using lme4. *Journal of Statistical Software*, *67*(1), 1-48.

Bedell, H., & Yang, J. (2001). The attenuation of perceived image smear during saccades. *Vision Research*, *41*(4), 521–528.

Bridgeman, B., & Macknik, S. (1995). Saccadic suppression relies on luminance information. *Psychological research*, *58*(3), 163–168.

Bridgeman, B., Van der Heijden, A. H. C., & Velichkovsky, B. M. (1994). A theory of visual stability across saccadic eye movements. *Behavioral and Brain Sciences*, *17*(2), 247–258.

Brooks, B., Yates, J., & Coleman, R. (1980). Perception of images moving at saccadic velocities during saccades and during fixation. *Experimental Brain Research*, *40*(1), 71–78.

Burr, D., Morrone, M., & Ross, J. (1994). Selective suppression of the magnocellular visual pathway during saccadic eye movements. *Nature*, *371*(6497), 511–513.

Burr, D., & Ross, J. (1982). Contrast sensitivity at high velocities. *Vision research*, *22*(4), 479–484.

Campbell, F., & Wurtz, R. (1978). Saccadic omission: why we do not see a grey-out during a saccadic eye movement. *Vision research*, *18*(10), 1297–1303.

Carrasco, M., & McElree, B. (2001). Covert attention accelerates the rate of visual information processing. *Proceedings of the National Academy of Sciences*, *98*(9), 5363–5367.

Castet, E. (2010). Perception of intra-saccadic motion. In *Dynamics of visual motion processing, chapter 10* (pp. 213–238). Springer.

Castet, E., Jeanjean, S., & Masson, G. (2002). Motion perception of saccade-induced retinal translation. *Proceedings of the National Academy of Sciences*, *99*(23), 15159–15163.

Comets, E., Lavenu, A., & Lavielle, M. (2017). Parameter estimation in nonlinear mixed effect models using saemix, an R implementation of the SAEM algorithm. *Journal of Statistical Software*, *80*(3), 1–41. doi: 10.18637/jss.v080.i03

Duyck, M., Collins, T., & Wexler, M. (2016). Masking the saccadic smear. *Journal of vision*, *16*(10), 1.

Engbert, R., & Kliegl, R. (2003). Microsaccades uncover the orientation of covert attention. *Vision research*, *43*(9), 1035–1045.

Engbert, R., & Mergenthaler, K. (2006). Microsaccades are triggered by low retinal image slip. *Proceedings of the National Academy of Sciences*, *103*(18), 7192-7197.

Geisler, W. (1999). Motion streaks provide a spatial code for motion direction. *Nature*, *400*(6739), 65-69.

Hollingworth, A., & Franconeri, S. L. (2009). Object correspondence across brief occlusion is established on the basis of both spatiotemporal and surface feature cues. *Cognition*, *113*(2), 150–166.

Hollingworth, A., Richard, A. M., & Luck, S. J. (2008). Understanding the function of visual short-term memory: transsaccadic memory, object correspondence, and gaze correction. *Journal of experimental psychology. General*, *137*(1), 163–181.

Jarosz, A. F., & Wiley, J. (2014). What are the odds? a practical guide to computing and reporting bayes factors. *The Journal of Problem Solving*, *7*(1), 2.

Kahneman, D., Treisman, A., & Gibbs, B. (1992). The reviewing of object files: Object-specific integration of information. *Cognitive Psychology*, *265*, 175-219.

Kleiner, M., Brainard, D., Pelli, D., Ingling, A., Murray, R., & Broussard, C. (2007). What is new in psychtoolbox-3. *Perception*, *36*(14), 1-16.

Knöll, J., Binda, P., Morrone, M. C., & Bremmer, F. (2011). Spatiotemporal profile of peri-saccadic contrast sensitivity. *Journal of vision*, *11*(14), 15.

MacKay, D. M. (1973). Visual stability and voluntary eye movements. In *Central processing of visual information a: integrative functions and comparative data* (pp. 307–331). Springer.

Matin, E., Clymer, A., & Matin, L. (1972). Metacontrast and saccadic suppression. *Science*, *178*(4057), 179–182.

Mitrani, L., & Yakimoff, N. (1970). Smearing of the retinal image during voluntary saccadic eye movements. *Vision Research*, *10*(5), 405–409.

Mitroff, S. R., & Alvarez, G. A. (2007). Space and time, not surface features, guide object persistence. *Psychonomic Bulletin & Review*, *14*(6), 1199–1204.

Pelli, D. (1997). The videotoolbox software for visual psychophysics: Transforming numbers into movies. *Spatial vision*, *10*(4), 437–442.

R Core Team. (2015). *R: A language and environment for statistical computing*. R Foundation for Statistical Computing, Vienna, Austria. Retrieved from `http://www.R-project.org/` (ISBN 3-900051-07-0)

Richard, A., Luck, S., & Hollingworth, A. (2008). Establishing object correspondence across eye movements: Flexible use of spatiotemporal and surface feature information. *Cognition*, *109*(1), 66–88.

Ross, J., Morrone, M., Goldberg, M., & Burr, D. (2001). Changes in visual perception at the time of saccades. *Trends in neurosciences*, *24*(2), 113–121.

Schweitzer, R., & Rolfs, M. (2019). An adaptive algorithm for fast and reliable online saccade detection. *Behavior research methods*, 1–18.

Schweitzer, R., & Rolfs, M. (2020). Intra-saccadic motion streaks as cues to linking object locations across saccades. *Journal of Vision*, *20*(4), 17. doi: 10.1167/jov.20.4.17

Volkmann, F. C. (1986). Human visual suppression. *Vision research*, *26*(9), 1401–1416.

Wood, S. N. (2003). Thin plate regression splines. *Journal of the Royal Statistical Society: Series B (Statistical Methodology)*, *65*(1), 95–114.

Wood, S. N. (2017). *Generalized additive models: an introduction with R*. Chapman and Hall/CRC.

Wurtz, R. H. (2008). Neuronal mechanisms of visual stability. *Vision research*, *48*(20), 2070–2089.

Wyart, V., Nobre, A., & Summerfield, C. (2012). Dissociable prior influences of signal probability and relevance on visual contrast sensitivity. *Proceedings of the National Academy of Sciences*, *109*(9), 3593-3598.

5.1.5 Study V

Manuscript in preparation:

Schweitzer, R., Watson, T., Balsdon, T., & Rolfs, M. (in preparation). The reference frame of intra-saccadic vision.

Conference presentations:

Schweitzer, R., Watson, T., Balsdon, T., & Rolfs, M. (August, 2019). Formation of world-centered perception of intra- saccadic motion streaks. Poster at the *20th European Conference on Eye Movements*, Alicante, Spain.

Schweitzer, R., Watson, T., Balsdon, T., & Rolfs, M. (May, 2018). From retinal to world-centered perception of intra-saccadic motion streaks: Evidence for high-fidelity eye position information during saccades. Poster at the *18th Annual Meeting of the Vision Sciences Society*, St. Petersburg (FL), USA.

Pre-registration:

Experiment 1: `https://osf.io/3kpq4/?view_only=044fb911e0dd414ebfbd1ddc122180af`

Experiment 2: `https://osf.io/95w8v/?view_only=d2e12749d79248df8dee6c9fee948ee2`

Experiment 3: `https://osf.io/kmqzc/?view_only=783112b9a06e4258b6300e1bed82f43f`

Featured code:

Direction-based detection of post-saccadic oscillations:
`https://github.com/richardschweitzer/OnlineSaccadeDetection`

Manuscript in preparation, work in progress
Ver. 1 (July, 2020)

ISSN XXX-XXXX-XXXX

The reference frame of intra-saccadic vision

Richard Schweitzer[1,2,3], Tamara Watson[4], Tarryn Balsdon[5,6], & Martin Rolfs[1,2,3]

(1) Department of Psychology, Humboldt-Universität zu Berlin, Berlin, Germany; (2) Berlin School of Mind and Brain, Humboldt-Universität zu Berlin, Berlin, Germany; (3) Bernstein Center for Computational Neuroscience, Berlin, Germany; (4) School of Social Sciences and Psychology, Western Sydney University, Sydney, Australia; (5) Laboratoire des systèmes perceptifs, Département d'études cognitives, École normale supérieure, CNRS, Paris, France; (6) Laboratoire de neurosciences cognitives computationelles, Département d'études cognitives, École normale supérieure, INSERM, Paris, France

Even though saccades constantly cause rapidly changing retinal input to be sent along the retinotopically organized visual processing pathways, human observers usually have little trouble to represent visual stimuli in world-centered coordinates, which suggests the need of combining retinal with eye position information. By presenting rapid, unpredictable, and strictly intra-saccadic target motion using a 1440-fps projection system, we investigated the subjective appearance and localization of motion streaks induced by simultaneous eye and stimulus movement, reported by unconstrained computer mouse drawings. We found that observers did not simply report the retinal trajectory of the motion streak, but produced trajectories which followed a systematically different pattern and – in specific cases – were even strikingly similar to world-centered target trajectories. Even though these response patterns differed to some degree between experiments, they were unaffected by varying visual field location, background luminance and structure, and even additional large-field background motion injected during saccades. By modeling the underlying eye position signal for each response, we found that overall localization, appearance, and time course of perceived trajectories could be well explained by the assumption that retinal locations sampled over time were combined with an early-onset, but slowly changing representation of physical eye position, which is compatible with various results from the peri-saccadic flash localization literature. However, to sufficiently explain response patterns, crucial visual factors, such as motion direction and target contrast, had to be taken into account. Our results suggest that motion streaks emanate from retinotopic processing, but can be (imperfectly) localized in a world-centered reference frame.

Keywords: active vision, saccades, motion streaks, intra-saccadic vision, visual localization

Introduction

It seems to come naturally to most intelligent agents to tell whether a sensory change is caused by an external event in the environment or as a consequence of self-motion. Thanks to this capability, the agent is able to navigate around and act upon objects in the world. An impressive example of that capability is the human visual system: Even though rapid eye movements – so-called saccades – are made to constantly re-orient the non-homogeneous retina and retinotopically organized early visual processing hierachies towards objects of interest, objects are seamlessly localized in world-centered coordinates, so that we can readily point towards or grasp them. In addition to that, saccade-induced visual consequences, that is, both the constantly changing retinal locations of each object in the visual scene and the large amount of motion blur that should occur when projections of objects are rapidly shifted across the retina, are largely omitted from perception. In order to achieve a stable, world-centered perception of the world, the retinal signal is therefore thought to be combined with a reference signal providing information on eye (and head) position which could be recruited from proprioceptive ("inflow") and motor ("outflow") signals (Bridgeman, Van der Heijden, & Velichkovsky, 1994; MacKay, 1973; Mittelstaedt, 1990; Wurtz, 2008), or even purely from visual context (Gibson, 1966), while most evidence favors the view that copies of motor commands – known as efference copy (Von Holst & Mittelstaedt, 1950) or corollary discharge (Sperry, 1950) – serve as the basis of this reference signal (Sommer & Wurtz, 2008; Wurtz, 2018). Although it is ulti-

Correspondence should be addressed to Richard Schweitzer, Department of Psychology, Humboldt-Universität zu Berlin, Rudower Chaussee 18, 12489 Berlin, Germany, *E-mail:* richard.schweitzer@hu- berlin.de.

mately unclear how retinal information and eye position information are combined (for a number of possible approaches, see Bridgeman et al., 1994), the "elimination" approach assumes that any retinal change can be compensated for – by simple subtraction – if the size of the change in eye position is known. In fact, if the visual system had access to a near-perfect representation of eye position at any time point, this information could be sufficient not only to perform saccadic omission of saccade-induced motion, but also to compute object correspondence across saccades.

Although the accuracy of the eye position signal was thoroughly investigated in previous studies using peri-saccadic localization tasks, such as perceptual flash localization relative to visual scales (e.g., Bischof & Kramer, 1968; Honda, 1989; Mateeff, 1978; L. Matin, Matin, & Pola, 1970; Morrone, Ross, & Burr, 1997) or double-step tasks, in which secondary saccades were made to flashed targets (e.g., Dassonville, Schlag, & Schlag-Rey, 1992; Hallett & Lightstone, 1976a, 1976b), we apply a different approach in this study: Using a projection system operating with a temporal resolution of 1440 Hz, we gaze-contingently displayed targets that moved rapidly and unpredictably strictly during saccades, and asked observers' to report the phenomenological appearance of the resulting blurred motion trajectory – the motion streak (Geisler, 1999). Even though intra-saccadic motion smear is thought to be attenuated by active, extra-retinal mechanisms of saccadic suppression (for reviews, see Binda & Morrone, 2018; E. Matin, 1974; Ross, Morrone, Goldberg, & Burr, 2001; Volkmann, 1986), the perception of intra-saccadic motion is in principle possible (Castet, 2010; Castet, Jeanjean, & Masson, 2002; Castet & Masson, 2000) and motion streaks can be readily perceived when pre- and post-saccadic masking is alleviated (Brooks, Impelman, & Lum, 1981; Campbell & Wurtz, 1978; Duyck, Collins, & Wexler, 2016; Duyck, Wexler, Castet, & Collins, 2018; E. Matin, Clymer, & Matin, 1972; Schweitzer & Rolfs, 2020b). If a target stimulus moves rapidly during a saccade, then the target's retinal trajectory is the vector sum of stimulus and eye movement vectors. Depending on the extent to which target motion can be compensated for by the eye position signal, the perceived motion trajectory may be more similar to the world-centered (i.e., the motion trajectory displayed on the screen) or retinal motion trajectory (i.e., the motion trajectory on the retina). More specifically, if the eye position signal were a perfectly accurate representation of the ongoing saccade then observers would presumably report the world-centered trajectory of the stimulus, whereas if no eye position information were available then the retinal trajectory would be reported. To probe the accuracy of the eye position signal during saccades, the investigation of intra-saccadic motion streaks might thus be a useful tool, as they allow the assessment of the change in perceived stimulus position over time throughout the saccade. In three experiments, we investigate whether and to what extent observers were able to perceive unpredictable, strictly intra-saccadic stimulus motion in world-centered coordinates, systematically manipulating the effects of stimulus movement distance and duration, visual field location, background motion, as well as background type and luminance. Results are modeled and discussed in the context of damped eye position representations that enable the visual system to transform retinal coordinates to world-centered coordinates.

Experiment 1

In Experiment 1, we tested observers' ability to localize and report the phenomenological appearance of intra-saccadic motion streaks induced by rapidly moving noise patch target stimuli presented gaze-contingently during horizontal saccades on a uniform, grey background. Notably, motion streaks were unpredictable for observers, as target motion trajectories could start at nine screen locations, be directed in 12 different directions, and travel three different distances (**Figure 1a**). Observers responded using a standard computer mouse, if a motion streak was perceived in a given trial, and could skip their response if none was perceived.

Methods

Apparatus. Stimuli were projected onto a 16:9 (200 x 113 cm) video-projection screen (Celexon HomeCinema, Tharston, Norwich, UK) with a distance of 270 cm measured from the observer's eyes, using a ProPixx DLP projector (Vpixx Technologies, Saint-Bruno, QC, Canada) running at a refresh rate of 1440 Hz and a resolution of 960 x 540 pixels. The experimental code was implemented in MATLAB 2016b (Mathworks, Natick, MA, USA), using the Psychophysics and Eyelink toolboxes (Cornelisen, Peters, & Palmer, 2002; Kleiner et al., 2007) and was run on a Dell Precision T7810 Workstation with a Debian 8 operating system. Eye movements of both eyes were recorded using an EyeLink II head-mounted system (SR Research, Osgoode, ON, Canada) at a sampling rate of 500 Hz (without CR tracking and without heuristic link filter). Observers rested their head on a chin rest. Responses were collected with a standard computer mouse and US-english keyboard.

Participants. Ten observers were tested in four 1-hour sessions (on separate days) and received 35 Euros as remuneration. Written informed consent was obtained from all participants prior to the first session. The study was conducted in agreement with the Declaration of Helsinki (2013) and approved by the Ethics Committee of the German Society for Psychology. All observers (5 female; mean age: 26; age range: 19 – 37) had normal or corrected-to-normal vision (20/20 ft acuity in the Snellen test; one observer wore glasses and four observers wore contact lenses). Six of ten observers had right ocular dominance (established by a variant of the Porta test), only one of ten observers was left-handed. The

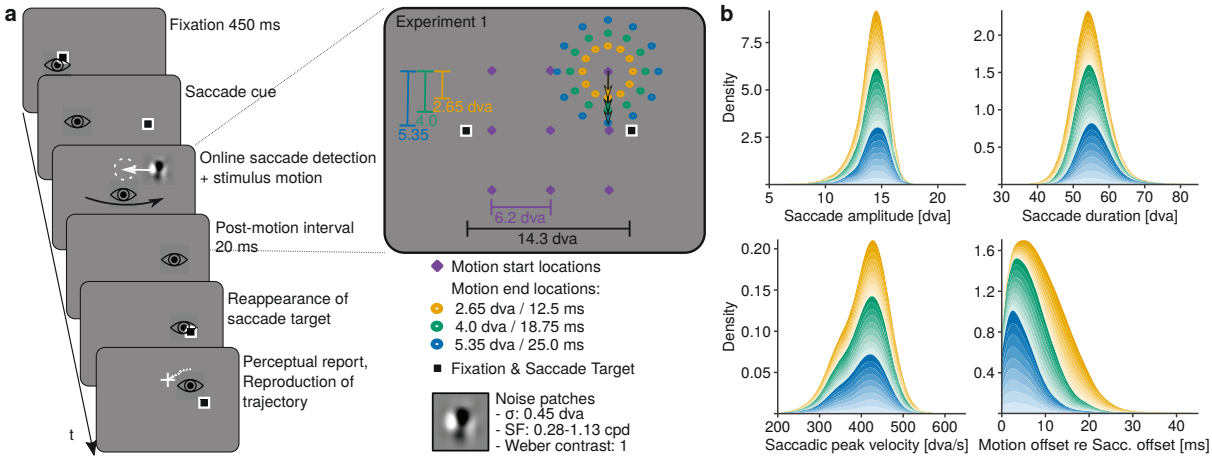

Figure 1. **a** Task procedure in Experiment 1. Observers made 14.3-dva horizontal saccades, during which unpredictable high-speed motion of a low-SF noise patch stimulus was displayed. Motion started at one of nine screen locations (violet diamonds) and could be directed in one of 12 directions. Stimuli traveled distances of 2.65 (orange), 4 (green), or 5.35 (blue) dva at constant velocities. After each saccade, observers reproduced motion trajectories using a computer mouse. **b** Distributions of saccade metrics. Varying color alpha levels represent different starting locations. Saccades had an average amplitude of 14.2 dva (SD = 0.8), taking on average 54.6 ms (SD = 2.0) with a peak velocity of 409.9 dva/s (SD = 40.8). Across observers, 25-ms motion ended 4.8 ms (SD = 2.1) prior to saccade offset, whereas 18.75-ms and 12.5-ms motion ended 8.2 ms (SD = 1.6 ms) and 13.5 ms (SD = 2.1 ms) prior to to saccade offset, respectively.

experiment was pre-registered at the Open Science Framework (OSF): `https://osf.io/3kpq4/`.

Task Procedure. Each trial started with a fixation control, using a fixation boundary with 1.3 dva radius. Observers fixated the fixation target for 450 milliseconds on the either left or right side on the screen (6-8 dva horizontal eccentricity from screen center). Upon successful fixation control plus a varying delay of 50-150 ms, the fixation target jumped to the location on the other side of the screen (14.3 dva horizontal eccentricity), which constituted the saccade target and the temporal cue to make a saccade. Observers made either rightward and leftward saccades (2 levels) and received ons creen feedback when saccades did not land within an area 1.8 dva around the saccade target or if two or more saccades – instead of one – were made to reach the saccade target. Saccades were detected using a velocity-based online saccade detection algorithm (Schweitzer & Rolfs, 2020a), using a direction restriction of ϑ=25 and three threshold settings, i.e., k=1 and λ=20, k=3 and λ=15, or k=5 and λ=10, to increase the temporal variance of stimulus presentations throughout the saccade. Upon saccade detection, a noise patch stimulus (see **Stimuli**) was rapidly moved across the screen, starting at one of nine screen locations – so-called stimulus anchors, organized in a grid in which individual starting locations were separated by 6.2 dva (9 levels) – and going in one of twelve directions (0: in saccade direction, 30, 60, 90: upwards, 120, 150, 180: against saccade direction, 210, 240, 270: downwards, 300, 330; 12 levels), as illustrated in **Figure** 1**a**, whereas in 10% of all trials no stimulus motion was presented. The distance travelled by moving stimuli varied between 2.65, 4, and 5.35 dva, with corresponding motion durations of 12.5, 18.75, and 25.0 ms (i.e., 18, 27, or 36 frames at a refresh rate of 1440 Hz; 3 levels). Thus, motion speed remained constant in all conditions at approximately 214 dva/s. During stimulus motion, the saccade target was removed, but reappeared 20 ms after stimulus motion offset. At 150 ms after the offset of stimulus motion, a crosshair mouse cursor appeared on the screen, allowing observers to draw their perceived motion trajectory from start to end. By clicking and holding the left or right mouse button, observers drew a white, dotted line, representing the perceived trajectory. This process could be repeated until observers were satisfied with the reproduction of the trajectory. By pressing the RightArrow key, observers accepted their latest drawing, thus ending the trial. By pressing LeftArrow, they indicated that no stimulus motion was perceived during the saccade, and the trial ended without any mouse response. All experimental conditions (2160 trials in total) were counter-balanced and trials were presented in a random and interleaved fashion, thus making stimulus motion and location entirely unpredictable. Observers had no knowledge about motion trajectories and were instructed to freely reproduce whatever they perceived during the saccade, defining the task as purely phenomenological. No feedback was given on responses. A slow-motion

video (i.e., 60 instead of 1440 frames per second) of the task procedure can be found at `https://osf.io/5vb4h/`.

Stimuli. Target stimuli were achromatic noise patches bandpass-filtered from 0.28 to 1.125 cpd, displayed on a uniform grey background. All noise patches were scaled to 100% Michelson contrast with maximum luminance twice the background luminance (Weber contrast: 1). Bandpass-filtered noise patches were enveloped in a Gaussian aperture with a standard deviation of 0.45 dva. Fixation and saccade targets were 0.4-dva quadratic black squares with white edging.

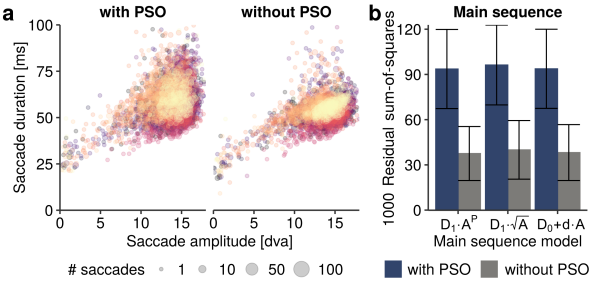

Figure 2. Evaluation of saccade offset without taking post-saccadic oscillations (PSOs) into account. **a** Relationship between saccade amplitude and saccade duration (uncleaned data from Experiment 1). Different colors indicate data from different observers (n = 10). Left: PSOs were included into saccade duration. Right: PSOs were detected and removed from the the saccade duration. **b** Three prominent main sequence models were fitted to the data (Becker, 1989; Collewijn, Erkelens, & Steinman, 1988; Lebedev, Van Gelder, & Tsui, 1996). As indicated by the residual sum-of-squares, all three models better described the data when PSO were excluded from saccade duration. Error bars denote one standard deviation.

Pre-processing. Prior to saccade detection, all trials were excluded that contained unsuccessful fixation controls, dropped presentation frames, or incorrect response keys. Saccades were detected within a time window of 200 ms before saccade cue onset until 100 ms after intra-saccadic stimulus motion offset, using the Engbert-Kliegl algorithm (Engbert & Kliegl, 2003; Engbert & Mergenthaler, 2006) with a scaling factor of 5 and a minimal duration of 12 samples. The algorithm was run on both eyes' data, but only saccades the observer's dominant eye were used for further analyses, unless that data was unavailable. To achieve a conservative estimate of saccade offset, we detected the peak of a post-saccadic oscillation (PSO; Hooge, Nyström, Cornelissen, & Holmqvist, 2015; Nyström, Hooge, & Holmqvist, 2013) using a custom direction-based method, which was made available on Github: `https://github.com/richardschweitzer/OnlineSaccadeDetection`. We first identified the overall direction of the saccade which served as the direction criterion. As a second step, using the online saccade detection algorithm by Schweitzer and Rolfs (2020a), we sequentially tested all saccade samples whether their direction was the same as the overall saccade direction. Crucially, a direction inversion usually takes place in the second half of the PSO, causing direction-based saccade detection to fail. This inversion point was then defined as the more conservative saccade offset. Indeed, excluding the second half of the PSO led to a considerable reduction in saccade duration (M=-4.16 ms, CI 95% [-5.36, -2.95], t(9)=-7.78, p<.001) and, as shown in **Figure** 2**a**, to a more realistic saccadic main sequence. Indeed, across three main sequence models, i.e., an exponential model (Becker, 1989), a square-root model (Lebedev et al., 1996), and a linear model (Collewijn et al., 1988), removing the second part of the PSO drastically reduced the residual sum-of-squares ($F(1,9)=38.2$, $\eta_i^2=0.62$, $p<.001$), suggesting that the corrected saccade duration more closely followed the main sequence (**Figure** 2**b**). Using this estimate for saccade offset, we excluded all trials, in which stimulus motion ended after saccade offset, taking into account a video latency of 8.3 ms of the Propixx projection system (Schweitzer & Rolfs, 2020a), as well as trials in which saccades could not be detected (e.g., due to blinks or missing samples) or online saccade detection was erroneously triggered prior to actual saccade onset (detected offline). As motion usually occurred relatively late throughout the saccade (see **Figure** 1**b**), 18.4% (SD = 8.5) of all trials had to be excluded from further analyses.

Prior to analysis, computer mouse responses underwent a spatial resampling procedure that produced equal distances between individual samples along the trajectory. Owing to the fact that human hand movements are not executed at constant velocity, mouse samples were more densely sampled at low velocities, such as at the beginning and end of each trajectory. Furthermore, due to the limited sampling rate and spatial resolution of the mouse, nonunique values would also occur and substantially distort the spatial representation of the drawing. After having removed these nonunique values from the data, the spatial distance between each pair of subsequently sampled mouse positions was filled with linearly interpolated, equidistant samples. Finally, a number (equal to the number of frames during presentation) of equidistant points between the first and last samples were chosen. Importantly, this procedure did not change the shape of the drawn trajectory, but allowed for a more accurate and unbiased comparison to the retinal and world-centered stimulus position vectors.

Analysis. To quantify whether drawn responses were more similar to world-centered (i.e., on-screen) or retinal stimulus trajectories, we computed two metrics capable of describing world-centered, retinal, and perceived trajectories.

First, we identified the angle of each trajectory by computing the median direction of all available samples relative to the first sample, as illustrated in **Figure** 3. This metric was

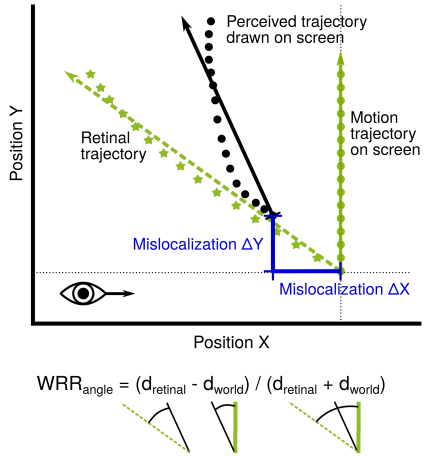

Figure 3. Simple illustration of the computation of the world-retinal-ratio (WRR) and mislocalization metrics. The observer makes a saccade to the right while upward stimulus motion (green circles, solid green line) is presented. The resulting retinal trajectory (green stars) is the difference of gaze and stimulus positions. The retinal direction (dashed green line) is defined as the median direction of the retinal trajectory. Similarly, the perceived direction (solid black line) is defined as the median direction of the drawn trajectory (black circles). The WRR of the perceived angle is the normalized difference between the angular difference between retinal and perceived direction and the angular difference between world-centered and perceived direction, respectively. Mislocalization in X and Y dimensions is defined as the spatial offset between the perceived and actual motion start position.

agnostic to the position, length, and curvature of each trajectory. Second, we computed a metric of path similarity, using the *scasim* algorithm implemented by von der Malsburg and Vasishth (2011). The algorithm aligns two paths using the Needleman-Wunsch algorithm and applies substitution penalties based on spatial distance and duration, whereas duration was not taken into account here. Paths were centered on top of each other, so that like trajectory angle, this metric was agnostic to position, but, unlike angle, was sensitive to the curvature and length of the trajectory. Given that world-centered and retinal trajectories could be more or less similar to each other depending on the experimental condition, relative similarity was computed using the world-retinal-ratio (WRR), which is defined as: $WRR = \frac{d_{retinal} - d_{world}}{d_{retinal} + d_{world}}$, where $d_{retinal}$ and d_{world} denote the dissimilarity (i.e., angular difference or path dissimilarity) of the perceived trajectory to the retinal and world-centered trajectory, respectively (**Figure** 3). According to the above definition, WRRs larger than zero indicate that the drawn trajectory was more similar to the world-centered than to the retinal trajectory, whereas WRRs below zero indicate the opposite. As both similarity metrics were (on purpose) agnostic to the spatial position of the drawn trajectory, mislocalization in vertical and horizontal dimensions were defined as the spatial offset between the world-centered position of motion onset and the perceived position of motion onset, i.e., the first position of the drawn trajectory. On the horizontal plane, positive values indicate mislocalizations in the direction of the saccade, whereas on the vertical plane, positive values indicate mislocalizations towards the lower visual field.

Results

Perceived motion trajectories. **Figure** 4**a** shows the average retinal trajectories of the target (across screen locations, saccade directions and observers) for the presented motion directions and amplitudes/durations. As expected, retinal trajectories differed to a large extent from the world-centered trajectories presented on the screen, as the ongoing saccade would rapidly shift the target across the retina in the opposite direction of the saccade. Therefore, motion streaks by targets moving in the opposite direction of the saccade induced a motion streak greatly extended in space, whereas targets moving the direction of the saccade induced a shortened motion streak, as the target's motion velocity (amounting to 214 dva/s) would counteract the saccade-induced retinal motion velocity, which ranged from 259.1 dva/s (SD = 28.9) at a motion duration of 25 ms to 317.6 dva/s (SD = 28.8) at a motion duration of 12.5 ms. The grand average reported trajectories (**Figure 4b**) suggest that what was perceived by observers resembled neither the world-centered nor the retinal motion trajectory of the target, but a trajectory in between the two. Strikingly, at longer motion amplitudes/durations reported trajectories seemed to increasingly resemble world-centered trajectories. Localization of the target was on average reasonably accurate (dotted lines in **Figure 4** represent the actual position of motion onset on the screen), but slightly biased towards the target's motion direction, as well as towards the lower visual field, especially when stimuli were presented in the upper visual field (**Figure 4c**, upper row).

Similarity to world-centered trajectories. To quantify similarity of the reported trajectory to the world-centered versus retinal trajectories, we computed the WRR (see **Analysis** and **Figure** 3) separately for the angle and path similarity of each drawn trajectory, and subsequently ran repeated-measures ANOVAs (motion duration × vertical visual field location × horizontal visual field location) on the subject-level aggregates. Using WRR as dependent variable revealed that perceived trajectories were indeed more similar to world-centered trajectories at longer motion durations (*WRR Angle*: $M_{12.5}$ = 0.02, $SEM_{12.5}$ = 0.05, $M_{18.75}$ = 0.11, $SEM_{18.75}$ = 0.05, $M_{25.0}$ = 0.15, $SEM_{25.0}$ = 0.06; $F(2,18) = 29.14$, $\eta_i^2 = 0.11$, $p < .001$, $p_{GG} < .001$; *WRR Path similarity*: $M_{12.5}$ = 0.10, $SEM_{12.5}$ = 0.05, $M_{18.75}$ = 0.19, $SEM_{18.75}$ = 0.04, $M_{25.0}$ = 0.18, $SEM_{25.0}$

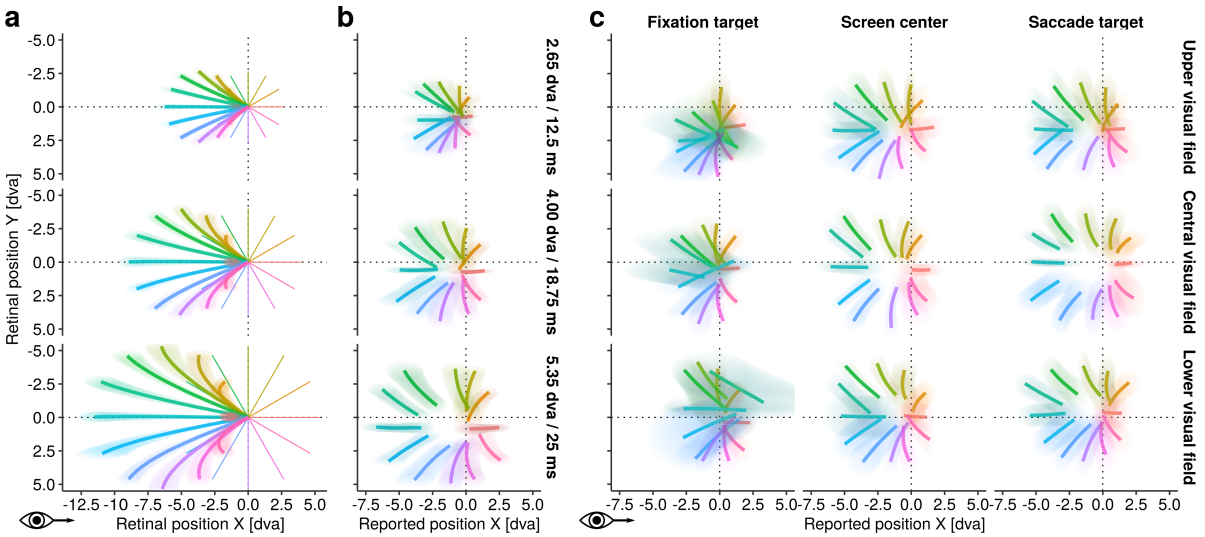

Figure 4. Average retinal and perceived trajectories in Experiment 1. **a** Average intra-saccadic retinal (solid lines) and corresponding world-centered (thin lines) stimulus trajectories for three motion amplitudes/durations. Spectral colors indicate motion direction relative to the saccade direction (normalized for rightward saccades). **b** Average perceived motion trajectories as indicated by computer mouse responses relative to the physical motion onset location (dotted lines). **c** Perceived motion trajectories (averaged across motion amplitudes/durations) for all nine stimulus anchor locations. Shaded areas indicate within-subject $\pm SEM$.

= 0.06; F(2,18) = 12.94, η_i^2= 0.10, p < .001, p_{GG}= .001). As shown in **Figure 5a** and **b**, the extent of world-centeredness depended strongly on motion direction: Trajectories of targets moving in the opposite of the saccade direction were on average more similar to world-centered trajectories than those moving orthogonal to the saccade direction. Moreover, as indicated by **Figure 4c**, reports were more similar to world-centered trajectories when motion originated from the screen center or close to the saccade target than when they originated close to the fixation target (*WRR Angle*: M_{fixtar} = 0.02, SEM_{fixtar} = 0.05, M_{center} = 0.13, SEM_{center} = 0.05, M_{sactar} = 0.12, SEM_{sactar} = 0.05; F(2,18) = 25.65, η_i^2= 0.11, p < .001, p_{GG}< .001; *WRR Path similarity*: M_{fixtar} = 0.1, SEM_{fixtar} = 0.04, M_{center} = 0.21, SEM_{center} = 0.04, M_{sactar} = 0.16, SEM_{sactar} = 0.04; F(2,18) = 33.09, η_i^2= 0.12, p < .001, p_{GG}< .001), and when motion was presented in the central visual field compared to the upper or lower visual field (*WRR Angle*: M_{upper} = 0.08, SEM_{upper} = 0.06, $M_{central}$ = 0.13, $SEM_{central}$ = 0.06, M_{lower} = 0.06, SEM_{lower} = 0.05; F(2,18) = 24.30, η_i^2= 0.04, p < .001, p_{GG}< .001; *WRR Path similarity*: M_{upper} = 0.14, SEM_{upper} = 0.04, $M_{central}$ = 0.18, $SEM_{central}$ = 0.04, M_{lower} = 0.15, SEM_{lower} = 0.05; F(2,18) = 11.18, η_i^2= 0.02, p < .001, p_{GG}< .001). Averaged across all conditions, trajectories were slightly, but in only one of two cases significantly more similar to world-centered than to retinal trajectories (*WRR Angle*: M = 0.09, SD = 0.17; F(1,9) = 4.97, η_i^2= 0.26, p = .052; *WRR Path similarity*: M = 0.16, SD = 0.14; F(1,9) = 20.40, η_i^2= 0.61, p = .001). No other higher-level interactions were significant, after applying Greenhouse-Geisser corrections for sphericity.

Spatial localization. On the horizontal plane, motion onset positions were globally (i.e., across all motion directions) mislocalized by -0.52 dva (SEM = 0.59), suggesting that motion streaks were perceived as slightly shifted towards the fixation target. This small bias was however not significantly different from zero (F(1,9) = 1.19, η_i^2= 0.08, p = .302). In fact, a localization bias against saccade direction was only present when motion was not displayed near the fixation target (M_{fixtar} = 0.42, SEM_{fixtar} = 0.58, M_{center} = -1.11, SEM_{center} = 0.63, M_{sactar} = -0.87, SEM_{sactar} = 0.44; F(2,18) = 7.33, η_i^2= 0.13, p = .005, p_{GG}= .008). Neither vertical visual field locations (F(2,18) = 2.08, η_i^2= 0.003, p = .153) nor motion duration (F(2,18) = 0.18, η_i^2< 0.001, p = .836) had an effect global mislocalization, and no interaction terms were significant. As shown in **Figure 5c**, however, the motion onset position was routinely mislocalized in the direction of the target motion. This effect was especially prominent for targets moving in the opposite direction of the saccade and increased in size at longer motion durations/amplitudes ($M_{12.5}$ = -0.37, $SEM_{12.5}$ = 0.69, $M_{18.75}$ = -1.41, $SEM_{18.75}$ = 0.35, $M_{25.0}$ = -2.19, $SEM_{25.0}$ = 0.72). A similar, but smaller effect was found on the vertical plane (**Figure 5d**): With increasing motion duration, targets moving upward were mislocalized towards the upper visual field ($M_{12.5}$ = 0.59, $SEM_{12.5}$ = 0.44, $M_{18.75}$ = 0.04, $SEM_{18.75}$ = 0.62, $M_{25.0}$ = -0.24, $SEM_{25.0}$ = 0.72), whereas targets mov-

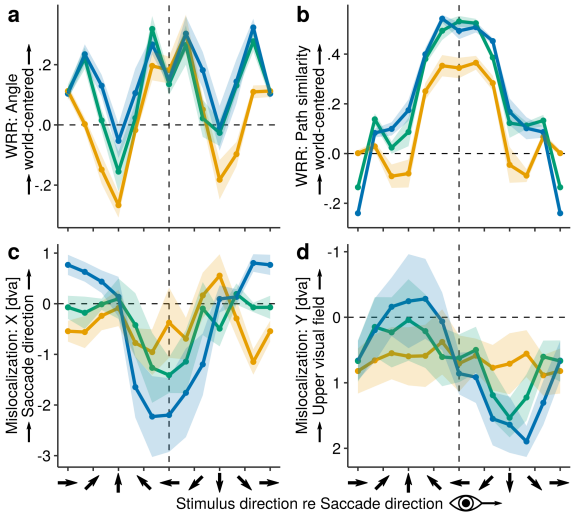

Figure 5. Average similarity and mislocalization metrics for motion directions relative to saccade direction (rightward) and 12.5-ms (orange), 18.75-ms (green), and 25.0-ms (blue) motion, respectively. Vertical dashed lines indicate stimulus motion against the direction of the saccade. **a-b** WRRs for angle and path similarity metrics. Positive values signify that drawn trajectories were more similar to world-centered than retinal trajectories. **c** Average motion onset mislocalization on horizontal dimension. Positive values indicate mislocalization in the direction of the saccade. **d** Mislocalization on vertical dimension. Here positive values indicate mislocalization towards the upper visual field.

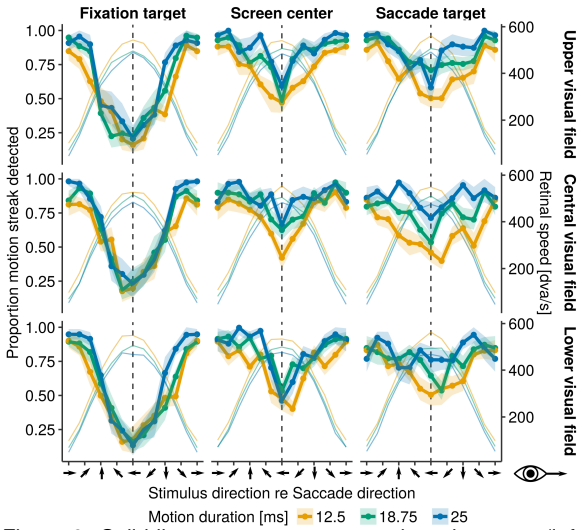

Figure 6. Solid lines represent average detection rates (left ordinate) as a function of motion direction (relative to saccade direction), motion duration, and stimulus anchor location. Thin lines show the average retinal velocity of the stimulus in each condition (right ordinate), i.e., the combined velocity of the eye and the target stimulus.

ing downward were mislocalized towards the lower visual field ($M_{12.5}$ = 0.71, $SEM_{12.5}$ = 0.46, $M_{18.75}$ = 1.53, $SEM_{18.75}$ = 0.30, $M_{25.0}$ = 1.64, $SEM_{25.0}$ = 0.43). On the vertical plane, motion onset positions were significantly globally mislocalized towards the lower visual field by on average 0.65 dva (SEM = 0.47; F(1,9) = 72.93, η^2= 0.25, p < .001). This global mislocalization was stronger in the upper visual field (M_{upper} = 1.91, SEM_{upper} = 0.44, $M_{central}$ = 0.49, $SEM_{central}$ = 0.19, M_{lower} = -0.44, SEM_{lower} = 0.39; F(2,18) = 8.48, η^2= 0.42, p = .002, p_{GG}= .015), as well as near the fixation target (M_{fixtar} = 0.82, SEM_{fixtar} = 0.45, M_{center} = 0.64, SEM_{center} = 0.46, M_{sactar} = 0.50, SEM_{sactar} = 0.49; F(2,18) = 17.17, η^2= 0.013, p < .001, p_{GG}< .001). No interactions were present.

Detection performance. On average, intra-saccadic motion streaks were detected in 70.8% (SEM = 6.2) of all trials. Detection improved with increasing motion duration ($M_{12.5}$ = 0.65, $SEM_{12.5}$ = 0.06, $M_{18.75}$ = 0.74, $SEM_{18.75}$ = 0.04, $M_{25.0}$ = 0.78, $SEM_{25.0}$ = 0.04; F(2,18) = 32.09, η^2= 0.10, p < .001, p_{GG}< .001) and was impaired when target motion was presented near the fixation target, i.e., the saccade starting point (M_{fixtar} = 0.60, SEM_{fixtar} = 0.05, M_{center} = 0.80, SEM_{center} = 0.05, M_{sactar} = 0.77, SEM_{sactar} = 0.06; F(2,18) = 24.12, η^2= 0.22, p < .001, p_{GG}< .001), whereas vertical visual field position did not affect detection performance (F(2,18) = 0.71, η^2= 0.004, p = .505, p_{GG}= .461) and no interaction terms were significant. Importantly, **Figure 6** shows clearly that detection performance varied strongly across motion directions and was inversely related to the target's retinal speed during intra-saccadic presentation: Mean detection performance was lowest when targets moved opposite to saccade direction (M = 0.44, SEM = 0.11), when induced retinal speeds were extremely high (M = 510.5 dva/s, SEM = 12.5). Similarly, detection performance was at its peak when targets moved in the same direction as the saccade (M = 0.88, SEM = 0.08) and corresponding retinal speeds were lower (M = 74.7 dva/s, SEM = 8.84).

Discussion

In this first experiment observers were tasked with drawing the appearance of randomly occurring intra-saccadic motion streaks to investigate to which extent and under which conditions motion streaks – that emanate from the individual retinal dynamics in each trial – could be localized and reported in world-centered coordinates. This novel paradigm proved feasible, as observers detected (and thus reported) the majority of presented motion streaks. As noise patches contained mostly low spatial frequencies, they remained resolvable even at very high retinal speeds that were close to

or above saccadic peak velocities (Burr & Ross, 1982; Castet et al., 2002). Prolonged motion duration led to increased detection rates for motion streaks (Schweitzer & Rolfs, 2020b), likely also due to decreasing retinal speeds toward the end of the saccade, as well as to an increased similarity of the reported trajectory to the actual world-centered target trajectory. Across all presented motion durations and directions no convincing evidence for a world-centered representation of motion streaks was found, instead perceived trajectories appeared as if consisting of both retinal and world-centered components, especially when targets moved orthogonal to the saccade vector. Clearly, however, trajectories of targets moving in the opposite direction of the saccade – even though they were harder to detect due to their high retinal velocities – were more similar to their world-centered trajectories. When evaluating only the angle of the reported trajectory, it may be hard to differentiate between the quite similar angles of retinal and world-centered trajectories, respectively. However, when evaluating path similarity (i.e., a metric that takes into account the length of the trajectory), it becomes evident that observers did not reproduce the elongated streak that would have been projected onto the retina when target-induced and saccade-induced retinal motion were additively combined, but a trajectory that more closely resembled the trajectory presented on the screen. Similarly, targets that moved in the same direction as the saccade would still be shifted in the opposite direction of the saccade, as their velocity (on the horizontal plane) was lower than the saccade. Yet, the perceived angle of these trajectories were closer to the presented angle than to the retinal angle, suggesting that the retinal signal must have been compensated to some extent.

With respect to the localization of the onset of each motion streak, it may appear surprising that no mislocalization in the direction of the saccade was found, as several previous studies on perisaccadic flash localization would suggest (e.g., Dassonville et al., 1992; Mateeff, 1978; L. Matin et al., 1970; Morrone et al., 1997; Schlag & Schlag-Rey, 1995). Instead, global mislocalization was small, only present for motion presented around screen center and saccade target, and opposite to saccade direction. Mislocalization in the opposite direction of the saccade was found in the context of perisaccadic compression of visual space, but was only present when flashes occurred beyond the saccade target (Morrone et al., 1997; Ostendorf, Fischer, Gaymard, & Ploner, 2006; Ross, Morrone, & Burr, 1997), which was not the case in our paradigm. Alternatively, there are reports of transient mislocalizations in the opposite direction of the saccade when target where flashed immediately before saccade offset (Honda, 1989, 1991, 1993), which may well have occurred in this experiment, as most presentations of target motion – especially those of longer durations – ended briefly prior to saccade offset. In these reports, however, mislocalizations were of much larger effect size than the barely significant global mislocalization found here. Importantly, effects of global mislocalization (computed as an average across motion directions) were most likely driven by the finding that motion streaks were routinely mislocalized in the direction of motion, especially at longer motion durations and when targets moved in the opposite direction of the saccade, i.e., in the direction of the saccade-induced retinal motion. This finding is reminiscent of the Fröhlich effect (Fröhlich, 1929), that is that the initial position of an unexpectedly presented moving object – e.g., when appearing from behind an aperture – is perceived as shifted in its motion direction, a phenomenon that was explained in terms of increased perceptual latency around the sudden motion onset (Whitney, 2002).

Finally, there was little evidence that localization and appearance of intra-saccadic motion streaks varied considerably across the nine possible motion anchors on the screen. Although world-centered reporting of motion streaks was slightly impaired around the fixation target compared to the screen center and saccade target, this effect was likely caused by not only the fact that in this condition (due to lower detection rates) less trials were available, but also greater retinal eccentricity: As the majority of targets were presented in the second half of the saccade, targets presented around screen center and saccade target were most likely able to benefit more from near-foveal processing. Further evidence for this view is provided by the finding that a similar benefit was found in the vertical plane where central screen locations (which were largely located along the saccade trajectory) were related to increased WRR compared to upper and lower field locations. Follow-up experiments should therefore try to improve online saccade detection to achieve an earlier presentation onset, thus allowing motion streaks to occur around saccadic peak velocity and when gaze position crosses the midline between fixation and saccade target.

Experiment 2

Even though we found that intra-saccadic motion streaks were perceived in neither retinal nor world-centered coordinates, suggesting that an incomplete compensation of the retinal signal must have taken place, it remains yet unclear what type of information could be used to perform such compensation. Whereas most studies of peri-saccadic flash localization suggest an extra-retinal signal (e.g., Honda, 1991; Pola, 2004, 2011; Ross et al., 1997), there is convincing evidence that mislocalization may occur in the absence of saccades when saccade-like motion is presented to the fixating eye. For instance, MacKay (1970) found that flashes were mislocalized in the direction opposite to the displayed motion, in other words, mislocalization in the direction of the “saccade”. Notably, this mislocalization even occurred prior to the motion onset, an effect which was recurrently attributed to a predictive extra-retinal signal that anticipates saccade onset (for reviews, see Ross et al., 2001; Volkmann, 1986). In

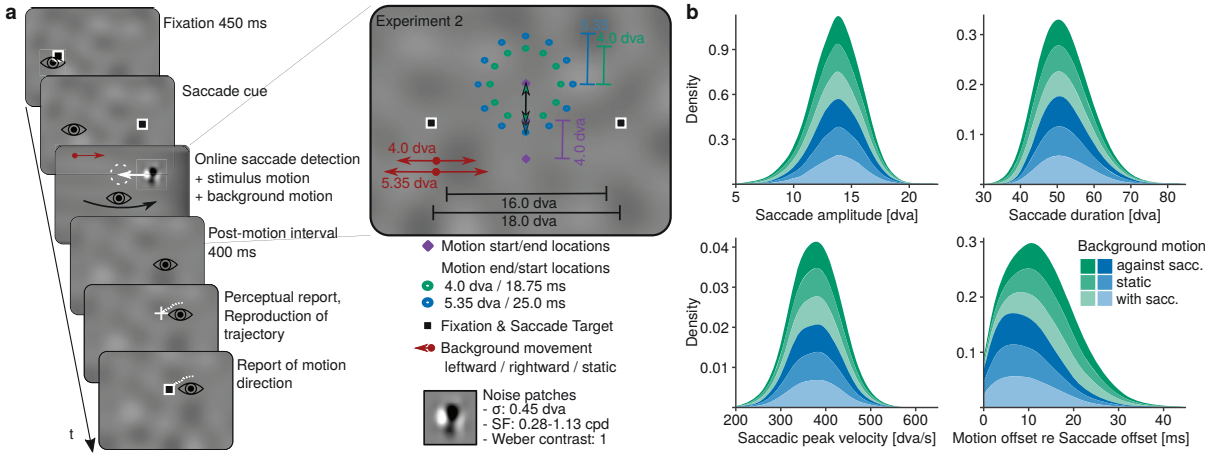

Figure 7. **a** Task procedure in Experiment 2 was largely similar to Experiment 1 (see **Task procedure**). To manipulate visual reference during and across saccades, we injected additional intra-saccadic motion parallel to the saccade direction by moving a lowS F patterned background horizontally in or against the direction of the saccade. **b** Distributions of saccade metrics. Varying color alpha levels represent different background motion conditions. Saccades in Experiment 2 had an average amplitude of 13.6 dva (SD = 0.7), took on average 51.8 ms (SD = 3.4), and had a peak velocity of 378.9 dva/s (SD = 30.8). Across observers, 18.75-ms and 25-ms motion ended 14.9 ms (SD = 3.5) and 10.0 ms (SD = 2.9) prior to to saccade offset, respectively.

addition, Sperling (1990) reported that image displacement was sufficient for mislocalization to occur, as also apparent or inverted motion produced the effect, as long as motion start and end points were available. Finally, Ostendorf et al. (2006) showed that the time course and size of even peri-saccadic compression of visual space could be found with both real and simulated saccades, suggesting that the latter could be a purely visual phenomenon.

In Experiment 2, we thus investigated the possibility that intra-saccadic large-field motion could have acted as a visual reference signal. On the one hand, a direct, extra-retinal representation of eye position may be available to compensate for the rapidly changing retinal location of the target. On the other hand, the target may have been localized relative to its visual reference frame, i.e., the illuminated screen, whose intra-saccadic motion is lawfully related to the ongoing eye movement. In the latter case, perception of intra-saccadic motion streaks should be sensitive to the retinal speed of the background, as it would represent an indicator of saccade velocity, direction and amplitude. Therefore, a full-field noise background (bandpass-filtered to low spatial frequencies, see **Figure 7a**) was introduced that could be moved in or against the direction of the saccade (or remain static), thereby effectively decreasing or increasing intra-saccadic retinal background velocity during target motion. If the subjective appearance and localization of motion streaks were dependent on the concurrent motion of visual references, then reported trajectories should be systematically altered across background motion conditions.

Methods

Apparatus. Stimuli were projected onto a 16:9 (250.2 x 141.0 cm) video-projection screen (Stewart Silver 5D Deluxe, Stewart Filmscreen, Torrance, CA), mounted on a wall at a distance of 340 cm in front of the participant. Like in Experiment 1, a PROPixx DLP projector (Vpixx Technologies, Saint-Bruno, QC, Canada) was used, running at 1440 Hz vertical refresh rate and a resolution of 960 x 540 pixels. The experimental code was also implemented in MATLAB (Mathworks, Natick, MA, USA), using the Psychophysics toolbox (Kleiner et al., 2007), as well as the custom TrackPixx toolbox (`https://github.com/richardschweitzer/TrackPixxToolbox`), and ran on a Dell Precision T7810 Workstation with a Ubuntu 18.04 operating system. Eye movements of both eyes are recorded via a TRACKPixx3 tabletop system (Vpixx Technologies, Saint-Bruno, QC, Canada) at a sampling rate of 2000 Hz, running firmware version 11. Participants rested their head on a chin rest and responses were collected with a standard computer mouse and US-english keyboard.

Participants. Ten observers were tested in three 1-hour sessions (on separate days) and received 26 Euros as remuneration, plus 2 Euros per 15 minutes overtime. Written informed consent was obtained from all participants prior to the first session. The study was conducted in agreement with the Declaration of Helsinki (2013) and was approved by the Ethics board of the Department of Psychology at Humboldt-Universität zu Berlin. All observers (8 female; mean age: 22; age range: 18 – 29) had normal or corrected-to-normal vision.

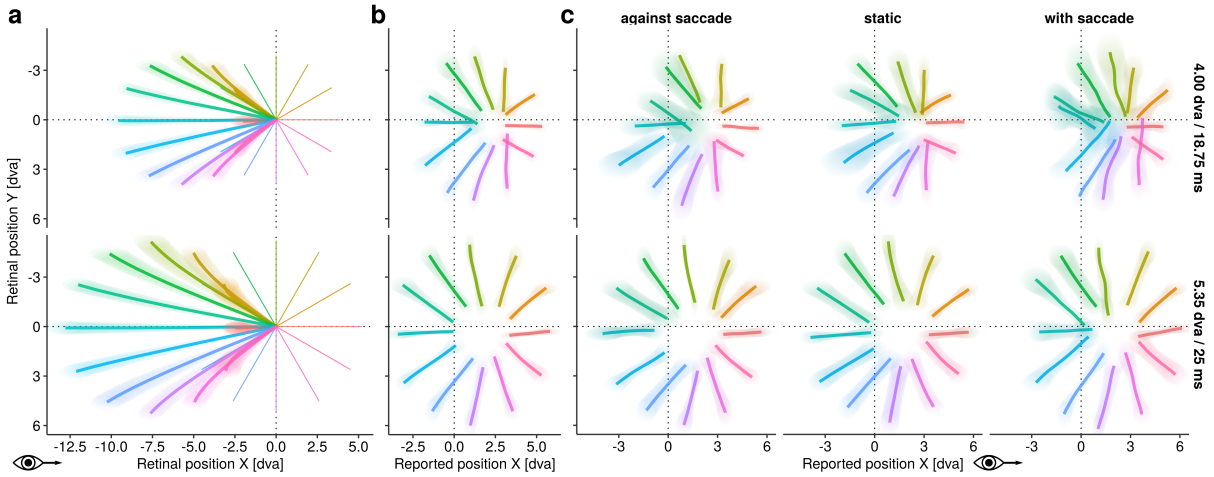

Figure 8. Average retinal and perceived trajectories for the two motion durations/amplitudes in Experiment 2 (upper row: 18.75 ms, lower row: 25 ms). **a** Average intra-saccadic retinal (solid lines) and world-centered (thin lines) stimulus trajectories for different motion directions relative to the saccade direction. **b** Average perceived motion trajectories. **c** Perceived motion trajectories for the three background motion conditions. Shaded areas indicate within-subject $\pm SEM$.

Two observers wore glasses and two observers wore contact lenses. Seven of ten observers had right ocular dominance, again one of ten observers was left-handed. The experiment was pre-registered at the Open Science Framework (OSF): `https://osf.io/95w8v/`. According to pre-registered inclusion criteria, two observers had to be replaced because they did not finish all three sessions.

Task Procedure. The task structure was largely the same as in Experiment 1, but a few important changes were introduced (see **Figure** 7**a**). First, to allow for earlier online saccade detection, we used the algorithm applied in Experiment 1 (Schweitzer & Rolfs, 2020a) with more liberal parameters (i.e., ϑ=40, k=2, λ=10) on data from both eyes. This binocular online saccade detection only detected saccades when velocity and direction criteria were fulfilled for both eyes, which increased robustness without additional latency. In addition to that, larger saccade amplitudes of 16 and 18 dva (2 levels) were instructed to achieve stimulus presentations around the time of the saccadic peak velocity. Second, the post-motion interval was prolonged to 400 ms, thus increasing the time until observers were allowed to respond after having made the saccade. Furthermore, as the reappearance of the saccade target could have acted as a landmark (Deubel, 2004), the saccade target remained removed until the end of the trial. Third, a two-alternative forced-choice response was introduced to assess observers' perceived direction of motion: Right after observers had drawn their perceived trajectory, a dot (similar to the saccade and fixation target) was displayed randomly at either end of the trajectory. Observers were asked to respond with the RightArrow key, if – according to their perceived motion direction – the presented dot location matched the final location of the motion trajectory, and with LeftArrow, if the dot matched the start of the motion trajectory. While in Experiment 1 stimuli moved strictly outward (i.e., away from their anchor), in Experiment 2 they were allowed to move both outward and inward (i.e., away from and toward their anchor; 2 levels). Intra-saccadic stimulus motion was present in 100% of all trials. Finally, to manipulate visual reference, a low-SF patterned background was displayed throughout the entire trial (see **Stimuli**), which – strictly during intra-saccadic target stimulus motion – was shifted horizontally either in the direction of the saccade or against the direction of the saccade, or remained static (3 levels). Amplitude and duration of horizontal background motion was always similar to target motion, i.e., 4.0 dva / 18.75 ms and 5.35 dva / 25.0 ms, thus moving at constant velocity. Naturally, when background motion was injected, the post-saccadic section of the background visible to the observer was different from the pre-saccadic section, but these shifts were rarely noticed, as the background always covered the entire screen. To reduce the number of counterbalanced conditions, only three stimulus anchors (separated vertically by 4.0 dva) were placed around screen center (**Figure** 7**a**) and only two motion durations were presented, i.e., 4.0 dva / 18.75 ms and 5.35 dva / 25.0 ms. Similar to Experiment 1, all experimental conditions (1728 trials in total) were again counter-balanced and presented in randomly interleaved order. Unlike Experiment 1, however, trials in which fixation controls were unsuccessful or observers did not reach an 3.5-dva radial boundary around the initial saccade target with one saccade, were repeated in the end of each experimental session, thus reducing the amount of data loss due to short or

inaccurate saccades.

Stimuli. Fixation and saccade targets, as well as noise patch stimuli were identical to those used in Experiment 1. As noise patches were presented upon a patterned background, their aperture was realized by a Gaussian alpha mask (SD = 0.45 dva). Full-field backgrounds consisted of Gaussian noise bandpass-filtered to low SFs with cut-offs at 0.07 and 0.28 cpd, as these low SFs remain resolvable even at high velocities (Burr & Ross, 1982). Backgrounds had an average Michelson contrast of 30% and their average luminance was half of the maximum luminance of the noise patch stimuli. For each observer 20 unique backgrounds were created which were randomly assigned to trials.

Pre-processing. Pre-processing of eye movement data and mouse responses followed the same procedure as in Experiment 1. As a consequence, 16.2% (SD = 10.3) of all trials were excluded. As the TrackPixx3 eye tracking system operated at a sampling rate of 2000 Hz, eye movement data was downsampled to 500 Hz using bandlimited interpolation, to match the sampling rate of the Eyelink 2. Due to the eye tracker's slightly elevated noise levels (as compared to the Eyelink 2), a scaling factor of 10 was supplied to the Engbert-Kliegl saccade detection algorithm.

Results

Perceived motion trajectories. Due to the application of TrackPixx3 eye tracking system, online saccade detection latency could be reduced to 4.0 ms (SD = 0.5) compared to the Eyelink II eye tracking system used in Experiment 1 (M = 12.8 ms, SD = 0.2), which led to an earlier presentation offset relative to saccade offset (**Figure 7b**). As a consequence, presentation onsets occurred closer to the time of saccadic peak velocity (*Mean eye velocity during presentation*: $M_{Exp.1}$ = 285.4, $SD_{Exp.1}$ = 16.4, $M_{Exp.2}$ = 326.7, $SD_{Exp.2}$ = 20.5), so that retinal trajectories were influenced to a larger degree by the eye movement, leading to even more horizontally elongated motion streaks than in Experiment 1 (**Figure 8a**). Even though retinal trajectories were more pronounced, reported trajectories did clearly resemble the world-centered trajectories to a larger degree than their corresponding retinal trajectories – especially at motion durations of 25 ms (**Figure 8b**). Trajectories drawn by observers furthermore appeared to contain less curvature and to be shifted globally in the direction of the saccade, while still being consistently offset along the target's motion direction.

Similarity to world-centered trajectories. On average across all conditions we found that reported trajectories were significantly more similar to world-centered than to retinal trajectories (*WRR Angle*: M = 0.1, SD = 0.16; F(1,9) = 7.32, η^2= 0.37, p = .024; *WRR Path similarity*: M = 0.22, SD = 0.1; F(1,9) = 138.62, η^2= 0.89, p < .001). Like in Experiment 1, this tendency was mostly driven by the longer motion durations of 25 ms (*WRR Angle*: $M_{18.75}$ = 0.005, $SEM_{18.75}$ = 0.03, $M_{25.0}$ = 0.20, $SEM_{25.0}$ = 0.04; F(1,9) = 36.36, η^2= 0.40, p < .001; *WRR Path similarity*: $M_{18.75}$ = 0.14, $SEM_{18.75}$ = 0.01, $M_{25.0}$ = 0.28, $SEM_{25.0}$ = 0.03; F(1,9) = 28.16, η^2= 0.49, p < .001). Similarly to results of the first experiment, using the path similarity metric, it was again evident that increased world-centeredness was mostly present when targets moved in the opposite direction of the saccade (**Figure 9a**), as observers did not reproduce the length of the streak. In contrast to Experiment 1, however, angles of trajectories produced by targets moving in directions orthogonal to the saccade tended to be more strongly represented in world-centered coordinates, but only at 25-ms motion durations ($M_{up,18.75}$ = -0.01, $SEM_{up,18.75}$ = 0.03, $M_{up,25.0}$ = 0.24, $SEM_{up,25.0}$ = 0.05; $M_{down,18.75}$ = -0.04, $SEM_{down,18.75}$ = 0.05, $M_{down,25.0}$ = 0.22, $SEM_{down,25.0}$ = 0.04). Crucial to the investigated hypothesis, however, no significant effect of background motion was found (**Figures 8c** and **9a**), neither as a main effect (*WRR Angle*: $M_{against}$ = 0.10, $SEM_{against}$ = 0.04, M_{static} = 0.09, SEM_{static} = 0.04, M_{with} = 0.10, SEM_{with} = 0.03; F(2,18) = 0.03, η^2= 0.001, p = .973, p_{GG} = .957; *WRR Path similarity*: $M_{against}$ = 0.22, $SEM_{against}$ = 0.02, M_{static} = 0.22, SEM_{static} = 0.02, M_{with} = 0.20, SEM_{with} = 0.02; F(2,18) = 3.92, η^2= 0.012, p = .039, p_{GG} = .053), nor as an interaction with motion duration (*WRR Angle*: F(2,18) = 0.13, η^2= 0.001, p = .872, p_{GG} = .835; *WRR Path similarity*: F(2,18) = 0.33, η^2= 0.003, p = .716, p_{GG} = .653).

Spatial localization. As shown in **Figure 9b**, motion streaks were globally mislocalized to a significant degree in the direction of the saccade by on average 1.97 dva (SEM = 0.76; F(1,9)=7.10, η^2= 0.41, p = .026), a bias that decreased in size at longer motion durations ($M_{18.75}$ = 2.28 dva, $SEM_{18.75}$ = 0.76, $M_{25.0}$ = 1.65, $SEM_{25.0}$ = 0.73; F(1,9) = 6.98, η^2= 0.02, p = .027), but was unaffected by background motion (F(2,18) = 1.41, η^2= 0.009, p = .271, p_{GG} = .272) and interactions of background motion and motion duration (F(2,18) = 0.38, η^2= 0.001, p = .684, p_{GG} = .640). On the vertical plane, small, but significant mislocalization occurred, as onset of motion streaks were offset by 0.46 dva (SEM = 0.29) towards the lower visual field (F(1,9) = 6.42, η^2= 0.21, p = .032), which was neither affected by motion duration (F(1,9) = 0.25, η^2= 0.004, p = .628) or background motion (F(2,18) = 0.18, η^2= 0.002, p = .835, p_{GG} = .779) nor their interaction (F(2,18) = 0.43, η^2= 0.02, p = .657, p_{GG} = .568).

Detection performance. Motion streaks were detected in 58% (SEM = 8.2) of all trials. As plotted in **Figure 10**, this detection rate depended strongly on motion duration ($M_{18.75}$ = 0.48, $SEM_{18.75}$ = 0.066, $M_{25.0}$ = 0.68, $SEM_{25.0}$ = 0.047; F(1,9) = 32.88, η^2= 0.24, p < .001). Although detection rate did not depend on background motion (F(2,18) = 1.33, η^2= 0.003, p = .287, p_{GG} = .287), the effect of motion duration was strongest when background motion was absent (F(2,18) = 4.93, η^2= 0.005, p = .019, p_{GG} = .020). Close inspection of **Figure 10** revealed that a small interaction between background motion and target motion: Background motion slightly

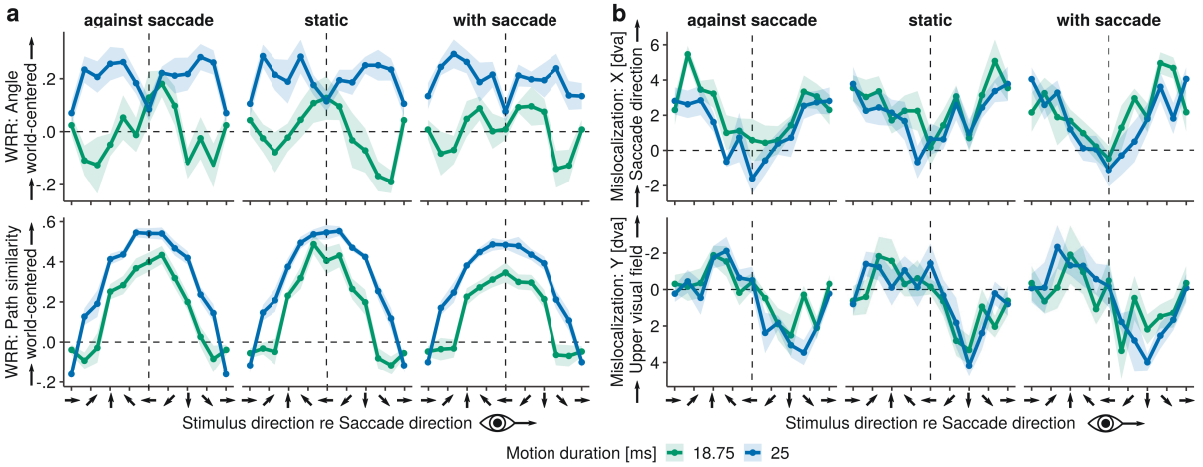

Figure 9. Average similarity and mislocalization metrics as a function of stimulus motion direction (relative to saccade direction), motion duration, and background motion in Experiment 2. **a** WRRs for angle and path similarity metrics. **b** Average motion onset mislocalization on horizontal and vertical dimensions. Positive values indicate mislocalization in the direction of the saccade and towards the upper visual field, respectively.

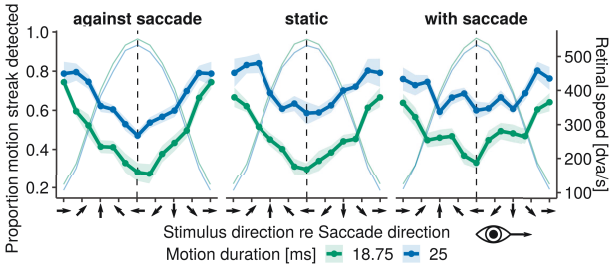

Figure 10. Average detection rates (solid lines, left ordinate) and retinal velocity during presentation (thin lines, right ordinate) as a function of motion direction, motion duration, and background motion in Experiment 2.

impaired detection of targets moving in the same direction as the background, while enhancing detection of targets moving in the opposite direction (relative to a static background). For instance, background motion in the direction of the saccade caused target motion in the direction of the saccade to be detected at a lower rate, while targets moving in the opposite direction of the saccade (even though generally harder to detect) were detected at a higher rate (M_{with} = 0.69, SEM_{with} = 0.067, $M_{against}$ = 0.46, $SEM_{against}$ = 0.065), as compared to when backgrounds were static (M_{with} = 0.73, SEM_{with} = 0.063, $M_{against}$ = 0.44, $SEM_{against}$ = 0.060). The effect was opposite for background motion against the saccade (M_{with} = 0.77, SEM_{with} = 0.056, $M_{against}$ = 0.38, $SEM_{against}$ = 0.064), thus representing a significant interaction between background and target motion direction in an addition repeated-measures ANOVA ($F(2,18) = 16.06$, $\eta_i^2 = 0.024$, $p < .001$, $p_{GG} = .002$).

Discussion

Experiment 2 investigated the possibility that intra-saccadic motion streaks are registered relative to the moving visual reference frame (MacKay, 1970, 1973; O'Regan, 1984). We hypothesized that if that were the case, then localization and appearance of reported trajectories should be affected by variations of retinal speed induced by motion of a full-field background at the time of target presentation. The background may not only act as a landmark (Deubel, 2004), but may also bias position relative to the observer's perceived midline, as shown by the Roelofs effect (Roelofs, 1935). In addition to that, perceived position can be heavily influenced by motion, as shown by motion-induced position shifts (Whitney & Cavanagh, 2000). With respect to the perception of intra-saccadic motion, however, no influence of additional motion injection was found, except for a marginally significant reduction of WRR when backgrounds moved in the same direction as the saccade. Importantly, this effect did not alter the overall appearance of the reported trajectories, instead, it is likely that this same-direction background motion introduced additional uncertainty into the localization process, as the background could be retinally stabilized when velocities of background and saccade were similar (Castet & Masson, 2000; Deubel, Elsner, & Hauske, 1987; García-Pérez & Peli, 2001). Apart from that, it seems unlikely that the presented background motion was taken into account when computing the world-centered positions of intra-saccadic target motion. One can only speculate why this is the case. First, given that the background grating was of low contrast (to further allow the detection of motion streaks induced by targets) and contained very low SFs, its signal may have been attenu-

ated by saccadic suppression, which has been shown to be especially effective in the low-SF domain (Burr, Holt, Johnstone, & Ross, 1982; Burr, Morrone, & Ross, 1994; Volkmann, Riggs, White, & Moore, 1978). Second, large-field background motion were likely masked by pre- and post-saccadic static retinal images (Campbell & Wurtz, 1978; Castet et al., 2002; Duyck et al., 2018), and could have – in the view of observers' reported unawareness of trans-saccadic background displacements – been affected by mechanisms similar to saccadic suppression of image displacement (Bridgeman, Hendry, & Stark, 1975). Third, it may well be possible that observers ignored background motion (as it was irrelevant to the task) and that the retinal shift of the illuminated screen in an otherwise dark environment acted as a visual reference frame to a sufficient degree to allow visual localization by computing relative motion of screen borders and target. This predictable shift of the visual reference frame as a consequence of the saccade may have been taken into account and could not be manipulated in the current setup, as Ganzfeld-like conditions or complete darkness would be needed to fully control for the potential influence of visual references. Although background motion did not alter the appearance of intra-saccadic motion streaks, it reduced the detectability of targets moving in the same direction as the background, i.e., when the relative motion of a target in front of its background was less salient, suggesting that background motion was most likely not entirely omitted from visual processing.

Background motion had no effect on global mislocalization, neither on the horizontal nor on the vertical dimension, which is in line with the results on phenomenological appearance described above. Interestingly though, a systematic global mislocalization was found in the direction of the saccade (unlike localization in Experiment 1) and could have been caused by earlier presentation onsets. This is likely, as in many studies perisaccadic mislocalization has been shown to be largest around saccade onset and to decrease (or even change its sign) towards saccade offset (e.g., Honda, 1991; Kennard, Hartmann, Kraft, & Glaser, 1971; Mateeff, 1978; Morrone et al., 1997; Schlag & Schlag-Rey, 1995). The small, but significant vertical mislocalization toward the lower visual field may however be best explained by means of visual field assymmetries (e.g., Abrams, Nizam, & Carrasco, 2012), as perisaccadic mislocalization does not occur for targets perpendicular to the saccade direction (Honda, 1993; Morrone et al., 1997).

Finally, despite the additional uncertainty about motion direction induced by background motion, a large increase in WRR was found as compared to the previous experiment, suggesting that under the conditions of Experiment 2 motion streaks were reproduced in a manner that more closely resembled the world-centered trajectory of the intra-saccadic target. This may be surprising, as target motion was detected with significantly less accuracy than in Experiment 1, most likely due to reduced effective target contrast introduced by the non-uniform background pattern. It is possible that the mere presence of a structured background facilitated the compensation of the retinal trajectory, which would suggest that world-centered perception of intra-saccadic motion streaks is at least to some extent visual. Alternatively, results might have been caused by a tradeoff between motion streak detection and judgment of appearance, or, in other words, by a bias for those motion streaks that were actually resolvable, e.g., due to lower retinal velocities. In fact, retinal velocities of detected targets was in a similar range as in Experiment 1, even though target presentations occurred earlier throughout the saccade. This suggests that a large proportion of motion streaks – especially those occurring in early stages of the saccade – were omitted from the results. As observers could not report motion streaks they could not detect, this question shall be addressed in the next experiment.

Experiment 3

Results of Experiment 2 suggested that (compared to Experiment 1) motion streaks were increasingly well perceived in world-centered coordinates and, beyond that, remained unaffected by the injection of intra-saccadic background motion. The definitive cause of these differences between experiments remains unclear, as changes were introduced not only in the paradigm (e.g., the structured background), but also to the experimental setup (e.g., eye tracking system and projection screen). Experiment 3 shall thus validate three important questions in a systematic within-subject design. First, do screen borders and visual context (i.e., the laboratory room) play a role as visual references? As they cannot be directly altered, their overall salience can be reduced by lowering background luminance to a point where a nearly dark environment is created. Second, does a structured background – directly compared to a uniform background of the same luminance – improve the world-centeredness of intra-saccadic perception? Third, what do phenomenological responses look like when intra-saccadic motion streaks can be detected at all times? By increasing target contrast by a factor of ten, observers should be able to report motion streaks which were unresolvable due to high retinal velocities in previous experiments. Importantly, Experiment 3 will apply the same task procedure and experimental setup that was used in Experiment 2 to maximize comparability between experiments.

Methods

Apparatus. The setup used was identical to the one used in Experiment 2, with the exception that the TRACKPixx3 firmware was updated to version 16 and a head rest (instead of a simple chin rest) was used to counteract comparably poor eye tracking quality of the TRACKPixx system in low-luminance conditions, which was likely related to increased pupil size. To match stimulus contrasts across background conditions, the luminance of all gray levels produced by the

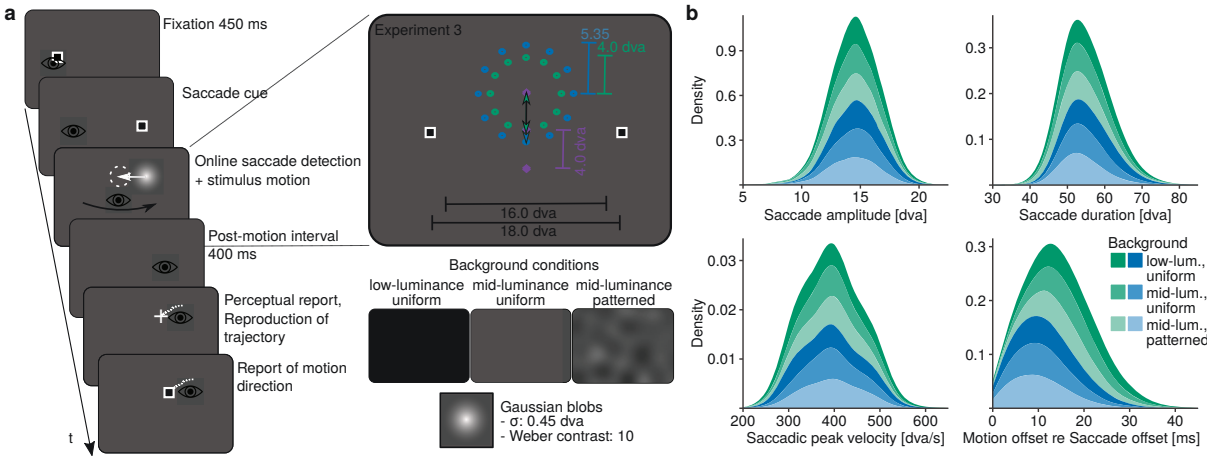

Figure 11. **a** Task procedure in Experiment 3 was identical to Experiment 2 with two relevant exceptions. First, to improve detection of intra-saccadic motion, Gaussian blobs with a Weber contrast of 10 were applied. Second, three different static backgrounds were presented in separate sessions to systematically investigate the potential role of background luminance and structure (while keeping target contrast constant), as well as the resulting saliency of screen borders. **b** Distributions of saccade metrics. Varying color alpha levels represent different background types. Saccades in Experiment 3 were of an average amplitude of 14.5 dva (SD = 1.1). Mean saccade duration amounted to 54.7 ms (SD = 3.7) and average peak velocity to 397.5 dva/s (SD = 54.3). Across observers, 18.75-ms and 25-ms motion ended 16.5 ms (SD = 3.8 ms) and 11.1 ms (SD = 3.6 ms) prior to to saccade offset, respectively.

PROPixx projection system was measured using a ColorCAL MKII Colorimeter (Cambridge Research Systems, Rochester, UK).

Participants. Ten observers were tested in three 1-hour sessions (on separate days) and received 26 Euros as remuneration, plus 2 Euros per 15 minutes overtime. Even though 12 observers were pre-registered (OSF link: `https://osf.io/kmqzc/`), only 10 observers could finish all three sessions due to the SARS-CoV-2-related closure of laboratory facilities. Written informed consent was obtained from all participants prior to the first session, and, just like Experiment 2, Experiment 3 was conducted in agreement with the Declaration of Helsinki (2013) and the Ethics board of the Department of Psychology at Humboldt-Universität zu Berlin. All observers (6 female; mean age: 26; age range: 21 – 33) had normal or corrected-to-normal vision. Two observers wore glasses. Seven of ten observers had right ocular dominance, all observers were right-handed.

Task Procedure. Design and task procedure was similar to Experiment 2, however, no background movement was presented during stimulus motion. As illustrated in **Figure** 11**a**, three background types (3 levels) were displayed: low-luminance uniform, mid-luminance uniform, and mid-luminance patterned (see **Stimuli**). Each background condition was assigned to one experimental session, but the order was randomly assigned and counterbalanced across observers (3 sessions, 6 permutations, 12 observers). Instead of noise patches, Gaussian blobs were presented to maximize intra-saccadic visibility. Their luminance was adjusted to match background luminance in order to keep Weber contrast constant across background conditions. Online saccade detection (parameters: ϑ=25, k=2, λ=15) was only run on observers' right eye, as (for an unknown reason) the right eye exhibited lower sample-to-sample noise levels in the TRACKPixx eye tracking system, therefore resulting in more reasonable velocity thresholds.

Stimuli. Stimuli were Gaussian blobs, enveloped in a Gaussian aperture with a standard deviation of 0.45 dva, which was again realized by the alpha channel of the noise patch. Depending on the background condition, stimuli were displayed on uniform backgrounds of low luminance (0.05 cd/m^2), uniform backgrounds of medium luminance (11.0 cd/m^2), or fullscreen noise backgrounds of the same luminance (on average 11.0 cd/m^2). The latter were of lower luminance but otherwise similar to the noise backgrounds used in Experiment 2, i.e., bandpass-filtered from 0.07 to 0.28 cpd and scaled to 30% Michelson contrast. All Gaussian blobs were presented at a Weber contrast of 10 relative to their respective background luminance. Target luminance thus amounted to 127.5 cd/m^2 on medium-luminance and 0.55 cd/m^2 on low-luminance backgrounds. Fixation and saccade targets were the similar to those used in the previous two experiments. Their luminance, as well as the luminance of inter-trial feedback, was equal to the target stimulus' luminance.

Pre-processing. Pre-processing procedures were identical to those used in Experiment 2. According to exclusion

criteria, 13.1% (SD = 6.8) of all trials had to be excluded.

Results

Perceived motion trajectories. We first tested whether saccade metrics (**Figure 11b**) and retinal trajectories (**Figure 12a**) were different from those found in Experiment 2 (see **Figure 7b** and **Figure 8a**, respectively). We found no significant differences with respect to saccade durations ($F(1,18) = 3.06$, $\eta_l^2 = 0.14$, $p = .097$) or saccadic peak velocities ($F(1,18) = 0.89$, $\eta_l^2 = 0.05$, $p = .357$), and only marginally longer saccade amplitudes in Experiment 3 ($F(1,18) = 4.54$, $\eta_l^2 = 0.20$, $p = .047$). Even though presentations had a slightly earlier onset in Experiment 2 ($M_{Exp.2} = 17.5$ ms, $SD_{Exp.2} = 0.6$, $M_{Exp.3} = 18.9$, $SD_{Exp.3} = 0.45$; $F(1,18) = 43.29$, $\eta_l^2 = 0.07$, $p < .001$), presentation offsets relative saccade offset did not differ ($F(1,18) = 0.74$, $\eta_l^2 = 0.04$, $p = .400$), and neither did the eye's velocity during stimulus presentation ($M_{Exp.2} = 326.7$ dva/s, $SD_{Exp.2} = 20.5$, $M_{Exp.3} = 349.7$ dva/s, $SD_{Exp.3} = 43.5$; $F(1,18) = 2.29$, $\eta_l^2 = 0.11$, $p = .147$). Despite average reported trajectories (**Figure 12b**) were strikingly different from previous results, that is, more elongated, curved and tilted opposite to saccade direction, in short, more similar to retinal trajectories. This effect was clearly present in all three background conditions (**Figure 12c**), even though slightly more pronounced in the low-luminance condition. Similar to Experiment 2, global mislocalization in the direction of the saccade was present, as well, which was also seemed largely unaltered by the type of background.

Similarity to world-centered trajectories. In contrast to the results of previous experiments, WRR was overall around or even significantly below zero (*WRR Angle*: $M = -0.17$, $SD = 0.16$; $F(1,9) = 13.97$, $\eta_l^2 = 0.55$, $p = .004$; *WRR Path similarity*: $M = 0.06$, $SD = 0.18$; $F(1,9) = 1.56$, $\eta_l^2 = 0.12$, $p = .243$), suggesting that reported trajectories were on trend more similar to the retinal than to the world-centered stimulus trajectory. Again, longer motion durations caused slightly more world-centered reproductions (*WRR Angle*: $M_{18.75} = -0.22$, $SEM_{18.75} = 0.04$, $M_{25.0} = -0.12$, $SEM_{25.0} = 0.05$; $F(1,9) = 17.69$, $\eta_l^2 = 0.08$, $p = .002$; *WRR Path similarity*: $M_{18.75} = -0.002$, $SEM_{18.75} = 0.05$, $M_{25.0} = 0.12$, $SEM_{25.0} = 0.05$; $F(1,9) = 23.32$, $\eta_l^2 = 0.13$, $p < .001$). More specifically, the effects of motion duration mostly pertained to the perceived angles of motion trajectories othogonal to saccade direction and to perceived length (indicated by path similarity) of motion trajectories opposite to the direction of the saccade (**Figure 13a**). Background type had no significant effect on angles of perceived trajectories (*WRR Angle*: $M_{low,uniform} = -0.20$, $SEM_{low,uniform} = 0.05$, $M_{mid,uniform} = -0.16$, $SEM_{mid,uniform} = 0.05$, $M_{mid,patterned} = -0.15$, $SEM_{mid,patterned} = 0.04$; $F(2,18) = 1.60$, $\eta_l^2 = 0.02$, $p = .230$, $p_{GG} = .237$), but path similarity to world-centered trajectories was slightly increased when mid-luminance and especially patterned backgrounds were used (*WRR Path similarity*: $M_{low,uniform} = 0.007$, $SEM_{low,uniform} = 0.05$, $M_{mid,uniform} = 0.06$, $SEM_{mid,uniform} = 0.05$, $M_{mid,patterned} = 0.11$, $SEM_{mid,patterned} = 0.05$; $F(2,18) = 5.87$, $\eta_l^2 = 0.07$, $p = .011$, $p_{GG} = .023$). No interactions between motion duration and background type were present (*WRR Angle*: $F(2,18) = 0.89$, $\eta_l^2 = 0.003$, $p = .425$, $p_{GG} = .377$; *WRR Path similarity*: $F(2,18) = 0.37$, $\eta_l^2 = 0.005$, $p = .693$, $p_{GG} = .678$).

Spatial localization. Just like in Experiment 2, motion onset was mislocalized in the direction of the saccade by 1.98 dva ($SEM = 0.63$; $F(1,9) = 10.12$, $\eta_l^2 = 0.51$, $p = .011$) and this mislocalization was stronger at shorter motion duration ($M_{18.75} = 2.21$ dva, $SEM_{18.75} = 0.59$, $M_{25.0} = 1.73$, $SEM_{25.0} = 0.65$; $F(1,9) = 10.09$, $\eta_l^2 = 0.014$, $p = .011$). Background type had a small, but insignificant effect on mislocalization (**Figure 13b**), as mislocalization was stronger in the low-luminance condition and decreased with luminance and background structure ($M_{low,uniform} = 2.30$ dva, $SEM_{low,uniform} = 0.54$, $M_{mid,uniform} = 1.94$ dva, $SEM_{mid,uniform} = 0.72$, $M_{mid,patterned} = 1.67$ dva, $SEM_{mid,patterned} = 0.65$; $F(2,18) = 2.37$, $\eta_l^2 = 0.02$, $p = .121$, $p_{GG} = .131$), and did not interact with motion duration ($F(2,18) = 2.95$, $\eta_l^2 = 0.004$, $p = .078$, $p_{GG} = .085$). As also found in previous experiments, a small, but significant localization bias toward the lower visual field was found ($M = 0.5$ dva, $SEM = 0.24$; $F(1,9) = 9.03$, $\eta_l^2 = 0.34$, $p = .014$), which decreased at longer motion durations ($M_{18.75} = 0.81$ dva, $SEM_{18.75} = 0.27$, $M_{25.0} = 0.18$, $SEM_{25.0} = 0.10$; $F(1,9) = 6.63$, $\eta_l^2 = 0.17$, $p = .030$), but was independent of background type ($M_{low,uniform} = 0.50$ dva, $SEM_{low,uniform} = 0.15$, $M_{mid,uniform} = 0.46$ dva, $SEM_{mid,uniform} = 0.14$, $M_{mid,patterned} = 0.53$ dva, $SEM_{mid,patterned} = 0.25$; $F(2,18) = 2.07$, $\eta_l^2 = 0.01$, $p = .155$, $p_{GG} = .171$).

Detection performance. Even though retinal speed during presentation was overall similar to previous experiments, detection of motion streaks now occurred in nearly 100% of all cases (**Figure 14**), regardless of motion duration ($M_{18.75} = 0.99$, $SEM_{18.75} = 0.004$, $M_{25.0} = 0.99$, $SEM_{25.0} = 0.002$) and background type ($M_{low,uniform} = 0.99$, $SEM_{low,uniform} = 0.006$, $M_{mid,uniform} = 0.99$, $SEM_{mid,uniform} = 0.002$, $M_{mid,patterned} = 0.99$, $SEM_{mid,patterned} = 0.001$).

Discussion

Experiment 3 undertook a systematic investigation of the potential effects of background luminance and structure on the subjective appearance of intra-saccadic motion streaks, while keeping target contrast constant across these conditions. Moreover, a tenfold increase of target contrast made it possible to assess the appearance of virtually all presented motion streaks. Results provide strong evidence that neither background luminance nor background structure had a relevant impact on reported trajectories. This finding is in principle compatible with previous research. For instance, Honda (1993) argued that flash localization in illuminated and structured backgrounds "is essentially the same as that reported for the 'dark'" (p. 715) by showing that background luminance

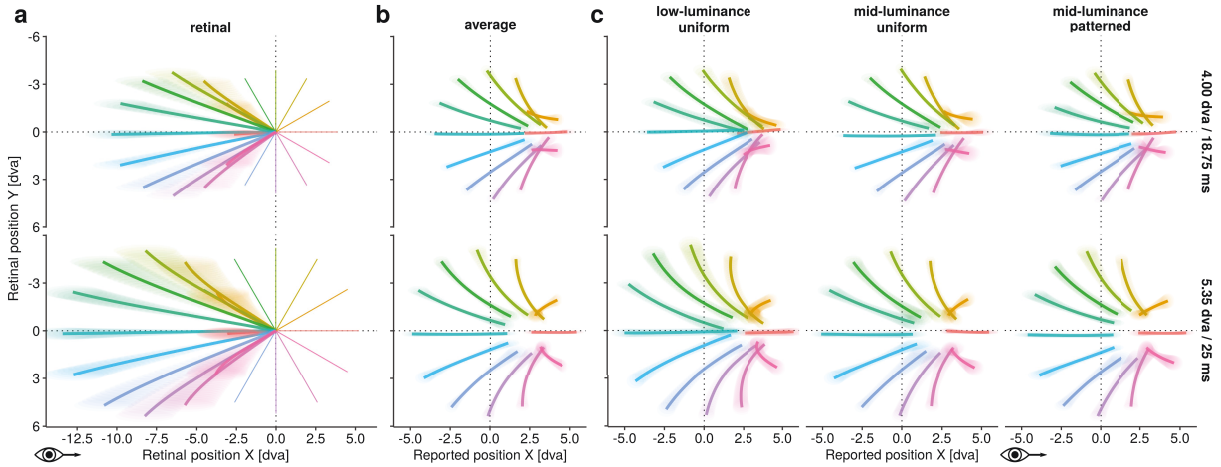

Figure 12. Average retinal and perceived trajectories for the two motion amplitudes/durations in Experiment 3 (upper row: 4 dva / 18.75 ms, lower row: 5.35 dva / 25 ms). **a** Average intra-saccadic retinal (solid lines) and world-centered (thin lines) stimulus trajectories for different motion directions relative to the saccade direction. **b** Average perceived motion trajectories. **c** Perceived motion trajectories for the three background type conditions tested in three separate sessions. Shaded areas indicate within-subject $\pm SEM$.

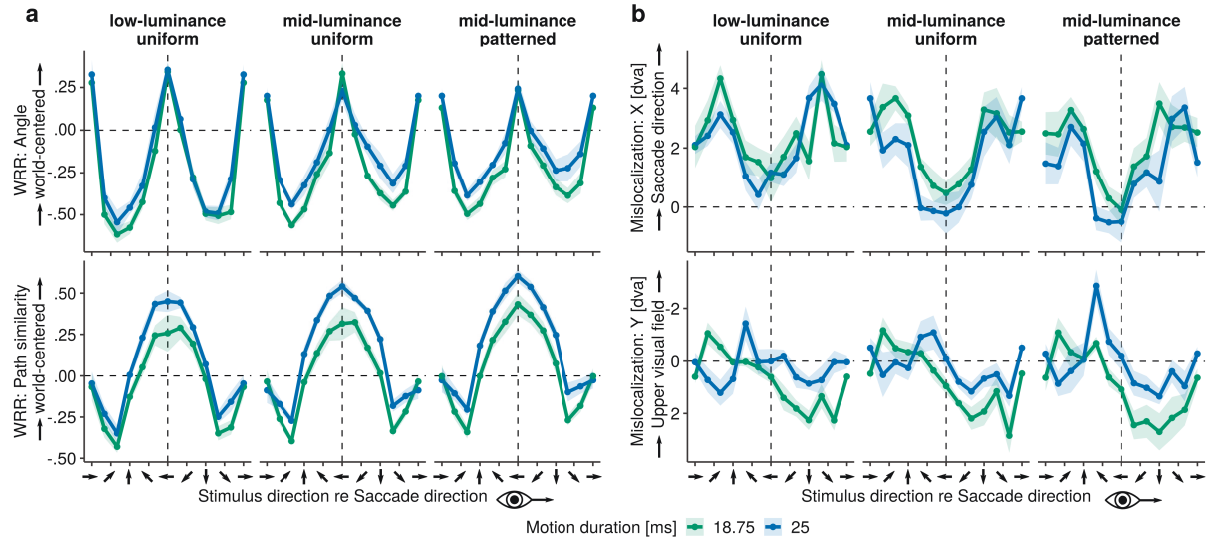

Figure 13. Average similarity and mislocalization metrics as a function of stimulus motion direction (relative to saccade direction), motion duration, and background type in Experiment 3. **a** WRRs for angle and path similarity metrics. **b** Average motion onset mislocalization on horizontal and vertical dimensions.

only quantitatively affected peri-saccadic localization: At low luminance, mislocalization occurred earlier relative to the onset of the saccade and had a larger effect size than with an illuminated background (for an extensive discussion, see Pola, 2011), while the overall localization patterned remained the same in both conditions. Crucially, Honda (1993) kept the luminance of the test flash constant across background luminance conditions, thus changing the Weber contrast of the target stimulus. Having kept the target's Weber contrast constant, our results now show that background luminance and structure had only a very limited effect on both mislocalization and subjective appearance of intra-saccadic motion streaks. Although we did find that reproduced paths were slightly more similar to world-centered trajectories when presented on a mid-luminance structured background, this result was most likely fully caused by a change in perceived streak length,

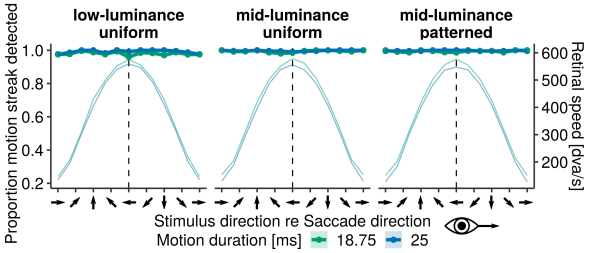

Figure 14. Average detection rates (solid lines, left ordinate) and retinal velocity during presentation (thin lines, right ordinate) as a function of motion direction, motion duration, and background type in Experiment 3.

given that in the low-luminance condition streaks were on average perceived as more elongated (**Figure 12c**). This may be a consequence of a reduction of the luminance-dependent size of saccadic suppression: Whereas saccadic suppression is virtually absent in near-complete darkness (Richards, 1969), it becomes more powerful as background luminance increases or structured backgrounds are introduced (Brooks & Fuchs, 1975; Chekaluk & Llewellyn, 1990; Mitrani & Yakimoff, 1971; Mitrani, Yakimoff, & Mateeff, 1973). Similarly, E. Matin et al. (1972) found that motion streaks appeared as more elongated, if they were induced by a target with higher luminance (see E. Matin, 1974, for a detailed analysis of this effect).

With respect to the initial motivation of this experiment, i.e., to determine whether visual references such as salient screen borders or a structured background facilitate or even drive world-centered perception of motion streaks, evidence suggests that it is quite unlikely that visual references are necessary to perform the task or that the introduction of a structured background could account for the increased dominance of world-centered representations in Experiment 2. Instead, increasing the target's contrast could provide an important clue to an alternative hypothesis that could explain both the increase of WRR in Experiment 2, as well as the uncanny decrease of WRR in Experiment 3. On the one hand, one could assume that motion streaks induced in the early stages of the saccade (when the eye's angular velocity is maximal) were underrepresented in the data, as observers were unable to detect them. Given that mislocalization has been shown to strongest around the onset of the saccade or image motion (e.g., MacKay, 1970; Mateeff, 1978; Ostendorf et al., 2006), motion streaks may be equally affected, causing them to more closely resemble their retinal trajectories. Increasing the target's contrast could thus have simply enabled the phenomenological access to these early motion streaks. Although possible, this is not likely, given target presentations in Experiment 2 and 3 had quite similar timing even when analyzing only trials in which successful detection took place: In Experiment 2, motion onset times remained unaltered (M_{all} = 17.5 ms, SD_{all} = 0.5, $M_{detected}$ = 17.9 ms, $SD_{detected}$ = 0.6) and motion offset times (prior to saccade offset) decreased only slightly (M_{all} = 12.5 ms, SD_{all} = 3.1, $M_{detected}$ = 10.8 ms, $SD_{detected}$ = 3.5) after excluding all those trials in which target motion was not detected. On the other hand, increased target contrast might have enhanced observers capability to report the inherent curvature of the motion streak caused by the sigmoidal profile of the saccade. That way, reports would be necessarily more similar to the equally curved retinal trajectories than to the linear world-centered trajectories. Although this may be the case, the largest differences between experiments were found when examining the angles of perceived trajectories, which were – for this reason – curvature-agnostic. Finally, as suggested by Pola (2004), target contrast may interact with extra-retinal position signals via visual persistence. Owing to the fact that visual processing delays must be accounted for when combining retinal with eye position information and higher luminance-contrast would increase the temporal persistence of the flash, high-contrast targets could be more prone not to mislocalization in space, but mislocalization in time (Sperling, 1990). This idea will be discussed in more detail at a later stage. Crucially, a fourth experiment should systematically investigate the role of target contrast in the perception of intra-saccadic motion streaks.

Modeling the eye position signal

Time-dependent appearance and localization. Perisaccadic localization follows a time course contingent upon the temporal dynamics of the saccade (Bischof & Kramer, 1968; Dassonville et al., 1992; Honda, 1989, 1991; Kennard et al., 1971; Mateeff, 1978; L. Matin, Matin, & Pearce, 1969; Morrone et al., 1997; Ostendorf et al., 2006; Schlag & Schlag-Rey, 1995). Unlike most flash localization studies – that sampled a large range of time points around the saccade – our experiment was designed to investigate strictly intra-saccadic presentations. If localization and appearance of intra-saccadic motion streaks followed a similar time course as flash localization, then perceptual reports would vary as a function of presentation onset relative to saccade onset and offset. To investigate this question, we fitted four linear mixed-effects regressions (including random slopes and intercepts for observers) that would model the relationship between each dependent variable and presentation onset time as a proportion of saccade duration (with 0.5 being the intercept of the model) in each experiment (dummy-coded, with Experiment 1 as the model intercept). Results are shown in **Figure 15**. Indeed, in Experiment 1 we found that angles of reported trajectories were increasingly similar to those of world-centered trajectories as presentations occurred closer to saccade offset (β = 1.73, t = 11.35, 95% CI [1.44, 2.02], p < .001). This relationship was less prominent in Experiment 2 (β = -1.26, t = -5.75, 95% CI [-1.68, -0.84], p < .001), but

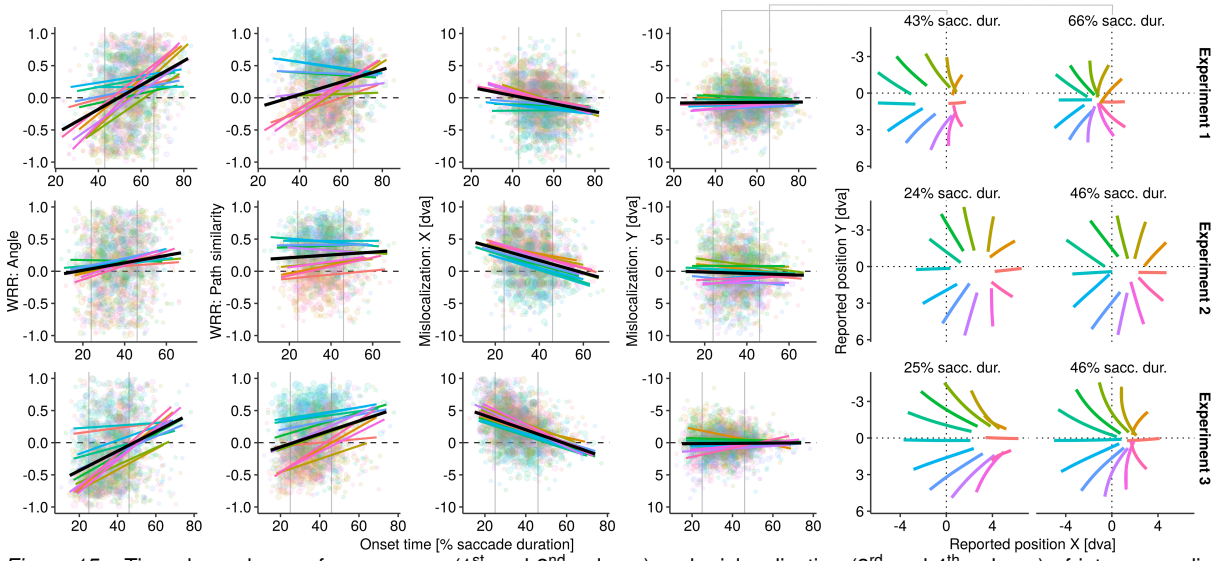

Figure 15. Time-dependence of appearance (1st and 2nd column) and mislocalization (3rd and 4th column) of intra-saccadic motion streaks in Experiments 1 (top row), 2 (middle row), and 3 (bottom row). Coloured lines represent prediction of linear regressions fitted for each motion direction, whereas solid black lines represents their average. Thin vertical lines indicate the 5% and 95% quantiles of each experiment's presentation onset time distribution. Average reports for these two time points are shown on the right. These average reports are based on predictions of mixed-effects generalized additive models (separately computed for each experiment, motion direction, and dimension) that include presentation onset time as a metric covariate.

unaltered in Experiment 3 (β = -0.27, t = -1.24, 95% CI [-0.68, 0.15], p = .224). Using path similarity as dependent variable, the same effect was found, even though less pronounced (*Experiment 1*: β = 0.83, t = 6.88, 95% CI [0.60, 1.06], p < .001; Δ*Experiment* 2: β = -0.63, t = -3.65, 95% CI [-0.97, -0.30], p = .001; Δ*Experiment* 3: β = -0.03, t = -0.17, 95% CI [-0.35, 0.30], p = .867). In Experiment 1, global mislocalization of motion streaks in the direction of the saccade decreased with later presentation onsets (β = -5.44, t = -4.91, 95% CI [-7.58, -3.32], p < .001), a trend which was also found in Experiment 2 (β = -1.32, t = -0.83, 95% CI [-4.36, 1.73], p = .413) and even increased in Experiment 3 (β = -4.07, t = -2.61, 95% CI [-7.07, -1.07], p = .015). No time-dependence of localization on the vertical plane was found (*Experiment 1*: β = -0.19, t = -0.45, 95% CI [-1.02, 0.64], p = .653; Δ*Experiment* 2: β = 1.29, t = 2.00, 95% CI [-0.05, 2.53], p = .054; Δ*Experiment* 3: β = 0.11, t = 0.18, 95% CI [-1.05, 1.26], p = .856). These results are not only compatible with most previous studies, but also suggest that the extent to which an intra-saccadic motion streaks are similar to world-centered target trajectories is inversely related to the amount of mislocalization in the direction is the saccade, which invites the hypothesis that both may have a common origin. In other words, the appearance of motion streaks could be operationalized as the sum of perceived target positions sampled over time.

The eye position model. The relatively simple eye position model assumes that, in order to localize a stimulus in world-centered coordinates, visual information (in retinal coordinates) must be combined with an eye position representation coding the egocentric direction or angle of the eye (Mittelstaedt, 1990). A simple formula captures this approach: $pos_{x,y}(t) = retinal_{x,y}(t) + eye_{x,y}(t)$. As retinal coordinates can be computed using stimulus and gaze positions over time, and subjective positions were reported by observers, the internal eye position signal can be estimated. We assume this eye position signal to follow the shape of a saccade and therefore chose to model it using an the extended version of a compressed exponential model, which has been successfully applied to approximate the position profiles of saccades (Han, Saunders, Woods, & Luo, 2013). The model has four parameters – amplitude, duration, delay, and tailedness – and is elucidated in **Figure 16**. We performed model fitting separately for each observer and condition using the stochastic approximation expectation maximization algorithm in a mixed-effects setting (Comets, Lavenu, & Lavielle, 2017), treating each individual trial as a random effect. Given that 18–36 position samples were already present in each trial, this procedure allowed an estimation of the four model parameters not only for each observer and condition, but also for every single trial. Note that only the horizontal dimension of the data was fitted, as localization of the vertical plane was on average veridical

and did not follow a saccade-contingent time course (**Figure 15**, see also Honda, 1993).

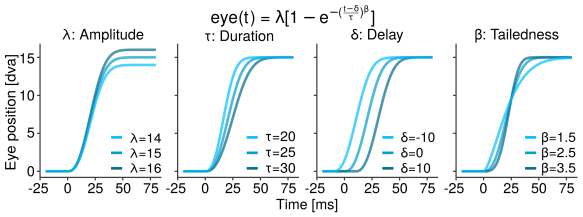

Figure 16. The (extended) compressed exponential model used to represent eye position over time. Four panels describe the respective effects of the four parameters (amplitude λ, duration τ, delay δ, and tailedness β) on the eye trajectory. Note that for the model formula $t > \delta$, else 0, applies.

Estimated eye position signals for each observer (averaged across experimental conditions) are shown in **Figure 17**. Like a variety of previous studies (e.g., Honda, 1991; Mateeff, 1978), our results – even though only intra-saccadic positions were assessed – also suggest an early-onset and slow-changing eye position signal, i.e., a "damped representation of eye displacement" (Dassonville et al., 1992, p. 261). More specifically, the represented eye position starts to change even up to one saccade duration prior to saccade onset (Delay δ [% saccade duration]: *Experiment 1*: M = -35.9, SD = 19.4; *Experiment 2*: M = -22.5, SD = 8.4; *Experiment 3*: M = -66.9, SD = 36.9) and continues changing even after saccade offset (Duration τ [% saccade duration]: *Experiment 1*: M = 100.3, SD = 22.5; *Experiment 2*: M = 72.1, SD = 18.6; *Experiment 3*: M = 119.9, SD = 33.9). For further analyses, we report the simplified same-amplitude variant of the eye position model (**Figure 17**, left column), since free-amplitude models estimated unrealistic amplitudes (**Figure 17**, right column), even though visual localization long before and after the saccade was usually accurate, which would suggests that the visual system has an adequate representation of saccade amplitude. Moreover, Pola (2004, 2011) defined extra-retinal signals in a conceptually quite similar fashion, namely by specifying a time delay and an nth-order lag that the saccadic signal must pass through. Finally, using the simplest model, we avoid the problem of overfitting and producing unnecessary complex predictions.

Compatibility of experimental data and model predictions. Can the eye position model account for experimental findings? In **Figure 18a** we predicted the appearance of motion streaks using the previously fitted eye position signals. Note that these predictions were performed individually on each trial's retinal trajectories, so that inherent differences between observers and experiments are accounted for. In principle, response patterns appear to be closely matched by the model predictions, especially when using eye position signals fitted separately for each motion direction (trial-level predic-

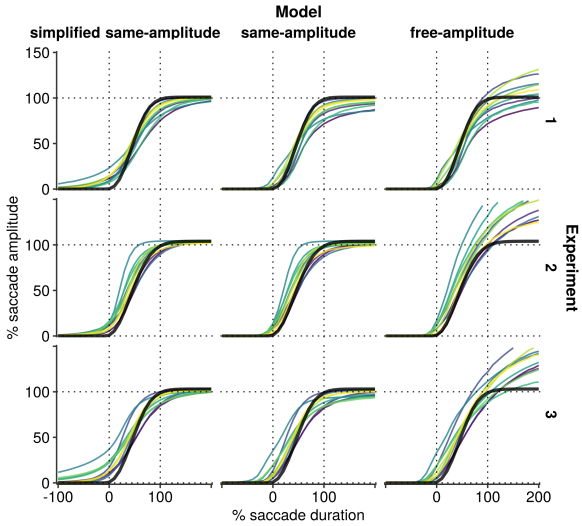

Figure 17. Estimated eye position signals of participants of Experiments 1 to 3 (top to bottom). Three variants of the extended compressed model were fitted. The free-amplitude variant of the model (right column) allowed for four free parameters and was prone to overestimations of amplitudes. The same-amplitude model (center column) fixed the amplitude to the amplitude of the respective saccade (solid black lines). The simplified same-amplitude model (left column) had only two free parameters, i.e., duration and delay.

tion in **Figure 18b**). In Experiments 1 and 3, the curvature of observers' responses were closely matched, suggesting that the mislocalization in the direction of the saccade which was stongest in the early stages of target motion and decreased over time (as indicated by the conspicuous tilt of the reported trajectory in the opposite direction of the saccade) is most likely a consequence of the eye position signal's time course relative to the saccade-contingent retinal input. More specifically, since the eye position signal has an earlier onset (encoding an eye position that has not yet been reached by the eye) early target positions were mislocalized in the direction of the saccade, whereas later target positions were localized in the opposite direction of the saccade once the eye overtakes the more sluggish eye position signal. This explanation would not only explain this data, but also previous findings. For instance, Kennard et al. (1971) – like later Honda (2006) – presented rapidly descending light spots around the time of horizontal saccades and had observers describe their motion path. As predicted by the eye position model, observers reported an inverted S-shaped trajectory exhibiting a large deviation in saccade direction around the onset of the eye movement, as well as a rebound in the opposite direction around its offset. Similarly, Mateeff (1978) presented upward vertical target motion with the same velocity profile as the ongo-

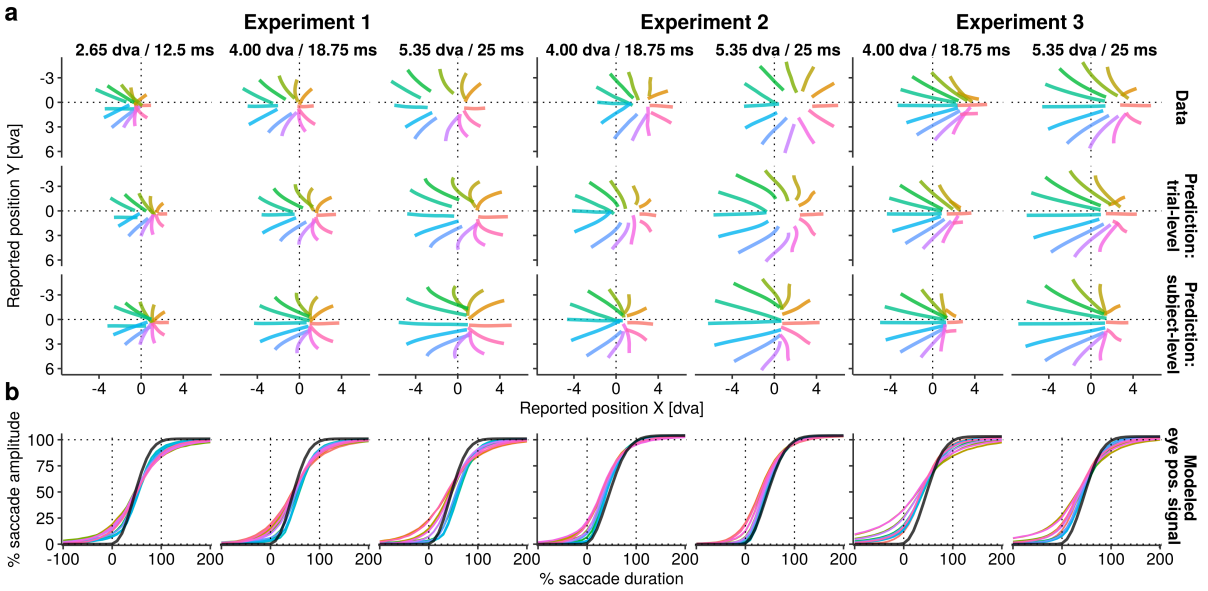

Figure 18. Appearance of intra-saccadic motion streaks as predicted by the eye position model. **a** Average experimental findings are shown in the top row. Two model predictions are shown: The trial-level prediction (middle row) uses the eye position signal estimated in each individual motion-direction condition to predict subjective trajectories, whereas the subject-level prediction (bottom row) assumes one prototypical eye position signal per observer, i.e., the eye position signal averaged across all 12 motion directions. **b** Average eye position signals fitted separately for each motion direction condition (spectral-colored lines), relative to the duration and amplitude of the corresponding saccade (solid black lines).

ing saccade and found a curved trajectory closely resembling observers' reports of upward motion presented here.

In addition to the curvature of reported trajectories, even the length of the perceived motion streak is closely matched in Experiment 3, which is less the case in Experiment 1. A probable explanation in favor of the eye position model would be that the streak length predicted by the model could not be resolved due to lower contrast. In fact, a reduction of peri-saccadic contrast sensitivity could have further amplified a well-known bias, that is that the length of intra-saccadic motion streaks is by trend underestimated (Bedell & Yang, 2001; E. Matin et al., 1972). This might also explain the relative poor performance of the model in Experiment 2 (**Figure 18a**), in which the model was unable to account for both the global mislocalization of trajectories in the direction of the saccade and the straightness of the reported trajectories, which should actually have the same origin. Therefore, modeled eye positions did exhibit an early onset (necessary to explain global mislocalization), but very little sluggishness (to account for relatively world-centered reports). Due to the inherent saccade-induced curvature of model predictions, trajectories were produced that very poorly reflect the data. Given that the data could in principle be approximated very well by the model (Experiment 3 in **Figure 18a**), it may however be the case that the predicted curvature might have been present in the data, but was rendered invisible due to the low effective target contrast. Indeed, likely for the same reason, some observers in Experiment 2 reported extremely short motion streak trajectories which were difficult to be fitted by the model.

As indicated by **Figure 18b**, eye position signals fitted separately for different motion directions were ordered in a consistent fashion, suggesting systematic differences. Owing to the fact that the intra-saccadic target's motion direction was unpredictable to the observer, it makes little sense that internal representations of eye position should depend on it. Instead, the varying onsets of the internal change in eye position indicate a separate phenomenon, namely the mislocalization of the motion onset position in the direction of motion – similar to the Fröhlich effect (Fröhlich, 1929). Importantly, this is indirect evidence that perceived position is not simply a product of retinotopic visual processing and extra-retinal eye position information, but that the retinal motion of the target (possibly also relative to a visual reference) is taken into account even during saccades (MacKay, 1970; O'Regan, 1984). Indeed, assuming one eye position signal per observer independent of motion direction (subject-level prediction in **Figure 18a**), similarity to the experimental data is visibly reduced.

Finally, can the eye position model account for the effect of presentation onset on appearance and localization of motion

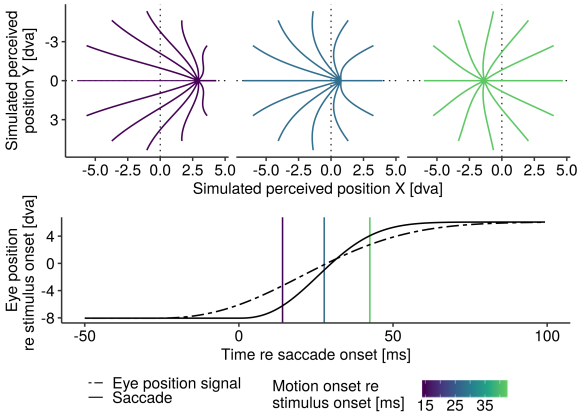

Figure 19. Simulated appearance of intra-saccadic motion streaks based on the eye position model. An early-onset, slow-changing eye position signal (λ = 14.1, δ = -27.2 ms, τ = 59.7 ms, β = 2.4) co-occurring with a horizontal saccade (λ = 14.1, δ = 0 ms, τ = 32.2 ms, β = 2.4) is assumed, during which 25-ms 5.35-dva target motion (starting at the origin of the coordinate system) in all 12 tested directions is presented at three different time points (14.1 ms, 27.7 ms, 42.5 ms).

streaks (**Figure 15**)? To investigate this question, a simple simulation was performed, whose results are shown in **Figure 19**. Target motion was set to start at three different time points, each time traveling a distance of 5.35 dva in 25 ms. When targets were presented at the earliest time point during the saccade, reports resembled the results of Experiment 3, featuring global mislocalization in the direction of the saccade and an elongation of trajectories in the opposite direction of the saccade. When presented right in the middle of the saccade, reports became more similar to those of Experiment 1, exhibiting a slightly higher similarity to world-centered than to retinal trajectories, as well as little global mislocalization – if any – in the opposite direction of the saccade. At the latest presentation onset time already close to saccade offset, reports are already extremely similar to world-centered trajectories, displaying mislocalization opposite to the direction of the saccade, presumably due to the sluggishness of the eye position signal. Note that these cases were mostly excluded from our experimental data, as presentation offset would occur only after saccade offsets. The eye position model suggests that both localization and appearance of intra-saccadic motion streaks are results of a temporal mismatch between assumed and actual eye position, and is thus able to conceptually explain a large proportion of variance in the data.

General Discussion

In this study we set out to study the phenomenological appearance of motion streaks induced by rapid and strictly intra-saccadic target motion that could be presented continuously and with high temporal fidelity using a 1440-fps projection system. Unlike previous paradigms that measured peri-saccadic localization psychophysically, we instructed observers to freely report the subjective appearance and location of motion streaks using a computer mouse – a tool that they have considerable experience with – to be able to assess the full extent of observers' perception. Whereas Experiments 1 and 2 provided surprising evidence showing that observers were able to report intra-saccadic target motion in nearly world-centered coordinates, suggesting that an accurate eye position signal must have been available even during saccades, Experiment 3 scrutinized these results using well-detectable high-contrast targets showing that this is not necessarily the case. Even though similarity of subjective reports to world-centered trajectories varied across experiments, response patterns were largely independent of the target's visual field location (Experiment 1), background luminance and structure (Experiment 3), and even intra-saccadic large-field background motion (Experiment 2). By modeling the latent eye position signal accompanying each saccade, we found that overall response patterns were to large extent explained by an early-onset, but slowly changing eye position signal, which has also served as an explanation of peri-saccadic mislocalization effects in previous studies (e.g., Dassonville et al., 1992; Honda, 1989, 1991, 1993, 2006; Mateeff, 1978; L. Matin et al., 1969, 1970). Importantly, we found consistent mislocalization of motion streaks in the direction of their inducing target motion, suggesting that motion signals could well bias position estimates (Whitney, 2002; Whitney & Cavanagh, 2000) – even during saccades.

The "world-centered" reference frame around saccades. Visual stimuli are routinely localized in world-centered coordinates, yet around the onset of saccades significant systematic mislocalizations occur, which have been throughly researched ever since the 1960s (Bischof & Kramer, 1968; L. Matin & Pearce, 1965; Sperling & Speelman, 1965). Most experimental results are compatible with the hypothesis that the visual system has access to only a damped eye position signal that causes peri-saccadic mislocalization, yet a notable exception are the double-step experiments by Hallett and Lightstone (1976a, 1976b). These experiments, which were conducted in complete darkness, showed that observers were able to make accurate secondary saccades to a target that was flashed strictly during an ongoing primary saccade and – e.g., at a presentation duration of 20 ms – even produced a considerable motion streak. In contrast to previous flash localization studies, these results suggested a high-fidelity representation of eye position, but Dassonville et al. (1992) later found that oculomotor mislocalization consistent with a dampened eye position signal also occurred when using the double-step paradigm. Recently, Watson, Schweitzer, Castet, Ohl, and Rolfs (2017)

provided evidence that localization of rapidly drifting gratings during saccades (rendered visible due to a reduction of retinal speed; Deubel et al. 1987; García-Pérez and Peli 2001) occurred consistently in world-centered coordinates, not only for oculomotor (saccade) but also for perceptual (computer mouse) responses. How could this be explained? One potentially relevant cue lies in the experimental paradigm: Whereas most mislocalization studies presented flashed targets across a large temporal range (i.e., up to ±400 milliseconds around saccade onset; Dassonville et al., 1992), studies that reported nearly world-centered localization (Hallett & Lightstone, 1976a, 1976b; Watson et al., 2017, and the experiments reported here) applied gaze-contingent stimulus presentations that occurred in (by comparison) very small temporal ranges, centering around the mid-point or peak velocity of the saccade. Comparing the fitted trajectories of saccades and eye position signals (e.g., **Figure 19**), it becomes obvious that – of course depending on stimulus type and system latencies of the setup – presentations may well occur within a temporal sweet spot where actual and assumed eye position are largely identical. In that case, averaged results would suggest a world-centered representation of stimulus position which may however only be the incidental outcome of intra-saccadic stimulus timing and would therefore still be compatible with damped eye position signals. Our results strongly speak in favor of this hypothesis: Even though target motion was presented upon the onset of the saccade after a (on average) fixed time delay (for a description of the incurring latencies, see Schweitzer & Rolfs, 2020a), we not only assessed positions over time by studying countinous motion streaks, but also systematically analyzed the effects of presentation onset time on appearance and localization, which were well consistent with the predictions of the time course of a damped eye position signal.

The plausibility of the eye position signal. One might furthermore raise the question whether a damped eye position signal is feasible and why it should be damped at all. Importantly, despite the earlier onset of the fitted eye position signal relative to saccade onset, the eye position signal does not need to be anticipatory. Instead, as shown in various simulations by Pola (2004), to match latencies that incur in visual processing pathways, the eye position signal used for visual localization must be significantly delayed in time, essentially occurring after the saccade. Note that, as no reliable estimate of visual latencies of motion streak stimuli could be made at this point, we ignored this aspect in our modeling, assuming that there was no visual latency or, similarly, that visual and eye position information had the exact same latency. If world-centered localization of intra-saccadic stimuli were possible, then two prerequisites should be met. First, the time course of the ongoing eye movement should be precisely known to allow for localization even at high angular velocities. Recent evidence suggests that this may not unreasonable. For instance, Smalianchuk, Jagadisan, and Gandhi (2018) provided evidence that neural activity in the superior colliculus – a midbrain structure also found to be implicated in the coding of amplitude and direction of impending saccades (Seideman, 2020) – was directly related not only to the peak velocity of a saccade (independently of amplitude), but also provided an accurate representation of the saccade's velocity profile. Interestingly, by computing cross-correlations between neural activity and instantanious saccade velocity, the authors estimated a delay of approximately 12 milliseconds. Furthermore, Herzfeld, Kojima, Soetedjo, and Shadmehr (2018) found that the population firing rate of cerebellar Purkinje cells precisely represented differences in shape of saccadic velocity profiles induced by saccadic adaptation. It could thus well be that the neural representation of the ongoing saccade trajectories may be sufficiently accurate to allow for intra-saccadic spatial localization in world-centered coordinates. This leads us to the second prerequisite, that is, the precise temporal synchronization of eye position signal and visual input. This, indeed, should be a difficult feat to achieve, as visual latencies may vary considerably depending on factors such as intensity (Mansfield & Daugman, 1978), retinal locus (Lichtenstein & White, 1961), or presence of motion (Allik & Kreegipuu, 1998). Given that it might be impossible to appropriately delay the eye position signal to match unpredictably varying visual latencies, the visual system may dampen the eye position signal. As suggested by Dassonville et al. (1992), the dampening of the eye position signal could have developed to minimize errors: By increasing the time window of position change – while accepting the drawback of prolonged spatial uncertainty and larger localization errors around saccade onset and offset (as shown by Honda, 1993) – it may be possible to remedy more drastic spatial localization errors that would occur if the eye position signal more closely matched the brief, step-like saccade profile. An alternative hypothesis assumes that it may not be the eye position signal that is damped, but the impulse response function to flashed stimuli, which could well produce a temporally extended representation over time due to visual persistence (Pola, 2004, 2011). Following this argument, mislocalization would occur as an artifact of using flashed targets mislocalized in time, not as a consequence of a damped eye position signal. This hypothesis cannot be ruled out, as afterimages have also been shown to be shifted in saccade direction (Grüsser, Krizic, & Weiss, 1987), but is incompatible with the finding that retinally stabilized visual targets continuously visible during saccades are still mislocalized in the direction of the saccade (Mateeff, 1978). Moreover, as shown by Schlag and Schlag-Rey (1995), continuously presented targets extinguished prior to saccade onset were not subject to mislocalization despite visual persistence that occurred in the dark. These authors also emphasized the point that motion streaks only occurred when targets were physically shifted on the

retina and never when they (illusionary) shifted positions after being flashed prior to saccade onset. Clearly, peri-saccadic mislocalization could originate from various, potentially additive sources. These include not only a delayed, most likely damped eye position signal, but also various visual factors, such as stimulus intensity, duration, and motion. Strong evidence for this assumption is provided by the result that a prototypical, observer-specific eye position signal could account neither for the motion direction-dependent localization biases found in all three experiments, nor for the drastic differences in motion streak appearance in Experiment 2 and 3.

The role of target contrast. Finally, by elaborating on the role of target contrast, an attempt shall be made to explain these large differences that have occurred between the three reported experiments. Experiment 3 applied a Weber contrast of 10 (by reducing background luminance) and targets in Experiments 1 and 2 each had a Weber contrast of 1, while effective target contrast in Experiment 2 was even lower due to the structured background. Strikingly, similarity to world-centered trajectories was largest in Experiment 2, slightly lower in Experiment 1, and lowest in Experiment 3 – thus displaying an inverted relationship to target contrast. Note that we planned to systematically investigate the effect of target contrast in a fourth experiment, which has not yet been initiated due to the SARS-CoV-2-related shutdown of laboratories. In the light of these preliminary findings, however, the hypothesis may be formulated that increasing target contrast led to a reduction of visual latency which then caused targets to be localized earlier in time. There is good evidence that contrast and visual latency have an inverted relationship. For example, V1 simple cell response latencies decrease in an exponential fashion as (log-)contrast increases (Reich, Mechler, & Victor, 2001). This effect already occurred on the retinal level when measured by the electroretinogram (Mansfield & Daugman, 1978). On a perceptual level, the effect could be demonstrated using the Hess effect, where high-luminance stimuli seemed to lead low-luminance stimuli, even though both move at the same velocity and are physically aligned (Williams & Lit, 1983). As outlined above, it might be impossible to accurately align the time courses of eye position and visual stimulation, as visual latency will be hard to predict: High-contrast targets will be processed with short latencies, whereas low-contrast targets (if detected at all) will need more time to reach the same point in the visual processing hierarchy. Both our experimental results (**Figure** 15) and simulations (**Figure** 19) emphasized not only that localization and appearance of motion streaks depend heavily on the stimulus' onset time relative to saccade onset, but also that responses to a target presented at a given time could strongly vary between experiments. A contrast-dependent change in visual latency could explain these results, if mislocalization had not occurred in space, but in time: High-contrast targets (with shorter visual latencies) were perceived as occurring earlier throughout the saccade, and were therefore localized in space using an earlier eye position representation (that overestimated the physical position of the eye). Indeed, as indicated by the fitted delays, the eye position signal started to change significantly earlier in Experiment 3 than in Experiments 1 and 2, indicating a larger relative shift of the synchronization of visual and position signals. This would also explain Honda's (1993) results which showed an earlier onset of the eye position signal when a target of a constant luminance was localized in front of a low-luminance background compared to a mid-luminance background, as, naturally, if presented in nearly complete darkness, the Weber contrast of any stimulus would be nearly infinite.

Conclusion. By studying the subjective appearance and localization of intra-saccadic motion streaks, we provided insights in how retinal input induced by concurrent eye and stimulus movement is localized in world-centered coordinates. Our results are well consistent with the hypothesis that retinal locations sampled over time are combined with a imperfect, damped representation of physical eye position, even though additional visual factors, such as direction of motion and contrast of the target, have to be taken into account to explain the data. Future studies are envisaged to scrutinize the possible roles of both visual latency (to ultimately estimate the delay of the eye position signal in perceptual tasks) and visual references (to explain the striking similarity between real and simulated saccades in some studies, e.g., MacKay, 1970; Ostendorf et al., 2006; Sperling, 1990). Finally, the oculomotor system may in principle have an accurate representation about the ongoing saccadic trajectory, but it seems unlikely that it could be adequately used to localize unpredictably appearing peri-saccadic visual input in space. Thus, it remains an open question to what extent eye position signals could contribute to the omission of the visual consequences of saccades or to trans-saccadic continuity.

Acknowledgements

We thank Jan-Niklas Klanke, Clara Kuper, Polina Arbuzova, Luke Pendergrass, Julius Krumbiegel, and Olga Shurygina for their help with running Experiment 1. R.S. was supported by the Studienstiftung des deutschen Volkes and the Berlin School of Mind and Brain. M.R. was supported by the Deutsche Forschungsgemeinschaft (DFG, grants RO3579/2-1, RO3579/8-1 and RO3579/10-1).

Author contributions

R.S., T.W., T.B., and M.R. conceived and designed the study. R.S. implemented and conducted experiments. R.S. analyzed data under M.R.'s and T.W.'s supervision. R.S. wrote the manuscript, and M.R., T.W., and T.B. will provide critical revisions.

References

Abrams, J., Nizam, A., & Carrasco, M. (2012). Isoeccentric locations are not equivalent: The extent of the vertical meridian asymmetry. *Vision Research*, *52*(1), 70–78.

Allik, J., & Kreegipuu, K. (1998). Multiple visual latency. *Psychological Science*, *9*(2), 135–138.

Becker, W. (1989). The neurobiology of saccadic eye movements. metrics. *Reviews of oculomotor research*, *3*, 13.

Bedell, H., & Yang, J. (2001). The attenuation of perceived image smear during saccades. *Vision Research*, *41*(4), 521–528.

Binda, P., & Morrone, M. C. (2018). Vision during saccadic eye movements. *Annual review of vision science*, *4*, 193–213.

Bischof, N., & Kramer, E. (1968). Untersuchung und überlegungen zur richtungswahrnehmung bei willkürlichen sakkadischen augenbewegungen [investigations and considerations of directional perception during voluntary saccadic eye movements]. *Psychologische Forschung*, *32*(3), 185–218.

Bridgeman, B., Hendry, D., & Stark, L. (1975). Failure to detect displacement of the visual world during saccadic eye movements. *Vision research*, *15*(6), 719–722.

Bridgeman, B., Van der Heijden, A. H. C., & Velichkovsky, B. M. (1994). A theory of visual stability across saccadic eye movements. *Behavioral and Brain Sciences*, *17*(2), 247–258.

Brooks, B. A., & Fuchs, A. F. (1975). Influence of stimulus parameters on visual sensitivity during saccadic eye movement. *Vision Research*, *15*(12), 1389–1398.

Brooks, B. A., Impelman, D., & Lum, J. (1981). Backward and forward masking associated with saccadic eye movement. *Perception & Psychophysics*, *30*(1), 62–70.

Burr, D., Holt, J., Johnstone, J., & Ross, J. (1982). Selective depression of motion sensitivity during saccades. *The Journal of physiology*, *333*(1), 1–15.

Burr, D., Morrone, M., & Ross, J. (1994). Selective suppression of the magnocellular visual pathway during saccadic eye movements. *Nature*, *371*(6497), 511–513.

Burr, D., & Ross, J. (1982). Contrast sensitivity at high velocities. *Vision research*, *22*(4), 479–484.

Campbell, F., & Wurtz, R. (1978). Saccadic omission: why we do not see a grey-out during a saccadic eye movement. *Vision research*, *18*(10), 1297–1303.

Castet, E. (2010). Perception of intra-saccadic motion. In *Dynamics of visual motion processing, chapter 10* (pp. 213–238). Springer.

Castet, E., Jeanjean, S., & Masson, G. (2002). Motion perception of saccade-induced retinal translation. *Proceedings of the National Academy of Sciences*, *99*(23), 15159–15163.

Castet, E., & Masson, G. (2000). Motion perception during saccadic eye movements. *Nature Neuroscience*, *2*, 177–183.

Chekaluk, E., & Llewellyn, K. R. (1990). Visual stimulus input, saccadic suppression, and detection of information from the postsaccade scene. *Perception & Psychophysics*, *48*(2), 135–142.

Collewijn, H., Erkelens, C. J., & Steinman, R. M. (1988). Binocular coordination of human horizontal saccadic eye movements. *The Journal of physiology*, *404*(1), 157–182.

Comets, E., Lavenu, A., & Lavielle, M. (2017). Parameter estimation in nonlinear mixed effect models using saemix, an R implementation of the SAEM algorithm. *Journal of Statistical Software*, *80*(3), 1–41. doi: 10.18637/jss.v080.i03

Cornelisen, F., Peters, E., & Palmer, J. (2002). The eyelink toolbox: eyetracking with matlab and the psychophysics toolbox. *Behaviour Research Methods*, *34*(4), 613–617.

Dassonville, P., Schlag, J., & Schlag-Rey, M. (1992). Oculomotor localization relies on a damped representation of saccadic eye displacement in human and nonhuman primates. *Visual neuroscience*, *9*(3-4), 261–269.

Deubel, H. (2004). Localization of targets across saccades: Role of landmark objects. *Visual Cognition*, *11*(2-3), 173–202.

Deubel, H., Elsner, T., & Hauske, G. (1987). Saccadic eye movements and the detection of fast-moving gratings. *Biological cybernetics*, *57*(1-2), 37–45.

Duyck, M., Collins, T., & Wexler, M. (2016). Masking the saccadic smear. *Journal of vision*, *16*(10), 1.

Duyck, M., Wexler, M., Castet, E., & Collins, T. (2018). Motion masking by stationary objects: a study of simulated saccades. *i-Perception*, *9*(3), 2041669518773111.

Engbert, R., & Kliegl, R. (2003). Microsaccades uncover the orientation of covert attention. *Vision research*, *43*(9), 1035–1045.

Engbert, R., & Mergenthaler, K. (2006). Microsaccades are triggered by low retinal image slip. *Proceedings of the National Academy of Sciences*, *103*(18), 7192-7197.

Fröhlich, F. W. (1929). *Die empfindungszeit: ein beitrag zur lehre von der zeit-, raum-und bewegungsempfindung*. G. Fischer.

García-Pérez, M. A., & Peli, E. (2001). Intrasaccadic perception. *Journal of Neuroscience*, *21*(18), 7313–7322.

Geisler, W. (1999). Motion streaks provide a spatial code for motion direction. *Nature*, *400*(6739), 65-69.

Gibson, J. J. (1966). *The senses considered as perceptual systems* (L. Carmichael, Ed.). George Allen & Unwin Ltd, London.

Grüsser, O.-J., Krizic, A., & Weiss, L.-R. (1987). Afterimage movement during saccades in the dark. *Vision Research*, *27*(2), 215–226.

Hallett, P. E., & Lightstone, A. (1976a). Saccadic eye movements to flashed targets. *Vision research*, *16*(1), 107–114.

Hallett, P. E., & Lightstone, A. D. (1976b). Saccadic eye movements towards stimuli triggered by prior saccades. *Vision research*, *16*(1), 99–106.

Han, P., Saunders, D. R., Woods, R. L., & Luo, G. (2013). Trajectory prediction of saccadic eye movements using a compressed exponential model. *Journal of Vision*, *13(8)*(27).

Herzfeld, D. J., Kojima, Y., Soetedjo, R., & Shadmehr, R. (2018). Encoding of error and learning to correct that error by the purkinje cells of the cerebellum. *Nature neuroscience*, *21*(5), 736–743.

Honda, H. (1989). Perceptual localization of visual stimuli flashed during saccades. *Perception & Psychophysics*, *45*(2), 162–174.

Honda, H. (1991). The time courses of visual mislocalization and of extraretinal eye position signals at the time of vertical saccades. *Vision research*, *31*(11), 1915–1921.

Honda, H. (1993). Saccade-contingent displacement of the apparent position of visual stimuli flashed on a dimly illuminated structured background. *Vision research*, *33*(5-6), 709–716.

Honda, H. (2006). Achievement of transsaccadic visual stability using presaccadic and postsaccadic visual information. *Vision Research*, *46*(20), 3483–3493.

Hooge, I., Nyström, M., Cornelissen, T., & Holmqvist, K. (2015). The art of braking: Post saccadic oscillations in the eye tracker signal decrease with increasing saccade size. *Vision research*, *112*, 55–67.

Kennard, D. W., Hartmann, R. W., Kraft, D. P., & Glaser, G. H. (1971). Brief conceptual (nonreal) events during eye movement. *Biological psychiatry*, *3*(3), 205.

Kleiner, M., Brainard, D., Pelli, D., Ingling, A., Murray, R., & Broussard, C. (2007). What is new in psychtoolbox-3. *Perception*, *36*(14), 1-16.

Lebedev, S., Van Gelder, P., & Tsui, W. H. (1996). Square-root relations between main saccadic parameters. *Investigative Ophthalmology & Visual Science*, *37*(13), 2750–2758.

Lichtenstein, M., & White, C. T. (1961). Relative visual latency as a function of retinal locus. *JOSA*, *51*(9), 1033–1034.

MacKay, D. M. (1970). Mislocation of test flashes during saccadic image displacements. *Nature*, *227*(5259), 731–733.

MacKay, D. M. (1973). Visual stability and voluntary eye movements. In *Central processing of visual information a: integrative functions and comparative data* (pp. 307–331). Springer.

Mansfield, R. J. W., & Daugman, J. G. (1978). Retinal mechanisms of visual latency. *Vision Research*, *18*(9), 1247–1260.

Mateeff, S. (1978). Saccadic eye movements and localization of visual stimuli. *Perception & Psychophysics*, *24*(3), 215–224.

Matin, E. (1974). Saccadic suppression: a review and an analysis. *Psychological bulletin*, *81*(12), 899.

Matin, E., Clymer, A., & Matin, L. (1972). Metacontrast and saccadic suppression. *Science*, *178*(4057), 179–182.

Matin, L., Matin, E., & Pearce, D. G. (1969). Visual perception of direction when voluntary saccades occur. i. relation of visual direction of a fixation target extinguished before a saccade to a flash presented during the saccade. *Perception & Psychophysics*, *5*(2), 65–80.

Matin, L., Matin, E., & Pola, J. (1970). Visual perception of direction when voluntary saccades occur: II. relation of visual direction of a fixation target extinguished before a saccade to a subsequent test flash presented before the saccade. *Perception & Psychophysics*, *8*(1), 9–14.

Matin, L., & Pearce, D. G. (1965). Visual perception of direction for stimuli flashed during voluntary saccadic eye movements. *Science*, *148*(3676), 1485–1488.

Mitrani, L., & Yakimoff, N. (1971). Is saccadic suppression really saccadic? *Vision Research*, *11*(10), 1157–1161.

Mitrani, L., Yakimoff, N., & Mateeff, S. T. (1973). Saccadic suppression in the presence of structured background. *Vision research*.

Mittelstaedt, H. (1990). Basic solutions to the problem of head-centric visual localization. In (pp. 267–287). Erlbaum Hillsdale, NJ.

Morrone, M. C., Ross, J., & Burr, D. (1997). Apparent position of visual targets during real and simulated saccadic eye movements. *J. Neurosci.*, *17*(20), 7941.

Nyström, M., Hooge, I., & Holmqvist, K. (2013). Post-saccadic oscillations in eye movement data recorded with pupil-based eye trackers reflect motion of the pupil inside the iris. *Vision research*, *92*, 59–66.

O'Regan, J. K. (1984). Retinal versus extraretinal influences in flash localization during saccadic eye movements in the presence of a visible background. *Perception & Psychophysics*, *36*(1), 1–14.

Ostendorf, F., Fischer, C., Gaymard, B., & Ploner, C. J. (2006). Perisaccadic mislocalization without saccadic eye movements. *Neuroscience*, *137*(3), 737–745.

Pola, J. (2004). Models of the mechanism underlying perceived location of a perisaccadic flash. *Vision research*, *44*(24), 2799–2813.

Pola, J. (2011). An explanation of perisaccadic compression of visual space. *Vision research*, *51*(4), 424–434.

Reich, D. S., Mechler, F., & Victor, J. D. (2001). Temporal coding of contrast in primary visual cortex: when, what, and why. *Journal of neurophysiology*, *85*(3), 1039–1050.

Richards, W. (1969). Saccadic suppression. *Journal of the*

Optical Society of America, *59*(5), 617–623.

Roelofs, C. O. (1935). Die optische lokalisation. *Archiv für Augenheilkunde*.

Ross, J., Morrone, M., Goldberg, M., & Burr, D. (2001). Changes in visual perception at the time of saccades. *Trends in neurosciences*, *24*(2), 113–121.

Ross, J., Morrone, M. C., & Burr, D. C. (1997). Compression of visual space before saccades. *Nature*, *386*(6625), 598–601.

Schlag, J., & Schlag-Rey, M. (1995). Illusory localization of stimuli flashed in the dark before saccades. *Vision research*, *35*(16), 2347–2357.

Schweitzer, R., & Rolfs, M. (2020a). An adaptive algorithm for fast and reliable online saccade detection. *Behavior research methods*, *52*(3), 1122-1139.

Schweitzer, R., & Rolfs, M. (2020b). Intra-saccadic motion streaks as cues to linking object locations across saccades. *Journal of Vision*, *20*(4), 17. doi: 10.1167/jov.20.4.17

Seideman, J. A. (2020). A dynamic, imperturbable link between midbrain activity and saccade velocity. *Journal of Neurophysiology*, *123*(2), 451–453.

Smalianchuk, I., Jagadisan, U. K., & Gandhi, N. J. (2018). Instantaneous midbrain control of saccade velocity. *Journal of Neuroscience*, *38*(47), 10156–10167.

Sommer, M. A., & Wurtz, R. H. (2008). Brain circuits for the internal monitoring of movements. *Annu. Rev. Neurosci.*, *31*, 317–338.

Sperling, G. (1990). Comparison of perception in the moving and stationary eye. *Eye movements and their role in visual and cognitive processes*, *4*, 307–351.

Sperling, G., & Speelman, R. G. (1965). Visual spatial localization during object motion, apparent object motion, and image motion produced by eye movements [abstract]. *Journal of the Optical Society of America*, *55*, 1576-1577.

Sperry, R. W. (1950). Neural basis of the spontaneous optokinetic response produced by visual inversion. *Journal of comparative and physiological psychology*, *43*(6), 482.

Volkmann, F. C. (1986). Human visual suppression. *Vision research*, *26*(9), 1401–1416.

Volkmann, F. C., Riggs, L., White, K., & Moore, R. (1978). Contrast sensitivity during saccadic eye movements. *Vision research*, *18*(9), 1193–1199.

von der Malsburg, T., & Vasishth, S. (2011). What is the scanpath signature of syntactic reanalysis? *Journal of Memory and Language*, *65*(2), 109-127.

Von Holst, E., & Mittelstaedt, H. (1950). Das reafferenzprinzip [the principle of reafference]. *Naturwissenschaften*, *37*(20), 464–476.

Watson, T., Schweitzer, R., Castet, E., Ohl, S., & Rolfs, M. (2017). Intra-saccadic localisation is consistently carried out in world-centered coordinates [abstract]. *Journal of Vision*, *17*(10), 1276–1276.

Whitney, D. (2002). The influence of visual motion on perceived position. *Trends in cognitive sciences*, *6*(5), 211–216.

Whitney, D., & Cavanagh, P. (2000). Motion distorts visual space: shifting the perceived position of remote stationary objects. *Nature neuroscience*, *3*(9), 954–959.

Williams, J. M., & Lit, A. (1983). Luminance-dependent visual latency for the hess effect, the pulfrich effect, and simple reaction time. *Vision research*, *23*(2), 171–179.

Wurtz, R. H. (2008). Neuronal mechanisms of visual stability. *Vision research*, *48*(20), 2070–2089.

Wurtz, R. H. (2018). Corollary discharge contributions to perceptual continuity across saccades. *Annu. Rev. Vis. Sci.*, *4*(1), 215–237. doi: 10.1146/annurev-vision-102016-061207